Branching processes and multiple term structure modeling

Guillaume Szulda

Université de Paris

ED 386 – École Doctorale Sciences Mathématiques de Paris Centre

Laboratoire de Probabilités, Statistique et Modélisation (LPSM)

Processus de branchement et modélisation des structures à terme multiples

Branching processes and multiple term structure modeling

Guillaume Szulda

Sous la direction de Prof. Claudio Fontana

Thèse de doctorat

Discipline : Mathématiques Appliquées

Présentée et soutenue à Paris le **vendredi 10 décembre 2021** devant le jury suivant :

Aurélien Alfonsi	PU	École des Ponts	Rapporteur
Antoine Jacquier	Reader	Imperial College	Rapporteur
Ying Jiao	PU	Université de Lyon	Examinatrice
Zorana Grbac	MCU	Université de Paris	Examinatrice
Mathieu Rosenbaum	PU	École Polytechnique	Examinateur
Claudio Fontana	Associate Professor	Università di Padova	Directeur
Alessandro Gnoatto	Associate Professor	Università di Verona	Invité

À ma famille

Processus de branchement et modélisation des structures à terme multiples

Guillaume Szulda

Résumé

Cette thèse est consacrée à la modélisation des structures à terme multiples à l'aide des processus de branchement à état continu avec immigration (processus CBI). Plus précisément, nous considérons deux marchés financiers où l'on peut observer la coexistence de structures à terme multiples : le marché des taux d'après-crise, où les courbes multiples de taux ont émergé depuis la crise financière des années 2007–2009, et le marché des taux de change, où de multiples devises sont échangées à l'aide de transactions au comptant ou par échanges de produits dérivés.

Cette thèse est divisée en cinq chapitres. Nous introduisons les sujets principaux de la thèse dans le chapitre 1. En particulier, nous présentons un cadre de travail général pour la modélisation des structures à terme multiples, nous motivons notre approche à l'aide des caractéristiques empiriques des marchés considérés, et définissons l'objectif principal que cette thèse cherche à atteindre.

La partie 1 se compose des chapitres 2 et 3, et est dédiée à la modélisation des courbes multiples de taux dans le marché des taux d'après-crise via processus CBI. Dans le chapitre 2, nous présentons un cadre de travail autonome pour les processus CBI. Ce cadre de travail contient une analyse des moments exponentiels des processus CBI, une étude des relations entre deux représentations stochastiques d'un processus CBI, et une vue d'ensemble des nombreux exemples de processus CBI qui peuvent être trouvés dans la litérature. Nous introduisons aussi une nouvelle spécification que l'on nomme *processus CBI stable et tempéré*.

Dans le chapitre 3, nous développons un modèle pour les courbes multiples de taux basé sur les processus CBI, motivé par les caractéristiques empiriques des "spreads" entre les taux interbancaires. Nous construisons une nouvelle classe de modèles à courbes multiples dépendant d'un *flux de processus CBI stables et tempérés*. Ces modèles sont particulièrement parcimonieux du point de vue du nombre de paramètres et maniables, et sont capables de générer des effets de contagion entre les différents spreads. L'approche proposée permet aussi une évaluation efficace des dérivés de taux linéaires, et assure l'existence de formules en forme close pour les produits non linéaires à l'aide de techniques basées sur la transformée de Fourier. Nous comparons numériquement deux méthodes de pricing basées sur l'algorithme FFT et la quantification, et montrons qu'une spécification de notre classe de modèles à courbes multiples peut être calibrée avec succès aux données du marché.

La partie 2 comprend les chapitres 4 et 5, et répond au problème de la modélisation des devises multiples dans le marché de change. Dans le chapitre 4, nous construisons une classe de processus à deux dimensions combinant processus CBI et processus de Lévy changés en temps, que l'on nomme *CBI-time-changed Lévy processes* (CBITCL). Nous développons un cadre de travail analytique étendant la plupart des résultats du chapitre 2, et appliqué à la modélisation des devises multiples au chapitre 5. En particulier, nous formulons un théorème de type Girsanov pour les processus CBITCL, qui aura des applications importantes pour la modélisation des devises multiples.

Dans le chapitre 5, nous développons un modèle à volatilité stochastique pour les devises multiples basé sur les processus CBITCL. En plus de capturer les facteurs de risque typiques du marché de change, et de préserver les symétries propres à ses taux, notre modèle est aussi capable de produire des processus de taux de change dont la volatilité peut s'exciter elle-même, provenant directement du comportement auto-excitant des processus CBI. L'approche proposée est maniable du point de vue analytique puisque celle-ci repose sur la technologie des processus affine, et permet de caractériser une classe de probabilités neutres au risque préservant la structure du modèle. Exploitant la préservation de la structure affine du modèle, nous assurons une formule de pricing de forme semi-close pour les options sur devises par le biais de techniques basées sur la transformée de Fourier. Enfin, nous testons notre modèle à l'aide d'une calibration à un triangle de change où deux types de calibration sont proposés : *standard* et *deep*, dont ce dernier utilise des techniques venant du deep learning.

Mots-clés: processus CBI, structures à terme multiples, marché des taux d'après-crise, modèles à courbes multiples, flux de processus CBI, quantification, marché forex, stabilité sous inversion, deep calibration, processus affines, SDEs, transformée de Lamperti, processus de Hawkes, processus stables et tempérés.

Branching processes and multiple term structure modeling

Guillaume Szulda

Abstract

This thesis is devoted to the modeling of multiple term structures in financial markets by relying on *continuous-state branching processes with immigration* (CBI). More specifically, we consider two financial markets where multiple term structures coexist: the post-crisis interest rate market, in which multiple yield curves have emerged since the 2007–2009 financial crisis; and the Foreign-Exchange market (FX), where multiple currencies are traded by spot and derivative transactions.

This manuscript is divided into five chapters. We start by introducing the main topics of the thesis in Chapter 1. In particular, we present a general multiple term structure framework, we then draw our motivation from the empirical features of the considered markets, and state the main objective that this thesis seeks to attain.

Part 1 consists of Chapters 2 and 3, and is dedicated to the modeling of multiple yield curves in the post-crisis interest rate market with CBI processes. In Chapter 2, we present a self-contained framework for CBI processes. This framework contains an analysis of exponential moments of CBI processes, a study of the relations between two stochastic representations of a CBI process, and an overview of several examples of CBI processes that can be found in the literature. We also introduce a new specification of a CBI process that we name *tempered-stable CBI process*.

In Chapter 3, we develop a modeling framework for multiple yield curves based on CBI processes, motivated by the empirical features of the spreads between interbank rates. We construct a new class of multi-curve models driven by a *flow of tempered-stable CBI processes*. Such models are especially parsimonious and tractable, and are able to generate contagion effects among different spreads. The proposed approach also allows for the explicit valuation of all linear interest rate derivatives, and ensures semi-closed-form formulae for non-linear products by means of Fourier techniques. We provide a numerical comparison of FFT and quantization-based pricing methodologies, and show that a simple specification of the proposed class of CBI-driven multi-curve models can be successfully calibrated to market data.

Part 2 comprises Chapters 4 and 5, and addresses the issue of modeling multiple currencies in the FX market. In Chapter 4, we construct a class of two-dimensional processes combining CBI processes with time-changed Lévy processes, which we name *CBI-time-changed Lévy processes* (CBITCL). We develop an analytical framework extending most of the results of Chapter 2 for CBI processes, which will be applied to multiple currency modeling in Chapter 5. In particular, we formulate a Girsanov-type theorem for CBITCL processes, which will reveal to have important applications in multiple currency modeling.

In Chapter 5, we develop a general stochastic volatility framework for multiple currencies based on CBITCL processes. Besides capturing the typical sources of risk in the FX market, and preserving the peculiar symmetries of FX rates, our framework allows for self-excitation in the volatility of FX rates, which derives from the self-exciting behavior of CBI processes. The proposed approach is analytically tractable since it relies on the technology of affine processes, and allows to characterize a class of risk-neutral measures that leave invariant the structure of the framework. By exploiting the preservation of the affine property, we derive a semi-closed-form pricing formula for currency options via Fourier techniques. Finally, we test our model by means of a calibration to an FX triangle where two types of calibration are proposed: *standard* and *deep*, the latter of which uses deep-learning techniques.

Keywords: CBI processes, multiple term structures, post-crisis interest rate market, multi-curve models, flow of CBI processes, quantization, FX market, stability under inversion, deep calibration, affine processes, SDEs, Lamperti transform, Hawkes processes, tempered-stable processes.

Acknowledgments

This thesis is the final outcome of four extremely demanding years that have greatly changed my person forever. During this journey of my life, and even now, several key people have been contributing to this achievement, and to whom I henceforth feel the duty to express my gratitude through these few, hopefully powerful, nonetheless humble words.

First and foremost, I would like to graciously thank, from the bottom of my heart, my doctoral supervisor, Professor Claudio Fontana, without whom I would not have ever been able to make such a life-changing accomplishment. I still remember how our collaboration started in May 2017, when everything was yet to be done. Since then, our teamwork has never ceased to expand, and I can now affirm that I have learned ever so much from you. I may especially mention your very rigorous scientific approach that I have inherited, along with your unfailing dedication to research which I can for now only admire and hope to acquire with time.

In June 2018, we were particularly delighted to welcome Professor Alessandro Gnoatto as a new crucial member of our collaboration. I would then like to seize this unique opportunity to show you my sincere appreciation. I have undoubtedly benefited enormously from our many fruitful discussions upon numerical analysis, without neglecting the long hours that we devoted to debugging our numerous lines of code one by one. I am also deeply grateful to you for making me feel at home whenever I came to Verona throughout these years.

I am truly indebted to several institutions for assisting me indirectly in making this achievement concrete: the *Laboratoire de Probabilités, Statistique et Modélisation* (LPSM), of which I gratefully acknowledge the hospitality; the *École Doctorale Sciences Mathématiques de Paris Centre* (ED386), to which I am immensely thankful for the financial support; the *Fondation Science Mathématiques de Paris* (FSMP), whose financial support permitted me to sojourn at the *University of Freiburg* where I researched alongside inspiring professionals; and lastly the *University of Verona*, whose hospitality and financial support were very much acknowledged.

This fulfillment has nevertheless been contingent upon the completion of the doctoral defense. In this regard, I would like to cordially thank Professors Aurélien Alfonsi and Antoine Jacquier for consenting to referee my thesis, of whom I have sincerely appreciated reading the detailed accounts. I am also grateful to Professors Ying Jiao, Zorana Grbac, and Mathieu Rosenbaum, for agreeing to take part in the jury. Furthermore, I would like to thank Professor Claudio Fontana again, for offering me the possibility to assume a post-doctoral position within his extremely dynamic research group at the *University of Padova*. I am utterly convinced that our teamwork will endure and give rise to further research projects in the future.

Last, but certainly not least, I want to seize this ultimate opportunity to express my gratitude to my family, the polar star of my life, and Sofía, for your indispensable moral support throughout the successive lockdowns of the last two years.

Thank you.

Table of contents

Introduction en Français

Summary. Ce chapitre constitue l'introduction de ce manuscrit et vise principalement à préparer le lecteur en vue des parties 1 et 2. Nous commençons par présenter un cadre de travail général pour la modélisation des structures à terme multiples, étendant notamment certaines idées initialement développées par [**JT98**]. Nous tirons ensuite notre motivation des caractéristiques empiriques des deux marchés considérés, et formulons l'objectif principal que cette thèse cherche à atteindre. Enfin, nous exposons les grandes lignes de l'approche proposée basée sur les processus de branchement à état continu avec immigration (processus CBI), et présentons l'organisation globale de la thèse.

Dans ce chapitre introductif, soit $\big(\Omega, \mathcal{F}, \mathbb{F}, \mathbb{Q}\big)$ un espace de probabilité satisfaisant les conditions usuelles, où $\mathbb{Q}$ est une mesure de probabilité et $\mathbb{F} = (\mathcal{F}_t)_{t\geqslant 0}$ est une filtration à laquelle tous les processus stochastiques considérés dans ce chapitre sont adaptés. Nous fixons $\mathcal{F} = \mathcal{F}_\infty$ et notons l'espérance sous $\mathbb{Q}$ par $\mathbb{E}$.

0.1. Un cadre de travail pour la modélisation des structures à terme multiples

Cette thèse a pour sujet la modélisation des structures à terme multiples dans les marchés financiers. D'abord, nous rappelons la définition classique d'une *structure à terme*.

Definition 0.1. Soit $t \geqslant 0$, on dit que la fonction $T \mapsto P(t,T)$ définit une *structure à terme* si pour tout $T \geqslant t$, $P(t,T)$ représente le prix à l'instant t d'un payoff délivré à maturité T.

Une structure à terme est par définition un objet infini-dimensionnel. Nous indiquons aussi que pour tout $T > 0$, $P(\cdot, T)$ représente le processus de prix du contrat de maturité T. Un exemple canonique est la structure à terme des obligations à coupon zéro $T \mapsto B(t,T)$, où $B(t,T)$ est le prix à l'instant t d'un payoff "unitaire" à maturité T (à savoir $B(T,T) = 1$). Les obligations à coupon zéro jouent un rôle fondamental dans la modélisation du marché des taux d'intérêts avant la crise (nous référons par exemple à [**Fil09**]). Toutefois, comme nous le verrons par la suite, la situation s'avère plus complexe dans l'environnement d'après-crise.

Plusieurs structures à terme peuvent coexister dans le même marché. Pour clarifier les idées, notons $N \in \mathbb{N}$ le nombre de structures à terme présentes dans le marché considéré. Pour chaque $1 \leqslant i \leqslant N$, $T \mapsto P^i(t,T)$ représente la $i^{\text{ème}}$ structure à terme du marché à l'instant t. Nous introduisons alors notre définition formelle d'un marché à structures à terme multiples.

Definition 0.2. Un *marché à structures à terme multiples* est un marché financier où N structures à terme sont échangées, c'est-à-dire pour chaque $1 \leqslant i \leqslant N$ et pour tout $T > 0$, $P^i(\cdot, T)$ est un actif échangé sur le marché.

Au cours de leurs travaux présentés dans [**JT98**], les auteurs ont postulé que tout marché à structures à terme multiples au sens de la définition 0.2 peut être expliqué par les processus stochastiques suivants :

- N structures à terme d'obligations à coupon zéro $T \mapsto B^i(\cdot, T)$, pour $1 \leqslant i \leqslant N$;
- Une famille de processus "spot" $S^i = (S^i_t)_{t\geqslant 0}$, pour $1 \leqslant i \leqslant N$.

Plus précisément, [**JT98**] ont développé un cadre de travail au pouvoir unificateur pour les structures à terme multiples où, à l'aide d'une simple transformation sans hypothèses initiales requises[1], ils en ont déduit la relation suivante :

$$P^i(t,T) = B^i(t,T)\, S^i_t, \tag{0.1}$$

pour tout $0 \leqslant t \leqslant T$ et pour chaque $1 \leqslant i \leqslant N$. Celle-ci donne lieu à une analogie avec le marché des taux de change, communément appelée *foreign exchange analogy* en Anglais, où

[1] Hormis la positivité stricte des processus de prix considérés.

- $B^i(\cdot, T)$ représente une obligation à coupon zéro exprimée dans une devise étrangère i;
- $S^i = (S^i_t)_{t\geqslant 0}$ est le taux de change entre la devise étrangère i et la monnaie domestique;
- $P^i(\cdot, T)$ correspond à l'obligation à coupon zéro $B^i(\cdot, T)$ convertie en monnaie domestique.

En appliquant la transformation (0.1) à d'autres marchés financiers, [**JT98**] ont montré que de nombreux marchés connus peuvent en réalité être considérés comme marchés à structures à terme multiples au sens de la définition 0.2, en particulier le marché des actions, le marché des taux d'intérêts d'avant-crise, ainsi que le marché des matières premières. Cette analogie avec le marché des taux de change a été ensuite exploitée par [**JT98**] en vue de réutiliser des techniques précédemment développées par [**AJ91**] afin de concevoir un cadre de travail dédié au pricing de produits dérivés en présence de structures à terme multiples.

L'objet des deux prochaines sections est de revisiter ces idées en les appliquant au marché forex ainsi qu'au marché des taux d'après-crise, ces derniers représentant les marchés financiers sujets à modélisation dans cette thèse. En particulier, nous allons fournir au lecteur l'intuition qui se cache derrière les objets que nous allons modéliser au cours des parties 1 et 2. Nous avons l'intime conviction que les marchés de l'électricité et du gaz peuvent être traités d'une manière similaire, ce qui fera l'objet de futures recherches.

0.2. Le marché forex

Le marché forex est un marché financier où de multiples devises sont échangées. Différentes économies y sont impliquées, où chacune d'entre elles est associée à une devise spécifique. Les $i^{\text{ème}}$ et $j^{\text{ème}}$ devises sont reliées par le taux de change $S^{i,j} = (S^{i,j}_t)_{t\geqslant 0}$, où $S^{i,j}_t$ représente la valeur à l'instant t d'une unité de la devise j exprimée dans la devise i.

Notons $N \geqslant 2$ le nombre de devises échangées sur le marché, un *marché à devises mutliples*, dont la définition formelle sera énoncée au chapitre 5, est un marché financier où pour chaque $1 \leqslant i \leqslant N$, les actifs suivants sont échangés au sein de la $i^{\text{ème}}$ économie :

- La structure à terme d'obligations à coupon zéro $T \mapsto B^i(\cdot, T)$;
- Pour chaque $1 \leqslant j \leqslant N$ avec $j \neq i$, la structure à terme des obligations à coupon zéro de la $j^{\text{ème}}$ économie exprimée dans la devise i, à savoir $S^{i,j}B^j(\cdot, T)$, pour tout $T > 0$.

Lors de la conception d'un modèle financier pour les devises multiples, une attention particulière doit être attribuée aux symétries des taux de change :

- Si nous inversons le taux de change $S^{i,j}$, alors nous devons retrouver $S^{j,i} = 1/S^{i,j}$, à savoir la valeur d'une unité de la devise i exprimée dans la devise j. Ceci constitue l'*inversion*;
- Considérons une devise k quelconque. Le taux de change $S^{i,j}$ doit alors pouvoir être retrouvé en multipliant $S^{i,k}$ et $S^{k,j}$: $S^{i,j} = S^{i,k} \times S^{k,j}$. Ceci constitue la *triangulation*.

En vue de préserver ces symétries, une approche couramment adoptée est de supposer l'exsitence d'une devise artificielle indéxée par 0 et d'exprimer chacune des devises échangées sur le marché par le biais de cette devise artificielle, donnant lieu ainsi à N taux de change artificiels $(S^{0,i})_{1\leqslant i\leqslant N}$.

Nous calculons alors les taux de change $S^{i,j} = (S_t^{i,j})_{t\geqslant 0}$, pour chaque $1 \leqslant i, j \leqslant N$, de la façon suivante :

$$S_t^{i,j} := \frac{S_t^{0,j}}{S_t^{0,i}}, \qquad \forall t \geqslant 0. \tag{0.2}$$

Cette approche est communément appelée "l'approche de la devise artificielle", en Anglais *artificial currency approach*, qui fut d'abord présentée par [**FH97, Dou07**], et appliquée par la suite par [**Dou12, DCGG13, GG14, BGP15**].

Un marché à devises multiples généré par une telle approche est alors un exemple de marché à structures à terme multiples au sens de la définition 0.2. En effet, pour chaque $1 \leqslant i \leqslant N$, la $i^{\text{ème}}$ structure à terme $T \mapsto P^i(t,T)$ est donnée par la structure à terme des taux de change "forward" entre la devise i et la devise artificielle (voir [**MR06**, Proposition 4.2.1]), comme suit :

$$P^i(t,T) = B^i(t,T)\, S_t^{0,i}, \tag{0.3}$$

pour tout $0 \leqslant t \leqslant T$ et pour chaque $1 \leqslant i \leqslant N$, sous l'hypothèse que $r^0 \equiv 0$, représentant le "taux court" de la devise artificielle (voir [**Fil09**]). En résumé, le marché à devises multiples peut être expliqué par les N taux de change artificiels $(S^{0,i})_{1\leqslant i\leqslant N}$, ainsi que par les N taux courts $(r^i)_{1\leqslant i\leqslant N}$, où r^i est le taux court de la $i^{\text{ème}}$ économie. Les processus spot $(S^{0,i})_{1\leqslant i\leqslant N}$ représenteront alors les principales quantités sujettes à modélisation du chapitre 5, où l'on ne considérera que des taux d'intérêts constants et déterministes.

0.3. Le marché des taux d'intérêts d'après-crise

Le marché des taux d'intérêts d'après-crise fait l'objet d'une segmentation en courbes multiples de taux depuis la crise financière des années 2007–2009. Les courbes de taux les plus importantes sont d'abord la courbe générée par les taux "Overnight Indexed Swaps" (OIS) $T \mapsto L^{\text{OIS}}(T,T,\delta)$, communément considérés comme les meilleurs représentants du taux "sans risque", où $L^{\text{OIS}}(T,T,\delta)$ est le taux OIS spot pour la période $[T, T+\delta]$ avec $\delta > 0$, et ensuite les courbes de taux générées par les taux dits "Interbank offered" (Ibor) $T \mapsto L(T,T,\delta)$ pour chaque durée δ d'un ensemble générique $\mathcal{G} := \{\delta_1, \ldots, \delta_m\}$ avec $0 < \delta_1 < \ldots < \delta_m$ pour $m \in \mathbb{N}$, où $L(T,T,\delta)$ est le taux Ibor spot pour la période $[T, T+\delta]$. Nous référons le lecteur au chapitre 3 pour plus de détails.

Parmis tous les produits dérivés construits sur les taux Ibor, les contrats couramment appelés "Forward Rate Agreements" (FRA) peuvent être considérés comme les plus basiques, un contrat FRA construit sur le taux Ibor spot $L(T,T,\delta)$ avec strike K est un contrat qui délivre le payoff $\delta\big(L(T,T,\delta) - K\big)$ à maturité $T+\delta$. Un *marché à courbes de taux multiples*, dont la définition formelle sera énoncée au chapitre 3, se compose des actif échangés suivants :

- Les obligations à coupon zéro de type OIS pour toute maturité $T > 0$;
- Les contrats FRA pour toute durée $\delta \in \mathcal{G}$, pour toute maturité $T > 0$, et pour un strike K fixé arbitrairement.[2]

[2]Par linéarité de la règle de pricing, n'importe quel contrat FRA de n'importe quel strike peut être déduit de ce contrat FRA avec strike K ainsi que des obligations à coupon zéro.

Représentons maintenant la structure à terme des obligations à coupon zéro par $T \mapsto B^{\mathrm{OIS}}(\cdot, T)$ ainsi que la structure à terme des contrats FRA par $T \mapsto P^{\mathrm{FRA}}(\cdot, T, \delta, K)$ pour chaque durée $\delta \in \mathcal{G}$ et strike K fixé, où $P^{\mathrm{FRA}}(\cdot, T, \delta, K)$ est le processus de prix du contrat FRA construit sur $L(T, T, \delta)$ avec strike K, nous pouvons alors vérifier qu'un marché à courbes de taux multiples est un marché à structures à terme multiples au sens de la définition 0.2 avec $N = 1 + |\mathcal{G}|$.

Afin de montrer que la relation (0.1) peut être appliquée au marché à courbes de taux multiples, nous introduisons le taux Ibor "forward" $L(t, T, \delta)$ à l'instant $t \leqslant T$, défini comme la valeur de K telle que le prix à l'instant t du contrat FRA est égal à zéro, ce qui donne

$$P^{\mathrm{FRA}}(t, T, \delta, K) = \delta \left(L(t, T, \delta) - K\right) B^{\mathrm{OIS}}(t, T + \delta), \qquad \forall t \leqslant T. \tag{0.4}$$

En procédant comme dans [**FGGS20**, Section 2], sans aucunes hypothèses supplémentaires, nous pouvons réécrire l'équation (0.4) comme suit :

$$P^{\mathrm{FRA}}(t, T, \delta, K) = S^{\delta}_t \, B^{\delta}(t, T) - \left(1 + \delta \, K\right) B^{\mathrm{OIS}}(t, T + \delta), \qquad \forall t \leqslant T, \tag{0.5}$$

où $S^{\delta} = (S^{\delta}_t)_{t \geqslant 0}$ est donné par

$$S^{\delta}_t := \frac{1 + \delta \, L(t, t, \delta)}{1 + \delta \, L^{\mathrm{OIS}}(t, t, \delta)}, \tag{0.6}$$

pour tout $t \geqslant 0$ et pour chaque $\delta \in \mathcal{G}$, et où $B^{\delta}(t, T)$ est égal à

$$B^{\delta}(t, T) := \frac{1 + \delta \, L(t, T, \delta)}{1 + \delta \, L(t, t, \delta)} \, \frac{B^{\mathrm{OIS}}(t, T + \delta)}{B^{\mathrm{OIS}}(t, t + \delta)}, \tag{0.7}$$

pour tout $0 \leqslant t \leqslant T$ et pour chaque $\delta \in \mathcal{G}$.

Nous observons ainsi que l'analogie avec le marché des taux de change, précédemment formulée par (0.1), reste satisfaite par la " floating leg" du contrat FRA où pour chaque durée $\delta \in \mathcal{G}$, $B^{\delta}(\cdot, T)$ peut être interprété comme une obligation à coupon zéro fictive exprimée dans une devise étrangère δ (remarquez que $B^{\delta}(T, T) = 1$, pour toute $\delta \in \mathcal{G}$ et toute $T > 0$), et $S^{\delta} = (S^{\delta}_t)_{t \geqslant 0}$ est le taux de change entre la devise δ et la monnaie domestique. Nous mentionnons que des analogies similaires ont été présentées par [**Bia10, NS15, CFG16, MM18**].

En adoptant la modélisation de [**JT98**], le marché à courbes de taux multiples peut être expliqué par les processus stochastiques suivants :

- La structure à terme des obligations à coupon zéro $T \mapsto B^{\mathrm{OIS}}(\cdot, T)$;
- Les processus spot $(S^{\delta})_{\delta \in \mathcal{G}}$.

Les processus spot $(S^{\delta})_{\delta \in \mathcal{G}}$ définis par (0.6) correspondent aux "spreads multiplicatifs" spot (en Anglais *spot multiplicative spreads*) entre les taux Ibor spot et les taux OIS spot. Ils représenteront, combinés avec le taux court OIS $r = (r_t)_{t \geqslant 0}$, les quantités principales de modélisation dans le chapitre 3. L'idée de modéliser les courbes multiples de taux à l'aide des spreads multiplicatifs est initialement due à [**Hen14**], et a été poursuivie par [**CFG16, CFG19b, EGG20, FGGS20**].

0.4. Motivation et objectif

Dans cette section, nous commençons par présenter les caractéristiques empiriques qui motivent le développment des modélisations des parties 1 and 2.

0.4.1. Les spreads multiplicatifs spot. Les processus spot $(S^\delta)_{\delta\in\mathcal{G}}$ définis par (0.6) peuvent être directement récupérés à partir des données du marché par construction. En conséquence, ils manisfestent plusieurs caractéristiques empiriques, pouvant aisément être visualisées sur le premier graphique de la figure 0.2 :

(i) Les spreads sont généralement plus grands que l'unité et croissants en fonction de la durée $\delta \in \mathcal{G}$;
(ii) La présence de mouvements simultanés prononcés (en particulier des sauts positifs) parmis les différents spreads;
(iii) La présence de clusters de volatilité pendant les périodes de crise, où les spreads prennent des valeurs de plus en plus grandes;
(iv) La persistance des valeurs de certains spreads à des niveaux relativement bas.

Nous référons le lecteur au chapitre 3 pour plus d'informations sur la source de ces caractéristiques empiriques. À notre connaissance, un modèle financier capable de capturer convenablement ces caractéristiques empiriques n'existe pas encore dans la littérature.

0.4.2. Les taux de change artificiels. Contrairement aux spreads multiplicatifs, les taux de change artificiels $(S^{0,i})_{1\leqslant i\leqslant N}$ représentent des quantités qui ne peuvent être observées dans la réalité. Toutefois, à la vue de l'équation (0.2), ils jouent un rôle important dans la construction des vrais taux de changes, connus pour manisfester les caractéristiques empiriques suivantes :

(i) Volatilité stochastique ainsi que des sauts;
(ii) Dépendance stochastique entre les différents taux de change;
(iii) Asymétrie d'ordre stochastique du smile de volatilité;
(iv) Potentiel comportement auto-excitant de la volatilité des taux de change.

Comme précédemment, nous référons le lecteur au chapitre 5 pour plus d'informations sur ces caractéristiques. Pour une visualisation du point (iv), le second graphique de la figure 0.2 représente la moyenne pondérée des volatilités implicites d'options call de maturité 1Y et strike ATM de trois paires de devises majeures (USDJPY, EURJPY, et EURUSD). Manisfestement, nous sommes en mesure d'observer des clusters de sauts successifs, ce qui indique la présence éventuelle d'un comportement auto-excitant de la volatilité des taux de change.

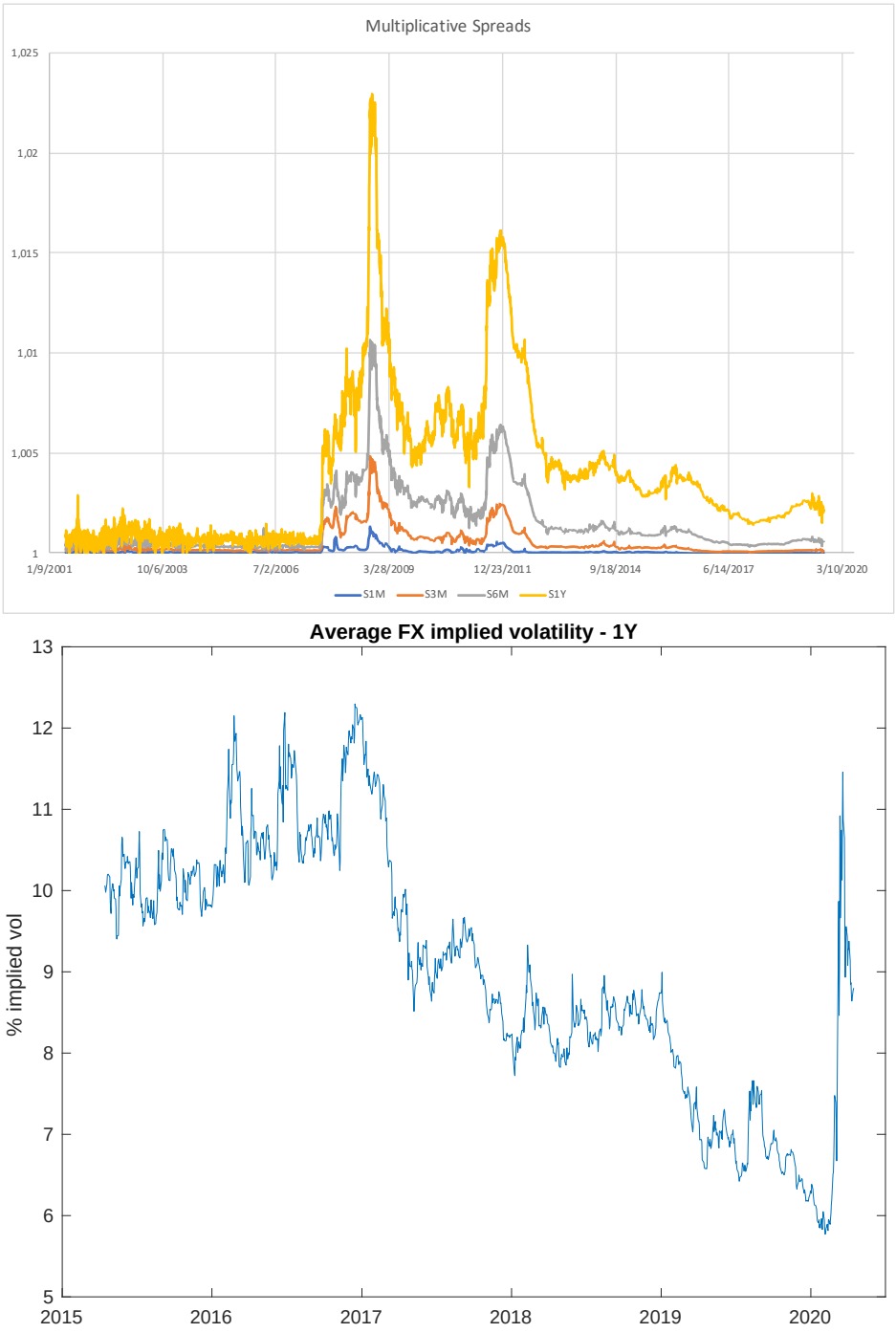

FIGURE 0.2. Visualisation des caractéristiques empiriques motivant le développement des modèles des parties 1 et 2.
Premier graphique: Spreads Euribor-OIS de 06/2001 à 09/2019.
Second graphique: Moyenne pondérée des volatilités implicites de trois paires de devises majeures (USDJPY, EURJPY, et EURUSD)..
Source: Bloomberg.

0.4.3. Formulation de notre objectif. Nous sommes désormais en position de formuler l'objectif principal que cette thèse cherche à atteindre. Nous insistons sur le fait que ce dernier est directement motivé par les caractéristiques empiriques présentées précédemment.

OBJECTIF	
Formulation:	Développer une approche pour la modélisation des structures à terme multiples combinant au mieux **maniabilité** du point de vue analytique et **cohérence** avec les caractéristiques empiriques vues précédemment.
Solution proposée:	*Processus de branchement à état continu avec immigration* (CBI).

0.5. L'approche proposée

Dans cette thèse, afin de répondre à l'objectif formulé ci-dessus, nous proposons une approche générale pour la modélisation des structures à terme multiples en se basant sur la classe des *processus de branchement à état continu avec immigration* (CBI). Comme mentionné précédemment, nous nous concentrons sur les courbes multiples de taux dans le marché des taux d'intérêts d'après-crise, et sur les devises multiples dans le marché forex. Nous développons alors deux modélisations, dont nous exposons maintenant les grandes lignes ci-dessous.

0.5.1. Partie 1. Les courbes multiples de taux. Dans cette partie, nous développons un modèle pour les courbes multiples de taux basé sur les processus CBI, capturant toutes les caractéristiques empiriques des spreads $(S^\delta)_{\delta\in\mathcal{G}}$ et, en même temps, permettant une évaluation efficace des produits dérivés de taux. En exploitant la propriété affine des processus CBI, nous concevons notre modèle dans le cadre des modèles affines multi-courbes récemment développés par [**CFG19b**], c'est-à-dire en prenant les spreads multiplicatifs spot $(S^\delta)_{\delta\in\mathcal{G}}$ et le taux court OIS $(r_t)_{t\geqslant 0}$ comme principales quantités de modélisation.

Par construction, le modèle est en parfaite adéquation avec les structures à terme observées, et garantit des spreads plus grand que l'unité ainsi que croissants en fonction de la durée $\delta \in \mathcal{G}$. Le modèle génére aussi une structure exponentiellement affine pour les obligations à coupon zéro de type OIS et les spreads multiplicatifs forward, permettant ainsi une évaluation explicite de tous les dérivés de taux linéaires.

Cependant, la construction du modèle exige une étude précise des moments exponentiels des processus CBI. À cette fin, nous effectuons une analyse détaillée de leurs moments exponentiels et donnons une caractérisation explicite et générale de leur instant d'explosion. De plus, nous définissons une nouvelle spécification que l'on nomme *processus CBI stable et tempéré*, qui, plus particulièrement, garantit une condition nécessaire et suffisante simple pour la finitude de leurs moments exponentiels.

Contrairement à [**CFG19b**], où l'accent a été mis sur les propriétés générales et théroriques du modèle, nous contribuons à travers la mise en place d'une nouvelle classe de modèles multi-courbes, dirigés par un *flux de processus CBI stables et tempérés*, dont l'introduction est particulièrement motivée par les caractéristiques empiriques vues précédemment. Ce flux, dont tous les aspects seront inspectés plus tard, génére des effets de contagion parmis les différents spreads ainsi que des périodes de clusters de volatilité, où le comportement auto-excitant typique des processus CBI s'avère être un ingrédient clé pour reproduire ces caractéristiques.

Nous établissons une formule de pricing de forme semi-close pour les caplets par le biais de techniques basées sur la transformée de Fourier. Plus précisément, nous implémentons deux méthodologies : la première repose sur une application directe de l'algorithme FFT (voir [**CM99**]), tandis que la seconde utilise un algorithme basé sur la quantification (voir [**CFG19a**]), qui est ici appliqué pour la première fois dans un contexte de taux d'intérêts. Lors d'une analyse numérique, ces deux méthodologies sont comparées et une spécification de la modélisation proposée avec deux durées est calibrée aux données du marché.

0.5.2. Partie 2. Les devises multiples. Dans cette partie, nous développons un modèle à volatilité stochastique pour les devises multiples produisant des processus de taux de change dont la volatilité peut s'exciter elle-même, tout en capturant les facteurs de risque typiques du marché de change (comme la dépendance stochastique entre les différentes devises et l'asymétrie stochastique du smile de volatilité), et préservant les symétries propres à ses taux (à savoir les symétries par inversion et triangulation).

Nous procédons en utilisant la technologie des *CBI-Time-Changed Lévy processes* (CBITCL), qui sont définis comme des processus à deux dimensions combinant le comportement auto-excitant typique des processus CBI et la généralité des processus de Lévy changés en temps. En exploitant leur structure affine, nous pouvons montrer que les processus CBITCL sont *cohérents* au sens de [**Gno17**]. Cela signifie que si un taux de change est modélisé par un processus CBITCL, alors le processus inversé appartient à la même classe de modèles.

Inspiré par [**Gno17**, Section 4] et en prenant en compte notre discussion précédente, nous construisons notre modèle en adoptant *l'approche de la devise artificielle*, c'est-à-dire en considérant les taux de change artificiels $(S^{0,i})_{1\leqslant i\leqslant N}$ comme les quantités principales à modéliser. À cet égard, les taux de change sont symétriques par inversion et triangulation par construction puisque ils sont définis comme quotients via la relation (0.2).

En formulant un résultat de type Girsanov pour les processus CBITCL, nous sommes capables de caractériser une classe de probabilités neutres au risque préservant la structure du modèle, ce qui constitue un prérequis indispensable pour le pricing d'options sur devises. En particulier, en exploitant la préservation de la structure affine du modèle, nous établissons une formule de pricing de forme semi-close pour les options sur devises, découlant d'une application directe de la méthode COS développée par [**FO09**].

Le modèle proposé peut aussi reproduire de nombreuses caractéristiques empiriques du marché forex. Plus particulièrement, il peut générer des relations de dépendance d'ordre stochastique entre les différentes devises, ainsi que entre les taux de change et leur volatilité. Nous insistons sur le fait que ce type de dépendance est connu pour jouer un rôle essentiel pour la création de smiles de volatilité manisfestant une asymétrie stochastique.

Nous évaluons la performance empirique du modèle à l'aide d'une calibration à un triangle de change se composant de trois paires de devises majeures (USDJPY, EURJPY, et EURUSD). Nous mettons en place deux calibrations : *standard* et *deep*, où cette dernière utilise des techniques provenant du deep learning et développées par [**HMT21**]. Ensuite, à l'aide des paramètres calibrés obtenus, nous effectuons une analyse des sensitivités sur les smiles de volatilité générés par le modèle. L'objectif de cette étude empirique est de déterminer l'impact des différents paramètres du modèle sur la forme moyenne du smile de volatilité.

0.6. Structure de la thèse

La suite est organisée autour de quatre chapitres. La partie 1 comprend les chapitres 2 et 3. Dans le chapitre 2, nous établissons un cadre de travail autonome pour les processus CBI incluant, en particulier, une analyse des moments exponentiels des processus CBI ainsi que la définition formelle des *processus CBI stables et tempérés*. Ce cadre de travail est ensuite appliqué lors du chapitre 3 au développement d'un modèle pour les courbes multiples de taux basé sur les processus CBI, où la construction de modèles multi-courbes dirigés par un *flux de processus CBI stables et tempérés* est menée à bien.

La partie 2 se compose des chapitres 4 et 5. Dans le chapitre 4, nous définissons formellement la classe des *CBI-Time-Changed Lévy processes* (CBITCL), pour lequel nous mettons en place un cadre de travail analytique. Le chapitre 5 contient ensuite le développement d'un modèle à volatilité stochastique pour les devises multiples, utilisant la technologie des processus CBITCL.

Pour conclure ce chapitre introductif, une brève comparaison des modèles développés dans les parties 1 et 2 peut être consultée dans le tableau 0.1.

	Modèle de la partie 1	Modèle de la partie 2
Type des structures à terme modélisées	Les courbes multiples de taux dans le marché d'après-crise	Les devises multiples dans le marché forex
Principales quantités de modélisation	Les spreads multiplicatifs spot $(S^{\delta})_{\delta\in\mathcal{G}}$ et le taux court OIS $(r_t)_{t\geqslant 0}$	Les taux de change artificiels $(S^{0,i})_{1\leqslant i\leqslant N}$
Processus utilisés	Flux de processus CBI stables et tempérés	CBI-time-changed Lévy processes (CBITCL)
Prérequis indispensable pour la construction	Finitude des moments exponentiels	Invariance du modèle sous les probabilités neutres au risque
La principale caractéristique empirique capturée	Effets de contagion entre les différents spreads	Comportement auto-excitant de la volatilité des taux de change
Techniques basées sur la transformée de Fourier pour le pricing	[**Lee04**] pour le pricing de caplets, FFT [**CM99**] ou quantification [**CFG19a**] pour l'approximation	La méthode COS [**FO09**] pour le pricing d'options sur devises
Évaluation numérique du modèle	Comparaison des algorithmes FFT et quantification pour le pricing, calibration aux données du marché	Deux types de calibration : standard et deep inspiré par [**HMT21**], analyse des sensitivités

TABLE 0.1. Comparaison des modèles développés dans les parties 1 et 2.

CHAPTER 1

Introduction

SUMMARY. This chapter constitutes the introduction of this manuscript and aims to provide the reader with some motivation and preliminaries in view of Parts 1 and 2. We start by introducing the multiple term structure framework, extending some of the ideas first introduced by [**JT98**] to the two financial markets considered in this thesis. We then draw our motivation from the empirical features of the considered markets, and state the main objective that this thesis seeks to attain. Finally, we outline the proposed modeling approach based on *Continuous-state Branching processes with Immigration* (CBI), and present the global organization of the thesis.

Contents

In this introductory chapter, let $\big(\Omega, \mathcal{F}, \mathbb{F}, \mathbb{Q}\big)$ be a stochastic basis satisfying the usual conditions, where $\mathbb{Q}$ is a probability measure and $\mathbb{F} = (\mathcal{F}_t)_{t\geqslant 0}$ is a filtration to which all stochastic processes are assumed to be adapted. We set $\mathcal{F} = \mathcal{F}_\infty$ and denote the expectation under $\mathbb{Q}$ by $\mathbb{E}$.

1.1. The multiple term structure framework

This thesis deals with the modeling of multiple term structures in financial markets. First, we recall the classical definition of a *term structure* as follows.

Definition 1.1. Let $t \geqslant 0$, the function $T \mapsto P(t,T)$ is said to represent a *term structure* if for all $T \geqslant t$, $P(t,T)$ denotes the price at time t of a payoff delivered at maturity T.

A term structure is by definition an infinite-dimensional object. We also point out that for all $T > 0$, $P(\cdot, T)$ stands for the price process of the contract with maturity T. A canonical example is the term structure of zero-coupon bonds $T \mapsto B(t,T)$, where $B(t,T)$ is the price at time t of a unit payoff at maturity T (and therefore $B(T,T) = 1$). Zero-coupon bonds play a fundamental role in the modeling of the pre-crisis interest rate market (see e.g. [**Fil09**]). However, as we shall see in the following, the situation reveals to be more complex in the post-crisis environment.

Multiple term structures may coexist in the same market. As an illustration, let $N \in \mathbb{N}$ denote the number of term structures in the market considered. For every $1 \leqslant i \leqslant N$, $T \mapsto P^i(t,T)$ represents the i^{th} term structure of the market at time t. We then introduce our formal definition of a generic *multiple term structure market*.

Definition 1.2. A *multiple term structure market* is a financial market where N term structures are traded, namely for every $1 \leqslant i \leqslant N$ and for all $T > 0$, $P^i(\cdot, T)$ is a traded asset.

In the early work [**JT98**], the authors postulated that any multiple term structure market in the sense of Definition 1.2 can be described by the following stochastic processes:

- N term structures of zero-coupon bonds $T \mapsto B^i(\cdot, T)$, for $1 \leqslant i \leqslant N$;
- A family of spot processes $S^i = (S^i_t)_{t\geqslant 0}$, for $1 \leqslant i \leqslant N$.

More specifically, [**JT98**] developed a unifying modeling framework for multiple term structures where, by a means of a simple transformation with no preliminary assumption required[1], they derived the following relation:

$$P^i(t,T) = B^i(t,T)\, S^i_t, \tag{1.1}$$

for all $0 \leqslant t \leqslant T$ and for every $1 \leqslant i \leqslant N$. This gives rise to a *foreign exchange analogy* where

- $B^i(\cdot, T)$ represents a zero-coupon bond denominated in units of a foreign currency i;
- $S^i = (S^i_t)_{t\geqslant 0}$ is the spot foreign exchange rate between currency i and the domestic one;
- $P^i(\cdot, T)$ corresponds to the domestic version of the zero-coupon bond $B^i(\cdot, T)$, namely measured in units of the domestic currency.

[1] Except for the strict positivity of the price processes considered.

By adopting the modeling approach of equation (1.1), [**JT98**] showed that many different financial markets can be recovered as special cases of Definition 1.2, in particular the equity market, the (pre-crisis) interest rate market, and the commodity market. This foreign exchange analogy was then exploited by [**JT98**] to utilize techniques previously developed by [**AJ91**] in order to design a derivative pricing framework in the context of multiple term structures.

In the next two sections, we revisit these ideas by applying them to the Foreign-Exchange (FX) market and the post-crisis interest rate market, which represent the financial markets investigated in this thesis. In these sections, we aim at providing the reader with some intuition on the modeling quantities that will be considered in Parts 1 and 2. We believe that the electricity and gas markets can also be treated in a similar manner, leaving it for further research.

1.2. The Foreign-Exchange (FX) market

The FX market is a financial market where multiple currencies are traded. Such a market involves different economies, each one associated to a specific currency. The i^{th} and j^{th} currencies are related by the spot FX rate process $S^{i,j} = (S_t^{i,j})_{t\geqslant 0}$, where $S_t^{i,j}$ denotes the value at time t of one unit of currency j measured in units of currency i.

Letting $N \geqslant 2$ be the number of currencies traded in the market, a *multiple currency market*, whose formal definition can be found in Chapter 5, is a financial market where for every $1 \leqslant i \leqslant N$, the following assets are traded in the i^{th} economy:

- The term structure of zero-coupon bonds $T \mapsto B^i(\cdot, T)$;
- For every $1 \leqslant j \leqslant N$ with $j \neq i$, the term structure of zero-coupon bonds of the j^{th} economy denominated in units of the i^{th} currency, namely $S^{i,j}B^j(\cdot, T)$, for all $T > 0$.

When constructing a financial model for multiple currencies, special attention has to be paid to the symmetries that FX rates typically satisfy as follows:

- If we invert the FX rate $S^{i,j}$, then we must obtain $S^{j,i} = 1/S^{i,j}$, which is the value of one unit of currency i measured in units of currency j. This is referred to as *inversion*;
- Take any additional currency k. The FX rate $S^{i,j}$ must be implied from $S^{i,k}$ and $S^{k,j}$ through multiplication: $S^{i,j} = S^{i,k} \times S^{k,j}$. This is called *triangulation*.

In view of satisfying these symmetries, a commonly adapted approach is to assume the existence of an artificial currency indexed by 0 and express each traded currency with respect to this artificial currency, giving rise to N artificial spot FX rates $(S^{0,i})_{1\leqslant i\leqslant N}$. We then compute the spot FX rate processes $S^{i,j} = (S_t^{i,j})_{t\geqslant 0}$, for every $1 \leqslant i, j \leqslant N$, as follows:

$$S_t^{i,j} := \frac{S_t^{0,j}}{S_t^{0,i}}, \qquad \forall t \geqslant 0. \tag{1.2}$$

This is typically referred to as the *artificial currency approach*, which was first introduced by [**FH97, Dou07**], and pursued by [**Dou12, DCGG13, GG14, BGP15**] among others.

A multiple currency market generated by an artificial currency approach can be recovered as a special case of Definition 1.2. Indeed, for every $1 \leqslant i \leqslant N$, the i^{th} term structure $T \mapsto P^i(t, T)$

is given by the term structure of *forward exchange rates* between currency i and the artificial one (see e.g. [**MR06**, Proposition 4.2.1]), as follows:

$$P^i(t,T) = B^i(t,T)\, S_t^{0,i}, \tag{1.3}$$

for all $0 \leqslant t \leqslant T$ and for every $1 \leqslant i \leqslant N$, under the assumption that $r^0 \equiv 0$, denoting the short rate of the artificial currency. In summary, the multiple currency market can be described by the N artificial spot FX rates $(S^{0,i})_{1\leqslant i\leqslant N}$, together with the N short rates $(r^i)_{1\leqslant i\leqslant N}$, where r^i is the short rate of the i^{th} economy. The spot processes $(S^{0,i})_{1\leqslant i\leqslant N}$ will constitute our main modeling quantities in Chapter 5, where we will consider constant and deterministic rates for simplicity.

1.3. The post-crisis interest rate market

The post-crisis interest rate market has been characterized by a segmentation into multiple yield curves since the 2007–2009 financial crisis. The most important curves are the Overnight Indexed Swaps (OIS) rates $T \mapsto L^{\text{OIS}}(T,T,\delta)$, typically considered as the best proxies for risk-free rates, where $L^{\text{OIS}}(T,T,\delta)$ is the OIS spot rate for the period $[T, T+\delta]$ with $\delta > 0$, and the interbank offered rates $T \mapsto L(T,T,\delta)$ for every tenor δ of a generic set $\mathcal{G} := \{\delta_1, \ldots, \delta_m\}$ with $0 < \delta_1 < \ldots < \delta_m$ for some $m \in \mathbb{N}$, where $L(T,T,\delta)$ is the spot interbank offered rate for the period $[T, T+\delta]$. We refer the reader to Chapter 3 for more details.

Among all financial derivatives written on interbank offered rates, Forward Rate Agreements (FRAs) can be regarded as the basic building blocks, a FRA written on the interbank offered rate $L(T,T,\delta)$ with strike K is a contract that delivers the payoff $\delta\big(L(T,T,\delta) - K\big)$ at maturity $T+\delta$. A *multiple yield curve market*, whose formal definition can be found in Chapter 3, consists of the following traded assets:

- OIS zero-coupon bonds for all maturities $T > 0$;
- FRAs for all tenors $\delta \in \mathcal{G}$, for all maturities $T > 0$, and for an arbitrary fixed strike K.[2]

Denoting now the OIS term structure by $T \mapsto B^{\text{OIS}}(\cdot, T)$ and the term structures of FRAs by $T \mapsto P^{\text{FRA}}(\cdot, T, \delta, K)$ for every tenor $\delta \in \mathcal{G}$ and fixed strike K, where $P^{\text{FRA}}(\cdot, T, \delta, K)$ stands for the price process of the FRA written on $L(T,T,\delta)$ with fixed strike K, it can be checked that a multiple yield curve market can be recovered as a special case of Definition 1.2 with $N = 1 + |\mathcal{G}|$.

In order to show that the foreign exchange analogy of equation (1.1) can be applied to the multiple yield curve market, let us introduce the forward interbank offered rate $L(t,T,\delta)$ at time $t \leqslant T$, defined as the value of K that makes the time-t price of the FRA equal to zero, thus yielding

$$P^{\text{FRA}}(t,T,\delta,K) = \delta\big(L(t,T,\delta) - K\big)\, B^{\text{OIS}}(t, T+\delta), \qquad \forall t \leqslant T. \tag{1.4}$$

Proceeding as in [**FGGS20**, Section 2], under no additional assumption, we are able to rewrite equation (1.4) as follows:

$$P^{\text{FRA}}(t,T,\delta,K) = S_t^\delta\, B^\delta(t,T) - \big(1 + \delta\, K\big)\, B^{\text{OIS}}(t, T+\delta), \qquad \forall t \leqslant T, \tag{1.5}$$

[2]By linearity of the pricing rule, all FRA prices for every strike can be derived from the FRA price with this arbitrary fixed strike and OIS bonds.

where $S^\delta = (S^\delta_t)_{t\geqslant 0}$ is given by

$$S^\delta_t := \frac{1+\delta\, L(t,t,\delta)}{1+\delta\, L^{\mathrm{OIS}}(t,t,\delta)}, \tag{1.6}$$

for all $t \geqslant 0$ and $\delta \in \mathcal{G}$, and where $B^\delta(t,T)$ is given by

$$B^\delta(t,T) := \frac{1+\delta\, L(t,T,\delta)}{1+\delta\, L(t,t,\delta)}\, \frac{B^{\mathrm{OIS}}(t,T+\delta)}{B^{\mathrm{OIS}}(t,t+\delta)}, \tag{1.7}$$

for all $0 \leqslant t \leqslant T$ and $\delta \in \mathcal{G}$.

We observe that the foreign exchange analogy, as formulated in equation (1.1), remains satisfied by the floating leg of a FRA where for every tenor $\delta \in \mathcal{G}$, $B^\delta(\cdot,T)$ can be interpreted as a fictitious zero-coupon bond measured in units of a foreign currency δ (note that $B^\delta(T,T) = 1$, for all $\delta \in \mathcal{G}$ and $T > 0$), and $S^\delta = (S^\delta_t)_{t\geqslant 0}$ is the spot exchange rate between currency δ and the domestic one. Similar foreign exchange analogies have been discussed by [**Bia10, NS15, CFG16, MM18**].

Adopting the modeling paradigm of [**JT98**], the multiple yield curve market can be described by the following processes:

- The OIS term structure $T \mapsto B^{\mathrm{OIS}}(\cdot,T)$;
- The spot processes $(S^\delta)_{\delta\in\mathcal{G}}$.

The spot processes $(S^\delta)_{\delta\in\mathcal{G}}$ as given by (1.6) correspond to the *spot multiplicative spreads* between (normalized) spot interbank offerd rates and (normalized) OIS spot rates. They will represent, together with the *OIS short rate* $r = (r_t)_{t\geqslant 0}$, our main modeling quantities in Chapter 3. The idea of modeling multiple yield curve markets via multiplicative spreads is initially due to [**Hen14**], and has been pursued by [**CFG16, CFG19b, EGG20, FGGS20**] among others.

1.4. Motivation and objective

In this section, we first discuss the empirical features that motivate the development of the modeling frameworks in Parts 1 and 2.

1.4.1. The spot multiplicative spreads. The spot processes $(S^\delta)_{\delta\in\mathcal{G}}$ as given by (1.6) can be directly retrieved from market quotes by construction as spreads between different interbank rates. In this respect, they exhibit several empirical features, which can be easily visualized from the top panel of Figure 1.1 as follows:

(i) Spreads are typically greater than one and non-decreasing with respect to the tenor;
(ii) There are strong co-movements (in particular, common upward jumps) among spreads associated to different tenors;
(iii) Relatively large values of the spreads are associated to high volatility, showing volatility clustering zones during crisis periods;
(iv) Low values of some spreads can persist for prolonged periods of time.

We refer the reader to Chapter 3 for further details on the source of these features. To the best of our knowledge, a financial model that can adequately reproduce all these empirical features does not yet exist in the related literature.

1.4.2. The artificial spot FX rates. Unlike the spot multiplicative spreads, the artificial spot FX rates $(S^{0,i})_{1\leqslant i\leqslant N}$ are modeling quantities that cannot be observed in reality. However, in view of equation (1.2), they play an important role in the construction of spot FX rates, which are known to exhibit the following empirical features:

(i) Stochastic volatility and jumps;
(ii) Stochastic dependence among FX rates;
(iii) Stochastic skewness of the FX volatility smile;
(iv) Potential presence of self-excitation in the volatility of FX rates.

As before, we refer the reader to Chapter 5 for further details on these features. In view of a visualization of feature (iv), the bottom panel of Figure 1.1 illustrates the weighted average of the 1Y ATM call-implied volatilities of three major currency pairs (USDJPY, EURJPY, and EURUSD). Notably, we can observe successive jump clusters, which suggests the potential presence of self-excitation in the volatility of FX rates.

1.4.3. Statement of the objective. At this point, we are in a position to state the principal objective that the present thesis seeks to attain. We emphasize that the latter is directly motivated by the empirical features discussed above.

OBJECTIVE	
Formulation:	Elaborate a modeling approach for multiple term structures capable of combining **analytical tractability** and **consistency** with the empirical features previously mentioned.
Proposed solution:	*Continuous-state Branching processes with Immigration* (CBI).

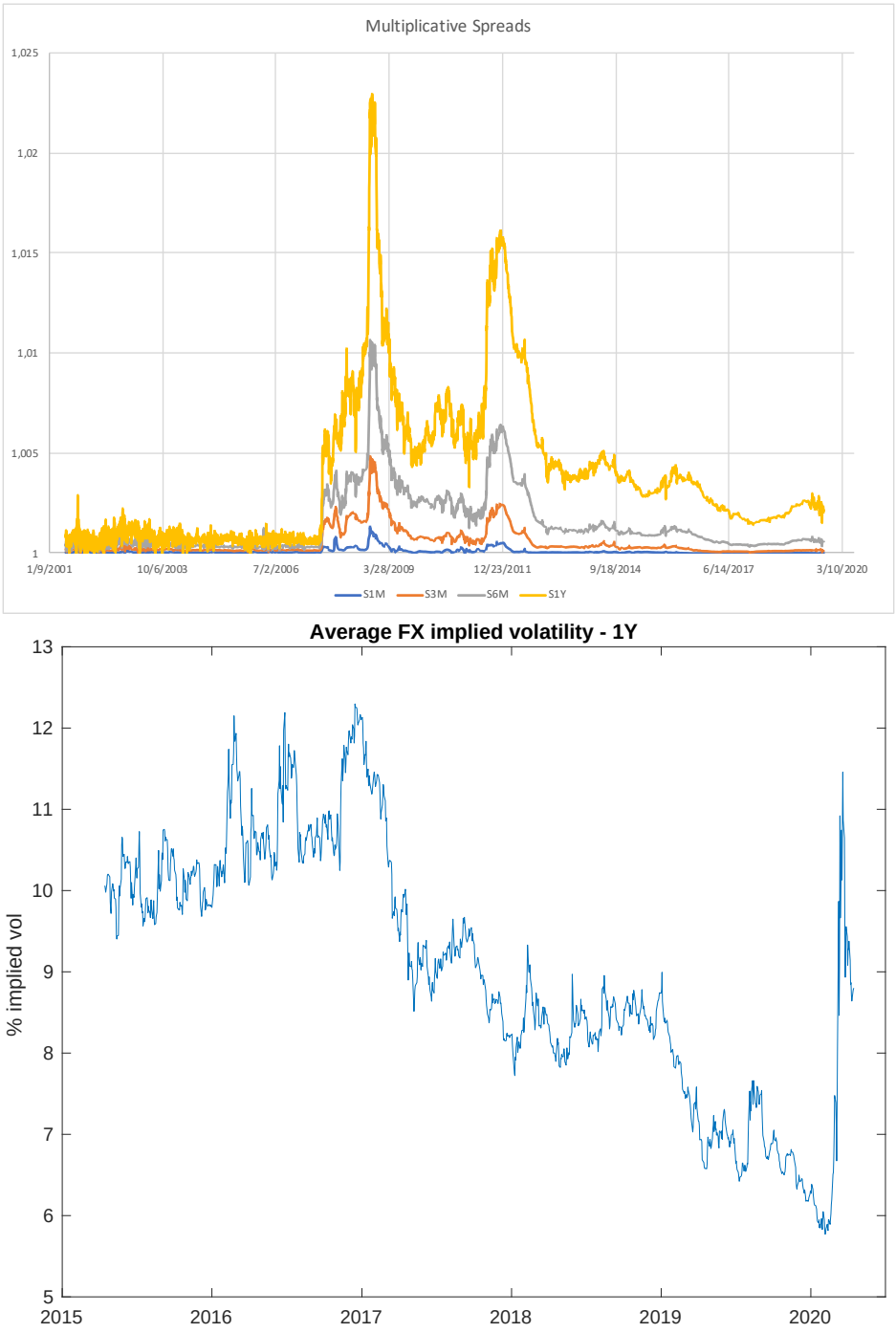

FIGURE 1.1. Illustration of the empirical features that motivate the development of the modeling framework of Parts 1 and 2.
On the top panel: Euribor-OIS spreads from 06/2001 to 09/2019.
On the bottom panel: Weighted average of the implied volatilities of three major currency pairs (USDJPY, EURJPY, and EURUSD).
Source: Bloomberg.

1.5. The proposed approach

In this thesis, we propose a general modeling approach for multiple term structures driven by *Continuous-state Branching processes with Immigration* (CBI), which is specifically motivated by addressing the objective stated above. As mentioned previously, we focus on multiple yield curves in the post-crisis interest rate market, and multiple currencies in the FX market. We then develop two modeling frameworks in Parts 1 and 2, devoted to the modeling of these two financial markets. Let us now briefly outline the principal contributions of each part separately as follows.

1.5.1. Part 1. Multiple yield curves. In this part, we develop a modeling framework for multiple yield curves based on CBI processes, which captures all the relevant empirical features of the spreads $(S^\delta)_{\delta\in\mathcal{G}}$ and, at the same time, permits an efficient valuation of interest rate derivatives. By exploiting the affine property of CBI processes, we design our modeling framework in the context of the affine multi-curve models recently introduced by [**CFG19b**], namely taking the spot multiplicative spreads $(S^\delta)_{\delta\in\mathcal{G}}$ and the OIS short rate $(r_t)_{t\geqslant 0}$ as main modeling quantities.

By construction, the model achieves a perfect fit to the observed term structures, and ensures spreads greater than one and non-decreasing with respect to the tenor. The model also generates an exponentially-affine structure for OIS zero-coupon bonds and forward multiplicative spreads, allowing for the explicit valuation of all linear interest rate derivatives.

However, the construction of the model requires a precise investigation of the finiteness of exponential moments of CBI processes. To this effect, we provide a detailed analysis of exponential moments and derive an explicit and general characterization of their time of explosion. Moreover, we define a new specification that we name *tempered-stable CBI process*, which, in particular, ensures a simple necessary and sufficient condition for the finiteness of exponential moments.

While [**CFG19b**] focused on the general theoretical properties of the model, we contribute by introducing a novel class of tractable and flexible multi-curve models driven by a *flow of tempered-stable CBI processes*, which are specifically motivated by the empirical features discussed above. Such a flow of CBI processes, which we will clarify later, generates strong co-movements among spreads such as common upwards jumps and jump clustering, where the characteristic self-exciting behavior of CBI processes proves to be a key ingredient to reproduce these features.

We derive semi-closed-form pricing formulae for caplets via Fourier techniques. More precisely, we implement two pricing methodologies: the former relies on a direct application of the FFT algorithm (see [**CM99**]), while the latter utilizes a quantization-based algorithm (see [**CFG19a**]), which is here applied for the first time to an interest rate setting. In a numerical analysis, these two pricing methodologies are compared and a specification of the proposed model with two tenors is calibrated to market data, demonstrating an excellent fit to market data.

1.5.2. Part 2. Multiple currencies. In this part, we develop a general stochastic volatility modeling framework for multiple currencies that allows for self-excitation in the volatility of FX rates, while capturing the typical sources of risk in the FX market (such as stochastic dependence among FX rates and stochastic skewness of the FX volatility smile), and preserving the peculiar symmetries of FX rates (i.e. symmetries under inversion and triangulation).

We proceed by relying on the technology of *CBI-Time-Changed Lévy processes* (CBITCL), which are defined as two-dimensional processes combining the self-exciting behavior of CBI process with the generality of time-changed Lévy processes. By exploiting their affine structure, we can show that CBITCL processes are *coherent* in the sense of [**Gno17**]. This means that if an FX rate is modeled by a CBITCL process, then the inverse FX rate belongs to the same modeling class.

Inspired by [**Gno17**, Section 4] and taking into account our previous discussion, we design our modeling framework by adopting the *artificial currency approach*, namely taking the artificial spot FX rates $(S^{0,i})_{1\leqslant i\leqslant N}$ as main modeling quantities. In this regard, FX rates satisfy the inversion and triangulation symmetries by construction since they are defined as ratios by relation (1.2).

By formulating a Girsanov-type result for CBITCL processes, we can characterize a class of risk-neutral measures that leave invariant the structure of the framework, which is an indispensable requirement for pricing options written on FX rates. In particular, by exploiting the preservation of the affine property of CBITCL processes, we provide a semi-closed-form pricing formula for currency options, deriving from a direct application of the COS method developed by [**FO09**].

The proposed model can also reproduce several features of the FX market. More specifically, it allows for non-trivial stochastic dependence between the different currencies, and for non-trivial dependence between FX rates and their volatilities. We emphasize that this type of dependence is known to play a relevant role in generating FX volatility smiles that exhibit stochastic skewness.

We assess the empirical performance of our model via a calibration to an FX triangle consisting of three major currency pairs (USDJPY, EURJPY, and EURUSD). We perform two calibrations: *standard* and *deep*, where the latter uses deep-learning techniques developed by [**HMT21**]. Then, by retaining the calibrated values of the model parameters, we carry out a sensitivity analysis on model-implied volatility smiles. The purpose of this empirical study is to determine the impact of the different model parameters on the shape of the FX volatility smile.

1.6. Structure of the thesis

The sequel is organized around four chapters. Part 1 comprises Chapters 2 and Chapter 3. In Chapter 2, we provide a self-contained framework for CBI processes including, in particular, an analysis of the exponential moments of CBI processes and the formal definition of *tempered-stable CBI processes*. This framework is applied in Chapter 3 to the development of a modeling framework for multiple yield curves based on CBI processes, where the construction of multi-curve models driven by a *flow of tempered-stable CBI processes* is performed in full details.

Part 2 consists of Chapters 4 and 5. In Chapter 4, we formally define *CBI-Time-Changed Lévy processes* (CBITCL), for which we give an analytical framework. Chapter 5 contains the development of a general stochastic volatility modeling framework for multiple currencies, utilizing CBITCL processes as driving processes.

As a conclusion to this introductory chapter, a brief comparative overview of the modeling frameworks developed in Parts 1 and 2 is reported in Table 1.1.

	Modeling framework of Part 1	Modeling framework of Part 2
Type of the multiple term structures modeled	Multiple yield curves in the post-crisis interest market	Multiple currencies in the FX market
Main modeling quantities	Spot multiplicative spreads $(S^\delta)_{\delta\in\mathcal{G}}$ and OIS short rate $(r_t)_{t\geqslant 0}$	Artificial spot FX rates $(S^{0,i})_{1\leqslant i\leqslant N}$
Driving processes	Flow of tempered-stable CBI processes	CBI-time-changed Lévy processes (CBITCL)
Indispensable requirement for the construction of the model	Finiteness of exponential moments	Invariance under the risk-neutral measures of the FX market
Most relevant empirical feature reproduced	Contagion effects among spreads	Self-excitation in the volatility of FX rates
Fourier techniques used for the pricing of non-linear products	[**Lee04**] for caplet pricing, FFT [**CM99**] or quantization [**CFG19a**] for approximation	The COS method [**FO09**] for currency option pricing
Numerical assessment of the model	Comparison of FFT and quantization pricing methods, calibration to market data	Two types of calibration: standard and deep inspired by [**HMT21**], sensitivity analysis

TABLE 1.1. Comparative overview of the modeling frameworks of Parts 1 and 2.

Part 1

Multiple yield curves

CHAPTER 2

Continuous-state branching processes with immigration

SUMMARY. We present a self-contained framework for CBI processes, which will be applied to multiple yield curve modeling in Chapter 3. We first provide an analysis of exponential moments of CBI processes. We then study the relations between two representations of a CBI process: the stochastic integral equation of Dawson and Li [**DL06**], and the stochastic time change equation in the sense of Lamperti [**ECPGUB13**]. We also derive a correspondence between CBI processes and (marked) Hawkes processes. In particular, we refine the time change Poisson representation of general point processes for the specific case of Hawkes processes, providing a proof that only relies on the theory of CBI processes. Finally, we propose a new specification that we name *tempered-stable CBI process*, which is well suited to multiple yield curve modeling.

Contents

2.1. Introduction

Continuous-state Branching processes with Immigration (CBI) were first introduced by [**KW71**], where they were obtained by letting the population size of normalized *Bienaymé–Galton–Watson branching processes with immigration* tend to infinity (see [**Bie45, WG75**]). CBI processes extend the class of *Continuous-state Branching processes* (CB), which were introduced by [**Fel51**] under the name of *Feller diffusions*, and later revisited by [**Jir58, Lam67b, Sil69, Gri74**] among others.

After their original application to population dynamics (see [**Par16**]), CBI processes have been adopted with success in finance. Especially for their non-negativity, branching structure, and Feller property, CBI processes have found an application in interest rate modeling. This began with the work of [**Fil01**], where CBI processes extended the class of *Cox–Ingersoll–Ross processes* (CIR, see [**CIR85**]) by allowing for jumps in their dynamics. More generally, CBI processes belong to the class of *affine processes* that were studied by [**DFS03**].

CBI processes exhibit a characteristic self-exciting behavior: the occurrence of a large (upward) jump increases the likelihood of subsequent jumps. This has been exploited by several contributions in order to capture volatility clustering. In [**JMS17**], an alpha-stable extension of the CIR process was proposed as a single-curve interest rate model. The same stochastic process was then used by [**JMSZ21**] for stochastic volatility modeling, extending the Heston model [**Hes93**]. We also mention [**JMSS19, CMS19**], where CBI processes have been applied to energy markets.

In this chapter, we present a self-contained framework for CBI processes with the objective of modeling multiple yield curves (see Chapter 3). For general accounts on CB and CBI processes, we refer the reader to [**Li11**, Chapter 3], [**Kyp14**, Chapter 12], and [**Li20**]. First, we define CBI processes and show their link with affine processes (Section 2.2). Next, we provide an analysis of exponential moments of CBI processes. In particular, we extend the domain of their Laplace transform, refining some results of [**KRM15**] (Section 2.3), and prove a general characterization of the time of explosion of exponential moments of a CBI process, by specializing techniques of [**KR11**]. This analysis will play a fundamental role in Chapter 3, where the finiteness of exponential moments will represent an indispensable requirement.

In the literature on CBI processes, there exist two main representations of a CBI process: the stochastic integral equation of Dawson and Li (see [**DL06**]), and the stochastic time change equation in the sense of Lamperti (first introduced by [**Lam67a**] for CB processes, later revisited by [**ECPGUB13**] for CBI processes). The main result of Section 2.5 (see Theorem 2.12) shows the equivalence (in a weak sense) between these two different representations of a CBI process. In Section 2.6, we present several examples of CBI processes. We first discuss the CIR process and its alpha-stable extension. We then derive a correspondence between CBI processes and *(marked) Hawkes processes* (see [**Haw71, HO74**]), extending [**BS20**, Proposition 7.2]. Moreover, we refine the time change Poisson representation of general point processes for the specific case of Hawkes processes. Finally, we introduce a novel specification that we name *tempered-stable CBI process* (Section 2.7), which is well suited to multiple yield curve modeling (see Chapter 3).

2.2. Definition and affine property

We fix a stochastic basis $\big(\Omega, \mathcal{F}, \mathbb{F}, \mathbb{Q}\big)$ satisfying the usual conditions, where $\mathbb{Q}$ is a probability measure and $\mathbb{F} = (\mathcal{F}_t)_{t\geqslant 0}$ a filtration to which all stochastic processes are assumed to be adapted. We set $\mathcal{F} = \mathcal{F}_\infty$ and denote the expectation under $\mathbb{Q}$ by $\mathbb{E}$.

We start with the standard definition of a CBI process, which can be found for example in [**Li11**, Chapter 3] and [**Li20**].

- Let the function $\Psi : \mathbb{R}_- \to \mathbb{R}$ be given by

$$\Psi(x) := \beta\, x + \int_0^{+\infty} \big(e^{\,x\,z} - 1\big)\, \nu(\mathrm{d}z), \qquad \forall x \leqslant 0, \tag{2.1}$$

  where $\beta \geqslant 0$ and ν is a Lévy measure on $\mathbb{R}_+$ such that $\int_0^1 z\, \nu(\mathrm{d}z) < +\infty$;
- Let the function $\Phi : \mathbb{R}_- \to \mathbb{R}$ be given by

$$\Phi(x) := -\,b\, x + \frac{1}{2}\,(\sigma\, x)^2 + \int_0^{+\infty} \big(e^{\,x\,z} - 1 - x\, z\big)\, \pi(\mathrm{d}z), \qquad \forall x \leqslant 0, \tag{2.2}$$

  where $b \in \mathbb{R}$, $\sigma \geqslant 0$, and π is a Lévy measure on $\mathbb{R}_+$ such that $\int_1^{+\infty} z\, \pi(\mathrm{d}z) < +\infty$.

Definition 2.1. A Markov process $X = (X_t)_{t\geqslant 0}$ with initial value X_0 and state space $\mathbb{R}_+$ is said to be a *Continuous-state Branching process with Immigration* (CBI) with immigration mechanism Ψ and branching mechanism Φ if its Laplace transform is given by

$$\mathbb{E}[e^{\,x\,X_T}] = \exp\left(\int_0^T \Psi\big(\mathcal{V}(s,x)\big)\, \mathrm{d}s + \mathcal{V}(T,x)\, X_0\right), \tag{2.3}$$

for all $x \leqslant 0$ and $T \geqslant 0$, where the function $\mathcal{V}(\cdot, x) : \mathbb{R}_+ \to \mathbb{R}_-$ is the unique solution to

$$\frac{\partial \mathcal{V}}{\partial t}(t,x) = \Phi\big(\mathcal{V}(t,x)\big), \qquad \mathcal{V}(0,x) = x. \tag{2.4}$$

From now on, any CBI process in the sense of Definition 2.1 will be denoted by $\mathrm{CBI}\big(X_0, \Psi, \Phi\big)$. We emphasize that this definition corresponds to a conservative, stochastically continuous CBI process in the sense of [**KW71**, Theorems 1.1 and 1.2], where more general CBI processes were considered in their Definition 1.1. In the present setting, we refer to Definition 2.1 as the standard definition of CBI processes. This implies that CBI processes are non-negative, strongly Markov (Feller), with càdlàg trajectories, and conservative.

From the perspective of financial modeling, the analytical tractability of CBI processes is ensured by their fundamental and well-known link with affine processes (see [**Fil01, DFS03**]). This is the content of the next result, which provides the joint conditional Laplace transform of the CBI process $X = (X_t)_{t\geqslant 0}$ and its time integral $Y_t := \int_0^t X_s\, \mathrm{d}s$, for all $t \geqslant 0$.

Lemma 2.2. *Let $X = (X_t)_{t\geqslant 0}$ be a $\mathrm{CBI}\big(X_0, \Psi, \Phi\big)$. Then, the joint process $(X_t, Y_t)_{t\geqslant 0}$ is affine with initial value $(X_0, 0)$, state space $\mathbb{R}_+^2$, and joint conditional Laplace transform*

$$\mathbb{E}\big[e^{\,x_1\,X_T + x_2\,Y_T} \,\big|\, \mathcal{F}_t\big] = \exp\big(\mathcal{U}(T-t, x_1, x_2) + \mathcal{V}(T-t, x_1, x_2)\, X_t + x_2\, Y_t\big), \tag{2.5}$$

for all $(x_1, x_2) \in \mathbb{R}_-^2$ *and* $0 \leqslant t \leqslant T < +\infty$, *where the functions* $\mathcal{U}(\cdot, x_1, x_2) : \mathbb{R}_+ \to \mathbb{R}$ *and* $\mathcal{V}(\cdot, x_1, x_2) : \mathbb{R}_+ \to \mathbb{R}_-$ *solve the following* CBI Riccati system:

$$\mathcal{U}(t, x_1, x_2) = \int_0^t \Psi\big(\mathcal{V}(s, x_1, x_2)\big)\, \mathrm{d}s, \tag{2.6}$$

$$\frac{\partial \mathcal{V}}{\partial t}(t, x_1, x_2) = \Phi\big(\mathcal{V}(t, x_1, x_2)\big) + x_2, \qquad \mathcal{V}(0, x_1, x_2) = x_1, \tag{2.7}$$

Proof. A direct application of [**KR09**, Theorem 4.10] yields the desired result, exploiting the affine property of the CBI process $X = (X_t)_{t \geqslant 0}$. □

2.3. Laplace transform domain extension

In this section, we extend the domain of the conditional Laplace transform (2.5) of the affine process $(X_t, Y_t)_{t \geqslant 0}$. To proceed, we rely on some techniques developed by [**KRM15**]. Let us first define the set $\mathcal{D}_1$:

$$\mathcal{D}_1 := \left\{ x \in \mathbb{R} : \int_1^{+\infty} e^{x\, z}\, (\nu + \pi)(\mathrm{d}z) < +\infty \right\}. \tag{2.8}$$

Observe that $\mathcal{D}_1$ is the effective domain of the immigration and branching mechanism functions Ψ and Φ. By using standard results on exponential moments of Lévy measures (see e.g. [**Sat99**, Theorem 25.17] and [**EK20**, Theorem 2.20]), we can extend Ψ and Φ, as finite-valued convex functions, to the set $\mathcal{D}_1$. Before applying such an extension to the conditional Laplace transform (2.5), we need to define an extended version of the Riccati system (2.6)–(2.7), In a similar way to [**KRM15**, Definition 2.10].

Definition 2.3. For $(x_1, x_2) \in \mathcal{D}_1 \times \mathbb{R}_-$, a solution $\big(\mathcal{U}(\cdot, x_1, x_2), \mathcal{V}(\cdot, x_1, x_2)\big)$ to the *extended CBI Riccati system* is defined as a solution to the following system:

$$\begin{aligned} \mathcal{U}(t, x_1, x_2) &= \int_0^t \Psi\big(\mathcal{V}(s, x_1, x_2)\big)\, \mathrm{d}s, \\ \frac{\partial \mathcal{V}}{\partial t}(t, x_1, x_2) &= \Phi\big(\mathcal{V}(t, x_1, x_2)\big) + x_2, \qquad \mathcal{V}(0, x_1, x_2) = x_1, \end{aligned} \tag{2.9}$$

up to a time $\mathrm{T}^{(x_1,x_2)} \in [0, +\infty]$, where $\mathrm{T}^{(x_1,x_2)}$ denotes the maximum joint lifetime of the functions $\mathcal{U}(\cdot, x_1, x_2) : [0, \mathrm{T}^{(x_1,x_2)}) \to \mathbb{R}$ and $\mathcal{V}(\cdot, x_1, x_2) : [0, \mathrm{T}^{(x_1,x_2)}) \to \mathcal{D}_1$.

Definition 2.3 extends the CBI Riccati system (2.6)–(2.7) by taking into account the possibility of explosion in finite time. For this reason, for each initial value $(x_1, x_2) \in \mathcal{D}_1 \times \mathbb{R}_-$, the lifetime $\mathrm{T}^{(x_1,x_2)}$ has to be introduced. In some cases, this lifetime can be infinite, which means that no explosion occurs (this holds true for example when $(x_1, x_2) \in \mathbb{R}_-^2$).

It is well known that the branching mechanism function Φ is locally Lipschitz continuous on the interior of $\mathcal{D}_1$, but it may fail to be so at the boundary of $\mathcal{D}_1$, denoted by $\partial\mathcal{D}_1$. Hence, a solution $\mathcal{V}(\cdot, x_1, x_2) : [0, \mathrm{T}^{(x_1,x_2)}) \to \mathcal{D}_1$ to equation (2.9) may not be unique when it starts at the boundary of $\mathcal{D}_1$ (i.e. when $x_1 \in \partial\mathcal{D}_1$) or reaches it at a later time. In order to overcome this issue,

the finiteness of the derivative of Φ, denoted by Φ', at the boundary $\partial\mathcal{D}_1$ does suffice to guarantee that $\Phi \in \mathcal{C}^1(\mathcal{D}_1, \mathbb{R})$. To formalize this observation, let us introduce two quantities:

$$\psi := \sup\{x \geqslant 0 : \Psi(x) < +\infty\} \in [0, +\infty] \quad \text{and} \quad \phi := \sup\{x \geqslant 0 : \Phi(x) < +\infty\} \in [0, +\infty]. \tag{2.10}$$

Since $\mathcal{D}_1$ is a convex set containing $\mathbb{R}_-$, it can be written as $\mathcal{D}_1 = (-\infty, \psi \wedge \phi)$ or $(-\infty, \psi \wedge \phi]$ when $\psi \wedge \phi < +\infty$ and $\Psi(\psi \wedge \phi) \vee \Phi(\psi \wedge \phi) < +\infty$ (or equivalently $\int_1^{+\infty} e^{(\psi \wedge \phi)z}(\nu + \pi)(\mathrm{d}z) < +\infty$). By a differentiability result for convex functions (see e.g. [**Roc70**, Theorem 25.5]), the function Φ is differentiable almost everywhere on the interior of $\mathcal{D}_1$ (i.e. $\mathcal{D}_1^\circ$), with derivative given by

$$\Phi'(x) = -b + \sigma^2 x + \int_0^{+\infty} z\,(e^{x\,z} - 1)\,\pi(\mathrm{d}z), \qquad \forall x \in \mathcal{D}_1^\circ. \tag{2.11}$$

When $\psi \wedge \phi = +\infty$, we have $\mathcal{D}_1 = \mathbb{R}$ and then $\Phi \in \mathcal{C}^1(\mathbb{R}, \mathbb{R})$. When $\psi \wedge \phi < +\infty$, Φ' may diverge at $\partial\mathcal{D}_1 = \{\psi \wedge \phi\}$. Under the following assumption, we have $\Phi'(\psi \wedge \phi) < +\infty$ and then $\Phi \in \mathcal{C}^1(\mathcal{D}_1, \mathbb{R})$.

Assumption 2.4. If $\psi \wedge \phi < +\infty$, then $\int_1^{+\infty} z\, e^{(\psi \wedge \phi)z}\, \pi(\mathrm{d}z) < +\infty$.

Under Assumption 2.4, there exists a unique solution $\big(\mathcal{U}(\cdot, x_1, x_2), \mathcal{V}(\cdot, x_1, x_2)\big)$ to the extended CBI Riccati system, for all $(x_1, x_2) \in \mathcal{D}_1 \times \mathbb{R}_-$. This enables us to refine the second assertion of [**KRM15**, Theorem 2.14] for the specific case of CBI processes.

Proposition 2.5. *Let $(X_t)_{t \geqslant 0}$ be a $\mathrm{CBI}\big(X_0, \Psi, \Phi\big)$. Suppose that Assumption 2.4 holds true. Then, the conditional Laplace transform* (2.5) *can be extended to $\mathcal{D}_1 \times \mathbb{R}_-$ as follows:*

$$\mathbb{E}\big[e^{x_1 X_T + x_2 Y_T} \,\big|\, \mathcal{F}_t\big] = \exp\big(\mathcal{U}(T - t, x_1, x_2) + \mathcal{V}(T - t, x_1, x_2)\, X_t + x_2\, Y_t\big), \tag{2.12}$$

for all $(x_1, x_2) \in \mathcal{D}_1 \times \mathbb{R}_-$ and $0 \leqslant t \leqslant T < \mathrm{T}^{(x_1, x_2)}$, where $\big(\mathcal{U}(\cdot, x_1, x_2), \mathcal{V}(\cdot, x_1, x_2)\big)$ is the unique solution to the extended CBI Riccati system starting from $(x_1, x_2) \in \mathcal{D}_1 \times \mathbb{R}_-$ and up to $\mathrm{T}^{(x_1, x_2)}$.

Proof. Under Assumption 2.4, it holds that $\Phi \in \mathcal{C}^1(\mathcal{D}_1, \mathbb{R})$. Hence, for all $(x_1, x_2) \in \mathcal{D}_1 \times \mathbb{R}_-$, the extended CBI Riccati system has a unique solution $\big(\mathcal{U}(\cdot, x_1, x_2), \mathcal{V}(\cdot, x_1, x_2)\big)$ up to $\mathrm{T}^{(x_1, x_2)}$. The extension of (2.5) to $\mathcal{D}_1 \times \mathbb{R}_-$ then follows from [**KRM15**, Theorem 2.14]. □

Remark 2.6. In the setting of Proposition 2.5, we can state another important property of the maximum lifetime $\mathrm{T}^{(x_1, x_2)}$ of the unique solution $\big(\mathcal{U}(\cdot, x_1, x_2), \mathcal{V}(\cdot, x_1, x_2)\big)$ to the extended CBI Riccati system. By [**KRM15**, Proposition 3.3], for all $(x_1, x_2) \in \mathcal{D}_1 \times \mathbb{R}_-$, the lifetime $\mathrm{T}^{(x_1, x_2)}$ also characterizes the finiteness of real exponential moments:

$$\mathrm{T}^{(x_1, x_2)} = \sup\Big\{t \geqslant 0 : \mathbb{E}\big[e^{x_1 X_t + x_2 Y_t}\big] < +\infty\Big\}. \tag{2.13}$$

Remark 2.7. [**KRM15**] also provides a complex extension of the joint conditional Laplace transform (2.12), which will be needed later in Chapter 3 for the pricing of non-linear derivatives by means of Fourier techniques. To this effect, let $\mathcal{O}_1 := \big\{u \in \mathbb{C} : \mathrm{Re}(u) \in \mathcal{D}_1^\circ\big\}$, with $\mathrm{Re}(u)$ denoting the real part of u. For all $(u_1, u_2) \in \mathcal{O}_1 \times \mathbb{C}_-$, Assumption 2.4 guarantees the existence of a unique solution to the extended CBI Riccati system, starting from $(\mathrm{Re}(u_1), \mathrm{Re}(u_2)) \in \mathcal{D}_1^\circ \times \mathbb{R}_-$ and defined up to the lifetime $\mathrm{T}^{(\mathrm{Re}(u_1), \mathrm{Re}(u_2))}$. By using [**KRM15**, Theorem 2.26], the joint conditional Laplace (–Fourier) transform (2.12) holds for all $(u_1, u_2) \in \mathcal{O}_1 \times \mathbb{C}_-$, where we have to replace Ψ and Φ by

their analytic extensions to the complex domain $\mathcal{O}_1$ (see [**KRM15**, Proposition 2.21]). However, this extension is only valid up to a time $\mathrm{T}^{(u_1,u_2)}$, which verifies $\mathrm{T}^{(u_1,u_2)} \geqslant \mathrm{T}^{(\mathrm{Re}(u_1),\mathrm{Re}(u_2))}$ (see [**KRM15**, Proposition 5.1]). We refer the reader to Chapter 4 for further details.

2.4. Finiteness of exponential moments

In this section, we provide an explicit and general characterization of the lifetime $\mathrm{T}^{(x_1,x_2)}$, for all $(x_1,x_2) \in \mathcal{D}_1 \times \mathbb{R}_-$. In view of (2.13), this characterization is intimately related to the finiteness of exponential moments of CBI processes. Especially for pricing purposes, it is important to know whether exponential moment explosion happens in finite time or not. Our result specializes [**KR11**, Theorem 4.1], but does not require the CBI process $X = (X_t)_{t\geqslant 0}$ to be subcritical (i.e. $b > 0$). For $x_2 \in \mathbb{R}_-$, let us introduce the following notation:

$$\mathcal{S} := \Big\{ x \in \mathcal{D}_1 : \Phi(x) + x_2 \leqslant 0 \Big\} \quad \text{and} \quad \chi := \sup \mathcal{S}.$$

We can then formulate the following theorem.

THEOREM 2.8. *Let $(X_t)_{t\geqslant 0}$ be a $\mathrm{CBI}\big(X_0, \Psi, \Phi\big)$. Suppose that Assumption 2.4 holds true. Then, for all $(x_1,x_2) \in \mathcal{D}_1 \times \mathbb{R}_-$, the lifetime $\mathrm{T}^{(x_1,x_2)}$ is characterized as follows:*

(i) *If $x_1 \leqslant \chi$, then $\mathrm{T}^{(x_1,x_2)} = +\infty$;*

(ii) *If $x_1 > \chi$, then*

$$\mathrm{T}^{(x_1,x_2)} = \int_{x_1}^{\psi\wedge\phi} \frac{\mathrm{d}x}{\Phi(x) + x_2}. \tag{2.14}$$

PROOF. In view of characterizing $\mathrm{T}^{(x_1,x_2)}$, we can decompose it as $\mathrm{T}^{(x_1,x_2)} = \mathrm{T}^{\mathcal{U}} \wedge \mathrm{T}^{\mathcal{V}}$, where

$$\mathrm{T}^{\mathcal{U}} := \inf\big\{ t \geqslant 0 : \mathcal{V}(t,x_1,x_2) = \psi \big\} \quad \text{and} \quad \mathrm{T}^{\mathcal{V}} := \inf\big\{ t \geqslant 0 : \mathcal{V}(t,x_1,x_2) = \phi \big\}, \tag{2.15}$$

where $\mathrm{T}^{\mathcal{U}}$ corresponds to the maximum lifetime of the function $\mathcal{U}(\cdot,x_1,x_2)$ and $\mathrm{T}^{\mathcal{V}}$ to that of the function $\mathcal{V}(\cdot,x_1,x_2)$. Let us first consider the trivial case $\Phi \equiv 0$ ($\phi = +\infty$). The CBI process $X = (X_t)_{t\geqslant 0}$ then degenerates into a non-decreasing Lévy process whose Lévy exponent is given by Ψ. Then, it is straightforward to see that, for all $(x_1,x_2) \in \mathcal{D}_1 \times \mathbb{R}_-$, the unique solution $\mathcal{V}(\cdot,x_1,x_2)$ to equation (2.9) is given by $\mathcal{V}(t,x_1,x_2) = x_1 + x_2\, t$, for all $t \geqslant 0$, thus leading to $\mathrm{T}^{\mathcal{V}} = +\infty$. In addition, we have $\mathcal{S} = \big\{ x \in \mathcal{D}_1 : x_2 \leqslant 0 \big\} = \mathcal{D}_1$, where $\mathcal{D}_1 = (-\infty, \psi)$ (or $(-\infty,\psi]$ when $\psi < +\infty$ and $\Psi(\psi) < +\infty$), and then $\chi = \psi$. Therefore, for all $x_1 \leqslant \chi$, the function $\mathcal{V}(\cdot,x_1,x_2)$ is non-increasing and never reaches the explosion point of the function Ψ, which yields $\mathrm{T}^{\mathcal{U}} = +\infty$ and therefore $\mathrm{T}^{(x_1,x_2)} = +\infty$ for all $x_1 \leqslant \chi$.

Frown now on, let us suppose that there exists at least one point $x \in \mathcal{D}_1$ such that $\Phi(x) \neq 0$. Given that $\Phi(0) = 0$, the set $\mathcal{S}$ is non-empty since it always contains zero. Then, we can write $\chi = \sup \mathcal{S} \in [0, \psi \wedge \phi]$ and $\Phi(\chi) + x_2 \leqslant 0$ due to the continuity of Φ. Figure 2.1 illustrates some possible shapes of the function Φ over $\mathcal{D}_1$, where the solid curves refer to the case $\psi \wedge \phi < +\infty$ and the dashed ones to the case $\psi \wedge \phi = +\infty$. The determination of $\mathrm{T}^{(x_1,x_2)}$, for $(x_1,x_2) \in \mathcal{D}_1 \times \mathbb{R}_-$ relies on the location of χ, which is illustrated graphically in Figure 2.1 as the intersection point of the function Φ with the horizontal line $y = -x_2$, whenever this intersection is non-empty. Consider now the following cases:

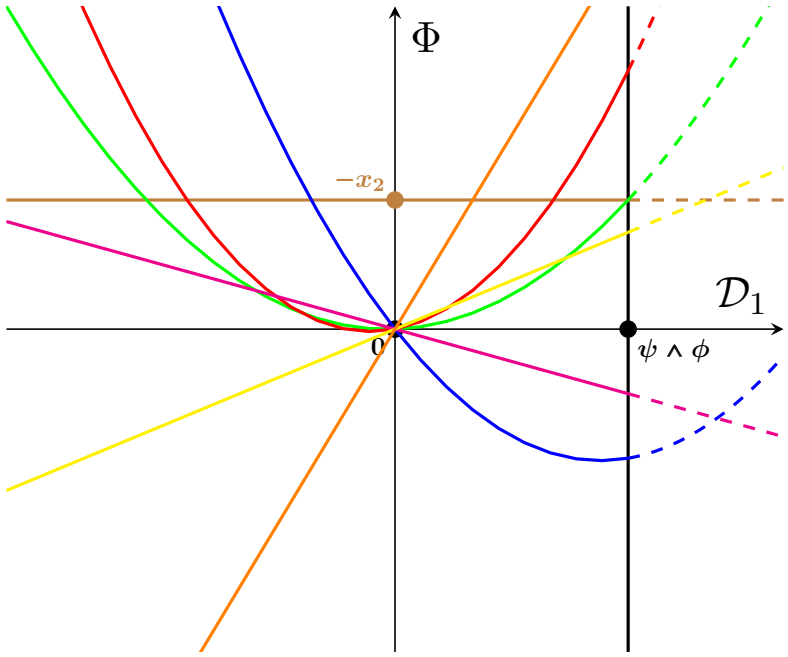

FIGURE 2.1. Some possible shapes of the function Φ over $\mathcal{D}_1$, where the solid curves refer to $\psi \wedge \phi < +\infty$ and the dashed ones to $\psi \wedge \phi = +\infty$.

(1) $\Phi(\chi) + x_2 = 0$, corresponding to the green curve ($\chi = \psi \wedge \phi$ when $\psi \wedge \phi < +\infty$), the red curve and the orange line (linear case $\Phi(x) = -b\,x$ with $b < 0$). In this case, we have $\mathcal{V}(\cdot, \chi, x_2) \equiv \chi$ as the unique solution to equation (2.9), which implies $\mathrm{T}^{(\chi, x_2)} = +\infty$. Then, for all $x_1 \leqslant \chi$, in view of (2.13), we have $\mathrm{T}^{(x_1, x_2)} = +\infty$ since $\mathbb{E}\big[e^{x_1 X_t + x_2 Y_t}\big] \leqslant \mathbb{E}\big[e^{\chi X_t + x_2 Y_t}\big] < +\infty$, for all $t \geqslant 0$;

(2) Consider again the case $\Phi(\chi) + x_2 = 0$, but when $x_1 > \chi$. By convexity of Φ, we have that $\Phi(x_1) + x_2 > 0$, implying by equation (2.9) that the unique solution $\mathcal{V}(\cdot, x_1, x_2)$ starting from $x_1 > \chi$ is strictly increasing with values in $[x_1, \phi]$. At this point, following standard extension results (see e.g. [**Har82**, Theorem II.3.1] whose main hypothesis can be reduced to the continuity of the function Φ), $\mathcal{V}(\cdot, x_1, x_2)$ can be extended to a maximal interval of existence $[0, \mathrm{T}')$ such that one of the following two situations occurs:

$$\Big\{\mathrm{T}' = +\infty\Big\} \qquad \text{or} \qquad \Big\{\mathrm{T}' < +\infty \quad \text{and} \quad \lim_{t \to \mathrm{T}'} \mathcal{V}(t, x_1, x_2) = \phi\Big\}. \tag{2.16}$$

Suppose that $\mathrm{T}' = +\infty$. Since the function $\mathcal{V}(\cdot, x_1, x_2)$ is strictly increasing, it must admit a limit $\lim_{t \to +\infty} \mathcal{V}(t, x_1, x_2) = l$ with values in $(\chi, \phi] \cup \{+\infty\}$. Assume that $l < +\infty$, i.e. the line $y = l$ is an horizontal asymptote for $\mathcal{V}(\cdot, x_1, x_2)$ as $t \to +\infty$. This implies that $\frac{\partial \mathcal{V}}{\partial t}(t, x_1, x_2) \underset{t \to +\infty}{\to} 0$. Then, letting t go to infinity on both sides of equation (2.9) yields $\Phi(l) + x_2 = 0$, contradicting $\Phi(x_1) + x_2 > 0$ for all $x_1 > \chi$. Therefore, the limit l must necessarily be infinite, in which case we have $\phi = +\infty$. In particular, this can be reduced to $\lim_{t \to \mathrm{T}'} \mathcal{V}(t, x_1, x_2) = \phi$ with $\mathrm{T}' = +\infty$ and $\phi = +\infty$. Therefore, T' is equivalent to the lifetime

$\mathrm{T}^{\mathcal{V}}$ of the function $\mathcal{V}(\cdot, x_1, x_2)$ given by (2.15). Let $(\mathrm{T}_n)_{n\geqslant 0}$ be an increasing sequence such that $\mathrm{T}_n \underset{n\to+\infty}{\to} \mathrm{T}^{\mathcal{V}}$. Due to the continuity of $\mathcal{V}(\cdot, x_1, x_2)$, we have $\lim_{n\to+\infty} \mathcal{V}(\mathrm{T}_n, x_1, x_2) = \phi$. In view of equation (2.9), we can write

$$\mathrm{T}_n = \int_{x_1}^{\mathcal{V}(\mathrm{T}_n, x_1, x_2)} \frac{\mathrm{d}x}{\Phi(x) + x_2}, \tag{2.17}$$

for all $n \in \mathbb{N}$. Letting n go to infinity on both sides of equation (2.17) yields

$$\mathrm{T}^{\mathcal{V}} = \int_{x_1}^{\phi} \frac{\mathrm{d}x}{\Phi(x) + x_2}.$$

So far, $\mathrm{T}^{\mathcal{V}}$ only represents the lifetime of $\mathcal{V}(\cdot, x_1, x_2)$. In order to recover the joint lifetime of both $\mathcal{U}(\cdot, x_1, x_2)$ and $\mathcal{V}(\cdot, x_1, x_2)$, for all $x_1 > \chi$, we have to distinguish two additional cases:

(i) The case $\phi \leqslant \psi$. This means that $\mathcal{U}(\cdot, x_1, x_2)$ never explodes in finite time before $\mathcal{V}(\cdot, x_1, x_2)$, thus yielding for all $x_1 > \chi$

$$\mathrm{T}^{(x_1,x_2)} = \mathrm{T}^{\mathcal{V}} = \int_{x_1}^{\phi} \frac{\mathrm{d}x}{\Phi(x) + x_2}; \tag{2.18}$$

(ii) The case $\phi > \psi$, meaning that $\mathcal{U}(\cdot, x_1, x_2)$ explodes in finite time before $\mathcal{V}(\cdot, x_1, x_2)$ at time $\mathrm{T}^{\mathcal{U}}$. In this case, we can assume that there exists $n \in \mathbb{N}$ such that $\mathrm{T}_n = \mathrm{T}^{\mathcal{U}}$ and $\mathcal{V}(\mathrm{T}^{\mathcal{U}}, x_1, x_2) = \psi$. By (2.17), we have for all $x_1 > \chi$

$$\mathrm{T}^{(x_1,x_2)} = \mathrm{T}^{\mathcal{U}} = \int_{x_1}^{\psi} \frac{\mathrm{d}x}{\Phi(x) + x_2}. \tag{2.19}$$

Combining both cases, we obtain formula (2.14) for $\mathrm{T}^{(x_1,x_2)}$, for all $x_1 > \chi$;

(3) Consider now the case $\Phi(\chi) + x_2 < 0$. This means that the function Φ never crosses the line $y = -x_2$ after zero, thus yielding $\chi = \psi \wedge \phi$. In Figure 2.1, this case corresponds to the blue curve (when $\psi \wedge \phi < +\infty$), the yellow line (when $\psi < +\infty$) and the magenta line ($\chi = +\infty$ when $\psi = +\infty$), both of which correspond to the linear case $\Phi(x) = -\,b\,x$ with $b \neq 0$ and $\phi = +\infty$. In this linear case, for all $(x_1, x_2) \in \mathcal{D}_1 \times \mathbb{R}_-$, the solution $\mathcal{V}(\cdot, x_1, x_2)$ to equation (2.9) is given by $\mathcal{V}(t, x_1, x_2) = \left(x_1 - \frac{x_2}{b}\right) e^{-\,b\,t} + \frac{x_2}{b}$, for all $t \geqslant 0$, which then gives $\mathrm{T}^{\mathcal{V}} = +\infty$ by (2.15). Concerning $\mathrm{T}^{\mathcal{U}}$, its determination depends on the sign of the parameter $b \neq 0$ as follows:

(i) If $b < 0$, then the function Φ crosses the line $y = -x_2$ at $x = \frac{x_2}{b} \in \mathbb{R}_+$. In this case ($\Phi(\chi) + x_2 < 0$), we necessarily have $\chi < \frac{x_2}{b}$, implying that for all $x_1 \leqslant \chi$, the function $\mathcal{V}(\cdot, x_1, x_2)$ is strictly decreasing and never reaches the explosion point of the function Ψ, thus yielding $\mathrm{T}^{\mathcal{U}} = +\infty$ and $\mathrm{T}^{(x_1,x_2)} = +\infty$ for all $x_1 \leqslant \chi$;

(ii) If $b > 0$, then the function Φ crosses the line $y = -x_2$ at $x = \frac{x_2}{b} \in \mathbb{R}_-$. In this case, for all $\frac{x_2}{b} < x_1 \leqslant \chi$, the function $\mathcal{V}(\cdot, x_1, x_2)$ is strictly decreasing and never reaches the explosion point of the function Ψ, thus yielding $\mathrm{T}^{\mathcal{U}} = +\infty$ and $\mathrm{T}^{(x_1,x_2)} = +\infty$ for all $\frac{x_2}{b} < x_1 \leqslant \chi$. Similarly, as in the case $\Phi(\chi) + x_2 = 0$, we have $\mathrm{T}^{(x_1,x_2)} = +\infty$ for all $x_1 \leqslant \frac{x_2}{b}$ in view of (2.13).

Consider now a non-linear branching mechanism Φ. Similarly to the case $\Phi(x) = -b\,x$ with $b > 0$, there exists a unique $\xi \in \mathbb{R}_-$ such that $\Phi(\xi)+x_2 = 0$. Hence, for all $\xi < x_1 \leqslant \chi$, we have $\Phi(x_1) + x_2 < 0$. The function $\mathcal{V}(\cdot, x_1, x_2)$ is then strictly decreasing and by integrating on both sides of equation (2.9), we obtain

$$t = \int_{\mathcal{V}(t,x_1,x_2)}^{x_1} \frac{-\,\mathrm{d}x}{\Phi(x) + x_2}. \tag{2.20}$$

Letting t go to infinity on both sides of this identity, given $\Phi(\xi) + x_2 = 0$, we obtain $\lim_{t\to+\infty} \mathcal{V}(t, x_1, x_2) = \xi$ and $\xi < \mathcal{V}(\cdot, x_1, x_2) \leqslant x_1$, for all $\xi < x_1 \leqslant \chi$, yielding $\mathrm{T}^{\mathcal{V}} = +\infty$. Since Ψ is non-decreasing on $\mathcal{D}_1$, we have $t\,\Psi(\xi) \leqslant \mathcal{U}(t, x_1, x_2) \leqslant t\,\Psi(x_1)$, for all $t \geqslant 0$, then $\mathrm{T}^{\mathcal{U}} = +\infty$. We obtain $\mathrm{T}^{(x_1,x_2)} = +\infty$ for all $\xi < x_1 \leqslant \chi$ and for all $x_1 \leqslant \xi$ by (2.13).

□

Under an additional assumption, the next result provides a simple necessary and sufficient condition for the finiteness of the exponential moment $\mathbb{E}\big[e^{\,x_1\,X_T\,+\,x_2\,Y_T}\big]$, for all $(x_1, x_2) \in \mathcal{D}_1 \times \mathbb{R}_-$ and $T > 0$. This result will be useful for the construction of the modeling framework in Chapter 3.

Corollary 2.9. *Let $(X_t)_{t\geqslant 0}$ be a $\mathrm{CBI}\big(X_0, \Psi, \Phi\big)$. Suppose that Assumption 2.4 holds true. Under $\psi \wedge \phi + \Psi(\psi \wedge \phi) < +\infty$, $\mathrm{T}^{(x_1,x_2)} = +\infty$ for all $(x_1, x_2) \in \mathcal{D}_1 \times \mathbb{R}_-$ if and only if $\Phi(\psi \wedge \phi) \leqslant 0$.*

Proof. Combining Assumption 2.4 with $\psi \wedge \phi < +\infty$ necessarily yields $\Phi(\psi \wedge \phi) < +\infty$. Suppose further that $\Psi(\psi \wedge \phi) < +\infty$, we then have $\mathcal{D}_1 = (-\infty, \psi \wedge \phi]$. We proceed as follows:

- If $\Phi(\psi \wedge \phi) \leqslant 0$, then we have $\chi = \psi \wedge \phi$ automatically, therefore the first assertion of Theorem 2.8 implies that $\mathrm{T}^{(x_1,x_2)} = +\infty$, for all $(x_1, x_2) \in \mathcal{D}_1 \times \mathbb{R}_-$;
- Conversely, suppose that $\mathrm{T}^{(x_1,x_2)} = +\infty$ for all $(x_1, x_2) \in \mathcal{D}_1 \times \mathbb{R}_-$. This holds in particular for $x_1 = \psi \wedge \phi$ and $x_2 = 0$ since $\psi \wedge \phi \in \mathcal{D}_1$. We now prove that $\Phi(\psi \wedge \phi) \leqslant 0$ by contradiction. If $\Phi(\psi \wedge \phi) > 0$, then $\chi = 0$ since $x_2 = 0$ and in view of the properties of the function Φ. The second assertion of Theorem 2.8 asserts that $\mathrm{T}^{(\psi\wedge\phi,0)}$ is given by formula (2.14), i.e. $\mathrm{T}^{(\psi\wedge\phi,0)} = 0$, thus leading to a contradiction.

□

2.5. Stochastic representations

In the literature, there exist two representations of a $\mathrm{CBI}\big(X_0, \Psi, \Phi\big)$: the stochastic integral equation by Dawson and Li (see [**DL06**, Section 5]), and the stochastic time change equation in the sense of Lamperti (see [**ECPGUB13**]). The purpose of this section is to show that these two representations are equivalent in a weak sense. We begin with the Dawson–Li representation, where we suppose that the stochastic basis $\big(\Omega, \mathcal{F}, \mathbb{F}, \mathbb{Q}\big)$ is equipped with the following objects:

- A standard Brownian motion $B = (B_t)_{t\geqslant 0}$;
- A Poisson random measure $N_0(\mathrm{d}t, \mathrm{d}x)$ on $\mathbb{R}_+ \times \mathbb{R}_+$ with compensator $\mathrm{d}t\,\nu(\mathrm{d}x)$ and compensated measure $\widetilde{N}_0(\mathrm{d}t, \mathrm{d}x) := N_0(\mathrm{d}t, \mathrm{d}x) - \mathrm{d}t\,\nu(\mathrm{d}x)$;
- A Poisson random measure $N_1(\mathrm{d}t, \mathrm{d}u, \mathrm{d}x)$ on $\mathbb{R}_+ \times \mathbb{R}_+ \times \mathbb{R}_+$ with compensator $\mathrm{d}t\,\mathrm{d}u\,\pi(\mathrm{d}x)$ and compensated measure $\widetilde{N}_1(\mathrm{d}t, \mathrm{d}u, \mathrm{d}x) := N_1(\mathrm{d}t, \mathrm{d}u, \mathrm{d}x) - \mathrm{d}t\,\mathrm{d}u\,\pi(\mathrm{d}x)$.

In addition, we assume that B, N_0, and N_1 are mutually independent. We can then write, for any $X_0 \geqslant 0$, the following stochastic integral equation:

$$\begin{aligned} X_t &= X_0 + \int_0^t \big(\beta - b\, X_s\big)\, \mathrm{d}s + \sigma \int_0^t \sqrt{X_s}\, \mathrm{d}B_s \\ &\quad + \int_0^t \int_0^{+\infty} x\, N_0(\mathrm{d}s, \mathrm{d}x) + \int_0^t \int_0^{X_{s-}} \int_0^{+\infty} x\, \widetilde{N}_1(\mathrm{d}s, \mathrm{d}u, \mathrm{d}x), \qquad \forall t \geqslant 0. \end{aligned} \tag{2.21}$$

As a result of [**DL06**, Theorems 5.1 and 5.2], for any $X_0 \geqslant 0$, there exists a unique non-negative strong solution to equation (2.21), which is a $\mathrm{CBI}\big(X_0, \Psi, \Phi\big)$. The following statement represents our formal definition of a *Dawson–Li representation*.

Definition 2.10. A non-negative càdlàg stochastic process $X = (X_t)_{t\geqslant 0}$ with initial value X_0 admits a *Dawson–Li representation* if it is a weak solution to equation (2.21).

Following the characterization of [**Li11**, Theorem 9.31] and [**Li20**, Theorem 8.1], a non-negative càdlàg stochastic process $X = (X_t)_{t\geqslant 0}$ admits a Dawson–Li representation if and only if it is a $\mathrm{CBI}\big(X_0, \Psi, \Phi\big)$. In particular, we deduce that any $\mathrm{CBI}\big(X_0, \Psi, \Phi\big)$ can only jump upward.

In view of the Lamperti-type representation, we first recall that $Y_t := \int_0^t X_s\, \mathrm{d}s$, for all $t \geqslant 0$. Since $X = (X_t)_{t\geqslant 0}$ is non-negative with càdlàg trajectories, $Y = (Y_t)_{t\geqslant 0}$ is non-decreasing and almost surely finite at all times. It can then be utilized as a finite, continuous time change in the sense of [**KS02b**, Definition 2]. We assume that the stochastic basis $\big(\Omega, \mathcal{F}, \mathbb{F}, \mathbb{Q}\big)$ supports the following two independent processes:

- A non-decreasing Lévy process $L^\Psi = (L^\Psi_t)_{t\geqslant 0}$ with $L^\Psi_0 = 0$, whose Lévy exponent is given by Ψ and characterized by the Lévy triplet $(\beta, 0, \nu)$;
- A spectrally positive Lévy process $L^\Phi = (L^\Phi_t)_{t\geqslant 0}$ with $L^\Phi_0 = 0$ and finite first moment, whose Lévy exponent is given by Φ through the Lévy triplet $(-b, \sigma, \pi)$.

In this respect, we can define, for any $X_0 \geqslant 0$, the following stochastic time change equation:

$$X_t = X_0 + L^\Psi_t + L^\Phi_{Y_t}, \qquad \forall t \geqslant 0. \tag{2.22}$$

Following [**ECPGUB13**, Proposition 2 and Theorem 2], for any $X_0 \geqslant 0$, there is a unique non-negative strong solution to equation (2.22), which is a $\mathrm{CBI}\big(X_0, \Psi, \Phi\big)$. We can then give our formal definition of a *Lamperti-type representation*.

Definition 2.11. A non-negative càdlàg stochastic process $X = (X_t)_{t\geqslant 0}$ with initial value X_0 admits a *Lamperti-type representation* if it is a weak solution to equation (2.22).

We formulate the main result of this section, which relates the Dawson–Li stochastic integral representation to the Lamperti-type stochastic time change representation. We give a self-contained proof, whose techniques are also used for the characterization of CBITCL processes in Chapter 4.

Theorem 2.12. *A non-negative càdlàg stochastic process $X = (X_t)_{t\geqslant 0}$ with initial value X_0 admits a Dawson–Li representation if and only if it admits a Lamperti-type representation.*

PROOF. Let $X = (X_t)_{t\geqslant 0}$ admit a Lamperti-type representation, meaning that $X = (X_t)_{t\geqslant 0}$ is a weak solution to (2.22). Since $L^\Psi = (L^\Psi_t)_{t\geqslant 0}$ is a Lévy process with non-decreasing sample paths, its Lévy-Itô decomposition can be written as follows (see e.g. [**CT04**, Corollary 3.1]):

$$L^\Psi_t = \beta\, t + \int_0^t \int_0^{+\infty} x\, N_0(\mathrm{d}s, \mathrm{d}x), \qquad \forall t \geqslant 0, \tag{2.23}$$

where $N_0(\mathrm{d}t, \mathrm{d}x)$ is a Poisson random measure with compensator $\mathrm{d}t\, \nu(\mathrm{d}x)$. We proceed similarly with the Lévy process $L^\Phi = (L^\Phi_t)_{t\geqslant 0}$ where we take into account the time change $Y = (Y_t)_{t\geqslant 0}$:

$$L^\Phi_{Y_t} = -\, b\, Y_t + \sigma\, W_{Y_t} + \int_0^{Y_t} \int_0^{+\infty} x\, \widetilde{N}(\mathrm{d}s, \mathrm{d}x), \qquad \forall t \geqslant 0, \tag{2.24}$$

where $W = (W_t)_{t\geqslant 0}$ is a Brownian motion independent of the Poisson random measure $N(\mathrm{d}t, \mathrm{d}x)$ on $\mathbb{R}_+ \times \mathbb{R}_+$ with compensator $\mathrm{d}t\, \pi(\mathrm{d}x)$ and compensated measure $\widetilde{N}(\mathrm{d}t, \mathrm{d}x) := N(\mathrm{d}t, \mathrm{d}x) - \mathrm{d}t\, \pi(\mathrm{d}x)$. By the change of-variable formula of [**Jac79**, Theorem 10.27], we rewrite the stochastic integral by means of the time-changed random measure $N(X_t\, \mathrm{d}t, \mathrm{d}x)$ with compensator $X_{t-}\, \mathrm{d}t\, \pi(\mathrm{d}x)$:

$$\int_0^{Y_t} \int_0^{+\infty} x\, \widetilde{N}(\mathrm{d}s, \mathrm{d}x) = \int_0^t \int_0^{+\infty} x\, \widetilde{N}(X_s\, \mathrm{d}s, \mathrm{d}x), \qquad \forall t \geqslant 0.$$

Following [**IW89**, Theorem II.7.4], possibly on an enlarged probability space, there exists a Poisson random measure $N_1(\mathrm{d}t, \mathrm{d}u, \mathrm{d}x)$ with compensator $\mathrm{d}t\, \mathrm{d}u\, \pi(\mathrm{d}x)$ and compensated measure $\widetilde{N}_1(\mathrm{d}t, \mathrm{d}u, \mathrm{d}x) := N_1(\mathrm{d}t, \mathrm{d}u, \mathrm{d}x) - \mathrm{d}t\, \mathrm{d}u\, \pi(\mathrm{d}x)$ such that

$$\int_0^t \int_0^{+\infty} x\, \widetilde{N}(X_s\, \mathrm{d}s, \mathrm{d}x) = \int_0^t \int_0^{X_{s-}} \int_0^{+\infty} x\, \widetilde{N}_1(\mathrm{d}s, \mathrm{d}u, \mathrm{d}x), \qquad \forall t \geqslant 0.$$

Similarly, by [**IW89**, Theorem II.7.1'], there exists a Brownian motion $B = (B_t)_{t\geqslant 0}$ (possibly on an enlarged probability space) such that $W_{Y_t} = \int_0^t \sqrt{X_s}\, \mathrm{d}B_s$, for all $t \geqslant 0$. This directly implies that $X = (X_t)_{t\geqslant 0}$ is a weak solution to (2.21), thus admitting a Dawson–Li representation.

Conversely, suppose that $X = (X_t)_{t\geqslant 0}$ admits a Dawson–Li representation, meaning that $X = (X_t)_{t\geqslant 0}$ is a weak solution to (2.21). We first observe that the process $\big(\beta\, t + \int_0^t \int_0^{+\infty} x\, N_0(\mathrm{d}s, \mathrm{d}x)\big)_{t\geqslant 0}$ is a non-decreasing Lévy process with Lévy triplet $(\beta, 0, \nu)$, which we denote by $L^\Psi = (L^\Psi_t)_{t\geqslant 0}$. Let us then define the process $V = (V_t)_{t\geqslant 0}$ as follows:

$$V_t := -\, b\, Y_t + \sigma \int_0^t \sqrt{X_s}\, \mathrm{d}B_s + \int_0^t \int_0^{X_{s-}} \int_0^{+\infty} x\, \widetilde{N}_1(\mathrm{d}s, \mathrm{d}u, \mathrm{d}x), \qquad \forall t \geqslant 0.$$

In order to show that $V = (V_t)_{t\geqslant 0}$ is a time-changed Lévy process, we follow the scheme of the proof of [**Kal06**, Theorem 3.2]. Without loss of generality, we can suppose that the underlying stochastic basis already supports a spectrally positive Lévy process $L = (L_t)_{t\geqslant 0}$ with $L_0 = 0$ and finite first moment, whose Lévy exponent is given by Φ and characterized by the Lévy triplet $(-b, \sigma, \pi)$.

Let $Y_\infty := \lim\limits_{t\to+\infty} Y_t$ and define the inverse time change $\tau = (\tau_z)_{z\geqslant 0}$ by $\tau_z := \inf\big\{t \geqslant 0 : Y_t > z\big\}$, for all $z \geqslant 0$. We recall that $X = (X_t)_{t\geqslant 0}$ is a $\mathrm{CBI}\big(X_0, \Psi, \Phi\big)$ by [**Li11**, Theorem 9.31] and [**Li20**, Theorem 8.1]. When $\Psi \equiv 0$, $X = (X_t)_{t\geqslant 0}$ becomes a CB process, for which zero is known to be an absorbing state (see [**Gre74**]). In this case, we may have $Y_\infty < +\infty$, which implies that $\tau = (\tau_z)_{z\geqslant 0}$ is infinite from time Y_∞ onward. Thus, the time-changed process $W = (W_z)_{z<Y_\infty}$ given

by $W_z := V_{\tau_z}$, for all $z < Y_\infty$, is a well-defined semimartingale, but only on the stochastic interval $[\![0, Y_\infty[\![$ (see [**Jac79**, Theorem 10.10]). Its characteristics, which we denote by $\big(A, B, C\big)$, can be computed as follows:

$$A_z = -\,b\,Y_{\tau_z} = -\,b\,z, \quad B_z = \sigma^2\,Y_{\tau_z} = \sigma^2\,z, \quad \text{and} \quad C_z(\mathrm{d}x) = \pi(\mathrm{d}x)\,Y_{\tau_z} = \pi(\mathrm{d}x)\,z,$$

for all $z < Y_\infty$, where $Y_{\tau_z} = z$ since $\tau = (\tau_z)_{z\geqslant 0}$ is strictly increasing on $[\![0, Y_\infty[\![$. The differential characteristics of $W = (W_z)_{z<Y_\infty}$ are then both deterministic and time-independent. Therefore, by [**Kal06**, Proposition 1], $W = (W_z)_{z<Y_\infty}$ is a Lévy process on $[\![0, Y_\infty[\![$ characterized by the Lévy triplet $(-b, \sigma, \pi)$.

In view of using [**Jac79**, Lemma 10.14], we show that $V = (V_t)_{t\geqslant 0}$ is constant on every interval $[r, s] \subseteq \mathbb{R}_+$ such that $Y_r = Y_s$. First, $Y_r = Y_s$ means that $\int_r^s X_t\,\mathrm{d}t = 0$, which, due to the non-negativity of $X = (X_t)_{t\geqslant 0}$, implies that $X_t = 0$ almost everywhere on $[r, s]$. We deduce that $[r, s] \subseteq \big\{t \geqslant 0 : X_t = 0\big\}$. We thus obtain $V_t = V_r$, for all $t \in [r, s]$, proving that $V = (V_t)_{t\geqslant 0}$ is constant on every interval of this type. Hence, we can write $V_t = W_{Y_t}$, for all $t \geqslant 0$. However, $W = (W_z)_{z<Y_\infty}$ is a Lévy process only on $[\![0, Y_\infty[\![$. In line with [**RY99**, Theorem V.1.7], we can construct the stochastic process $L^\Phi = (L^\Phi_z)_{z\geqslant 0}$ where $L^\Phi_z := W_z\,\mathbf{1}_{\{z<Y_\infty\}} + L_z\,\mathbf{1}_{\{z\geqslant Y_\infty\}}$, for all $z \geqslant 0$. $L^\Phi = (L^\Phi_z)_{z\geqslant 0}$ is a Lévy process characterized by the Lévy triplet $(-b, \sigma, \pi)$, which extends $W = (W_z)_{z<Y_\infty}$ to the entire $\mathbb{R}_+$. We then have $V_t = L^\Phi_{Y_t}$, for all $t \geqslant 0$, showing that $V = (V_t)_{t\geqslant 0}$ is a time-changed Lévy process. By inserting $L^\Psi = (L^\Psi_t)_{t\geqslant 0}$ and $L^\Phi = (L^\Phi_z)_{z\geqslant 0}$ into equation (2.21), we finally obtain that $X = (X_t)_{t\geqslant 0}$ admits a Lamperti-type representation. □

Remark 2.13. [**DL12**] also introduced another representation of a $\mathrm{CBI}\big(X_0, \Psi, \Phi\big)$, which is equivalent to the Dawson–Li representation. We suppose the existence of an independent Gaussian white noise $W(\mathrm{d}t, \mathrm{d}u)$ as in [**Wal86**, Chapters 1 and 2], defined on $\mathbb{R}_+ \times \mathbb{R}_+$ and with intensity $\mathrm{d}t\,\mathrm{d}u$. Consider then the stochastic integral equation

$$\begin{aligned} X_t = X_0 &+ \int_0^t \big(\beta - b\,X_s\big)\,\mathrm{d}s + \sigma \int_0^t \int_0^{X_s} W(\mathrm{d}s, \mathrm{d}u) \\ &+ \int_0^t \int_0^{+\infty} x\,N_0(\mathrm{d}s, \mathrm{d}x) + \int_0^t \int_0^{X_{s-}} \int_0^{+\infty} x\,\widetilde{N}_1(\mathrm{d}s, \mathrm{d}u, \mathrm{d}x), \qquad \forall t \geqslant 0. \end{aligned} \tag{2.25}$$

By [**DL12**, Theorem 3.1], for any $X_0 \geqslant 0$, there exists a unique non-negative strong solution to equation (2.25), which is a $\mathrm{CBI}\big(X_0, \Psi, \Phi\big)$. The peculiarity of representation (2.25) lies in its comparison property (see e.g. [**Li20**, Theorem 8.4]), which will be the starting point in the construction of multi-curve models driven by a *flow of CBI processes* (see Chapter 3).

Remark 2.14. Stochastic integral equation (2.25) makes evident the self-exciting behavior of a $\mathrm{CBI}\big(X_0, \Psi, \Phi\big)$. Indeed, the two martingale components (i.e. the stochastic integrals with respect to W and $\widetilde{N}_1$), depend on the current value of the process itself and, therefore, large values of the process give rise to episodes of high volatility. In particular, the jump intensity of N_1 increases whenever a jump occurs, thereby generating jump clustering effects. These features will have a particularly relevant role in Chapter 3.

2.6. Examples of CBI processes

We present several examples of CBI processes that can be found in the literature. We first mention the *Cox–Ingersoll–Ross process* (CIR), which is a continuous CBI processes. We also discuss its alpha-stable extension, which is a jump-type CBI process. We derive a correspondence between CBI processes and *Hawkes processes*, which we combine with Theorem 2.12 to refine the time change Poisson representation of general point processes for the specific case of Hawkes processes. Finally, we obtain similar results for *marked Hawkes processes*.

2.6.1. The CIR process. The diffusion (17) of [**CIR85**] is widely known in the literature as the *Cox–Ingersoll–Ross process* (CIR). This process is mostly used in interest rate modeling (see [**Fil01**]), in stochastic volatility modeling (e.g. the *Heston model* by [**Hes93**]), as well as for default intensity modeling.

This process can be recovered from a $\mathrm{CBI}\big(X_0, \Psi, \Phi\big)$ by letting $b > 0$, $\nu = 0$, and $\pi = 0$, i.e. a continuous subcritical CBI process. The affine property of the joint process $(X_t, Y_t)_{t\geqslant 0}$, where $X = (X_t)_{t\geqslant 0}$ is a CIR process and where $Y_t := \int_0^t X_s \,\mathrm{d}s$ for all $t \geqslant 0$, is ensured by Lemma 2.2 where the immigration and branching mechanisms Ψ and Φ become $\Psi(x) = \beta\, x$ and $\Phi(x) = -\,b\, x + \frac{1}{2}\,(\sigma\, x)^2$, for all $x \in \mathcal{D}_1$, with $\mathcal{D}_1 = \mathbb{R}$.

For the CIR process, the Dawson-Li representation (2.21) reduces to the CIR diffusion:

$$X_t = X_0 + b \int_0^t \left(\frac{\beta}{b} - X_s\right) \mathrm{d}s + \sigma \int_0^t \sqrt{X_s}\, \mathrm{d}B_s, \qquad \forall t \geqslant 0. \tag{2.26}$$

By using Theorem 2.12, which coincides here with the Dambis–Dubins–Schwarz theorem (see e.g. [**RY99**, Theorem V.1.6]), we can derive the following time change representation of the CIR process $X = (X_t)_{t\geqslant 0}$, which is equivalent to (2.26):

$$X_t = X_0 + b \int_0^t \left(\frac{\beta}{b} - X_s\right) \mathrm{d}s + \sigma\, W_{Y_t}, \qquad \forall t \geqslant 0, \tag{2.27}$$

where $W = (W_t)_{t\geqslant 0}$ is a Brownian motion. Since $b > 0$, the mean reversion of the CIR process $X = (X_t)_{t\geqslant 0}$ holds with long-term value β/b and speed b. We also recall the *Feller condition* for the inaccessibility of 0, which takes the form $2\,\beta \geqslant \sigma^2$ (see e.g. [**Fil09**, Section 5.4.2]).

2.6.2. The α-CIR process. A natural extension of (2.26), which can be found in the literature (see [**LM15, JMS17, JMSZ21**] among others), consists in adding jumps via a Lévy-driven stochastic integral as follows:

$$X_t = X_0 + b \int_0^t \left(\frac{\beta}{b} - X_s\right) \mathrm{d}s + \sigma \int_0^t \sqrt{X_s}\, \mathrm{d}B_s + \eta \int_0^t \sqrt[\alpha]{X_s}\, \mathrm{d}Z_s, \qquad \forall t \geqslant 0, \tag{2.28}$$

where $\eta \geqslant 0$ serves as a volatility parameter for the jump part and $Z = (Z_t)_{t\geqslant 0}$ is an independent, spectrally positive compensated stable Lévy process with Lévy measure $C_\alpha\, z^{-1-\alpha}\, \mathbf{1}_{\{z>0\}}\, \mathrm{d}z$, where $\alpha \in (1, 2)$ is called *stability index* and $C_\alpha \geqslant 0$ is a normalization constant depending on α.

By [**FL10**, Corollary 6.3], there exists a unique strong solution to (2.28), which is a *stable Cox–Ingersoll–Ross process* (or *α-CIR process*) and is a jump-type CBI process with $b > 0$, $\nu = 0$, and $\pi(\mathrm{d}z) = \eta^\alpha\, C_\alpha\, z^{-1-\alpha}\, \mathbf{1}_{\{z>0\}}\, \mathrm{d}z$. Lemma 2.2 implies the affine property of the joint process

$(X_t, Y_t)_{t\geqslant 0}$ with $X = (X_t)_{t\geqslant 0}$ being an α-CIR process, where the immigration mechanism Ψ is given by $\Psi(x) = \beta\, x$ and the branching mechanism Φ by

$$\Phi(x) = -\,b\,x + \frac{1}{2}\,(\sigma\,x)^2 + C_\alpha\,\Gamma(-\alpha)\,(-\,\eta\,x)^\alpha, \qquad \forall x \in \mathcal{D}_1, \tag{2.29}$$

where Γ denotes the Gamma function extended to $\mathbb{R}\backslash\mathbb{Z}_-$ (see [**Leb72**, Section 1.1]). In this case, we have $\mathcal{D}_1 = \mathbb{R}_-$, implying that the process $X = (X_t)_{t\geqslant 0}$ does not admit finite exponential moments of any order in the sense that Theorem 2.8 yields $\mathbb{E}\big[e^{\,x\,X_T}\big] = +\infty$, for all $x > 0$ and $T > 0$.

By [**Li11**, Theorem 9.32] and [**Li20**, Theorem 8.6], if $X = (X_t)_{t\geqslant 0}$ is a $\mathrm{CBI}\big(X_0, \Psi, \Phi\big)$ with $b > 0$, $\nu = 0$, and $\pi(\mathrm{d}z) = \eta^\alpha\, C_\alpha\, z^{-1-\alpha}\, \mathbf{1}_{\{z>0\}}\,\mathrm{d}z$, then $X = (X_t)_{t\geqslant 0}$ is a weak solution to (2.28) and coincides, on an enlarged space, with the corresponding α-CIR process. By Theorem 2.12, we can obtain a time change representation of the α-CIR process, equivalent to (2.28):

$$X_t = X_0 + b\int_0^t \left(\frac{\beta}{b} - X_s\right)\mathrm{d}s + \sigma\, W_{Y_t} + \eta\, L_{Y_t}, \qquad \forall t \geqslant 0, \tag{2.30}$$

where $W = (W_t)_{t\geqslant 0}$ is a Brownian motion and $L = (L_t)_{t\geqslant 0}$ is a compensated, spectrally positive stable Lévy process with Lévy measure $C_\alpha\, z^{-1-\alpha}\, \mathbf{1}_{\{z>0\}}\,\mathrm{d}z$. These two processes are taken independent of each other (a similar representation was derived by [**JMSZ21**] by relying on [**KS02b**, Theorems 2 and 3]). Finally, it has been shown in [**JMS17**, Proposition 3.4], by relying on the results of [**FUB14, DFM14**] for general CBI processes, that the Feller condition for the α-CIR process is identical to that of the CIR process recalled above, i.e. $2\,\beta \geqslant \sigma^2$.

2.6.3. The Hawkes process. First introduced by [**Haw71, HO74**], and extensively used in finance (see e.g. [**Haw18**]), a *Hawkes process*[1] is a counting process $(N_t)_{t\geqslant 0}$ whose intensity $X = (X_t)_{t\geqslant 0}$ satisfies the following stochastic integral equation:

$$X_t = X_0 + \kappa\int_0^t \big(\lambda - X_s\big)\,\mathrm{d}s + \eta\, N_t, \qquad \forall t \geqslant 0, \tag{2.31}$$

where we fix $\lambda = X_0$ for simplicity. By Itô's formula, this equation can be solved as follows:

$$X_t = X_0 + \eta\int_0^t e^{\,-\,\kappa\,(t-s)}\,\mathrm{d}N_s, \qquad \forall t \geqslant 0. \tag{2.32}$$

We denote the couple (X, N) by $\mathrm{Hawkes}\big(X_0, \kappa, \eta\big)$, where we suppose that $\kappa > \eta$ always holds. This is known in the literature on Hawkes processes as the *stability condition*, ensuring the finite activity of the process together with its long-run stability (see e.g. [**BM96, DFZ14**]).

Equation (2.32) makes clear the self-exciting behavior of $(N_t)_{t\geqslant 0}$ as follows: its intensity at time t, for all $t \geqslant 0$, is an affine function of the events of the counting process that occurred before t, where $\eta \geqslant 0$ serves as a volatility parameter measuring the contribution of the self-excitation, while $\kappa > 0$ controls the dampening, over time, of the effect of the past events. Note that when $\eta = 0$, the process $(N_t)_{t\geqslant 0}$ reduces to a Poisson process with constant intensity $X \equiv X_0$.

The next result, which extends [**BS20**, Proposition 7.2], provides a correspondence between (subcritical) CBI processes and Hawkes processes as defined above.

[1] We restrict our attention to univariate Hawkes processes with single-factor exponentially-decaying intensity, i.e. setting $g(v) = \eta\, e^{\,-\,\kappa\, v}$, $\forall v \geqslant 0$, with $\kappa > 0$ and $\eta \geqslant 0$ in the notation of [**Haw71**, Section 3].

PROPOSITION 2.15. *The following implications hold:*

(i) *Let* $X = (X_t)_{t\geqslant 0}$ *be a* $\mathrm{CBI}\big(X_0, \Psi, \Phi\big)$. *If* $b > 0$, $\sigma = 0$, $\nu = 0$, $\pi = \delta_\eta$ *with* $\eta > 0$, *and* $X_0 = \frac{\beta}{b+\eta}$, *then there exists a counting process* $(N_t)_{t\geqslant 0}$ *with intensity* $X = (X_t)_{t\geqslant 0}$ *such that* (X, N) *is a* $\mathrm{Hawkes}\big(\frac{\beta}{b+\eta}, b+\eta, \eta\big)$;

(ii) *Let* (X, N) *be a* $\mathrm{Hawkes}\big(X_0, \kappa, \eta\big)$ *with* $\eta > 0$. *Then,* $X = (X_t)_{t\geqslant 0}$ *is a* $\mathrm{CBI}\big(X_0, \Psi, \Phi\big)$ *with* $\beta = \kappa\, X_0$, $b = \kappa - \eta$, $\sigma = 0$, $\nu = 0$, *and* $\pi = \delta_\eta$.

PROOF. The first implication follows along the lines of [**BS20**, Proposition 7.2]. Starting from the Dawson–Li representation, we fix $b > 0$, $\sigma = 0$, $\nu = 0$, and $\pi = \delta_\eta$, where δ_η is the Dirac measure at $\eta > 0$. The stochastic integral with respect to $\widetilde{N}_1$ then becomes

$$\int_0^t \int_0^{X_{s-}} \int_0^{+\infty} x\, \widetilde{N}_1(\mathrm{d}s, \mathrm{d}u, \mathrm{d}x) = \eta \int_0^t \int_0^{X_{s-}} \widetilde{N}_1(\mathrm{d}s, \mathrm{d}u), \qquad \forall t \geqslant 0,$$

where $N_1(\mathrm{d}t, \mathrm{d}u)$ is a Poisson random measure on $\mathbb{R}_+ \times \mathbb{R}_+$ with compensator $\mathrm{d}t\,\mathrm{d}u$ and compensated measure $\widetilde{N}_1(\mathrm{d}t, \mathrm{d}u) := N_1(\mathrm{d}t, \mathrm{d}u) - \mathrm{d}t\,\mathrm{d}u$. In this case, we can separate the pure jump integral from its compensator, which gives

$$X_t = X_0 + \big(b+\eta\big) \int_0^t \left(\frac{\beta}{b+\eta} - X_s\right) \mathrm{d}s + \eta \int_0^t \int_0^{X_{s-}} N_1(\mathrm{d}s, \mathrm{d}u), \qquad \forall t \geqslant 0.$$

Fixing now $X_0 = \frac{\beta}{b+\eta}$ and defining the counting process $(N_t)_{t\geqslant 0}$ as $N_t := \int_0^t \int_0^{X_{s-}} N_1(\mathrm{d}s, \mathrm{d}u)$, for all $t \geqslant 0$, whose intensity clearly coincides with $X = (X_t)_{t\geqslant 0}$, we recover equations (2.31) and (2.32) by Itô's formula, which provides the couple (X, N) with the Hawkes property.

We prove the second assertion. Let (X, N) be a Hawkes(X_0, κ, η) with $\eta > 0$. We rewrite equation (2.31) by means of the measure $N(\mathrm{d}t, \mathrm{d}x)$ with compensator $X_{t-}\,\mathrm{d}t\,\delta_\eta(\mathrm{d}x)$, as follows:

$$X_t = X_0 + \int_0^t \Big(\kappa\, X_0 - \big(\kappa - \eta\big)\, X_s\Big)\, \mathrm{d}s + \int_0^t \int_0^{+\infty} x \Big(N(\mathrm{d}s, \mathrm{d}x) - X_{s-}\, \mathrm{d}s\, \delta_\eta(\mathrm{d}x)\Big), \qquad \forall t \geqslant 0.$$

By using [**IW89**, Theorem II.7.4], possibly on an extension of the probability space, there exists a Poisson random measure $N_1(\mathrm{d}t, \mathrm{d}u, \mathrm{d}x)$ with compensator $\mathrm{d}t\,\mathrm{d}u\,\delta_\eta(\mathrm{d}x)$ and compensated measure $\widetilde{N}_1(\mathrm{d}t, \mathrm{d}u, \mathrm{d}x) := N_1(\mathrm{d}t, \mathrm{d}u, \mathrm{d}x) - \mathrm{d}t\,\mathrm{d}u\,\delta_\eta(\mathrm{d}x)$ such that we have

$$X_t = X_0 + \int_0^t \Big(\kappa\, X_0 - \big(\kappa - \eta\big)\, X_s\Big)\, \mathrm{d}s + \int_0^t \int_0^{X_{s-}} \int_0^{+\infty} x\, \widetilde{N}_1(\mathrm{d}t, \mathrm{d}u, \mathrm{d}x), \qquad \forall t \geqslant 0.$$

Therefore, $X = (X_t)_{t\geqslant 0}$ has a Dawson–Li representation with $\beta = \kappa\, X_0$, $b = \kappa - \eta$, $\sigma = 0$, $\nu = 0$, and $\pi = \delta_\eta$, and thus [**Li11**, Theorem 9.31] and [**Li20**, Theorem 8.1] yield the desired result. □

It is well-known in point process theory that any counting process, under mild conditions on its compensator, can be represented by a time-changed Poisson process with unit intensity (see [**DVJ08**, Theorem 7.4.I] for the general theorem and [**GT05**] for the converse). We now refine this result for the specific case of Hawkes processes by relying on CBI processes. More precisely, we provide a self-contained proof that only makes use of Proposition 2.15 and Theorem 2.12.

COROLLARY 2.16. *Let* (X, N) *be a* Hawkes(X_0, κ, η). *Then, there exists a unit-intensity Poisson process* $N' = (N'_t)_{t\geqslant 0}$ *such that* $N_t = N'_{Y_t}$ *where* $Y_t := \int_0^t X_s\, \mathrm{d}s$, *for all* $t \geqslant 0$.

PROOF. Let (X, N) be a Hawkes$\big(X_0, \kappa, \eta\big)$. We now distinguish two cases. The first one is trivial and reduces to $\eta = 0$, when $N = (N_t)_{t\geqslant 0}$ degenerates into a Poisson process with constant intensity $X \equiv X_0$. The desired result then follows from the time-rescaling theorem in its most basic form, i.e. relating inhomogeneous Poisson processes to (deterministic) time-changed homogeneous Poisson processes: $N_t = N'_{X_0\, t} = N'_{Y_t}$, where $N' = (N'_t)_{t\geqslant 0}$ is a Poisson process with unit intensity.

Let $\eta > 0$. By using the second assertion of Proposition 2.15, the process $X = (X_t)_{t\geqslant 0}$ is a CBI$\big(X_0, \Psi, \Phi\big)$ with $\beta = \kappa\, X_0$, $b = \kappa - \eta$, $\sigma = 0$, $\nu = 0$, and $\pi = \delta_\eta$. By [**Li11**, Theorem 9.31] and [**Li20**, Theorem 8.1], $X = (X_t)_{t\geqslant 0}$ admits a Dawson–Li representation, which is weakly equivalent to the Lamperti-type representation by Theorem 2.12. Without loss of generality, we can suppose that the stochastic basis already supports two independent Lévy processes $L^\Psi = (L^\Psi_t)_{t\geqslant 0}$ and $L^\Phi = (L^\Phi_t)_{t\geqslant 0}$ such that $X_t = X_0 + L^\Psi_t + L^\Phi_{Y_t}$, for all $t \geqslant 0$. By applying the Lévy-Itô decomposition, and then inserting the parameters specified above, we obtain

$$\begin{aligned} L^\Psi_t &= \kappa\, X_0\, t, \qquad \forall t \geqslant 0, \\ L^\Phi_t &= \big(\eta - \kappa\big)\, t + \int_0^t \int_0^{+\infty} x\, \widetilde{N}'(\mathrm{d}s, \mathrm{d}x), \qquad \forall t \geqslant 0, \end{aligned}$$

where $N'(\mathrm{d}t, \mathrm{d}x)$ is a Poisson random measure defined on $\mathbb{R}_+ \times \mathbb{R}_+$ with compensator $\mathrm{d}t\, \delta_\eta(\mathrm{d}x)$ and compensated measure $\widetilde{N}'(\mathrm{d}t, \mathrm{d}x) := N'(\mathrm{d}t, \mathrm{d}x) - \mathrm{d}t\, \delta_\eta(\mathrm{d}x)$. Similarly to Proposition 2.15, the stochastic integral with respect to $\widetilde{N}'$ reduces to

$$\int_0^t \int_0^{+\infty} x\, \widetilde{N}'(\mathrm{d}s, \mathrm{d}x) = \eta\, \widetilde{N}'_t, \qquad \forall t \geqslant 0,$$

where $N' = (N'_t)_{t\geqslant 0}$ is a unit-intensity Poisson process with compensated version $\widetilde{N}'_t := N'_t - t$, for all $t \geqslant 0$. Hence, by inserting both Lévy processes $L^\Psi = (L^\Psi_t)_{t\geqslant 0}$ and $L^\Phi = (L^\Phi_t)_{t\geqslant 0}$ into the Lamperti-type representation of $X = (X_t)_{t\geqslant 0}$, we can rewrite it as follows:

$$X_t = X_0 + \kappa \int_0^t \big(X_0 - X_s\big)\, \mathrm{d}s + \eta\, N'_{Y_t},$$

where we finally identify $N_t = N'_{Y_t}$ by (2.31), for all $t \geqslant 0$. □

2.6.4. The marked Hawkes process. The previous results can be readily extended to the class of *marked Hawkes processes*, whose terminology is taken from [**BSS18**] (see also [**DVJ08**, Section 6.4] for general marked point processes), obtained by randomizing η as follows:

$$X_t = X_0 + \kappa \int_0^t \big(X_0 - X_s\big)\, \mathrm{d}s + \int_0^t \int_0^{+\infty} x\, N(\mathrm{d}s, \mathrm{d}x), \qquad \forall t \geqslant 0, \tag{2.33}$$

which, through Itô's formula, can be solved by

$$X_t = X_0 + \int_0^t \int_0^{+\infty} x\, e^{-\kappa\,(t-s)}\, N(\mathrm{d}s, \mathrm{d}x), \qquad \forall t \geqslant 0. \tag{2.34}$$

The counting measure $N(\mathrm{d}t, \mathrm{d}x)$, whose compensator is $X_{t-}\, \mathrm{d}t\, \mu(\mathrm{d}x)$ where μ is a probability distribution on $\mathbb{R}_+$ with finite first moment, generates two different processes that share the same stochastic intensity $X = (X_t)_{t\geqslant 0}$:

- The *marked Hawkes process* denoted by the counting process $N_t := \int_0^t \int_0^{+\infty} N(\mathrm{d}s, \mathrm{d}x)$, for all $t \geqslant 0$;
- The *compound Hawkes process* defined by $M_t := \int_0^t \int_0^{+\infty} x\, N(\mathrm{d}s, \mathrm{d}x)$, for all $t \geqslant 0$.

We refer to [**BSS18**] and [**Swi21, SZZ21**] for further details on marked Hawkes processes and compound Hawkes processes, respectively. In this case, the stability condition becomes $\kappa > m$, where $m := \int_0^{+\infty} x\, \mu(\mathrm{d}x)$ (see e.g. [**DVJ08**, Proposition 6.4.VII]).

We now extend Proposition 2.15 and Corollary 2.16 to marked Hawkes processes. We first derive a correspondence between (subcritical) CBI processes and marked Hawkes process. Then, we refine the representation of compound Hawkes processes as time-changed compound Poisson processes by providing a self-contained proof that only relies on the theory of CBI processes.

Corollary 2.17. *The following implications hold:*

(i) *Let $X = (X_t)_{t\geqslant 0}$ be a $\mathrm{CBI}\big(X_0, \Psi, \Phi\big)$. If $b > 0$, $\sigma = 0$, $\nu = 0$, π a probability distribution on $\mathbb{R}_+$ with finite first moment m, and $X_0 = \frac{\beta}{b+m}$, then there exists a counting process $(N_t)_{t\geqslant 0}$ with intensity $X = (X_t)_{t\geqslant 0}$ such that $(N_t)_{t\geqslant 0}$ is a marked Hawkes process with $X_0 = \frac{\beta}{b+m}$, $\kappa = b + m$, and $\mu = \pi$;*

(ii) *Let $(N_t)_{t\geqslant 0}$ be a marked Hawkes process and $M = (M_t)_{t\geqslant 0}$ be a compound Hawkes process with intensity $X = (X_t)_{t\geqslant 0}$. Then, there exists a unit-intensity compound Poisson process $M' = (M'_t)_{t\geqslant 0}$ with mark distribution μ such that $M_t = M'_{Y_t}$ where $Y_t := \int_0^t X_s\, \mathrm{d}s$, for all $t \geqslant 0$, and where $X = (X_t)_{t\geqslant 0}$ is a $\mathrm{CBI}\big(X_0, \Psi, \Phi\big)$ with $\beta = \kappa\, X_0$, $b = \kappa - m$, $\sigma = 0$, $\nu = 0$, and $\pi = \mu$.*

Proof. The proof of the first assertion follows along the lines of the first part of the proof of Proposition 2.15. We first rewrite the Dawson–Li representation of $X = (X_t)_{t\geqslant 0}$ with $b > 0$, $\sigma = 0$, $\nu = 0$, and π is a probability distribution on $\mathbb{R}_+$ with finite first moment $m := \int_0^{+\infty} x\, \pi(\mathrm{d}x) < +\infty$. We then separate the pure jump integral from its compensator, which gives

$$X_t = X_0 + \big(b + m\big) \int_0^t \left(\frac{\beta}{b+m} - X_s \right) \mathrm{d}s + \int_0^t \int_0^{X_{s-}} \int_0^{+\infty} x\, N_1(\mathrm{d}s, \mathrm{d}u, \mathrm{d}x), \qquad \forall t \geqslant 0,$$

We finally fix $X_0 = \frac{\beta}{b+\eta}$ and define the counting process $N_t := \int_0^t \int_0^{X_{s-}} \int_0^{+\infty} N_1(\mathrm{d}s, \mathrm{d}u, \mathrm{d}x)$, for all $t \geqslant 0$, whose intensity is $X = (X_t)_{t\geqslant 0}$, thus showing that $N = (N_t)_{t\geqslant 0}$ is a marked Hawkes process.

The proof of the converse is similar to the second part of the proof of Proposition 2.15. We start by inserting the first moment m of the distribution μ into (2.33) as follows:

$$X_t = X_0 + \int_0^t \Big(\kappa\, X_0 - \big(\kappa - m\big)\, X_s \Big)\, \mathrm{d}s + \int_0^t \int_0^{+\infty} x \Big(N(\mathrm{d}s, \mathrm{d}x) - X_{s-}\, \mathrm{d}s\, \mu(\mathrm{d}x) \Big), \qquad \forall t \geqslant 0.$$

We then use [**IW89**, Theorem II.7.4], which ensures, possibly on an enlarged probability space, the existence of a Poisson random measure $N_1(\mathrm{d}t, \mathrm{d}u, \mathrm{d}x)$ with compensator $\mathrm{d}t\, \mathrm{d}u\, \mu(\mathrm{d}x)$ and compensated measure $\widetilde{N}_1(\mathrm{d}t, \mathrm{d}u, \mathrm{d}x) := N_1(\mathrm{d}t, \mathrm{d}u, \mathrm{d}x) - \mathrm{d}t\, \mathrm{d}u\, \mu(\mathrm{d}x)$ such that

$$X_t = X_0 + \int_0^t \Big(\kappa\, X_0 - \big(\kappa - m\big)\, X_s \Big)\, \mathrm{d}s + \int_0^t \int_0^{X_{s-}} \int_0^{+\infty} x\, \widetilde{N}_1(\mathrm{d}t, \mathrm{d}u, \mathrm{d}x), \qquad \forall t \geqslant 0.$$

[**Li11**, Theorem 9.31] and [**Li20**, Theorem 8.1] therefore provide the CBI property of $X = (X_t)_{t\geqslant 0}$.

At this point, we can apply Theorem 2.12 as in the proof of Corollary 2.16, which yields the Lamperti-type representation of $X = (X_t)_{t\geqslant 0}$ as follows:

$$X_t = X_0 + \kappa \int_0^t \big(X_0 - X_s\big)\,\mathrm{d}s + \int_0^{Y_t}\int_0^{+\infty} x\, M'(\mathrm{d}s, \mathrm{d}x), \qquad \forall t \geqslant 0,$$

where $Y_t := \int_0^t X_s\,\mathrm{d}s$, for all $t \geqslant 0$, and $M'(\mathrm{d}t, \mathrm{d}x)$ is a Poisson random measure defined on $\mathbb{R}_+ \times \mathbb{R}_+$ with compensator $\mathrm{d}t\,\mu(\mathrm{d}x)$. Let us now define the stochastic process $M' = (M'_t)_{t\geqslant 0}$ by $M'_t := \int_0^t \int_0^{+\infty} x\, M'(\mathrm{d}s, \mathrm{d}x)$, for all $t \geqslant 0$. $M' = (M'_t)_{t\geqslant 0}$ is then a unit-intensity compound Poisson process with mark law μ such that $M_t = M'_{Y_t}$ by (2.33), for all $t \geqslant 0$. □

2.7. Tempered-stable CBI processes

We recall that when $X = (X_t)_{t\geqslant 0}$ is an α-CIR process with $\alpha \in (1, 2)$, Theorem 2.8 yields $\mathbb{E}\big[e^{\,x\,X_T}\big] = +\infty$, for all $x > 0$ and $T > 0$. This represents a drawback of the class of α-CIR processes in view of the modeling of Chapter 3, where the finiteness of exponential moments will represent an indispensable requirement. In order to overcome this issue, we develop a new specification of the CBI process that we name *tempered-stable CBI process*. This process can be constructed either from an α-CIR process by means of an equivalent change of probability (see e.g. [**JMS17**, Proposition 4.1]), or as a solution to a certain stochastic time change equation. Let us proceed with the latter approach.

To this purpose, the stochastic basis $\big(\Omega, \mathcal{F}, \mathbb{F}, \mathbb{Q}\big)$ is supposed to be equipped with the following two independent stochastic processes:

- A standard Brownian motion $W = (W_t)_{t\geqslant 0}$;
- A compensated, spectrally positive tempered-stable Lévy process $L = (L_t)_{t\geqslant 0}$ with Lévy measure $C_\alpha\, z^{-1-\alpha}\, e^{-\theta\, z}\, \mathbf{1}_{\{z>0\}}\,\mathrm{d}z$, where $C_\alpha \geqslant 0$, $\theta > 0$ and $\alpha < 2$ (or $\theta = 0$ and $\alpha \in (1, 2)$).

Definition 2.18. A non-negative càdlàg stochastic process $X = (X_t)_{t\geqslant 0}$ with initial value X_0 is said to be a *tempered-stable CBI process* if it satisfies the stochastic time change equation

$$X_t = X_0 + \int_0^t \big(\beta - b\, X_s\big)\,\mathrm{d}s + \sigma\, W_{Y_t} + \eta\, L_{Y_t}, \qquad \forall t \geqslant 0, \tag{2.35}$$

where $Y_t := \int_0^t X_s\,\mathrm{d}s$, for all $t \geqslant 0$, $b \in \mathbb{R}$, $\beta \geqslant 0$, $\sigma \geqslant 0$, and $\eta \geqslant 0$.

The stochastic time change equation (2.35) is obtained by extending equation (2.30) as follows:

(i) The positivity constraint of the parameter b is relaxed:
(ii) The jumps of the stable process are tempered exponentially via the parameter θ;
(iii) The stable-type behavior of the jumps is preserved and still controlled by α.

A tempered-stable CBI process in the sense of Definition 2.18 cannot be represented by a Lévy-driven stochastic integral equation in the form of (2.28), which contrasts with an α-CIR process. This is due to the fact that the symmetry/self-similarity property of the stable process is not preserved by the exponential tempering.

The exponential tempering enables the Lévy process $L = (L_t)_{t\geqslant 0}$ to have finite moments of any order (see e.g. [**CT04**, Section 4.5]), regardless of the value of α. Moreover, it also allows α to

be extended to the whole $\mathbb{R}_-$, where the interval in which the value of α lies determines the path properties of the process $L = (L_t)_{t\geqslant 0}$ as follows:

(i) If $\alpha < 0$, then $L = (L_t)_{t\geqslant 0}$ is a compensated compound Poisson process;
(ii) If $\alpha \in [0, 1)$, then $L = (L_t)_{t\geqslant 0}$ has infinite activity and finite variation;
(iii) If $\alpha \in [1, 2)$, then $L = (L_t)_{t\geqslant 0}$ has infinite activity and infinite variation.

We rely on the findings of [**CW03**] and [**Orn14**] and set $\alpha \in [0, 2)$. However, in view of not limiting ourselves to Lévy processes with finite variation, we shall focus on $\alpha \in (1, 2)$ (while excluding $\alpha = 1$ for simplicity).

We fix $\eta > 0$, where we recall that η serves as a volatility parameter for the jump part (see Section 2.6.2). By [**ECPGUB13**, Proposition 2 and Theorem 2], there exists a unique non-negative strong solution to equation (2.35) for any $X_0 \geqslant 0$, which is a $\mathrm{CBI}\big(X_0, \Psi, \Phi\big)$ with Lévy measures $\nu = 0$ and $\pi(\mathrm{d}z) = \eta^\alpha\, C_\alpha\, z^{-1-\alpha}\, e^{-\frac{\theta}{\eta}\, z}\, \mathbf{1}_{\{z>0\}}\, \mathrm{d}z$. In this regard, for a tempered-stable CBI process in the sense of Definition 2.18, we have $\mathcal{D}_1 = (-\infty, \theta/\eta]$. Indeed, for all $x \in \mathbb{R}$, $x \in \mathcal{D}_1$ if and only if $\int_1^{+\infty} z^{-1-\alpha}\, e^{\,(x-\theta/\eta)\, z}\, \mathrm{d}z < +\infty$, which holds true if and only if $x \leqslant \theta/\eta$. Since $\nu = 0$, the immigration mechanism Ψ of a tempered-stable CBI process reduces to $\Psi(x) = \beta\, x$. The branching mechanism Φ is explicitly described in the following lemma.

Lemma 2.19. *For $\eta > 0$, $C_\alpha \geqslant 0$, $\theta \geqslant 0$, and $\alpha \in (1, 2)$, the branching mechanism Φ of a tempered-stable CBI process is explicitly given by*

$$\Phi(x) = -\,b\, x + \frac{1}{2}\,(\sigma\, x)^2 + C_\alpha\, \Gamma(-\alpha)\Big(\big(\theta - \eta\, x\big)^\alpha - \theta^\alpha + \alpha\, \theta^{\alpha-1}\, \eta\, x\Big), \tag{2.36}$$

for all $x \leqslant \theta/\eta$. Moreover, the branching mechanism Φ is non-increasing with respect to the tempering parameter θ, and Assumption 2.4 is satisfied.

Proof. Let us first consider the case $\theta = 0$, which amounts to $\pi(\mathrm{d}z) = \eta^\alpha\, C_\alpha\, z^{-1-\alpha}\, \mathbf{1}_{\{z>0\}}\, \mathrm{d}z$. This corresponds to a non-tempered stable CBI process in the sense of Section 2.6.2, whose branching mechanism Φ is given by

$$\Phi(x) = -\,b\, x + \frac{1}{2}\,(\sigma\, x)^2 + C_\alpha\, \Gamma(-\alpha)\,(-\,\eta\, x)^\alpha, \qquad \forall x \leqslant 0.$$

Henceforth, consider $\theta > 0$. Our starting point is the integral appearing in (2.2), where we replace the exponential $e^{\,x\, z}$ with its Maclaurin series:

$$\int_0^{+\infty} \big(e^{\,x\, z} - 1 - x\, z\big)\, \pi(\mathrm{d}z) = \eta^\alpha\, C_\alpha \int_0^{+\infty} \sum_{n=2}^{+\infty} \frac{(xz)^n}{n!}\, z^{-1-\alpha}\, e^{-\frac{\theta}{\eta}\, z}\, \mathrm{d}z,$$

for all $x \leqslant \theta/\eta$. By restricting x such that $|x| < \theta/\eta$, we can apply Fubini's theorem to interchange summation and integration:

$$\eta^\alpha\, C_\alpha \int_0^{+\infty} \sum_{n=2}^{+\infty} \frac{(xz)^n}{n!}\, z^{-1-\alpha}\, e^{-\frac{\theta}{\eta}\, z}\, \mathrm{d}z = \theta^\alpha\, C_\alpha \sum_{n=2}^{+\infty} \frac{(\eta\, x/\theta)^n}{n!} \int_0^{+\infty} z^{n-\alpha-1}\, e^{-z}\, \mathrm{d}z.$$

By using the Gamma function, we can write

$$\theta^\alpha\, C_\alpha \sum_{n=2}^{+\infty} \frac{(\eta\, x/\theta)^n}{n!} \int_0^{+\infty} z^{n-\alpha-1}\, e^{-z}\, \mathrm{d}z = \theta^\alpha\, C_\alpha \sum_{n=2}^{+\infty} \frac{(\eta\, x/\theta)^n}{n!}\, \Gamma(n-\alpha),$$

which is well defined for every $n \geqslant 2$ since $\alpha \in (1,2)$. At this point, by inserting, for every $n \geqslant 2$, $\Gamma(n-\alpha) = (-1)^n\, n!\, \binom{\alpha}{n}\, \Gamma(-\alpha)$ into the expression above, where $\binom{\alpha}{n}$ denotes the generalized binomial coefficient, we obtain

$$\theta^\alpha\, C_\alpha \sum_{n=2}^{+\infty} \frac{(\eta\, x/\theta)^n}{n!}\, \Gamma(n-\alpha) = \theta^\alpha\, C_\alpha\, \Gamma(-\alpha) \sum_{n=2}^{+\infty} \binom{\alpha}{n} \Big(-\frac{\eta\, x}{\theta}\Big)^n.$$

We can identify the binomial series associated to the Maclaurin series expansion of the function $x \mapsto (1+x)^\alpha$, whose convergence is ensured when $|x| < 1$. Therefore:

$$\theta^\alpha\, C_\alpha\, \Gamma(-\alpha) \sum_{n=2}^{+\infty} \binom{\alpha}{n} \Big(-\frac{\eta\, x}{\theta}\Big)^n = C_\alpha\, \Gamma(-\alpha) \Big(\big(\theta - \eta\, x\big)^\alpha - \theta^\alpha + \alpha\, \theta^{\alpha-1}\, \eta\, x \Big).$$

The branching mechanism Φ is then given by

$$\Phi(x) = -\, b\, x + \frac{1}{2}\, (\sigma\, x)^2 + C_\alpha\, \Gamma(-\alpha) \Big(\big(\theta - \eta\, x\big)^\alpha - \theta^\alpha + \alpha\, \theta^{\alpha-1}\, \eta\, x \Big),$$

for all x such that $|x| < \theta/\eta$. We can then continuously extend the function Φ to the whole interval $\mathcal{D}_1 = (-\infty, \theta/\eta]$. Now, by computing the derivative of $\Phi(x)$ with respect to the tempering parameter θ, we have

$$\frac{\partial \Phi(x)}{\partial \theta} = \alpha\, \theta^{\alpha-1}\, C_\alpha\, \Gamma(-\alpha) \left(\Big(1 - \frac{\eta}{\theta}\, x\Big)^{\alpha-1} - 1 + \big(\alpha - 1\big)\, \frac{\eta}{\theta}\, x \right).$$

By recalling that $\Gamma(-\alpha) > 0$ when $\alpha \in (1,2)$, and using Bernoulli's inequality, which here takes the form $\big(1 - \eta\, x/\theta\big)^{\alpha-1} \leqslant 1 - (\alpha-1)\, \eta\, x/\theta$, it then holds that $\frac{\partial \Phi(x)}{\partial \theta} \leqslant 0$, implying that Φ is non-increasing with respect to the tempering parameter θ. Finally, we can differentiate the function Φ on the open interval $(-\infty, \theta/\eta)$ as follows:

$$\Phi'(x) = -\, b + \sigma^2\, x + \alpha\, \eta\, C_\alpha\, \Gamma(-\alpha) \left(\theta^{\alpha-1} - \big(\theta - \eta\, x\big)^{\alpha-1} \right),$$

for all $x < \theta/\eta$, which proves to be finite when $x = \theta/\eta$, thus verifying Assumption 2.4. □

We show that the well-known Feller condition for CIR processes (see Sections 2.6.1 and 2.6.2), applies with the same form to tempered-stable CBI process. We rely on [**JMS17**, Proposition 3.4], where an analogous result was obtained for the α-CIR process. In particular, we exploit the non-increasing behavior of the branching mechanism Φ with respect to θ.

PROPOSITION 2.20. *Let $X = (X_t)_{t \geqslant 0}$ be a tempered-stable CBI process with $\eta \geqslant 0$, $C_\alpha \geqslant 0$, $\theta \geqslant 0$, and $\alpha \in (1,2)$. Then, 0 is inaccessible by the process $X = (X_t)_{t \geqslant 0}$ if and only if $2\, \beta \geqslant \sigma^2$.*

PROOF. Throughout this proof, we use the techniques of [**FUB14**, Corollary 6] and [**DFM14**, Theorem 2] for general CBI processes. First, there exist two trivial cases: $\eta = 0$, which corresponds to a CIR process and where the Feller condition is given by $2\, \beta \geqslant \sigma^2$. The second case is $\theta = 0$, which is a non-tempered stable CBI process (weakly equivalent to an α-CIR process), and for which [**JMS17**, Proposition 3.4] shows that the Feller condition takes the form $2\, \beta \geqslant \sigma^2$.

Let us now set $\eta > 0$ and $\theta > 0$. We start by exploiting the non-increasing behavior of the branching mechanism Φ with respect to θ by writing $\Phi^{\alpha-\mathrm{CIR}} \geqslant \Phi$, where $\Phi^{\alpha-\mathrm{CIR}}$ corresponds to the non-tempered case $\theta = 0$ given by (2.29). Next, by Bernoulli's inequality, we have $\Phi \geqslant \Phi^{\mathrm{CIR}}$,

where Φ^{CIR} denotes the branching mechanism of a CIR process given by $\Phi(x) = -b\,x + \frac{1}{2}(\sigma\,x)^2$. Define, for some $\rho < 0$ such that $\Phi(x) > 0$ for all $x \leqslant \rho$ by convexity of Φ, the quantity

$$\Xi\big(\Phi\big) := \int_{-\infty}^{\rho} \exp\left(\int_x^{\rho} \frac{-\Psi(y)}{\Phi(y)}\,\mathrm{d}y\right) \frac{\mathrm{d}x}{\Phi(x)}.$$

where we recall that $\Psi(x) = \beta\,x$, for all $x \leqslant \theta/\eta$, which is non-decreasing on $\mathcal{D}_1$. By [**FUB14**, Corollary 6] and [**DFM14**, Theorem 2], $\Xi(\Phi) = \infty$ if and only if 0 is inaccessible by the CBI process $X = (X_t)_{t\geqslant 0}$ associated to the branching mechanism Φ. Therefore, in view of inequality $\Phi^{\alpha-\mathrm{CIR}} \geqslant \Phi \geqslant \Phi^{\mathrm{CIR}}$, we can write

$$\Xi\big(\Phi^{\alpha-\mathrm{CIR}}\big) \leqslant \Xi\left(\Phi\right) \leqslant \Xi\big(\Phi^{\mathrm{CIR}}\big).$$

First, if $2\,\beta \geqslant \sigma^2$, then by [**JMS17**, Proposition 3.4], 0 is inaccessible by the α-CIR process of branching mechanism $\Phi^{\alpha-\mathrm{CIR}}$, which gives $\Xi\big(\Phi^{\alpha-\mathrm{CIR}}\big) = \infty$ and $\Xi\big(\Phi\big) = \infty$ as well. Hence, 0 is also inaccessible for the tempered-stable CBI process $X = (X_t)_{t\geqslant 0}$. Conversely, if 0 is inaccessible for $X = (X_t)_{t\geqslant 0}$, then $\Xi\big(\Phi\big) = \infty$, yielding $\Xi\big(\Phi^{\mathrm{CIR}}\big) = \infty$. In this case, given that Φ^{CIR} is the branching mechanism of a CIR process, we have $2\,\beta \geqslant \sigma^2$, which finally concludes the proof. □

The next proposition provides a simple necessary and sufficient condition on the parameter b for the finiteness of the exponential moment $\mathbb{E}\big[e^{\,x_1\,X_T\,+\,x_2\,Y_T}\big]$, for all $x_1 \leqslant \theta/\eta$, $x_2 \leqslant 0$, and $T > 0$, where $X = (X_t)_{t\geqslant 0}$ is a tempered-stable CBI process and $Y_t := \int_0^t X_s\,\mathrm{d}s$, for all $t \geqslant 0$.

Proposition 2.21. *Let $X = (X_t)_{t\geqslant 0}$ be a tempered-stable CBI process with $\eta > 0$, $C_\alpha > 0$, $\theta > 0$, and $\alpha \in (1,2)$. Then, we have $\mathbb{E}\big[e^{\,x_1\,X_T\,+\,x_2\,Y_T}\big] < +\infty$, for all $x_1 \leqslant \theta/\eta$, $x_2 \leqslant 0$, and $T > 0$, if and only if $b \geqslant \frac{1}{2}\,\sigma^2\,\frac{\theta}{\eta} + \eta\,C_\alpha\,\Gamma(-\alpha)\,\theta^{\alpha-1}\,(\alpha-1)$.*

Proof. It suffices to apply Corollary 2.9 to the tempered-stable CBI process $X = (X_t)_{t\geqslant 0}$, knowing that Assumption 2.4 is satisfied by Lemma 2.19. It then yields $\mathbb{E}\big[e^{\,x_1\,X_T\,+\,x_2\,Y_T}\big] < +\infty$, for all $x_1 \leqslant \theta/\eta$, $x_2 \leqslant 0$, and $T > 0$, if and only if $\Phi(\theta/\eta) \leqslant 0$, where Φ is given by (2.36). By computing $\Phi(\theta/\eta)$, we can recover the equivalence: $\Phi(\theta/\eta) \leqslant 0 \iff b \geqslant \frac{1}{2}\,\sigma^2\,\frac{\theta}{\eta} + \eta\,C_\alpha\,\Gamma(-\alpha)\,\theta^{\alpha-1}\,(\alpha-1)$. □

Remark 2.22. By combining Remark 2.7 with Proposition 2.21, for a tempered-stable CBI process $X = (X_t)_{t\geqslant 0}$ where $b \geqslant \frac{1}{2}\,\sigma^2\,\frac{\theta}{\eta} + \eta\,C_\alpha\,\Gamma(-\alpha)\,\theta^{\alpha-1}\,(\alpha-1)$, we also obtain the finiteness of the complex exponential moment $\mathbb{E}\big[e^{\,u_1\,X_T\,+\,u_2\,Y_T}\big]$, for all $u_1 \in \mathbb{C}$ such that $\mathrm{Re}(u_1) < \theta/\eta$, $u_2 \in \mathbb{C}_-$, and $T > 0$. Indeed, the extension of the joint conditional Laplace transform (2.12) to all the couples (u_1, u_2) of this kind holds only up to a time $\mathrm{T}^{(u_1,u_2)}$ such that $\mathrm{T}^{(u_1,u_2)} \geqslant \mathrm{T}^{(\mathrm{Re}(u_1),\mathrm{Re}(u_2))}$ (see Remark 2.7). However, under Proposition 2.21, we have $\mathrm{T}^{(x_1,x_2)} = +\infty$, for all $x_1 \leqslant \theta/\eta$ and $x_2 \leqslant 0$, if and only if $b \geqslant \frac{1}{2}\,\sigma^2\,\frac{\theta}{\eta} + \eta\,C_\alpha\,\Gamma(-\alpha)\,\theta^{\alpha-1}\,(\alpha-1)$. As a result, we obtain $\mathrm{T}^{(u_1,u_2)} = +\infty$, for all u_1 such that $\mathrm{Re}(u_1) < \theta/\eta$ and $u_2 \in \mathbb{C}_-$, by the previous inequality. This will play an important role for the application of Fourier-based pricing methods (see Chapter 3).

In conclusion to this chapter, a brief overview of all the examples of CBI processes that have been considered in Sections 2.6 and 2.7 is reported in Table 2.1. For each example in the table:

- The first column lists the parameters to specify from a general CBI process;
- The second column highlights the principal features of the example considered.

	Parameters	Features
CIR process ([**CIR85**])	$b > 0$, $\nu = 0$, and $\pi = 0$	Continuous CBI process Feller condition
α-CIR process, ([**LM15, JMS17, JMSZ21**])	$b > 0$, $\nu = 0$, and $\pi(\mathrm{d}z) = \eta^\alpha\, C_\alpha\, z^{-1-\alpha}\, \mathbf{1}_{\{z>0\}}\, \mathrm{d}z$, with $\eta \geqslant 0$, $C_\alpha \geqslant 0$, and $\alpha \in (1,2)$	Lévy-driven integral equation $\mathbb{E}\big[e^{\,x\,X_T}\big] = +\infty$, $\forall x > 0$, $\forall T > 0$ Feller condition applies
Hawkes process ([**Haw71, HO74, Haw18**])	$b > 0, \sigma = 0$, $\nu = 0$, $\pi = \delta_\eta$ with $\eta > 0$, and $X_0 = \frac{\beta}{b+\eta}$	Stochastic intensity Self-exciting counting process Time-changed Poisson formulation
Marked Hawkes process ([**BNT02, BM02**])	$b > 0, \sigma = 0$, $\nu = 0$, π probability distribution on $\mathbb{R}_+$, with $\int_0^{+\infty} x\, \pi(\mathrm{d}x) < \infty$, $X_0 = \frac{\beta}{b+\eta}$	One mark per event (with law π) Amplified self-exciting behavior Time-changed compound Poisson
Tempered-stable CBI process (see Section 2.7)	$\nu = 0$, and for all $z > 0$: $\pi(\mathrm{d}z) = \eta^\alpha\, C_\alpha\, z^{-1-\alpha}\, e^{-\frac{\theta}{\eta}\, z}\, \mathrm{d}z$, $\eta > 0$, $C_\alpha \geqslant 0$, $\theta \geqslant 0$, $\alpha \in (1,2)$	Stochastic time change equation $\mathbb{E}\big[e^{\,x\,X_T}\big] < +\infty$, $\forall x \leqslant \theta/\eta$, $\forall T > 0$ Feller condition applies

TABLE 2.1. Overview of the examples of CBI processes considered in this chapter.

CHAPTER 3

Multiple yield curve modeling with CBI processes

SUMMARY. We develop a modeling framework for multiple yield curves driven by *Continuous-state Branching processes with Immigration* (CBI). Exploiting the self-exciting behavior of jump-type CBI processes, this approach can reproduce the relevant empirical features of spreads between different interbank rates. In particular, we construct a novel class of multi-curve models by relying on a *flow of tempered-stable CBI processes*. Such models are especially parsimonious and tractable, and are able to generate contagion effects among different spreads. The proposed approach allows for the explicit valuation of all linear interest rate derivatives, and ensures semi-closed-form formulae for non-linear products via Fourier techniques. Finally, we provide a numerical comparison of FFT and quantization-based pricing methodologies, and then show that a simple specification of our CBI-driven multi-curve model can be successfully calibrated to market data. This chapter is based on the work *Multiple yield curve modelling with CBI processes*, co-authored with C. Fontana and A. Gnoatto, published in *Mathematics and Financial Economics*, volume 15, pages 579–610, 2021.

Contents

3.1. Introduction

3.1.1. Motivation and literature. The emergence of multiple yield curves can be rightfully considered as the most relevant feature of interest rate markets over the last decade, starting from the 2007–2009 financial crisis. While pre-crisis interest rate markets were adequately described by a single yield curve and Interbank offered rates[1] associated to different tenors were determined by simple no-arbitrage relations, this proves to be no longer valid in the post-crisis scenario, where yield curves associated to interbank rates of different tenors demonstrate a distinct behavior.

This phenomenon is reflected by the presence of tenor-dependent spreads between different yield curves. In the midst of the financial crisis, such spreads reached their peak beyond 200 basis points and since then, and still nowadays, they have continued to remain at non-negligible levels (see Figure 3.1). The credit, liquidity, and funding risks existing in the interbank market, which were deemed negligible prior to the financial crisis, reveal to be at the origin of this phenomenon (see for instance [**MU08, GKP11, CD13, GSS17**]).

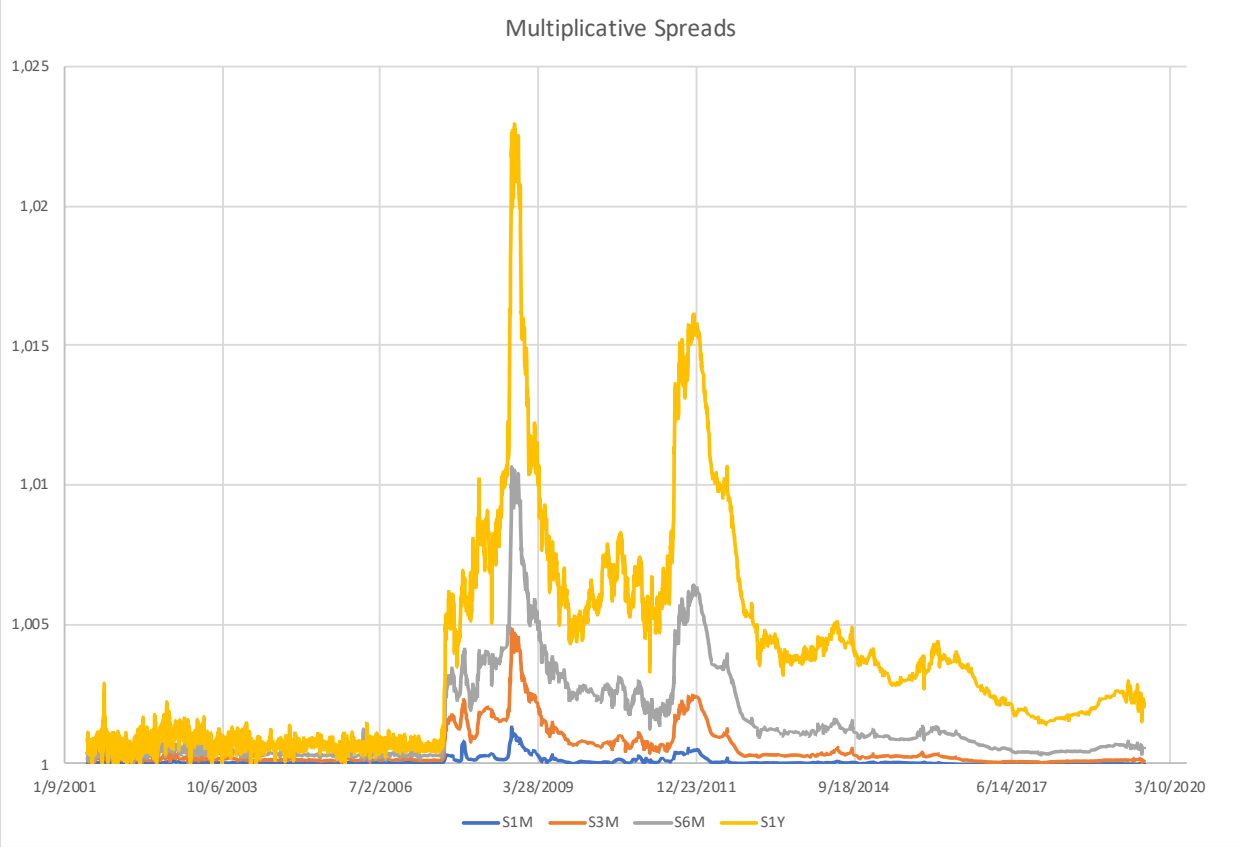

FIGURE 3.1. Euribor-OIS spreads from 06/2001 to 09/2019.
Source: Bloomberg.

[1]They are generally referred to as Ibor rates. The most relevant Ibor rates are represented by the Libor rates in the London interbank market and the Euribor rates in the Eurozone.

In all major jurisdictions, transaction-based backward-looking risk-free rates are currently being introduced as a replacement for Ibor rates (e.g. SOFR in the US market, €STR in the Eurozone, SONIA in the UK market), also as a response to the 2012 Libor manipulation scandal (see e.g. [**KS21**] for a brief examination of the alternative rate benchmarks). We can mention several works where the new reference rates intended to replace Ibor rates have been modeled. We start with [**Mer18b**], where a simple multi-curve short-rate model was extended to take SOFR rates into account. [**LM19**] presented an extension of the standard Libor market model to backward-looking rates. [**MS20**] introduced a class of rational savings account models for backward-looking rates, and [**AB20**] developed a modeling framework for interest rate spikes in view of SOFR derivative pricing. More recently, [**GS21**] have designed a SOFR short-rate model taking stochastic discontinuities explicitly into account, and [**SS21**] have constructed a novel class of dynamic term-structure models for SOFR futures by relying on historical data.

At the time of writing, definitive conclusions on the evolution of Ibor rates cannot be drawn. However, there seems to be a consensus on the fact that the multiple yield curve framework will remain relevant (and, possibly, even more relevant) in the future. Indeed, several authors have argued that a complete disappearence of Ibor rates, which are known to reflect the fluctuations in the unsecured term funding costs of banks, does not seem like a realistic scenario. Among others, we can in particular mention [**SS19**], who documented that multiple benchmark rates will coexist in the future. For instance, in some jurisdictions, Ibor benchmarks have been reformed and the "two-benchmark approach" of [**DS15**] has been adopted (e.g. in the Eurozone, the Euribor rate will not be abandoned, but only replaced by a reformed version that will coexist with the €STR rate as of 2022).

In this chapter, we propose a novel modeling approach to multiple yield curves, which is specifically motivated by the relevant empirical features of spreads between interbank rates. An inspection of Figure 3.1 provides an overview of these features (previously listed in Chapter 1):

(i) Spreads are typically greater than one and non-decreasing with respect to the tenor;
(ii) There are strong co-movements (in particular, common upward jumps) among spreads associated to different tenors;
(iii) Relatively large values of the spreads are associated to high volatility, showing volatility clustering zones during crisis periods;
(iv) Low values of some spreads can persist for prolonged periods of time.

As already postulated in Chapter 1, as far as we know, a multi-curve model that can adequately reproduce all these features does not yet exist in the related literature.

Prior to presenting our contribution, let us briefly discuss the literature on multi-curve models. We emphasize that we do not attempt a general overview of multi-curve modeling, referring instead to the volumes [**BM13, Hen14, GR15**] for detailed accounts on the topic. Multi-curve models, as extensions of standard single-curve interest rate models, can be categorized into four principal classes: short-rate models [**KTW09, Ken10, FT13, GM16**]; Heath–Jarrow–Morton (HJM) models [**FST11, MP14, CGNS15, CFG16**]; Libor market models [**Bia10, Mer10, Mer13, GPSS15**]; and finally pricing kernel models [**NS15, CMNS16, MM18**].

We can also add the following more recent contributions: [**CFG19b**], where the authors have developed *the affine framework* unifying all existing multi-curve models based on affine processes; [**BMSS19, AGS20**] have adopted a new short-rate approach modeling "roll-over risk" explicitly; [**EGG20**] have extended the Libor market model to allow for negative interest rates; [**FGGS20**] have constructed an HJM model taking stochastic discontinuities into account; [**LH20**] have introduced self-exciting features into the multiple yield curve framework through a reduced-form model of interbank credit risk by relying on self-exciting jump processes.

3.1.2. Contribution. By relying on the theory of *Continuous-state Branching processes with Immigration* (CBI), we develop a modeling framework that captures the relevant empirical features of spreads and, at the same time, guarantees an efficient valuation of interest rate derivatives written on Ibor rates. Exploiting the affine property of CBI processes, we design our modeling framework in the context of the affine multi-curve models recently introduced by [**CFG19b**], taking spot multiplicative spreads and the OIS short rate as fundamental modeling objects (see Chapter 1).

By construction, the model achieves a perfect fit to the observed term structures, and ensures spreads greater than one and non-decreasing with respect to the tenor. The model generates an exponentially-affine structure for OIS zero-coupon bonds and forward multiplicative spreads, allowing for the explicit valuation of all linear interest rate derivatives.

While [**CFG19b**] focused on the general theoretical properties of the framework, we contribute by introducing a novel class of tractable and flexible multi-curve models driven by a *flow of tempered-stable CBI processes*, which are specifically motivated by the empirical features discussed above. The adoption of a flow of CBI processes (see [**DL12**]) enables us to capture strong comovements among spreads such as common upwards jumps and jump clustering. In particular, the self-exciting behavior of CBI processes proves to be a key ingredient to reproduce these features.

The choice of *tempered-stable CBI processes*, as presented in Section 2.7, offers a remarkable trade-off between flexibility and analytical tractability, and allows for an explicit characterization of several important properties of the model. More specifically, tempered-stable CBI processes provide a simple necessary and sufficient condition for the finiteness of exponential moments, which will represent an indispensable requirement.

We derive semi-closed-form pricing formulae for caplets via Fourier techniques. More precisely, we implement two pricing methodologies based on FFT and quantization, where the latter is here applied for the first time to an interest rate setting. Finally, in a numerical analysis (Section 3.5), our two pricing methodologies are compared and a specification of the proposed model with two tenors is calibrated to market data, demonstrating an excellent fit to market data. We believe that the introduction of such models driven by a flow of CBI processes, can lead to further successful applications in other contexts where different term structures coexist.

3.1.3. Structure. Section 3.2 introduces the general modeling approach, which is then specialized in Section 3.3 to multi-curve models driven by a flow of tempered-stable CBI processes. Section 3.4 presents our pricing formulae for caplets. Section 3.5 contains numerical results, while Section 3.6 concludes. We finally simulate tempered-stable CBI processes in Appendix 3.A.

3.2. General modeling with CBI processes

As in Chapter 2, we fix a stochastic basis $\big(\Omega, \mathcal{F}, \mathbb{F}, \mathbb{Q}\big)$ satisfying the usual conditions, where $\mathbb{Q}$ is a probability measure whose role will be specified later, and where $\mathbb{F} = (\mathcal{F}_t)_{t\geqslant 0}$ is a filtration to which all stochastic processes are assumed to be adapted. By convention, we set $\mathcal{F} = \mathcal{F}_\infty$ and denote the expectation under $\mathbb{Q}$ by $\mathbb{E}$.

3.2.1. Preliminaries on the post-crisis interest rate market. The reference rates for overnight transactions are the EONIA (Euro Overnight Index Average) rate in the Eurozone and the Federal Funds rate in the US market. These rates are determined on the basis of actual overnight transactions of the interbank market, and represent the underlying of Overnight Indexed Swaps (OIS). These swaps are then quoted by their market swap rates, simply referred to as OIS rates, which are typically considered as the best proxies for risk-free rates.

By using bootstrapping techniques (see e.g. [**AB13**]), the OIS term structure $T \mapsto B(t,T)$ can be recovered from OIS rates, where $B(t,T)$ denotes the price at time t of an OIS zero-coupon bond with maturity T. We then represent the *OIS short rate* by the stochastic process $r = (r_t)_{t\geqslant 0}$, defined as the short end of the term structure of instantaneous forward rates implied by OIS zero-coupon bond prices. In market practice, the OIS short rate is usually approximated by the overnight rate associated to the shortest tenor and is often adopted as a collateral rate.

For $\delta \geqslant 0$ and $T \geqslant 0$, let us now introduce the simply-compounded (risk-free) OIS spot rate for the period $[T, T+\delta]$, which we denote by $L^{\mathrm{OIS}}(T,T,\delta)$. The latter is given by

$$L^{\mathrm{OIS}}(T,T,\delta) := \frac{1}{\delta}\left(\frac{1}{B(T,T+\delta)} - 1\right). \tag{3.1}$$

We point out that equation (3.1) is valid for all $\delta \geqslant 0$ and $T \geqslant 0$ as far as OIS rates are concerned. We also observe that the right-hand side of (3.1) used to be the pre-crisis textbook definition of the Interbank offered rate (Ibor) prevailing at time T for the period $[T, T+\delta]$.

Ibor rates represent the underlying of interest rate derivatives and are determined by a panel of primary financial institutions for unsecured lending (refer to [**GR15**, Chapter 1] for further details). We denote by $L(T,T,\delta)$ the spot Ibor rate for the period $[T, T+\delta]$, where the tenor δ is typically one day (1D), one week (1W), or several months (1M, 2M, 3M, 6M, 12M). We consider Ibor rates for a generic set $\mathcal{G} := \big\{\delta_1, \ldots, \delta_m\big\}$ of tenors, with $0 < \delta_1 < \ldots < \delta_m$, for some $m \in \mathbb{N}$. We emphasize that in the post-crisis environment, Ibor rates of different tenors exhibit a distinct behavior and are no longer determined by simple no-arbitrage relations. As in Section 3.1, this leads to non-negligible basis spreads and to the emergence of multiple yield curves.

Among all financial derivatives written on Ibor rates, Forward Rate Agreements (FRAs) can be regarded as the basic building blocks, owing to the fact that all linear interest rate products, such as interest rate swaps and basis swaps, can be represented as portfolios of FRAs (see e.g. [**CFG16**, Section 5.2]). We recall that a FRA written on the Ibor rate $L(T,T,\delta)$ with fixed strike K is a contract that delivers the payoff $\delta\big(L(T,T,\delta) - K\big)$ at maturity $T+\delta$. The forward Ibor rate $L(t,T,\delta)$ at time $t \leqslant T$ is defined as the value of K that makes the price at time t of the FRA equal to zero. We then formulate the definition of a multiple yield curve market as follows.

DEFINITION 3.1. A *multiple yield curve market* is a financial market where the following basic assets are traded:

- OIS zero-coupon bonds for all maturities $T > 0$;
- FRAs for all tenors $\delta \in \mathcal{G}$, for all maturities $T > 0$, and fixed strike K.

The natural question arising from Definition 3.1 concerns absence of arbitrage in this market. Recently, [**FGGS20**] have provided a formulation of the fundamental theorem of asset pricing for multiple yield curve markets. Indeed, by [**FGGS20**, Theorem 6.3], absence of arbitrage in the sense of *No Asymptotic Free Lunch with Vanishing Risk* (NAFLVR) is equivalent to the existence of an equivalent separating measure, thus extending the main result of [**CKT16**] to multiple curves and an infinite time horizon. In general, an equivalent separating measure cannot be replaced with *Equivalent Local martingale Measure* (ELMM), see [**FGGS20**, Remark 6.4]. However, by using Fatou's lemma, the existence of an ELMM always suffices to guarantee NAFLVR.

3.2.2. The general modeling framework. From now on, we adopt a martingale approach and directly define our modeling framework on the stochastic basis $\big(\Omega, \mathcal{F}, \mathbb{F}, \mathbb{Q}\big)$, where $\mathbb{Q}$ is assumed to be a *risk-neutral* measure for the multiple yield curve market. By definition, this means that all traded assets considered above are martingales under $\mathbb{Q}$ when discounted by the OIS bank account $B_t := e^{\int_0^t r_s \, \mathrm{d}s}$, for all $t \geqslant 0$, which therefore ensures NAFLVR for the multiple yield curve market by [**FGGS20**, Theorem 6.3].

OIS zero-coupon bond prices can be represented by

$$B(t,T) = \mathbb{E}\Big[e^{-\int_t^T r_s \, \mathrm{d}s} \,\Big|\, \mathcal{F}_t \Big], \tag{3.2}$$

for all $0 \leqslant t \leqslant T < +\infty$, and forward Ibor rates are given by

$$L(t,T,\delta) = \mathbb{E}^{T+\delta}\big[\, L(T,T,\delta) \,\big|\, \mathcal{F}_t \,\big], \tag{3.3}$$

for all $\delta \in \mathcal{G}$ and $0 \leqslant t \leqslant T < +\infty$, where $\mathbb{E}^{T+\delta}$ denotes the expectation under the $(T+\delta)$-forward probability measure $\mathbb{Q}^{T+\delta}$ with the OIS zero-coupon bond $B(\cdot, T+\delta)$ as a numéraire (see e.g. [**GEKR95**]). We also point out that equation (3.3) was first introduced by [**Mer10**, Section 4] as a definition of the FRA rate.

As mentioned in Section 3.1, we design our modeling framework in the context of the affine multi-curve models recently studied by [**CFG19b**]. Our main modeling quantities are the *OIS short rate* $r = (r_t)_{t \geqslant 0}$ and the *spot multiplicative spreads* between (normalized) spot Ibor rates and (normalized) simply-compounded OIS spot rates (refer also to Chapter 1), defined as follows:

$$S^\delta(t,t) := \frac{1 + \delta \, L(t,t,\delta)}{1 + \delta \, L^{\mathrm{OIS}}(t,t,\delta)}, \qquad \forall (\delta, t) \in \mathcal{G} \times \mathbb{R}_+. \tag{3.4}$$

In the post-crisis environment, multiplicative spreads are typically greater than one and non-decreasing with respect to the tenor. By abstracting from liquidity and funding issues, this can be ascribed to the fact that Ibor rates incorporate the risk that the average credit quality of an initial panel of creditworthy banks deteriorates over the term of the loan, while OIS rates, in turn, reflect the average credit quality of a periodically refreshed panel of banks (see e.g. [**CDS01, FT13**]).

The idea of modeling multiple yield curve markets via multiplicative spreads is due to [**Hen14**], and pursued by [**CFG16, CFG19b, EGG20, FGGS20**]. They can be directly inferred from quoted Ibor and OIS rates and, in comparison to additive spreads (see [**MX12, Mer13**]), admit a natural economic interpretation. Indeed, $S^\delta(t,t)$ can be considered as a market expectation (at time t) of the riskiness of the Ibor panel for the period $[t, t+\delta]$. In particular, this interpretation reveals to be related to the foreign exchange analogy that we derived in Chapter 1 (see also [**Bia10, NS15, CFG16, MM18**]).

Let us now suppose that the stochastic basis $\big(\Omega, \mathcal{F}, \mathbb{F}, \mathbb{Q}\big)$ supports a d-dimensional process $X = (X_t)_{t\geqslant 0}$ such that each component X^k is a $\mathrm{CBI}\big(X_0^k, \Psi^k, \Phi^k\big)$ in the sense of Chapter 2, whose branching mechanism Φ^k satisfies Assumption 2.4. We also assume that $X^1, \dots, X^d$ are mutually independent. Besides the driving process X, let us then introduce the following ingredients:

- A function $\ell : \mathbb{R}_+ \to \mathbb{R}$ such that $\int_0^T \big|\ell(u)\big| \,\mathrm{d}u < +\infty$, for all $T > 0$;
- A vector $\lambda \in \mathbb{R}_+^d$;
- A family of functions $\boldsymbol{c} = (c_1, \dots, c_m)$ with $c_i : \mathbb{R}_+ \to \mathbb{R}$, for every $1 \leqslant i \leqslant m$;
- A family of vectors $\boldsymbol{\gamma} = (\gamma_1, \dots, \gamma_m)$ with $\gamma_i \in \mathbb{R}^d$, for every $1 \leqslant i \leqslant m$.

Definition 3.2. The tuple $\big(X, \ell, \lambda, \boldsymbol{c}, \boldsymbol{\gamma}\big)$ is said to generate a *CBI-driven multi-curve model* if

$$r_t = \ell(t) + \lambda^\top X_t, \tag{3.5}$$

$$\log S^{\delta_i}(t,t) = c_i(t) + \gamma_i^\top X_t, \tag{3.6}$$

for all $t \geqslant 0$ and for every $1 \leqslant i \leqslant m$, and if the following conditions hold true:

$$\gamma_{i,k} \in \mathcal{D}_1^k \quad \text{and} \quad \mathrm{T}_k^{(\gamma_{i,k}, -\lambda_k)} = +\infty, \tag{3.7}$$

for every $1 \leqslant i \leqslant m$ and for every $1 \leqslant k \leqslant d$, where the set $\mathcal{D}_1^k$ is given by (2.8) and $\mathrm{T}_k^{(\gamma_{i,k}, -\lambda_k)}$ denotes the lifetime as in Theorem 2.8 applied to $x_1 = \gamma_{i,k}$ and $x_2 = -\lambda_k$, both with respect to the CBI process $X^k = (X_t^k)_{t\geqslant 0}$, for every $1 \leqslant k \leqslant d$.

Condition (3.7) guarantees that $\mathbb{E}\big[e^{-\int_0^T r_s \,\mathrm{d}s}\, S^\delta(T,T)\big] < +\infty$, for all $\delta \in \mathcal{G}$ and $T > 0$, thus ensuring that the model can be applied to arbitrarily large maturities (i.e. the expected value in (3.3) is always well-defined). The role of the time-dependent functions ℓ and $\boldsymbol{c}$ consists in allowing the model to perfectly fit the observed term structures (we refer the reader to [**CFG19b**, Proposition 3.18] for a precise characterization of this property).

A multi-curve model constructed as in Definition 3.2 inherits the properties of the CBI process, in particular its self-exciting behavior (see Remark 2.14). Moreover, it can easily generate common upward jumps in different spreads. In view of equations (3.6), this can be achieved by letting $\gamma_i^\top \gamma_j \neq 0$, for every $1 \leqslant i, j \leqslant m$ with $i \neq j$, meaning that the spreads associated to the tenors δ_i and δ_j are affected by common risk factors. As mentioned in Section 3.1, common upward jumps represent a particularly important empirical fact. We refer to Section 3.3 for a more specific discussion on the adequacy of this approach in reproducing the empirical features of Ibor-OIS spreads as exhibited by Figure 3.1.

REMARK 3.3. In general, there are no constraints on the choice of the dimension d of the driving process X. On the one hand, $d \geqslant m$ is needed to ensure non-trivial correlation structures among the m spreads. On the other hand, the case $d < m$ is in line with market practice, which often assumes for simplicity the existence of linear (possibly time-varying) dependence among different spreads. Let us also mention that models driven by a vector of independent CBI processes have been recently applied to spot and forward energy prices in [**JMSS19**] and [**CMS19**], respectively.

3.2.3. Features of the model. As shown in [**CFG16, CFG19b**], the basic building blocks for the valuation of interest rate derivatives in a multi-curve setting are represented by OIS zero-coupon bond prices and *forward multiplicative spreads* $S^{\delta}(t,T)$, defined as follows:

$$S^{\delta}(t,T) := \frac{1+\delta\, L(t,T,\delta)}{1+\delta\, L^{\mathrm{OIS}}(t,T,\delta)}, \tag{3.8}$$

for all $\delta \in \mathcal{G}$ and $0 \leqslant t \leqslant T < +\infty$, where $L(t,T,\delta)$ is the forward Ibor rate and $L^{\mathrm{OIS}}(t,T,\delta)$ is the simply-compounded (risk-free) OIS forward rate given by

$$L^{\mathrm{OIS}}(t,T,\delta) := \frac{1}{\delta}\left(\frac{B(t,T)}{B(t,T+\delta)} - 1\right). \tag{3.9}$$

We mention that by equation (3.3), the forward multiplicative spread process $(S^{\delta}(t,T))_{t\leqslant T}$ is a martingale under the T-forward measure $\mathbb{Q}^T$, for all $\delta \in \mathcal{G}$ and $T > 0$ (see [**CFG16**, Lemma 3.11]).

In the next result, we show that in a CBI-driven multi-curve model, OIS zero-coupon bonds and forward multiplicative spreads admit an exponentially-affine structure. As a consequence, all linear interest rate derivatives such as FRAs, interest rate swaps, and basis swaps, can be priced in closed form by relying on the general valuation formulae stated in [**CFG16**, Section 5.2].

LEMMA 3.4. *Let $\big(X, \ell, \lambda, \mathbf{c}, \boldsymbol{\gamma}\big)$ generate a CBI-driven multi-curve model. Then:*

(i) *For all $0 \leqslant t \leqslant T < +\infty$, the OIS zero-coupon bond price $B(t,T)$ is given by*

$$B(t,T) = \exp\big(\mathcal{A}_0(t,T) + \mathcal{B}_0(T-t)^{\top} X_t\big), \tag{3.10}$$

where $\mathcal{A}_0(t,T)$ and $\mathcal{B}_0(T-t) = \big(\mathcal{B}_0^1(T-t), \ldots, \mathcal{B}_0^d(T-t)\big)^{\top}$ are given by

$$\mathcal{A}_0(t,T) := -\int_0^{T-t}\left(\ell(s+t) + \sum_{k=1}^{d} \Psi^k\left(\mathcal{V}^k(s,0,-\lambda_k)\right)\right)\mathrm{d}s,$$

$$\mathcal{B}_0^k(T-t) := \mathcal{V}^k(T-t,0,-\lambda_k), \qquad \text{for every } 1 \leqslant k \leqslant d;$$

(ii) *For every $1 \leqslant i \leqslant m$ and for all $0 \leqslant t \leqslant T < +\infty$, the forward multiplicative spread $S^{\delta_i}(t,T)$ is given by*

$$S^{\delta_i}(t,T) = \exp\big(\mathcal{A}_i(t,T) + \mathcal{B}_i(T-t)^{\top} X_t\big), \tag{3.11}$$

where $\mathcal{A}_i(t,T)$ and $\mathcal{B}_i(T-t) = \big(\mathcal{B}_i^1(T-t), \ldots, \mathcal{B}_i^d(T-t)\big)^{\top}$ are given by

$$\mathcal{A}_i(t,T) := c_i(T) + \sum_{k=1}^{d}\int_0^{T-t}\left(\Psi^k\left(\mathcal{V}^k(s,\gamma_{i,k},-\lambda_k)\right) - \Psi^k\left(\mathcal{V}^k(s,0,-\lambda_k)\right)\right)\mathrm{d}s,$$

$$\mathcal{B}_i^k(T-t) := \mathcal{V}^k(T-t,\gamma_{i,k},-\lambda_k) - \mathcal{V}^k(T-t,0,-\lambda_k), \qquad \text{for every } 1 \leqslant k \leqslant d.$$

PROOF. Due to condition (3.7) and the independence of the processes $X^1, \dots, X^d$, equations (3.10) and (3.11) can be easily obtained by relying on the affine property of the CBI process. First, equation (3.10) for the OIS zero-coupon bond price $B(t,T)$, for all $0 \leqslant t \leqslant T < +\infty$, follows from (3.2) and a direct application of Lemma 2.2 for each CBI process $X^k = (X^k_t)_{t \geqslant 0}$. Then, equation (3.11) for the forward multiplicative spread $S^{\delta_i}(t,T)$, for every $1 \leqslant i \leqslant m$ and for all $0 \leqslant t \leqslant T < +\infty$, follows from the martingale property of $(S^{\delta_i}(t,T))_{t \leqslant T}$ under the T-forward measure $\mathbb{Q}^T$, and an application of Proposition 2.5 for each CBI process $X^k = (X^k_t)_{t \geqslant 0}$. □

As mentioned previously, in typical post-crisis market scenarios, multiplicative spreads are greater than one and non-decreasing with respect to the tenor. The next lemma shows that these features can be easily reproduced by a CBI-driven multi-curve model. While this result can be recovered as a special case of the general statement in [**CFG19b**, Proposition 3.7], here we provide a short self-contained proof that relies on the specific properties of CBI processes.

LEMMA 3.5. *Let $\big(X, \ell, \lambda, \mathbf{c}, \boldsymbol{\gamma}\big)$ generate a CBI-driven multi-curve model. Then:*

(i) *For every $1 \leqslant i \leqslant m$, if $\gamma_i \in \mathbb{R}^d_+$ and $c_i(t) \geqslant 0$, for all $t \geqslant 0$, then $S^{\delta_i}(t,T) \geqslant 1$ a.s. for all $0 \leqslant t \leqslant T < +\infty$;*

(ii) *For every $1 \leqslant i \leqslant m-1$, if $\gamma_{i+1} - \gamma_i \in \mathbb{R}^d_+$ and $c_i(t) \leqslant c_{i+1}(t)$, for all $t \geqslant 0$, then $S^{\delta_i}(t,T) \leqslant S^{\delta_{i+1}}(t,T)$ a.s. for all $0 \leqslant t \leqslant T < +\infty$.*

PROOF. Arguing as in [**Li11**, Proposition 3.1] and [**Li20**, Proposition 2.11], it can be shown that the function $\mathcal{V}^k$ is increasing in its second coordinate on $\mathcal{D}^k_1$, for every $1 \leqslant k \leqslant d$. In addition, we know from Chapter 2 that each immigration mechanism Ψ^k is non-decreasing. Hence, since X takes values in $\mathbb{R}^d_+$, the result is a direct consequence of part (ii) of Lemma 3.4. □

REMARK 3.6. Recently, negative short rates have been observed to coexist with non-negative spreads (see e.g. [**EGG20**]). Since the function ℓ in equation (3.5) is allowed to take negative values, our framework does not exclude this possibility. A slight extension of Definition 3.2 permits to generate OIS short rates not bounded from below by the function ℓ. It suffices to replace the process X with a $(d+1)$-dimensional process $X' = (X, Y)$ such that X' is an affine process with $\mathbb{Q}(Y_t < 0) > 0$, for all $t \geqslant 0$, where Y is not restricted to be independent of X. Equation (3.5) is then replaced by $r_t = \ell(t) + \lambda^\top X_t + Y_t$, while multiplicative spreads remain given by (3.6).

3.3. A new class of multi-curve models

In this section, we introduce a class of multi-curve models driven by a *flow of tempered-stable CBI processes*. The proposed specification is motivated by the most relevant features of the spreads (see Figure 3.1), and reveals to be particularly parsimonious and tractable for our purposes.

3.3.1. Flow of tempered-stable CBI processes. Let us first suppose that the stochastic basis $\big(\Omega, \mathcal{F}, \mathbb{F}, \mathbb{Q}\big)$ is equipped with the following two independent objects:

- A Gaussian white noise $W(\mathrm{d}t, \mathrm{d}u)$ as in [**Wal86**] on $\mathbb{R}_+ \times \mathbb{R}_+$ and with intensity $\mathrm{d}t\,\mathrm{d}u$;
- A Poisson random measure $N_1(\mathrm{d}t, \mathrm{d}u, \mathrm{d}x)$ on $\mathbb{R}_+ \times \mathbb{R}_+ \times \mathbb{R}_+$ with compensator $\mathrm{d}t\,\mathrm{d}u\,\pi(\mathrm{d}x)$ and compensated measure $\widetilde{N}_1(\mathrm{d}t, \mathrm{d}u, \mathrm{d}x) := N_1(\mathrm{d}t, \mathrm{d}u, \mathrm{d}x) - \mathrm{d}t\,\mathrm{d}u\,\pi(\mathrm{d}x)$.

As in Section 3.2, we fix a generic set $\mathcal{G} := \{\delta_1, \ldots, \delta_m\}$ of tenors, with $0 < \delta_1 < \ldots < \delta_m$, for some $m \in \mathbb{N}$. In this sense, for all $\delta \in \mathcal{G}$, consider the following stochastic integral equation:

$$\begin{aligned} Y_t(\delta) = Y_0(\delta) + \int_0^t \big(\beta(\delta) - b\, Y_s(\delta)\big)\, \mathrm{d}s + \sigma \int_0^t \int_0^{Y_s(\delta)} W(\mathrm{d}s, \mathrm{d}u) \\ + \int_0^t \int_0^{Y_{s-}(\delta)} \int_0^{+\infty} x\, \widetilde{N}_1(\mathrm{d}s, \mathrm{d}u, \mathrm{d}x), \qquad \forall t \geqslant 0, \end{aligned} \tag{3.12}$$

for $b \in \mathbb{R}$, $\sigma \geqslant 0$, and where the following hold:

- $Y_0 : \mathcal{G} \to \mathbb{R}_+$ and $\beta : \mathcal{G} \to \mathbb{R}_+$ are both deterministic and non-decreasing on $\mathcal{G}$;
- $\pi(\mathrm{d}z) = \eta^\alpha\, C_\alpha\, z^{-1-\alpha}\, e^{-\frac{\theta}{\eta} z}\, \mathbf{1}_{\{z>0\}}\, \mathrm{d}z$, with $\eta > 0$, $C_\alpha > 0$, $\theta > 0$, and $\alpha \in (1, 2)$.

By [**DL12**, Theorem 3.1], for all $\delta \in \mathcal{G}$, there exists a unique non-negative strong solution to equation (3.12), which is a CBI$\big(Y_0(\delta), \Psi^\delta, \Phi\big)$ (see also Remark 2.13). More precisely, for all $\delta \in \mathcal{G}$, $Y(\delta) = (Y_t(\delta))_{t\geqslant 0}$ is a tempered-stable CBI process as in Section 2.7 with immigration mechanism $\Psi^\delta(x) = \beta(\delta)\, x$ and branching mechanism Φ given in Lemma 2.19, where we recall that the function Φ automatically satisfies Assumption 2.4.

The two-parameter process $\{Y_t(\delta) : t \geqslant 0, \delta \in \mathcal{G}\}$ defines an instance of a *flow of tempered-stable CBI processes* (we refer the reader to [**DL12**, Section 3] for further details). All the components of the flow have a common branching mechanism Φ, given by (2.36), while the immigration mechanism of $Y(\delta)$ is equal to $\Psi^\delta(x) = \beta(\delta)\, x$, for all $\delta \in \mathcal{G}$. Observe also that the processes $\{Y(\delta) : \delta \in \mathcal{G}\}$ share the same volatility coefficients σ and η, where we recall that η serves as a volatility parameter for the jump part (see Definition 2.18). They also share the same jump measure π and the same speed of mean reversion b. Only the long-run value $\beta(\delta)/b$ (when $b > 0$) is specific for each process $Y(\delta) = (Y_t(\delta))_{t\geqslant 0}$, for all $\delta \in \mathcal{G}$. Furthermore, we highlight the fact that the martingale terms in equation (3.12) are generated by common sources of randomness W and $\widetilde{N}_1$, while depending on the current value of each process $Y(\delta) = (Y_t(\delta))_{t\geqslant 0}$, which therefore implies a non-trivial dependence structure among the processes $\{Y(\delta) : \delta \in \mathcal{G}\}$. This observation will be made more precise below.

3.3.2. Construction of the multi-curve models. Let us now formalize the notion of *multi-curve models driven by a flow of tempered-stable CBI process*. To this end, we define the factor process $Y = (Y_t)_{t\geqslant 0}$ by $Y_t := \big(Y_t(\delta_1), \ldots, Y_t(\delta_m)\big)^\top$, $\forall t \geqslant 0$, and introduce the following ingredients:

- A function $\ell : \mathbb{R}_+ \to \mathbb{R}$ such that $\int_0^T \big|\ell(u)\big|\, \mathrm{d}u < +\infty$, for all $T > 0$;
- A vector $\mu \in \mathbb{R}_+^m$;
- A family of functions $\boldsymbol{c} = (c_1, \ldots, c_m)$ with $c_i : \mathbb{R}_+ \to \mathbb{R}_+$, for every $1 \leqslant i \leqslant m$.

Definition 3.7. The tuple $\big(Y, \ell, \mu, \boldsymbol{c}\big)$ is said to generate a *multi-curve model driven by a flow of tempered-stable CBI processes* if

$$r_t = \ell(t) + \mu^\top Y_t, \tag{3.13}$$

$$\log S^{\delta_i}(t, t) = c_i(t) + Y_t(\delta_i), \tag{3.14}$$

for all $t \geqslant 0$ and for every $1 \leqslant i \leqslant m$, and if the following conditions hold true:

$$\theta > \eta \quad \text{and} \quad b \geqslant \frac{1}{2}\,\sigma^2\,\frac{\theta}{\eta} + \eta\,C_\alpha\,\Gamma(-\alpha)\,\theta^{\alpha-1}\,(\alpha-1)\,. \tag{3.15}$$

The second part of (3.15) corresponds to the condition provided by Proposition 2.21 for tempered-stable CBI processes, which is common to all the processes $\big\{Y(\delta) : \delta \in \mathcal{G}\big\}$. In this regard, $\theta > \eta$ suffices to guarantee that $\mathbb{E}\big[e^{Y_t(\delta)}\big] < +\infty$, for all $\delta \in \mathcal{G}$ and $t > 0$.

Under Definition 3.7, multiplicative spreads are by construction greater than one. Moreover, thanks to the properties of a flow of CBI processes, monotonicity of multiplicative spreads can be easily achieved, provided that the initially-observed spreads are non-decreasing in the tenor.

PROPOSITION 3.8. *Let $\big(Y, \ell, \mu, \boldsymbol{c}\big)$ generate a multi-curve model driven by a flow of tempered-stable CBI processes. Suppose that $c_i(t) \leqslant c_{i+1}(t)$, for every $1 \leqslant i \leqslant m-1$ and all $t \geqslant 0$. Then, it holds that $S^{\delta_i}(t,T) \leqslant S^{\delta_{i+1}}(t,T)$ a.s., for every $1 \leqslant i \leqslant m-1$ and all $0 \leqslant t \leqslant T < +\infty$.*

PROOF. Since both functions $Y_0 : \mathcal{G} \to \mathbb{R}_+$ and $\beta : \mathcal{G} \to \mathbb{R}_+$ are non-decreasing on $\mathcal{G}$, [**DL12**, Theorem 3.2] implies that for every $1 \leqslant i \leqslant m-1$, $\mathbb{Q}\big(Y_t(\delta_i) \leqslant Y_t(\delta_{i+1}), \forall t \geqslant 0\big) = 1$. Hence, if in addition we have $c_i(t) \leqslant c_{i+1}(t)$, for every $1 \leqslant i \leqslant m-1$ and all $t \geqslant 0$, it follows that $S^{\delta_i}(t,t) \leqslant S^{\delta_{i+1}}(t,t)$ a.s. for every $1 \leqslant i \leqslant m-1$ and all $t \geqslant 0$. The claim follows from the fact that the process $(S^{\delta_i}(t,T))_{t \leqslant T}$ is a martingale under the T-forward probability measure $\mathbb{Q}^T$. □

The processes $\big\{Y(\delta) : \delta \in \mathcal{G}\big\}$ possess the characteristic self-exciting behavior of CBI processes. This translates directly into a self-exciting property of spreads: for every $1 \leqslant i \leqslant m$, a large value of $S^{\delta_i}(t,t)$ increases the likelihood of further upward jumps of the spread itself. As discussed in Remark 2.14, a large value of $S^{\delta_i}(t,t)$ increases the volatility of the spread process itself, thereby generating volatility clustering zones in correspondence of large values of the spreads.

Under the conditions of Proposition 3.8, there is a further *self-exciting effect among different spreads*: a large value of $S^{\delta_i}(t,t)$ increases the likelihood of upward jumps of all other spreads with tenor δ_j, for every $j > i$, which reflects the higher risk implicit in Ibor rates with longer tenors. As pointed out in Section 3.1 (see in particular Figure 3.1), these contagion effects among spreads represent empirically relevant features of the post-crisis multi-curve interest rate market.

Figure 3.2 shows a sample trajectory of a multi-curve model in the sense of Definition 3.7 with $\mathcal{G} = \big\{3\mathrm{M}, 6\mathrm{M}\big\}$, providing a clear evidence of jump clustering phenomena. The sample paths have been generated by exploiting the simulation scheme for tempered-stable CBI processes described in Appendix 3.A, using the calibrated parameters reported in Table 3.3.

In Definition 3.7, each process $Y(\delta) = (Y_t(\delta))_{t \geqslant 0}$ drives the multiplicative spread with tenor δ, while all the processes $\big\{Y(\delta) : \delta \in \mathcal{G}\big\}$ can affect the OIS short rate given by (3.13). This generates a non-trivial dependence between the OIS short rate and the multiplicative spreads, and among the spreads themselves, in line with the dynamics observed on market data. The quadratic co-variation of log-spreads of tenors δ_i and δ_j, such that $i < j$, can be computed as follows:

$$\Big[\log S^{\delta_i}(\cdot,\cdot), \log S^{\delta_j}(\cdot,\cdot)\Big]_t = \sigma^2 \int_0^t Y_s(\delta_i)\,\mathrm{d}s + \int_0^t \int_0^{Y_{s-}(\delta_i)} \int_0^{+\infty} x^2\,N_1(\mathrm{d}s, \mathrm{d}u, \mathrm{d}x), \tag{3.16}$$

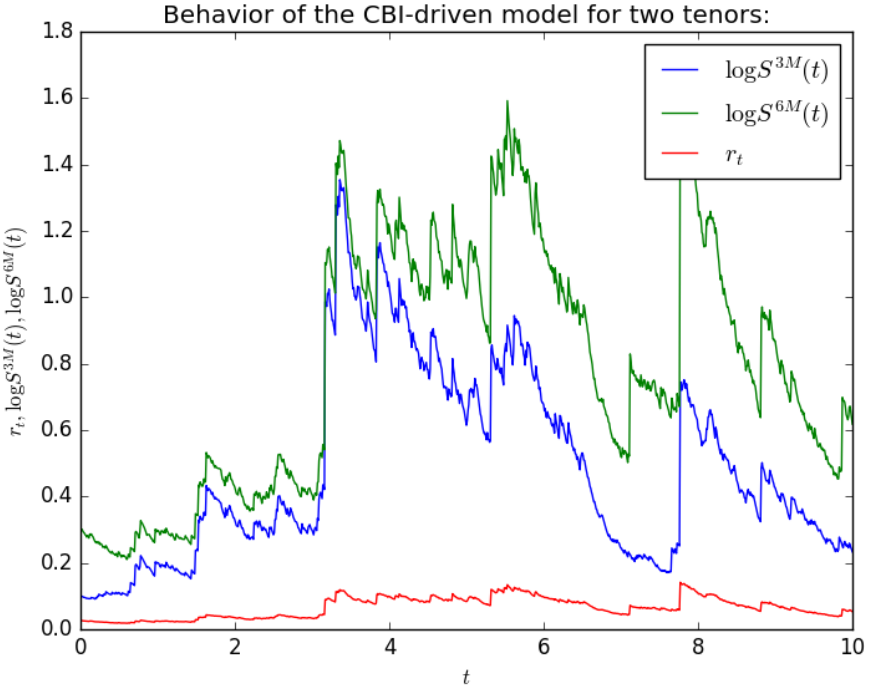

FIGURE 3.2. One sample path of the short rate (red line) and the multiplicative spreads for two tenors (3M in blue and 6M in green) given in Definition 3.7.

for all $t \geqslant 0$. This representation of the quadratic co-variation between log-spreads shows that common jumps arise due to the presence of the common random measure N_1. The presence of common upward jumps is consistent with the contagion effects reported in Section 3.1 (see also Figure 3.1), and is clearly visible in the simulated paths of Figure 3.2.

Figure 3.2 exhibits prolonged periods of time during which spreads remain at relatively low levels. This behavior is also observed in Figure 3.1, and can be achieved by small values of α in $(1, 2)$, common to all the processes $\{Y(\delta) : \delta \in \mathcal{G}\}$. Indeed, for all $\delta \in \mathcal{G}$, a smaller value of α implies a stronger compensation effect in $\widetilde{N}_1$, corresponding to a stronger negative drift after a large jump of the process $Y(\delta) = (Y_t(\delta))_{t \geqslant 0}$. This leads to a sharp reduction of the jump intensity, which then increases the likelihood of a persistence of low values for the spread $S^{\delta}(t, t)$.

REMARK 3.9. By adapting [**BBSS21**, Proposition 5] to our setting, we can show that the flow of processes $\{Y(\delta) : \delta \in \mathcal{G}\}$ as defined above, is closed under a wide class of equivalent changes of probability. Indeed, we can construct an equivalent probability measure $\mathbb{P}$ as follows:

$$\left.\frac{\mathrm{d}\mathbb{P}}{\mathrm{d}\mathbb{Q}}\right|_{\mathcal{F}_t} = \mathcal{E}\left(\xi \int_0^{\cdot}\int_0^{Y_s(\delta_m)} W(\mathrm{d}s, \mathrm{d}u) + \int_0^{\cdot}\int_0^{Y_{s-}(\delta_m)}\int_0^{+\infty} \left(e^{\zeta x} - 1\right) \widetilde{N}_1(\mathrm{d}s, \mathrm{d}u, \mathrm{d}x)\right)_t, \tag{3.17}$$

for all $t \geqslant 0$, for some $\xi \in \mathbb{R}$ and $\zeta \leqslant \theta/\eta$, where the stochastic exponential is a true martingale under $\mathbb{Q}$ as a direct consequence of [**KMK10**, Corollary 3.9]. The stochastic exponential has been

expressed with respect to the process $Y(\delta_m) = (Y_t(\delta_m))_{t\geqslant 0}$ of longest tenor δ_m in the set $\mathcal{G}$, so as to preserve the structural properties of the flow $\big\{Y(\delta) : \delta \in \mathcal{G}\big\}$ under $\mathbb{P}$. Additionally, as a direct consequence of Girsanov's theorem (see e.g. [**EK20**, Section 3.12]), the processes $\big\{Y(\delta) : \delta \in \mathcal{G}\big\}$, for all $\delta \in \mathcal{G}$, remain tempered-stable CBI processes under $\mathbb{P}$ up to parameter rescaling.

3.3.3. Embedding of the multi-curve models. The components of the flow of tempered-stable CBI processes $\big\{Y(\delta) : \delta \in \mathcal{G}\big\}$ are highly dependent. Hence, the multi-curve models of Definition 3.7, in their present form, do not seem to belong to the general class of CBI-driven multi-curve models as introduced by Definition 3.2. However, an easy transformation allows to consider the present specification as an instance of the general modeling framework of Section 3.2.

THEOREM 3.10. *Let $\big(Y, \ell, \mu, \boldsymbol{c}\big)$ generate a multi-curve model driven by a flow of tempered-stable CBI processes. Consider the following objects:*

- *The m-dimensional process $X = (X_t)_{t\geqslant 0}$ defined by*

$$X^i_t := Y_t(\delta_i) - Y_t(\delta_{i-1}), \qquad \forall t \geqslant 0, \tag{3.18}$$

  for every $1 \leqslant i \leqslant m$, with $Y(\delta_0) \equiv 0$ and $\beta(\delta_0) := 0$;
- *The vector $\lambda \in \mathbb{R}^m_+$ given by*

$$\lambda_i := \sum_{k=i}^{m} \mu_k, \qquad \text{for every } 1 \leqslant i \leqslant m; \tag{3.19}$$

- *The family of vector $\boldsymbol{\gamma} = (\gamma_1, \ldots, \gamma_m) \in \mathbb{R}^{m\times m}_+$ given by*

$$\gamma_{i,j} := \mathbf{1}_{\{j\leqslant i\}}, \qquad \text{for every } 1 \leqslant i, j \leqslant m. \tag{3.20}$$

Then, the tuple $\big(X, \ell, \lambda, \boldsymbol{c}, \boldsymbol{\gamma}\big)$ generates a CBI-driven multi-curve model such that

(i) *for every $1 \leqslant i \leqslant m$, the process $X^i = (X^i_t)_{t\geqslant 0}$ is a tempered-stable CBI process with branching mechanism Φ and immigration mechanism $\Psi^i(x) = \big(\beta(\delta_i) - \beta(\delta_{i-1})\big)\, x$;*
(ii) *the processes $X^1, \ldots, X^m$ are mutually independent;*
(iii) *the OIS short rate and multiplicative spreads are given by (3.13) and (3.14), respectively.*

PROOF. Parts (i) and (ii) are direct consequences of the properties of the flow of processes $\{Y(\delta) : \delta \in \mathcal{G}\}$ (see [**DL12**, Theorems 3.2 and 3.3]). To prove part (iii), it suffices to observe that, due to the definitions of λ and $\boldsymbol{\gamma}$ in (3.19) and (3.20), respectively, it holds that

$$\lambda^\top X_t = \mu^\top Y_t \qquad \text{and} \qquad \gamma_i^\top X_t = Y_t(\delta_i),$$

for all $t \geqslant 0$ and for every $1 \leqslant i \leqslant m$. Note that condition (3.7) is implied by condition (3.15), since $\mathcal{D}^i_1 = (-\infty, \theta/\eta]$, for every $1 \leqslant i \leqslant m$, where we have $\Phi(\theta/\eta) \leqslant 0$ with $\theta > \eta$. □

In view of Theorem 3.10, the multi-curve models of Definition 3.7 driven by the flow of tempered-stable CBI processes $\big\{Y(\delta) : \delta \in \mathcal{G}\big\}$ can be equivalently described in terms of a family of mutually-independent risk factors $X^1, \ldots, X^m$ where each factor X^i is affecting all spreads with tenor $\delta_j \geqslant \delta_i$ (and, possibly, the OIS short rate). In particular, the presence of common risk factors

among different spreads accounts for the possibility of common upward jumps, as mentioned above, in line with the contagion effects reported in Section 3.1 (see also Figure 3.1).

Another consequence of Theorem 3.10 is that multi-curve models as in Definition 3.7 can generate OIS zero-coupon bonds and forward multiplicative spreads that admit an exponentially-affine structure (see Lemma 3.4). As a result, in the context of a multi-curve model driven by a flow of tempered-stable CBI processes, all linear interest rate derivatives can be explicitly priced.

COROLLARY 3.11. *Let $\big(Y, \ell, \mu, \boldsymbol{c}\big)$ generate a multi-curve model driven by a flow of tempered-stable CBI processes. Consider the m-dimensional process $X = (X_t)_{t\geqslant 0}$ defined by* (3.18)*. Then:*

(i) *For all $0 \leqslant t \leqslant T < +\infty$, the OIS zero-coupon bond price $B(t,T)$ is given by*

$$B(t,T) = \exp\big(\mathcal{A}_0(t,T) + \mathcal{B}_0(T-t)^\top X_t\big), \tag{3.21}$$

where $\mathcal{A}_0(t,T)$ and $\mathcal{B}_0(T-t) = \big(\mathcal{B}_0^1(T-t), \dots, \mathcal{B}_0^m(T-t)\big)^\top$ are given by

$$\mathcal{A}_0(t,T) := -\int_0^{T-t} \ell(s+t)\,\mathrm{d}s + \sum_{i=1}^m \big(\beta(\delta_i) - \beta(\delta_{i-1})\big) \int_0^{T-t} \mathcal{V}\bigg(s, 0, -\sum_{k=i}^m \mu_k\bigg)\mathrm{d}s,$$

$$\mathcal{B}_0^i(T-t) := \mathcal{V}\bigg(T-t, 0, -\sum_{k=i}^m \mu_k\bigg), \qquad \text{for every } 1 \leqslant i \leqslant m;$$

(ii) *For every $1 \leqslant i \leqslant m$ and for all $0 \leqslant t \leqslant T < +\infty$, the forward multiplicative spread $S^{\delta_i}(t,T)$ is given by*

$$S^{\delta_i}(t,T) = \exp\big(\mathcal{A}_i(t,T) + \mathcal{B}_i(T-t)^\top X_t\big), \tag{3.22}$$

where $\mathcal{A}_i(t,T)$ and $\mathcal{B}_i(T-t) = \big(\mathcal{B}_i^1(T-t), \dots, \mathcal{B}_i^m(T-t)\big)^\top$ are given by

$$\mathcal{A}_i(t,T) = c_i(T) + \sum_{j=1}^i \big(\beta(\delta_j) - \beta(\delta_{j-1})\big) \int_0^{T-t} \bigg(\mathcal{V}\bigg(s, 1, -\sum_{k=j}^m \mu_k\bigg) - \mathcal{V}\bigg(s, 0, -\sum_{k=j}^m \mu_k\bigg)\bigg)\mathrm{d}s,$$

$$\mathcal{B}_i^j(T-t) = \bigg(\mathcal{V}\bigg(T-t, 1, -\sum_{k=j}^m \mu_k\bigg) - \mathcal{V}\bigg(T-t, 0, -\sum_{k=j}^m \mu_k\bigg)\bigg)\mathbf{1}_{\{j\leqslant i\}}, \qquad \text{for every } 1 \leqslant j \leqslant m.$$

PROOF. It suffices to apply Theorem 3.10 and Lemma 3.4, and then insert the definitions of λ and $\boldsymbol{\gamma}$ given by (3.19) and (3.20), respectively, into (3.10) and (3.11). □

Finally, observe that, unlike the general modeling framework of Section 3.2, the function $\mathcal{V}$ appearing in the above formulae is the same for every $1 \leqslant i, j \leqslant m$, due to the fact that the components of a flow of CBI processes $\big\{Y(\delta) : \delta \in \mathcal{G}\big\}$ share a common branching mechanism Φ. This results in additional analytical tractability of the proposed specification in comparison with the more general modeling framework of Section 3.2.

3.4. Valuation of non-linear products

In this section, we provide semi-closed-form formulae for non-linear interest rate derivatives via Fourier techniques. We place ourselves in the modeling framework of Section 3.3 and restrict our attention to caplets, referring the reader to [**CFG19b**, Section 4.2] where swaptions and

basis swaptions were priced in the context of affine multi-curve models by relying on a suitable approximation of the exercise region (see [**GCF17**]).

Let us first consider a caplet in the multiple yield curve market of Definition 3.1, written on the Ibor rate of tenor δ_i for some $1 \leqslant i \leqslant m$, with strike K, maturity T, and settled in arrears at time $T + \delta_i$. For simplicity of presentation, we fix a unitary notional amount and consider the pricing of the product at time $t = 0$. By using the general valuation formulae stated in [**CFG16**, Section 5.2], the arbitrage-free price of the caplet can be written as

$$\begin{aligned} P^{\mathrm{CPLT}}(0,T,\delta_i,K) &= P^{\mathrm{CPLT}}(T,\delta_i,K) = \delta_i\,\mathbb{E}\Big[\, e^{-\int_0^{T+\delta_i} r_s\,\mathrm{d}s}\,\Big(L(T,T,\delta_i)-K\Big)^+\,\Big] \\ &= B\big(0,T+\delta_i\big)\,\mathbb{E}^{T+\delta_i}\Big[\Big(e^{\,\mathcal{X}_T^i}-\big(1+\delta_i\,K\big)\Big)^+\,\Big], \end{aligned} \tag{3.23}$$

where the process $\mathcal{X}^i = (\mathcal{X}^i_t)_{t\geqslant 0}$ is defined by

$$\mathcal{X}^i_t := \log\left(\frac{S^{\delta_i}(t,t)}{B(t,t+\delta_i)}\right), \qquad \forall t \geqslant 0.$$

As a direct consequence of Theorem 3.10 and Corollary 3.11, the process $\mathcal{X}^i$ admits the explicit representation

$$\mathcal{X}^i_t = c_i(t) - \mathcal{A}_0(t,t+\delta_i) + \big(\gamma_i - \mathcal{B}_0(\delta_i)\big)^\top X_t, \qquad \forall t \geqslant 0,$$

where we recall that the vector γ_i is given by (3.20), the m-dimensional process $(X_t)_{t\geqslant 0}$ is defined by equation (3.18), and the functions $\mathcal{A}_0$ and $\mathcal{B}_0$ are given by (3.21).

We now present two pricing methodologies: the former relies on a direct application of the FFT algorithm (see [**CM99**]) and specializes [**CFG19b**, Section 4.1] to our setting, while the latter utilizes a quantization-based algorithm (see [**CFG19a**]), which is here applied for the first time to an interest rate setting.

3.4.1. Caplet pricing by FFT. Let us introduce the set

$$\Theta_i(T) := \Big\{u \in \mathbb{R} : \mathbb{E}^{T+\delta_i}\big[e^{\,u\,\mathcal{X}^i_T}\big] < +\infty\Big\}^\circ,$$

and the strip $\Lambda_i(T) := \big\{\zeta \in \mathbb{C} : -\mathrm{Im}(\zeta) \in \Theta_i(T)\big\}$. By using the independence of the processes $X^1,\dots,X^m$, together with condition (3.15), we can show that for $u \in \mathbb{R}$, $u \in \Theta_i(T)$ if and only if

$$\begin{cases} \mathcal{V}\big(\delta_i,0,-\lambda_j\big) + u\,\big(1-\mathcal{V}\big(\delta_i,0,-\lambda_j\big)\big) < \theta/\eta, & \text{for every } 1 \leqslant j \leqslant i, \\ \mathcal{V}\big(\delta_i,0,-\lambda_j\big) - u\,\mathcal{V}\big(\delta_i,0,-\lambda_j\big) < \theta/\eta, & \text{for every } i+1 \leqslant j \leqslant m, \end{cases}$$

where the vector λ is given by (3.19). Given that $\mathcal{V}(\delta_i,0,-\lambda_j) \leqslant 0$, for every $1 \leqslant j \leqslant m$, and the function $\mathcal{V}$ is increasing in its third coordinate on $\mathbb{R}_-$, it can checked that the condition

$$u < \frac{\theta/\eta - \mathcal{V}\big(\delta_i,0,-\lambda_1\big)}{1-\mathcal{V}\big(\delta_i,0,-\lambda_1\big)}, \tag{3.24}$$

is sufficient to ensure that $\mathcal{V}\big(\delta_i,0,-\lambda_j\big) + u\,\big(1-\mathcal{V}\big(\delta_i,0,-\lambda_j\big)\big) < \theta/\eta$, for every $1 \leqslant j \leqslant i$, while $u \leqslant 1$ suffices to guarantee that $\mathcal{V}\big(\delta_i,0,-\lambda_j\big) - u\,\mathcal{V}\big(\delta_i,0,-\lambda_j\big) < \theta/\eta$, for every $i+1 \leqslant j \leqslant m$.

Furthermore, since $\theta > \eta$, it always holds that $(-\infty, +1] \subseteq \Theta_i(T)$. Consequently, for all $\zeta \in \Lambda_i(T)$, the *modified characteristic function* of $\mathcal{X}_T^i$ can be defined and explicitly computed as follows:

$$\begin{aligned}\Xi_T^i(\zeta) &:= B\big(0, T+\delta_i\big)\, \mathbb{E}^{T+\delta_i}\left[e^{\mathsf{i}\,\zeta\,\mathcal{X}_T^i}\right] = \mathbb{E}\left[e^{-\int_0^T r_s\,\mathrm{d}s}\, B\big(T, T+\delta_i\big)\, e^{\mathsf{i}\,\zeta\,\mathcal{X}_T^i}\right] \\ &= \exp\left(-\int_0^T \ell(s)\,\mathrm{d}s + \mathcal{A}_0\big(T, T+\delta_i\big) + \mathsf{i}\,\zeta\left(c_i(T) - \mathcal{A}_0\big(T, T+\delta_i\big)\right)\right) \\ &\times \exp\left(\sum_{j=1}^m \big(\beta(\delta_j) - \beta(\delta_{j-1})\big) \int_0^T \mathcal{V}\Big(s,\, \mathcal{B}_0^j(\delta_i) + \mathsf{i}\,\zeta\,\big(\gamma_{i,j} - \mathcal{B}_0^j(\delta_i)\big), -\lambda_j\Big)\mathrm{d}s\right) \\ &\times \exp\left(\sum_{j=1}^m \mathcal{V}\Big(T,\, \mathcal{B}_0^j(\delta_i) + \mathsf{i}\,\zeta\,\big(\gamma_{i,j} - \mathcal{B}_0^j(\delta_i)\big), -\lambda_j\Big)\, X_0^j\right),\end{aligned}$$

where the application of Proposition 2.5 in the complex domain is justified by Remark 2.7 since that $\zeta \in \Lambda_i(T)$ ensures that $\mathrm{Re}\big(\mathcal{B}_0^j(\delta_i) + \mathsf{i}\,\zeta\,\big(\gamma_{i,j} - \mathcal{B}_0^j(\delta_i)\big)\big) < \theta/\eta$, for every $1 \leqslant j \leqslant m$.

We state the caplet valuation formula, which is a consequence of [**Lee04**, Theorem 5.1] and allows for a straightforward application of the FFT algorithm by [**CM99**]. Note that, according to the notation used by [**Lee04**], we have that $G = G_1$ and $b_0 = b_1 = 1 \in \Theta_i(T)$ (since condition (3.15) holds). Let $\bar{K}_i := 1 + \delta_i\, K$ and $\xi \in \mathbb{R}$ such that $1 + \xi \in \Theta_i(T)$. The arbitrage-free price of the caplet written on the Ibor rate of tenor δ_i for some $1 \leqslant i \leqslant m$, of strike K, maturity T, and settled in arrears at time $T + \delta_i$, is given by

$$P^{\mathrm{CPLT}}(T, \delta_i, K) = R_T^i\left(\bar{K}_i, \xi\right) + \frac{1}{\pi}\int_{0-\mathsf{i}\,\xi}^{\infty-\mathsf{i}\,\xi} \mathrm{Re}\left(e^{-\mathsf{i}\,\zeta\,\log(\bar{K}_i)}\,\frac{\Xi_T^i(\zeta-\mathsf{i})}{-\zeta\,(\zeta-\mathsf{i})}\right)\mathrm{d}\zeta, \tag{3.25}$$

where Ξ_T^i has been explicitly computed above, and where $R_T^i(\bar{K}_i, \xi)$ is given by

$$R_T^i\left(\bar{K}_i, \xi\right) = \begin{cases} \Xi_T^i(-\mathsf{i}) - \bar{K}_i\,\Xi_T^i(0), & \text{if } \xi < -1, \\ \Xi_T^i(-\mathsf{i}) - \frac{\bar{K}_i}{2}\,\Xi_T^i(0), & \text{if } \xi = -1, \\ \Xi_T^i(-\mathsf{i}), & \text{if } -1 < \xi < 0, \\ \frac{1}{2}\,\Xi_T^i(-\mathsf{i}), & \text{if } \xi = 0, \\ 0, & \text{if } \xi > 0. \end{cases}$$

3.4.2. Caplet pricing via quantization. The analytical tractability of CBI processes allows for the development of a quantization-based pricing methodology, which is here proposed for the first time in an interest rate setting. In this section, we show that the Fourier-based quantization technique recently introduced by [**CFG19a**] can be easily applied for the pricing of caplets.

The key ingredient of this approach is represented by the *quantization grid* denoted by $\Gamma^N = \{x_1, \ldots, x_N\}$, with $x_1 < \ldots < x_N$, for some chosen $N \in \mathbb{N}$ (see [**GL00, Pag15**] for details). Once the quantization grid Γ^N has been determined, the random variable $e^{\mathcal{X}_T^i}$ appearing in the general caplet valuation formula (3.23) can be approximated by its *Voronoi* Γ^N*-quantization*, i.e.

the nearest neighbor projection $\widehat{e^{\mathcal{X}_T^i}}$ of $e^{\mathcal{X}_T^i}$ onto Γ^N, given by the discrete random variable

$$\widehat{e^{\mathcal{X}_T^i}} = \sum_{j=1}^{N} x_j \, \mathbf{1}_{\left\{x_j^- \leqslant e^{\mathcal{X}_T^i} \leqslant x_j^+\right\}},$$

where $x_j^- = (x_{j-1}+x_j)/2$ and $x_j^+ = (x_{j+1}+x_j)/2$, for every $1 \leqslant j \leqslant N$, with $x_1^- = 0$ and $x_N^+ = +\infty$. Formula (3.23) can then be approximated as follows:

$$P^{\mathrm{CPLT}}(T, \delta_i, K) \approx B\big(0, T+\delta_i\big) \sum_{j=1}^{N} \big(x_j - (1 + K\,\delta_i)\big)^+ \, \mathbb{Q}^{T+\delta_i}\Big(\widehat{e^{\mathcal{X}_T^i}} = x_j\Big),$$

where the *companion weights* $\mathbb{Q}^{T+\delta_i}\big(\widehat{e^{\mathcal{X}_T^i}} = x_j\big)$, for every $1 \leqslant j \leqslant N$, are computed by

$$\mathbb{Q}^{T+\delta_i}\Big(\widehat{e^{\mathcal{X}_T^i}} = x_j\Big) = \mathbb{Q}^{T+\delta_i}\Big(e^{\mathcal{X}_T^i} \leqslant x_j^+\Big) - \mathbb{Q}^{T+\delta_i}\Big(e^{\mathcal{X}_T^i} \leqslant x_j^-\Big). \tag{3.26}$$

The core of quantization consists in optimally determining the quantization grid Γ^N in such a way that the discrete distribution of $\widehat{e^{\mathcal{X}_T^i}}$ over Γ^N is a good approximation of the continuous distribution of $e^{\mathcal{X}_T^i}$. This is achieved by choosing a grid Γ that minimizes the following L^p-distance:

$$D_p\big(\Gamma\big) = D_p\Big(\big\{x_1, \ldots, x_N\big\}\Big) := \Big\| e^{\mathcal{X}_T^i} - \widehat{e^{\mathcal{X}_T^i}} \Big\|_{L^p\left(\mathbb{Q}^{T+\delta_i}\right)} = \mathbb{E}^{T+\delta_i}\left[\min_{j=1,\ldots,N} \Big| e^{\mathcal{X}_T^i} - x_j \Big|^p \right]^{1/p}. \tag{3.27}$$

In the present setting, it can be shown that this minimization problem admits a unique solution of full size N (see [**Pag15**, Proposition 1.1]). In practice, Γ^N is typically determined by searching for the critical points of the map $\Gamma \mapsto D_p\big(\Gamma\big)$ (called *sub-optimal* quantization grids). In view of [**CFG19a**, Theorem 1], a sub-optimal quantization grid $\Gamma^N = \big\{x_1, \ldots, x_N\big\}$ is given by the solution to the following equation:

$$\int_0^{+\infty} \mathrm{Re}\left[\Delta_T^i(u)\, e^{-\,\mathsf{i}\,u\,\log(x_j)} \left(\bar\beta\left(\frac{x_j^-}{x_j}, -\,\mathsf{i}\,u, p \right) - \bar\beta\left(\frac{x_j}{x_j^+}, 1-p+\mathsf{i}\,u, p \right) \right) \right] \mathrm{d}u = 0, \tag{3.28}$$

for every $1 \leqslant j \leqslant N$, where $\bar\beta$ is defined as

$$\bar\beta(x, a, b) = \int_x^1 t^{a-1}\,(1-t)^{b-1}\,\mathrm{d}t,$$

for $a \in \mathbb{C}$, $\mathrm{Re}(b) > 0$, and $x \in (0,1)$, and Δ_T^i stands for the $(T+\delta_i)$-forward characteristic function of $\mathcal{X}_T^i$:

$$\Delta_T^i(u) := \mathbb{E}^{T+\delta_i}\left[e^{\,\mathsf{i}\,u\,\mathcal{X}_T^i} \right] = \frac{\Xi_T^i(u)}{B\big(0, T+\delta_i\big)}.$$

Equation (3.28) can be efficiently solved by using algorithms of Newton–Raphson type. Indeed, in the present framework, the gradient ∇D_p of the function D_p can be analytically computed and the associated Hessian matrix $H\big[D_p\big]$ turns out to be tridiagonal. In order to initialize the algorithm, the starting grid $\Gamma_{(0)}^N$ can be constructed by using a regular spacing around the expectation of the state variable $e^{\mathcal{X}_T^i}$, which is directly determined by market observables:

$$\mathbb{E}^{T+\delta_i}\left[e^{\mathcal{X}_T^i} \right] = \mathbb{E}^{T+\delta_i}\left[\frac{S^{\delta_i}(T,T)}{B\big(T, T+\delta_i\big)} \right] = 1 + \delta_i\, L\big(0, T, \delta_i\big).$$

Starting from $\Gamma^N_{(0)}$, a basic formulation of the Newton–Raphson algorithm for the determination of a sub-optimal quantization grid Γ^N is then based on the following iterations:

$$\Gamma^N_{(n+1)} = \Gamma^N_{(n)} - \Big(H\big[D_p\big](\Gamma^N_{(n)})\Big)^{-1} \nabla D_p(\Gamma^N_{(n)}),$$

which is performed at each iteration $n \in \mathbb{N}$.

Remark 3.12. We stress the fact that the companion weights $\mathbb{Q}^{T+\delta_i}\big(\widehat{e^{\mathcal{X}^i_T}} = x_j\big)$, for every $1 \leqslant j \leqslant N$, as well as the density function of the random variable $e^{\mathcal{X}^i_T}$, needed for the computation of the function $D_p\big(\Gamma\big)$ in equation (3.27), can be recovered from the $(T+\delta_i)$-forward characteristic function Δ^i_T. More specifically, it holds that

$$\mathbb{Q}^{T+\delta_i}\big(e^{\mathcal{X}^i_T} \in \mathrm{d}x\big) = \left(\frac{1}{x\pi}\int_0^{+\infty} \mathrm{Re}\left(e^{-\,\mathsf{i}\,u\,\log(x)}\,\Delta^i_T(u)\right)\mathrm{d}u\right)\mathrm{d}x,$$

$$\mathbb{Q}^{T+\delta_i}\big(e^{\mathcal{X}^i_T} \leqslant x\big) = \frac{1}{2} - \frac{1}{\pi}\int_0^{+\infty} \mathrm{Re}\left(\frac{e^{-\,\mathsf{i}\,u\,\log(x)}\,\Delta^i_T(u)}{\mathsf{i}\,u}\right)\mathrm{d}u.$$

Similarly to Ξ^i_T as explicitly computed in Section 3.4.1, Δ^i_T can also be analytically expressed by relying on the affine property of the CBI-driven multi-curve model.

3.5. Numerical results

This section contains some numerical results. We proceed as follows: first, we compare the two pricing methodologies proposed in Sections 3.4.1 and 3.4.2. Then, we calibrate the specification introduced in Section 3.3 to market data relative to the 3M and 6M tenors.

3.5.1. Numerical comparison of pricing methodologies. In this section, we implement the FFT and quantization-based pricing methodologies as previously developed. In order to assess the reliability of both approaches, we compare them under different combinations of moneyness, maturities, and model parameters. We preliminarily validate the FFT methodology by means of Monte Carlo simulations and, by relying on the simulation method described in Appendix 3.A, we verify that caplet prices computed by FFT correspond to Monte Carlo prices. This validation procedure enables us to take FFT prices as benchmark in the sequel.

We then compare the FFT and quantization-based pricing methods. Table 3.1 shows the results of this comparison, reporting the percentage differences between FFT and quantization prices for caplets with strikes 1% and 2%, and maturities ranging from 1 up to 2 years. This comparison over different strikes and maturities allows us to evaluate the reliability of the quantization approach against the FFT methodology. In Table 3.1, we use an FFT with 4096 points and a quantization grid of 10 points. The two proposed methodologies have different computation times. For the parameter set considered in Table 3.3, FFT prices are obtained in 2 seconds for each maturity. Concerning the quantization-based pricing method, the computation time is initially lower (0.5 seconds) but then, as the maturity increases, quantization becomes computationally more expensive, with an average computation time of 3 seconds for larger maturities.

As a further example, we report in Table 3.2 a comparison between the two methodologies for a different parameter set, corresponding to increased volatility. More specifically, we increase the parameters σ and η by 50% with respect to the calibrated values reported in Table 3.3, and set $\alpha = 1.8$. The first run of the comparison was not totally satisfactory since we observed that the prices produced by quantization (using a grid with 10 points) were diverging from those obtained via FFT. This issue has been solved by increasing the number of points for the quantization from 10 to 20, leading to an accuracy comparable to Table 3.1. This analysis highlights the fact that some care should be taken when utilizing the quantization-based pricing methodology: for some parameter set, one needs to re-adjust the meta-parameters of the numerical scheme, which is a delicate task to carry out during the execution of a calibration. In summary, we consider the FFT approach more robust and more computationally efficient in view of the calibration of the model.

	FFT 2%	Quant. 2%	Difference 2%	FFT 1%	Quant. 1%	Difference 1%
1	0.0064146	0.0063414	1.1554%	0.0065360	0.0070082	−6.7368%
1.1	0.0064303	0.0063641	1.0404%	0.0065520	0.0070325	−6.8330%
1.2	0.0064460	0.0063868	0.92556%	0.0065679	0.0070569	−6.9292%
1.3	0.0064679	0.0064187	0.76738%	0.0065903	0.0070910	−7.0616%
1.4	0.0064983	0.0064626	0.55350%	0.0066212	0.0071381	−7.2408%
1.5	0.0065291	0.0065069	0.34038%	0.0066525	0.0071857	−7.4193%
1.6	0.0065600	0.0065516	0.12813%	0.0066839	0.0072335	−7.5972%
1.7	0.0065911	0.0065966	−0.083181%	0.0067157	0.0072818	−7.7743%
1.8	0.0066250	0.0066458	−0.31232%	0.0067502	0.0073345	−7.9664%
1.9	0.0066620	0.0070707	−5.7812%	0.0067878	0.0078016	−12.995%
2	0.0066992	0.0071339	−6.0934%	0.0068257	0.0078694	−13.264%

TABLE 3.1. Comparison of FFT and quantization prices for different maturities (strikes at 2% and 1%, differences in relative terms). Quantization with 10 points and FFT with 4096 points. The parameter set used here is reported in Table 3.3.

	FFT 2%	Quant. 2%	Difference 2%	FFT 1%	Quant. 1%	Difference 1%
1	0.0064262	0.0063429	1.3127%	0.0065478	0.0070095	−6.5867%
1.1	0.0064433	0.0063672	1.1951%	0.0065652	0.0070356	−6.6849%
1.2	0.0064605	0.0063917	1.0773%	0.0065827	0.0070618	−6.7832%
1.3	0.0064841	0.0064252	0.91574%	0.0066067	0.0070978	−6.9182%
1.4	0.0065162	0.0064710	0.69830%	0.0066394	0.0071468	−7.1000%
1.5	0.0065487	0.0065173	0.48133%	0.0066725	0.0071965	−7.2815%
1.6	0.0065814	0.0065641	0.26495%	0.0067058	0.0072466	−7.4625%
1.7	0.0066145	0.0066113	0.049213%	0.0067395	0.0072973	−7.6430%
1.8	0.0066505	0.0066628	−0.18451%	0.0067761	0.0073525	−7.8387%
1.9	0.0066896	0.0070315	−4.8632%	0.0068159	0.0077575	−12.138%
2	0.0067291	0.0070963	−5.1748%	0.0068561	0.0078270	−12.405%

TABLE 3.2. Comparison of FFT and quantization prices for different maturities (strikes at 2% and 1%, differences in relative terms). Quantization with 20 points and FFT with 4096 points. Starting from the parameters reported in Table 3.3, we increased σ and η by 50% and set $\alpha = 1.8$.

3.5.2. Model calibration. To illustrate the calibration of our model specification presented in Section 3.3, we start by describing the market data and the reconstruction of the term structures.

3.5.2.1. *Market data.* We consider market data for the EUR market as of 25 June 2018, which consists of both linear and non-linear interest rate derivatives. The set of tenors is $\mathcal{G} = \{3\mathrm{M}, 6\mathrm{M}\}$. Market data on linear products consist of OIS and interest rate swaps, from which the discount curve $T \mapsto B(0,T)$ along with the forward curves $T \mapsto L(0,T,\delta_i)$, for $\delta_1 = 3\mathrm{M}$ and $\delta_2 = 6\mathrm{M}$, are constructed by relying on the bootstrapping procedure from the Finmath Java library (see [**Fri21**]). The OIS discount curve is bootstrapped from OIS swaps, by using cubic spline interpolation on logarithmic discount factors with constant extrapolation. Similarly, the 3M and 6M forward curves are bootstrapped from market quotes of FRAs (for short maturities) and swaps (for maturities beyond two years), by using cubic spline interpolation on forwards with constant extrapolation. Figure 3.3 reports the resulting discount and forward curves. We notice that, for short maturities, discount factors are larger than one and forward rates are negative.

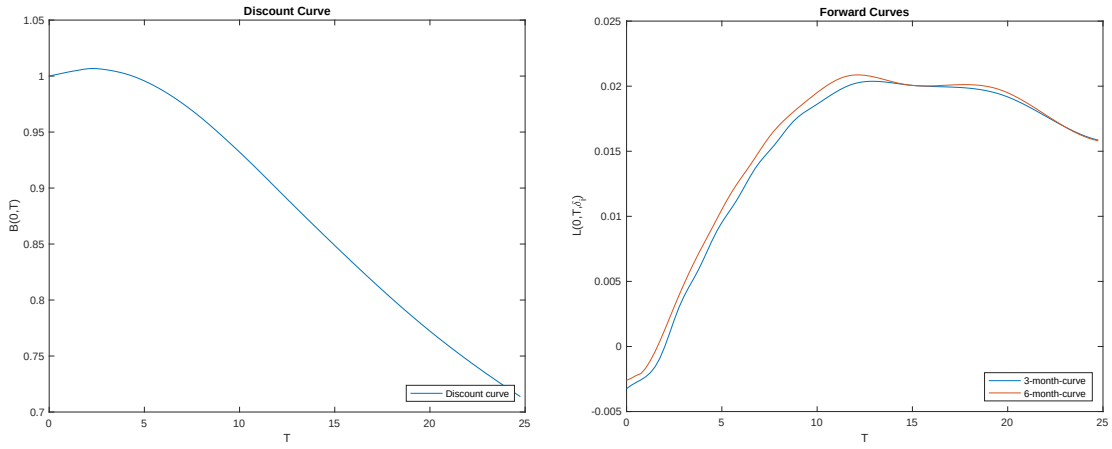

FIGURE 3.3. Discount and forward curves as of 25 June 2018.

As far as non-linear interest rate products are concerned, we focus on caplet market data, suitably bootstrapped from market cap volatilities. Consistently with the presence of negative interest rates, we also have market quotes for caps having a negative strike rate. Therefore, the boostrapped caplet volatility surface refers to strike prices ranging between -0.13% and 2%, and maturities between 6 months and 6 years. Caplets with maturity larger than two years are indexed to the 6-month rate, while those with shorter expiry are linked to the 3-month curve. Market data is given in terms of *normal* implied volatilities. More specifically, for a caplet written on the Ibor rate of tenor δ, of strike K, and maturity T, the normal implied volatility is obtained by searching for the value of $\sigma^{\mathrm{imp}}_{\mathrm{mkt}}(K, T+\delta)$ such that the Bachelier pricing formula

$$P^{\mathrm{CPLT}}_{Bac}(T,\delta,K) := B(0,T+\delta)\,\delta\,\sigma^{\mathrm{imp}}_{\mathrm{mkt}}(K,T+\delta)\,\sqrt{T}\left(\frac{1}{\sqrt{2\,\pi}}\,e^{-\frac{z^2}{2}} + z\,N(z)\right), \tag{3.29}$$

where we have

$$N(x) = \frac{1}{\sqrt{2\,\pi}}\int_{-\infty}^{x} e^{-\frac{y^2}{2}}\,\mathrm{d}y \qquad \text{and} \qquad z = \frac{L(0,T,\delta)-K}{\sigma_N\,\sqrt{T}},$$

provides the best fit to the market price of the caplet under consideration.

3.5.2.2. *Implementation.* For a certain vector p of model parameters belonging to the set $\mathcal{P}$ of admissible values (see Section 3.3), we compute model-implied caplet prices by means of the FFT pricing method presented in Section 3.4.1, where the numerical integration is performed along the lines of [**CM99**] with 32768 points and integration mesh size 0.05. For a fixed maturity, a single execution of the FFT routine yields a vector of model prices for several moneyness levels. Prices are then converted into normal implied volatilities by using formula (3.29).

Repeating this procedure for different maturities, we are able to generate a model-implied volatility $\sigma^{\mathrm{imp}}_{\mathrm{mod}}(K_k, T_j, p)$ for each strike K_k and each maturity T_j of the sample of market data under consideration. The purpose of the calibration is then to find the vector of parameters that solves the following minimization problem:

$$\min_{p\in\mathcal{P}} \sum_{j,k} \Big(\sigma^{\mathrm{imp}}_{\mathrm{mkt}}(K_k, T_j) - \sigma^{\mathrm{imp}}_{\mathrm{mod}}(K_k, T_j, p)\Big)^2. \tag{3.30}$$

3.5.2.3. *Calibration results.* We calibrate a two-tenor version of the model specification of Section 3.3. In view of the resolution of problem (3.30), we use the multi-threaded Levenberg–Marquardt optimizer of the Finmath Java library with 8 threads, while imposing the necessary parameter restrictions presented in Sections 3.3.1 and 3.3.2. We also fix the normalization constant C_α appearing in the measure π of the flow of tempered-stable CBI processes as follows:

$$C_\alpha := -\frac{1}{\Gamma(-\alpha)\cos(\alpha\,\pi/2)}.$$

The calibrated values of the model parameters are then reported in Table 3.3. In particular, we can observe that the results demonstrate an important role of the jump component, apparently more important than the diffusive component. The calibrated value of α is rather close to 1, thus showing evidence of persistence of low values (compare with the discussion before Remark 3.9 in Section 3.3.2). Together with the rather small value of θ, this also indicates a significant likelihood of large jumps, giving rise to potential jump clustering.

As illustrated by Figures 3.4, the model achieves a good fit to market data, across different strikes and maturities. Furthermore, we remark that, in terms of number of parameters, the specification under consideration, i.e. driven by a flow of tempered-stable CBI processes, is even more parsimonious than the simple specifications calibrated in [**CFG19b**].

Motivated by the presence of negative forward rates, we also calibrated a version of the model where the OIS short rate is affected by an auxiliary *Ornstein–Uhlenbeck process*, in line with Remark 3.6. However, this alternative specification did not yield a significant improvement of the quality of the fit. This seems to indicate that the deterministic-shift function ℓ, accounting for the initially-observed term structure of OIS zero-coupon bonds, does suffice to capture the negativity of the short rate. This is also in line with the widespread use of deterministic-shift extensions in the financial industry (see e.g. [**Mer18a**]).

b	0.05353	α	1.31753
σ	0.00582	Y_0	$(0.00495, 0.00507)^\top$
η	0.04070	β	$(9.99999E-4, 0.00340)^\top$
θ	0.05070	μ	$(1.49999, 1.00000)^\top$

TABLE 3.3. Calibrated values of the parameters.

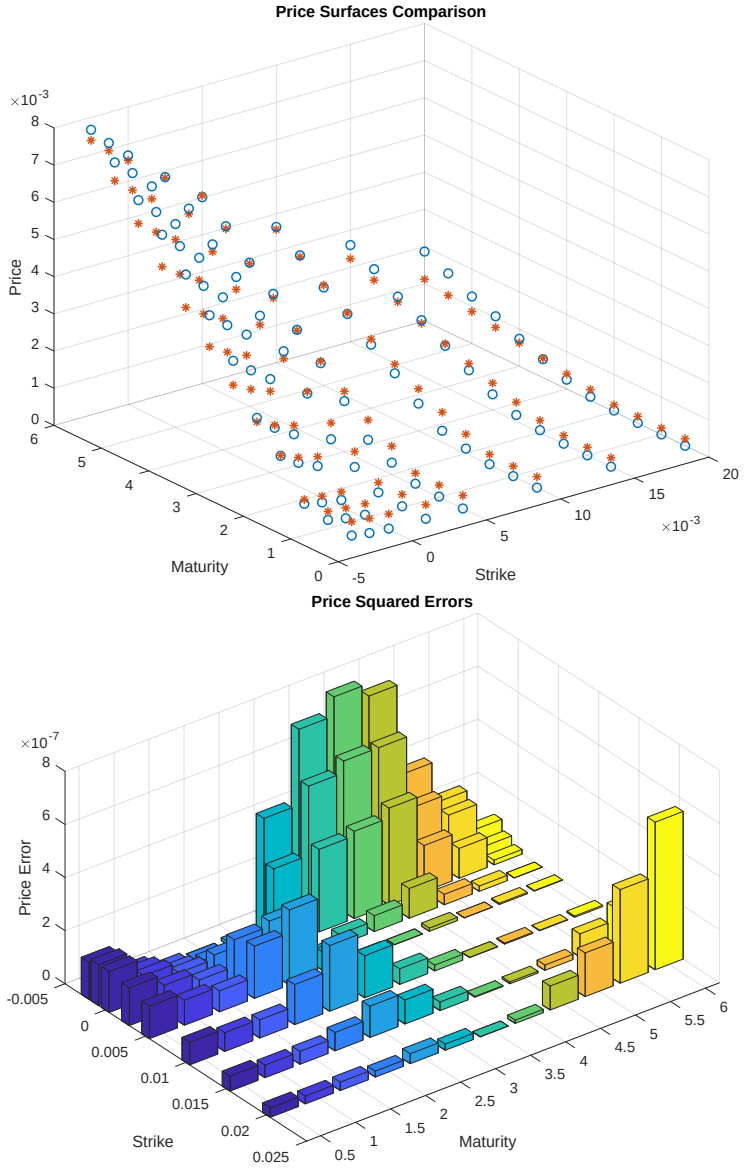

FIGURE 3.4. Model prices against market prices as of 25 June 2018.
On the top panel, market prices are represented by blue circles, while model prices by red stars. On the bottom panel, price squared errors are reported.

3.6. Conclusion

In the present paper, we have proposed a modeling framework for multiple yield curves based on CBI processes. The self-exciting behavior of jump-type CBI processes is consistent with most of the empirical features of spreads. At the same time, exploiting the fundamental link with affine processes, the proposed approach allows for an efficient valuation of interest rate derivatives.

Specifically motivated by capturing the relevant empirical features of the spreads between different interbank rates (see Figure 3.1), we have constructed a novel class of multi-curve models driven by a flow of tempered alpha-stable CBI processes.

In particular, we have shown that such multi-curve models represent a parsimonious way of modeling spreads in a realistic way, with a natural interpretation of the stochastic drivers in terms of risk factors. In our view, flows of CBI processes can lead to further interesting applications to financial markets where multiple term structures coexist.

3.A. Appendix: A simulation scheme

In this appendix, we describe a simulation scheme for tempered-stable CBI processes as presented in Section 2.7. We emphasize that this scheme has been used to generate the sample paths exhibited by Figure 3.2. Note that, by Theorem 3.10, and in view of simulating a multi-curve model driven by a flow of tempered-stable processes in the sense of Definition 3.7, it suffices to simulate m mutually-independent tempered-stable CBI processes. Consequently, we shall restrict our attention to the simulation of a one-dimensional tempered-stable CBI process $X = (X_t)_{t \leqslant \mathcal{T}}$, for some fixed time horizon $\mathcal{T} > 0$.

We can suppose, without loss of generality, that the underlying stochastic basis supports the following two independent objects:

- A standard Brownian motion $B = (B_t)_{t \leqslant \mathcal{T}}$;
- A Poisson random measure $N_1(\mathrm{d}t, \mathrm{d}u, \mathrm{d}x)$ on $[0, \mathcal{T}] \times \mathbb{R}_+ \times \mathbb{R}_+$ with compensator $\mathrm{d}t\, \mathrm{d}u\, \pi(\mathrm{d}x)$ and compensated measure $\widetilde{N}_1(\mathrm{d}t, \mathrm{d}u, \mathrm{d}x) := N_1(\mathrm{d}t, \mathrm{d}u, \mathrm{d}x) - \mathrm{d}t\, \mathrm{d}u\, \pi(\mathrm{d}x)$,

where we set $\pi(\mathrm{d}z) = \eta^\alpha\, C_\alpha\, z^{-1-\alpha}\, e^{-\frac{\theta}{\eta} z}\, \mathbf{1}_{\{z>0\}}\, \mathrm{d}z$, with $\eta > 0$, $C_\alpha > 0$, $\theta > 0$, and $\alpha \in (1, 2)$. For $X_0 \geqslant 0$, consider the stochastic integral equation

$$X_t = X_0 + \int_0^t \big(\beta - b\, X_s\big)\, \mathrm{d}s + \sigma \int_0^t \sqrt{X_s}\, \mathrm{d}B_s + \int_0^t \int_0^{X_{s-}} \int_0^{+\infty} x\, \widetilde{N}_1(\mathrm{d}s, \mathrm{d}u, \mathrm{d}x), \qquad \forall t \leqslant \mathcal{T}. \tag{3.31}$$

We recall from Section 2.5 that there exists a unique non-negative strong solution to equation (3.31), which is a tempered-stable CBI process (see Theorem 2.12 and Definition 2.18).

In order to simulate a sample path of the process $X = (X_t)_{t \leqslant \mathcal{T}}$, we resort to the regular Euler method for stochastic differential equations with jumps as described by [**PBL10**, Chapter 6]. We consider an equidistant partition of the time interval $[0, \mathcal{T}]$ with N steps (e.g. $N = 1000$). We let $\Delta := \mathcal{T}/N$ and $t_n := n\, \Delta$, for every $0 \leqslant n \leqslant N$, and denote by $\hat{X} = (\hat{X}_{t_n})_{0 \leqslant n \leqslant N}$, the approximation of the tempered-stable CBI process $X = (X_t)_{t \leqslant \mathcal{T}}$.

We start by approximating the Lévy measure π by its truncated version $\pi_\epsilon(\mathrm{d}z) := \pi(\mathrm{d}z)\,\mathbf{1}_{\{z \geqslant \epsilon\}}$, for a sufficiently small $\epsilon > 0$ (e.g. $\epsilon = 0.001$)[2]. The total mass of π_ϵ is given by

$$C_\epsilon := \pi_\epsilon(\mathbb{R}_+) = \eta^\alpha\, C_\alpha \int_\epsilon^{+\infty} z^{-1-\alpha}\, e^{-\frac{\theta}{\eta} z}\, \mathrm{d}z = \theta^\alpha\, C_\alpha\, \Gamma\big(-\alpha, \epsilon\,\theta/\eta\big),$$

where $\Gamma\big(-\alpha, \epsilon\,\theta/\eta\big) := \int_{\epsilon\theta/\eta}^{+\infty} u^{-\alpha-1}\, e^{-u}\, \mathrm{d}u$ denotes the incomplete Gamma function (see e.g. [**Leb72**, Problem 1.10]). For every $1 \leqslant n \leqslant N$, we approximate the number of jumps generated by the Poisson random measure N_1 in the time interval $[t_{n-1}, t_n]$ by a random variable J_n following a Poisson distribution with intensity

$$\int_{t_{n-1}}^{t_n} \int_0^{\hat{X}_{t_{n-1}}} \int_0^{+\infty} \mathrm{d}s\, \mathrm{d}u\, \pi_\epsilon(\mathrm{d}z) = C_\epsilon\, \hat{X}_{t_{n-1}}\, \Delta. \tag{3.32}$$

The random variables representing the sizes of the jumps generated by the Poisson random measure N_1 are drawn from a distribution with density f_ϵ, where

$$f_\epsilon(z) = \frac{1}{C_\epsilon}\, \frac{\pi_\epsilon(\mathrm{d}z)}{\mathrm{d}z} = \frac{\eta^\alpha}{\theta^\alpha\, \Gamma\big(-\alpha, \epsilon\,\theta/\eta\big)}\, z^{-1-\alpha}\, e^{-\frac{\theta}{\eta} z}\, \mathbf{1}_{\{z \geqslant \epsilon\}}. \tag{3.33}$$

In particular, observe that

$$f_\epsilon(z) \leqslant \frac{\eta^\alpha\, e^{-\epsilon\,\theta/\eta}}{\alpha\,(\epsilon\,\theta)^\alpha\, \Gamma\big(-\alpha, \epsilon\,\theta/\eta\big)}\, \alpha\, \epsilon^\alpha\, z^{-1-\alpha}\, \mathbf{1}_{\{z \geqslant \epsilon\}} = \frac{\eta^\alpha\, e^{-\epsilon\,\theta/\eta}}{\alpha\,(\epsilon\,\theta)^\alpha\, \Gamma\big(-\alpha, \epsilon\,\theta/\eta\big)}\, f_{\epsilon,\alpha}^{\mathrm{Par}}(z), \tag{3.34}$$

where $f_{\epsilon,\alpha}^{\mathrm{Par}}$ denotes the density function of a Pareto distribution with scale ϵ and shape α. In view of relation (3.34), we can simulate random variables with density f_ϵ by means of an acceptance-rejection scheme (see e.g. [**Pag15**, Section 1.4]) based on a Pareto distribution.

In order to construct the approximation $\hat{X} = (\hat{X}_{t_n})_{1 \leqslant n \leqslant N}$, we set $\hat{X}_0 := X_0$ and by means of successive iterations, for every $1 \leqslant n \leqslant N$, we write

$$\hat{X}_{t_n} := \hat{X}_{t_{n-1}} + \Big(\beta - \big(b + \eta\,\theta^{\alpha-1}\, C_\alpha\, \Gamma\big(1-\alpha, \epsilon\,\theta/\eta\big)\big)\, \hat{X}_{t_{n-1}}\Big)\, \Delta \,+\, \sigma \sqrt{\Delta \left(\hat{X}_{t_{n-1}}\right)^+}\, Z_n \,+\, \sum_{k=0}^{J_n} \xi_{n,k},$$

where $(Z_n)_{1 \leqslant n \leqslant N}$ is a sequence of i.i.d. standard Normal random variables, $(J_n)_{1 \leqslant n \leqslant N}$ is a sequence of independent random variables such that each J_n follows a Poisson distribution with intensity given by (3.32), and $(\xi_{n,k})_{1 \leqslant n \leqslant N,\, k \geqslant 0}$ is a family of i.i.d. random variables with common density f_ϵ as computed in (3.33).

[2] This truncation of the Lévy measure π serves to achieve integrability, at the expense of eliminating very small jumps. Along the lines of [**AR01**], the small jump component can be approximated by introducing a suitably-rescaled Brownian motion B', which is independent of the Brownian motion B appearing in (3.31).

Part 2

Multiple currencies

CHAPTER 4

CBI-time-changed Lévy processes

SUMMARY. We introduce a class of two-dimensional processes combining CBI processes with time-changed Lévy processes, which we name *CBI-time-changed Lévy processes* (CBITCL). We develop an analytical framework extending most of the results presented in Chapter 2 for CBI processes, which will be applied to multiple currency modeling in Chapter 5. We generalize the stochastic representations of a CBI processes, obtaining a characterization of CBITCL processes as weak solutions to a system of stochastic integral equations of Dawson–Li type. We show that CBITCL processes are affine, allowing for a precise analysis of exponential moments of CBITCL processes. Finally, we formulate a Girsanov-type theorem for CBITCL processes.

Contents

4.1. Introduction

Time-changed processes were first introduced in finance by [**Cla73**] as *subordinated processes*, where the base process was a Brownian motion and the stochastic clock a *subordinator* (i.e. a non-decreasing Lévy process). In order to relax the restrictions imposed by subordinators, [**AG00, GMY01**] introduced more general stochastic time changes. Moreover, [**AG00**] showed that the accumulated number of trades represents a better stochastic clock as a proxy for the market activity than the trading volume, as initially postulated by [**Cla73**].

In general, a stochastic time change is defined by a time integral of a non-negative càdlàg stochastic process. This integral denotes the accumulated number of trades, while the process to be integrated, also called *instantaneous activity rate*, represents the number of trades per unit of time (i.e. the speed at which the trading activity runs). As an illustration, if the speed of trading is high/low, then the stochastic clock elapses faster/slower, giving rise to stochastic volatility.

In this regard, [**CGMY03**] developed a class of stochastic volatility models based on more general time-changed processes, where the base process was allowed to be a Lévy process. Then, [**CW04**] presented an analytical framework for time-changed Lévy processes unifying almost all existing stochastic volatility approaches, also pointing out the possible use of CBI processes for modeling the activity rate. An empirical analysis of specifications of this general framework was performed by [**HW04**], restricting however the analysis to CIR-type activity rates. The authors concluded that a modern approach for modeling the activity rate should contain a high-frequency jump structure that can potentially excite itself.

In this chapter, we introduce a class of two-dimensional processes combining the self-exciting behavior of CBI process with the generality of time-changed Lévy processes, which we name *CBI-time-changed Lévy processes*. This class of processes will be applied to multiple currency modeling in Chapter 5. In Section 4.2, we start by defining CBITCL processes as solutions to a system of stochastic time change equations, where we extend the Lamperti-type stochastic time change representation of a CBI process. We then characterize CBITCL processes as weak solutions to a system of stochastic integral equations of Dawson–Li type.

We show in Section 4.3 that CBITCL processes are affine in the sense of [**DFS03**]. We exploit this result by deriving a complete analysis of exponential moments of CBITCL processes, which mostly generalizes the results previously obtained for CBI processes. Finally, by relying on the techniques of [**KS02a**] in Section 4.5, and by fixing a finite time horizon, we characterize a class of equivalent changes of probability of Esscher type that leave invariant the class of CBITCL processes. We formulate this result as a Girsanov-type theorem, which will find relevant applications in multiple currency modeling (see Chapter 5).

4.2. Construction and characterization

We fix a stochastic basis $\big(\Omega, \mathcal{F}, \mathbb{F}, \mathbb{Q}\big)$ satisfying the usual conditions, where $\mathbb{Q}$ is a probability measure and $\mathbb{F} = (\mathcal{F}_t)_{t\geqslant 0}$ a filtration to which all stochastic processes are assumed to be adapted. We set $\mathcal{F} = \mathcal{F}_\infty$ and denote the expectation under $\mathbb{Q}$ by $\mathbb{E}$.

We begin with the construction of CBITCL processes, extending the Lamperti-type stochastic time change representation of Definition 2.11. Recall from Chapter 2 that when $X = (X_t)_{t\geqslant 0}$ is a non-negative càdlàg stochastic process, its time integral $Y_t := \int_0^t X_s \,\mathrm{d}s$, for all $t \geqslant 0$, can be utilized as a finite, continuous time change. We then suppose that the stochastic basis $\big(\Omega, \mathcal{F}, \mathbb{F}, \mathbb{Q}\big)$ supports the following Lévy processes, assumed to be mutually independent:

- A non-decreasing Lévy process $L^\Psi = (L^\Psi_t)_{t\geqslant 0}$ with $L^\Psi_0 = 0$, whose Lévy exponent is denoted by Ψ, given by (2.1), and characterized by the Lévy triplet $(\beta, 0, \nu)$, where $\beta \geqslant 0$ and ν is a Lévy measure on $\mathbb{R}_+$ such that $\int_0^1 z\,\nu(\mathrm{d}z) < +\infty$;
- A spectrally positive Lévy process $L^\Phi = (L^\Phi_t)_{t\geqslant 0}$ with $L^\Phi_0 = 0$ and finite first moment, whose Lévy exponent is denoted by Φ, given by (2.2), and characterized by the Lévy triplet $(-b, \sigma, \pi)$, where $b \in \mathbb{R}$, $\sigma \geqslant 0$, and π is a Lévy measure on $\mathbb{R}_+$ such that $\int_1^{+\infty} z\,\pi(\mathrm{d}z) < +\infty$;
- A Lévy process $L^Z = (L^Z_t)_{t\geqslant 0}$ with $L^Z_0 = 0$, whose Lévy exponent $\Xi_Z : \mathrm{i}\,\mathbb{R} \to \mathbb{C}$ is determined by the Lévy triplet $(b_Z, \sigma_Z, \gamma_Z)$, where $b_Z \in \mathbb{R}$, $\sigma_Z \geqslant 0$, and γ_Z is a Lévy measure on $\mathbb{R}$. We recall that Ξ_Z is given by the *Lévy–Khintchine representation*

$$\Xi_Z(u) := b_Z\, u + \frac{1}{2}\,(\sigma_Z\, u)^2 + \int_{\mathbb{R}} \big(e^{z\,u} - 1 - z\,u\,\mathbf{1}_{\{|z|<1\}}\big)\,\gamma_Z(\mathrm{d}z), \qquad \forall u \in \mathrm{i}\,\mathbb{R}. \tag{4.1}$$

Definition 4.1. A joint process $(X_t, Z_t)_{t\geqslant 0}$, where

- $X = (X_t)_{t\geqslant 0}$ is a non-negative càdlàg stochastic process with initial value X_0;
- $Z = (Z_t)_{t\geqslant 0}$ is a càdlàg stochastic process with initial value $Z_0 = 0$,

is said to be a *CBI-time-changed Lévy process* (CBITCL) if it satisfies the following stochastic time change equations:

$$X_t = X_0 + L^\Psi_t + L^\Phi_{Y_t}, \tag{4.2}$$

$$Z_t = L^Z_{Y_t}, \tag{4.3}$$

for all $t \geqslant 0$, where $Y_t := \int_0^t X_s \,\mathrm{d}s$.

For any $X_0 \geqslant 0$, there exists a unique strong solution to system (4.2)–(4.3). Indeed, equation (4.2) corresponds to the *Lamperti-type representation* of a CBI process, for which there exists a unique non-negative strong solution $X = (X_t)_{t\geqslant 0}$, which is a $\mathrm{CBI}\big(X_0, \Psi, \Phi\big)$ of Definition 2.1 (see Section 2.5). Observe that the right-hand side of equation (4.3) does not depend on the process $Z = (Z_t)_{t\geqslant 0}$, but on the CBI process $X = (X_t)_{t\geqslant 0}$.

Any CBITCL process in the sense of Definition 4.1 will be denoted by $\mathrm{CBITCL}\big(X_0, \Psi, \Phi, \Xi_Z\big)$. Inspired by [**DL06**], we can also extend the Dawson–Li stochastic integral representation in the sense of Definition 2.10 to CBITCL processes. To this purpose, let us assume the existence of the following objects:

- Two standard Brownian motions $B^1 = (B^1_t)_{t\geqslant 0}$ and $B^2 = (B^2_t)_{t\geqslant 0}$;
- A Poisson random measure $N_0(\mathrm{d}t, \mathrm{d}x)$ on $\mathbb{R}_+ \times \mathbb{R}_+$ with compensator $\mathrm{d}t\,\nu(\mathrm{d}x)$ and compensated measure $\widetilde{N}_0(\mathrm{d}t, \mathrm{d}x) := N_0(\mathrm{d}t, \mathrm{d}x) - \mathrm{d}t\,\nu(\mathrm{d}x)$;
- A Poisson random measure $N_1(\mathrm{d}t, \mathrm{d}u, \mathrm{d}x)$ on $\mathbb{R}_+ \times \mathbb{R}_+ \times \mathbb{R}_+$ with compensator $\mathrm{d}t\,\mathrm{d}u\,\pi(\mathrm{d}x)$ and compensated measure $\widetilde{N}_1(\mathrm{d}t, \mathrm{d}u, \mathrm{d}x) := N_1(\mathrm{d}t, \mathrm{d}u, \mathrm{d}x) - \mathrm{d}t\,\mathrm{d}u\,\pi(\mathrm{d}x)$;
- A Poisson random measure $N_2(\mathrm{d}t, \mathrm{d}u, \mathrm{d}x)$ on $\mathbb{R}_+ \times \mathbb{R}_+ \times \mathbb{R}$ with compensator $\mathrm{d}t\,\mathrm{d}u\,\gamma_Z(\mathrm{d}x)$ and compensated measure $\widetilde{N}_2(\mathrm{d}t, \mathrm{d}u, \mathrm{d}x) := N_2(\mathrm{d}t, \mathrm{d}u, \mathrm{d}x) - \mathrm{d}t\,\mathrm{d}u\,\gamma_Z(\mathrm{d}x)$.

We suppose that B^1, B^2, N_0, N_1, and N_2 are mutually independent. Let us then define, for any $X_0 \in \mathbb{R}_+$, the following system of stochastic integral equations:

$$\begin{aligned} X_t &= X_0 + \int_0^t \big(\beta - b\,X_s\big)\,\mathrm{d}s + \sigma \int_0^t \sqrt{X_s}\,\mathrm{d}B^1_s \\ &\quad + \int_0^t \int_0^{+\infty} x\,N_0(\mathrm{d}s, \mathrm{d}x) + \int_0^t \int_0^{X_{s-}} \int_0^{+\infty} x\,\widetilde{N}_1(\mathrm{d}s, \mathrm{d}u, \mathrm{d}x), \qquad \forall t \geqslant 0, \end{aligned} \tag{4.4}$$

$$\begin{aligned} Z_t &= b_Z \int_0^t X_s\,\mathrm{d}s + \sigma_Z \int_0^t \sqrt{X_s}\,\mathrm{d}B^2_s + \int_0^t \int_0^{X_{s-}} \int_{|x|\geqslant 1} x\,N_2(\mathrm{d}s, \mathrm{d}u, \mathrm{d}x) \\ &\quad + \int_0^t \int_0^{X_{s-}} \int_{|x|<1} x\,\widetilde{N}_2(\mathrm{d}s, \mathrm{d}u, \mathrm{d}x), \qquad \forall t \geqslant 0, \end{aligned} \tag{4.5}$$

Since we do not assume finiteness of the first moment of the Lévy measure γ_Z, we cannot directly apply [**DL06**, Theorem 6.2] to system (4.4)–(4.5). However, it can be easily checked that for any $X_0 \geqslant 0$, there exists a unique strong solution to system (4.4)–(4.5). Indeed, equation (4.4) corresponds to the *Dawson–Li representation* of a CBI process, for which there is a unique non-negative strong solution $X = (X_t)_{t\geqslant 0}$, which is a $\mathrm{CBI}\big(X_0, \Psi, \Phi\big)$ (see Section 2.5). The existence of a unique strong solution follows from the fact that the right-hand side of (4.5) does not depend on the process $Z = (Z_t)_{t\geqslant 0}$, but only on the process $X = (X_t)_{t\geqslant 0}$.

The next result, which extends Theorem 2.12 and relies on similar techniques, characterizes the class of CBITCL processes as weak solutions to system (4.4)–(4.5). In particular, it provides an alternative way of defining a CBITCL process, which will be used in multiple currency modeling in Chapter 5.

LEMMA 4.2. *A joint process $(X_t, Z_t)_{t\geqslant 0}$ with initial value $(X_0, 0)$ is a $\mathrm{CBITCL}\big(X_0, \Psi, \Phi, \Xi_Z\big)$ if and only if it is a weak solution to system* (4.4)–(4.5).

PROOF. We follow the lines of the proof of Theorem 2.12, providing full details for the sake of completeness. Since $X = (X_t)_{t\geqslant 0}$ is a $\mathrm{CBI}\big(X_0, \Psi, \Phi\big)$, the weak equivalence between equations (4.2) and (4.4) follows directly from Theorem 2.12. We henceforth restrict our attention to the process $Z = (Z_t)_{t\geqslant 0}$. We then proceed as follows.

Let $Z = (Z_t)_{t\geqslant 0}$ be given by equation (4.3). By using the Lévy-Itô decomposition of the Lévy process $L^Z = (L^Z_t)_{t\geqslant 0}$, we obtain

$$Z_t = L^Z_{Y_t} = b_Z\,Y_t + \sigma_Z\,W_{Y_t} + \int_0^{Y_t} \int_{|x|\geqslant 1} x\,N(\mathrm{d}s, \mathrm{d}x) + \int_0^{Y_t} \int_{|x|<1} x\,\widetilde{N}(\mathrm{d}s, \mathrm{d}x), \qquad \forall t \geqslant 0, \tag{4.6}$$

where $W = (W_t)_{t\geqslant 0}$ is a Brownian motion independent of the Poisson random measure $N(\mathrm{d}t, \mathrm{d}x)$ with compensator $\mathrm{d}t\,\gamma_Z(\mathrm{d}x)$ and compensated measure $\widetilde{N}(\mathrm{d}t, \mathrm{d}x) := N(\mathrm{d}t, \mathrm{d}x) - \mathrm{d}t\,\gamma_Z(\mathrm{d}x)$. By using the change-of-variable formula of [**Jac79**, Theorem 10.27], we can rewrite both stochastic integrals appearing in (4.6) by means of the time-changed random measure $N(X_t\,\mathrm{d}t, \mathrm{d}x)$ with compensator $X_{t-}\,\mathrm{d}t\,\gamma_Z(\mathrm{d}x)$, yielding

$$\int_0^{Y_t}\int_{|x|\geqslant 1} x\,N(\mathrm{d}s, \mathrm{d}x) = \int_0^t\int_{|x|\geqslant 1} x\,N(X_s\,\mathrm{d}s, \mathrm{d}x),$$
$$\int_0^{Y_t}\int_{|x|< 1} x\,\widetilde{N}(\mathrm{d}s, \mathrm{d}x) = \int_0^t\int_{|x|< 1} x\,\widetilde{N}(X_s\,\mathrm{d}s, \mathrm{d}x),$$

for all $t \geqslant 0$. By [**IW89**, Theorem II.7.4], possibly on an enlarged probability space, there exists a Poisson random measure $N_2(\mathrm{d}t, \mathrm{d}u, \mathrm{d}x)$ with compensator $\mathrm{d}t\,\mathrm{d}u\,\gamma_Z(\mathrm{d}x)$ and compensated measure $\widetilde{N}_2(\mathrm{d}t, \mathrm{d}u, \mathrm{d}x) := N_2(\mathrm{d}t, \mathrm{d}u, \mathrm{d}x) - \mathrm{d}t\,\mathrm{d}u\,\gamma_Z(\mathrm{d}x)$ such that

$$\int_0^t\int_{|x|\geqslant 1} xN(X_s\,\mathrm{d}s, \mathrm{d}x) = \int_0^t\int_0^{X_{s-}}\int_{|x|\geqslant 1} x\,N_2(\mathrm{d}s, \mathrm{d}u, \mathrm{d}x)$$
$$\int_0^t\int_{|x|< 1} x\,\widetilde{N}(X_s\,\mathrm{d}s, \mathrm{d}x) = \int_0^t\int_0^{X_{s-}}\int_{|x|< 1} x\,\widetilde{N}_2(\mathrm{d}s, \mathrm{d}u, \mathrm{d}x)$$

for all $t \geqslant 0$. Similarly, there exists a Brownian motion $B^2 = (B^2_t)_{t\geqslant 0}$ such that $W_{Y_t} = \int_0^t \sqrt{X_s}\,\mathrm{d}B^2_s$ for all $t \geqslant 0$, thus showing that $Z = (Z_t)_{t\geqslant 0}$ is a weak solution to equation (4.5).

Conversely, suppose that $Z = (Z_t)_{t\geqslant 0}$ is a weak solution to (4.5). As we did in Section 2.5, in order to show that $Z = (Z_t)_{t\geqslant 0}$ is a time-changed Lévy process, we follow the scheme of the proof of [**Kal06**, Theorem 3.2]. Without loss of generality, we can suppose that the underlying stochastic basis already supports a Lévy process $L = (L_t)_{t\geqslant 0}$ with $L_0 = 0$, whose Lévy exponent is given by Ξ_Z and characterized by the Lévy triplet $(b_Z, \sigma_Z, \gamma_Z)$. Let $Y_\infty := \lim\limits_{t\to+\infty} Y_t$ and denote the inverse time change by $\tau = (\tau_z)_{z\geqslant 0}$, where $\tau_z := \inf\big\{t \geqslant 0 : Y_t > z\big\}$, for all $z \geqslant 0$. We recall that we may have $Y_\infty < +\infty$ when $\Psi \equiv 0$, which implies that $\tau = (\tau_z)_{z\geqslant 0}$ is infinite from time Y_∞ onward. As a result, the time-changed process $W = (W_z)_{z<Y_\infty}$ given by $W_z := Z_{\tau_z}$, for all $z < Y_\infty$, is a well-defined semimartingale, but on the stochastic interval $[\![0, Y_\infty[\![$. Its characteristics, which we denote by $\big(A, B, C\big)$, are given by

$$A_z = b_Z\,Y_{\tau_z} = b_Z\,z, \quad B_z = \sigma_Z^2\,Y_{\tau_z} = \sigma_Z^2\,z, \quad \text{and} \quad C_z(\mathrm{d}x) = \gamma_Z(\mathrm{d}x)\,Y_{\tau_z} = \gamma_Z(\mathrm{d}x)\,z,$$

for all $z < Y_\infty$, where we recall that $Y_{\tau_z} = z$ on $[\![0, Y_\infty[\![$. We can observe that $W = (W_z)_{z<Y_\infty}$ is a Lévy process on $[\![0, Y_\infty[\![$, and characterized by the Lévy triplet $(b_Z, \sigma_Z, \gamma_Z)$. As in the proof of Theorem 2.12, we need to show that $Z = (Z_t)_{t\geqslant 0}$ is constant on every interval $[r, s] \subseteq \mathbb{R}_+$ such that $Y_r = Y_s$. We recall from this proof that an interval of this type must verify $[r, s] \subseteq \big\{t \geqslant 0 : X_t = 0\big\}$, which yields $Z_t = Z_r$, for all $t \in [r, s]$. Then, we can write $Z_t = W_{Y_t}$, for all $t \geqslant 0$. However, $W = (W_z)_{z<Y_\infty}$ is a Lévy process only on $[\![0, Y_\infty[\![$. In order to overcome this issue, we construct the process $L^Z = (L^Z_z)_{z\geqslant 0}$ where $L^Z_z := W_z\,\mathbf{1}_{\{z<Y_\infty\}} + L_z\,\mathbf{1}_{\{z\geqslant Y_\infty\}}$, for all $z \geqslant 0$. $L^Z = (L^Z_z)_{z\geqslant 0}$ defines a Lévy process characterized by the Lévy triplet $(b_Z, \sigma_Z, \gamma_Z)$, which extends $W = (W_z)_{z<Y_\infty}$ to the entire $\mathbb{R}_+$. We then obtain $Z_t = L^Z_{Y_t}$, for all $t \geqslant 0$, thus satisfying equation (4.3). □

We conclude this section by discussing the self-exciting behavior of CBITCL processes, which can be seen from system (4.4)–(4.5) as follows:

- First, the CBI process $X = (X_t)_{t\geqslant 0}$ is self-exciting due to the presence of the stochastic integral with respect to $\widetilde{N}_1$. When a jump occurs, it increases the domain of integration. This in turn increases the jump intensity of N_1 and, therefore, the likelihood of subsequent jumps, thus generating jump clusters (see Remark 2.14);
- Second, the persistence of high values for the CBI process $X = (X_t)_{t\geqslant 0}$ has an impact on the stochastic integrals with respect to N_2 and $\widetilde{N}_2$. As before, when $X = (X_t)_{t\geqslant 0}$ increases, both domains of integration increase, which in turn increases the likelihood of volatility clusters in the dynamics of the process $Z = (Z_t)_{t\geqslant 0}$.

4.3. Affine property of CBITCL processes

In this section, we show that CBITCL processes are affine in the sense of [**DFS03**]. We mostly rely on a key result provided by [**KR09**, Theorem 4.16].

PROPOSITION 4.3. *Let $(X_t, Z_t)_{t\geqslant 0}$ be a* CBITCL$\big(X_0, \Psi, \Phi, \Xi_Z\big)$. *Consider the joint process $\big(X_t, Y_t, Z_t\big)_{t\geqslant 0}$, where $Y_t := \int_0^t X_s \,\mathrm{d}s$, for all $t \geqslant 0$. Then, it is an affine process with initial value $(X_0, 0, 0)$, state space $\mathbb{R}_+^2 \times \mathbb{R}$, and joint conditional Laplace–Fourier transform*

$$\mathbb{E}\Big[e^{\,u_1 X_T + u_2 Y_T + u_3 Z_T} \,\Big|\, \mathcal{F}_t\Big] = \exp\Big(\mathcal{U}(T-t, u_1, u_2, u_3) + \mathcal{V}(T-t, u_1, u_2, u_3)\, X_t + u_2\, Y_t + u_3\, Z_t\Big), \tag{4.7}$$

for all $(u_1, u_2, u_3) \in \mathbb{C}_-^2 \times \mathrm{i}\,\mathbb{R}$ and $0 \leqslant t \leqslant T < +\infty$, where the functions $\mathcal{U}(\cdot, u_1, u_2, u_3) : \mathbb{R}_+ \to \mathbb{C}$ and $\mathcal{V}(\cdot, u_1, u_2, u_3) : \mathbb{R}_+ \to \mathbb{C}_-$ solve the following CBITCL Riccati system:

$$\mathcal{U}(t, u_1, u_2, u_3) = \int_0^t \Psi\big(\mathcal{V}(s, u_1, u_2, u_3)\big)\,\mathrm{d}s, \tag{4.8}$$

$$\frac{\partial \mathcal{V}}{\partial t}(t, u_1, u_2, u_3) = \Phi\big(\mathcal{V}(t, u_1, u_2, u_3)\big) + u_2 + \Xi_Z(u_3), \qquad \mathcal{V}(0, u_1, u_2, u_3) = u_1, \tag{4.9}$$

where the functions $\Psi : \mathbb{C}_- \to \mathbb{C}$ and $\Phi : \mathbb{C}_- \to \mathbb{C}$ correspond to their analytic extensions to the complex domain $\mathbb{C}_-$.

PROOF. Lemma 2.2 yields the affine property of the joint process $(X_t, Y_t)_{t\geqslant 0}$, whose affine characteristics are given by

$$\Psi(u_1, u_2) := \Psi(u_1) \quad \text{and} \quad \Phi(u_1, u_2) := \Phi(u_1) + u_2, \qquad \forall (u_1, u_2) \in \mathbb{C}_-^2.$$

Consider now the Lévy process $L^Z = (L_t^Z)_{t\geqslant 0}$, appearing in the definition of the process $Z = (Z_t)_{t\geqslant 0}$ (see Definition 4.1). We emphasize that the latter is by construction independent of the CBI process $X = (X_t)_{t\geqslant 0}$. Following [**KR09**, Theorem 4.16], the joint process $\big(X_t, Y_t, Z_t\big)_{t\geqslant 0}$, where $Z_t = L^Z_{Y_t}$ for all $t \geqslant 0$ by equation (4.3), is affine with initial value $(X_0, 0, 0)$, state space $\mathbb{R}_+^2 \times \mathbb{R}$, and affine characteristics are given by

$$\begin{aligned}
\Psi(u_1, u_2, u_3) &:= \Psi\big(u_1, u_2 + \Xi_Z(u_3)\big) = \Psi(u_1), \\
\Phi(u_1, u_2, u_3) &:= \Phi\big(u_1, u_2 + \Xi_Z(u_3)\big) = \Phi(u_1) + u_2 + \Xi_Z(u_3),
\end{aligned}$$

for all $(u_1, u_2, u_3) \in \mathbb{C}_-^2 \times \mathrm{i}\,\mathbb{R}$. The claim then follows from [**DFS03**, Theorem 2.7], which enables us to derive the joint conditional Laplace–Fourier transform of the joint process $\big(X_t, Y_t, Z_t\big)_{t\geqslant 0}$, given by (4.7), and associated to the CBITCL Riccati system (4.8)–(4.9). □

Remark 4.4. In view of Proposition 4.3, CBITCL processes can be regarded as affine stochastic volatility models in the sense of [**KR11**, Definition 2.8], which were proved to be *coherent* by [**Gno17**]. This means that if an asset price process is modeled by a CBITCL process $(X_t, Z_t)_{t\geqslant 0}$, where $Z = (Z_t)_{t\geqslant 0}$ represents the discounted log-price process and $X = (X_t)_{t\geqslant 0}$ its stochastic volatility process, then the inverse asset price process, under a suitable equivalent change of probability, belongs to the same modeling class. This feature is fundamental for the construction of a modeling framework for multiple currencies, where foreign exchange rates and their inverse must be considered simultaneously (see Chapter 5).

4.4. Finiteness of exponential moments

This section generalizes the results of Sections 2.3 and 2.4 to CBITCL processes. In doing so, we mostly use techniques analogous to those employed in Sections 2.3 and 2.4, and rely on the results of [**KR11, KRM15**]. Let us first introduce, on top of $\mathcal{D}_1$ given by (2.8), the set $\mathcal{D}_2$ that we define as follows:

$$\mathcal{D}_2 := \left\{ x \in \mathbb{R} : \int_{|z|\geqslant 1} e^{\,x\,z}\,\gamma_Z(\mathrm{d}z) < +\infty \right\}. \tag{4.10}$$

While $\mathcal{D}_1$ represents the effective domain of the immigration and branching mechanisms Ψ and Φ, $\mathcal{D}_2$ denotes the effective domain of the Lévy exponent Ξ_Z, when restricted to real arguments. As in Section 2.3, by using standard results on exponential moments of Lévy measures (see e.g. [**Sat99**, Theorem 25.17]), we can extend Ξ_Z, as a finite-valued convex function, to $\mathcal{D}_2$. Let us now extend the CBITCL Riccati system (4.8)–(4.9), similarly to Definition 2.3.

Definition 4.5. For $(x_1, x_2, x_3) \in \mathcal{D}_1 \times \mathbb{R} \times \mathcal{D}_2$, a solution $\big(\mathcal{U}(\cdot, x_1, x_2, x_3), \mathcal{V}(\cdot, x_1, x_2, x_3)\big)$ to the *extended CBITCL Riccati system* is defined as a solution to the following system:

$$\begin{aligned} \mathcal{U}(t, x_1, x_2, x_3) &= \int_0^t \Psi\big(\mathcal{V}(s, x_1, x_2, x_3)\big)\mathrm{d}s, \\ \frac{\partial \mathcal{V}}{\partial t}(t, x_1, x_2, x_3) &= \Phi\big(\mathcal{V}(t, x_1, x_2, x_3)\big) + x_2 + \Xi_Z(x_3), \qquad \mathcal{V}(0, x_1, x_2, x_3) = x_1, \end{aligned} \tag{4.11}$$

up to a time $\mathrm{T}^{(x_1,x_2,x_3)} \in [0, +\infty]$, where $\mathrm{T}^{(x_1,x_2,x_3)}$ denotes the maximum joint lifetime of the functions $\mathcal{U}(\cdot, x_1, x_2, x_3) : [0, \mathrm{T}^{(x_1,x_2,x_3)}) \to \mathbb{R}$ and $\mathcal{V}(\cdot, x_1, x_2, x_3) : [0, \mathrm{T}^{(x_1,x_2,x_3)}) \to \mathcal{D}_1$.

By referring to Section 2.3, under Assumption 2.4, we know that there exists a unique solution $\big(\mathcal{U}(\cdot, x_1, x_2, x_3), \mathcal{V}(\cdot, x_1, x_2, x_3)\big)$ to the extended CBITCL Riccati system of Definition 4.5, for all $(x_1, x_2, x_3) \in \mathcal{D}_1 \times \mathbb{R} \times \mathcal{D}_2$. We are then allowed, similarly to Proposition 2.5, to refine the result of [**KRM15**, Theorem 2.14] for the specific case of CBITCL processes.

LEMMA 4.6. *Let $(X_t, Z_t)_{t\geqslant 0}$ be a* CBITCL$\big(X_0, \Psi, \Phi, \Xi_Z\big)$. *Suppose that Assumption 2.4 holds. Consider the joint process $\big(X_t, Y_t, Z_t\big)_{t\geqslant 0}$, where $Y_t := \int_0^t X_s \,\mathrm{d}s$, for all $t \geqslant 0$. Then, the joint conditional Laplace transform given by* (4.7) *can be extended to $\mathcal{D}_1 \times \mathbb{R} \times \mathcal{D}_2$ as follows:*

$$\mathbb{E}\Big[e^{\,x_1 X_T + x_2 Y_T + x_3 Z_T} \,\Big|\, \mathcal{F}_t\Big] = \exp\Big(\mathcal{U}(T-t, x_1, x_2, x_3) + \mathcal{V}(T-t, x_1, x_2, x_3)\, X_t + x_2\, Y_t + x_3\, Z_t\Big), \tag{4.12}$$

for all $(x_1, x_2, x_3) \in \mathcal{D}_1 \times \mathbb{R} \times \mathcal{D}_2$ and $0 \leqslant t \leqslant T < \mathrm{T}^{(x_1,x_2,x_3)}$, where $\big(\mathcal{U}(\cdot, x_1, x_2, x_3), \mathcal{V}(\cdot, x_1, x_2, x_3)\big)$ is the unique solution to the extended CBITCL Riccati system starting from (x_1, x_2, x_3), and defined up to the maximum joint lifetime $\mathrm{T}^{(x_1,x_2,x_3)}$.

PROOF. The proof follows the lines of the proof of Proposition 2.5, where the claim was obtained by applying [**KRM15**, Theorem 2.14]. □

We investigate the existence of complex exponential moments of CBITCL processes. We recall that they were briefly studied in Remark 2.7 for the specific case of CBI processes, but not totally treated in Section 2.3. To this purpose, let $\mathcal{O}_i = \{u \in \mathbb{C} : \mathrm{Re}(u) \in \mathcal{D}_i^\circ\}$, for $i = 1, 2$. Observe that $\mathcal{O}_1$ and $\mathcal{O}_2$ are open and connected. By relying on the principle of analytic continuation (see e.g. [**Die69**]), we can analytically extend the immigration and branching mechanisms Ψ and Φ from $\mathcal{D}_1^\circ$ to $\mathcal{O}_1$, as well as the Lévy exponent Ξ_Z from $\mathcal{D}_2^\circ$ to $\mathcal{O}_2$. We can then introduce a complex extended version of the CBITCL Riccati system (4.8)–(4.9).

DEFINITION 4.7. For $(u_1, u_2, u_3) \in \mathcal{O}_1 \times \mathbb{C} \times \mathcal{O}_2$, a solution $\big(\mathcal{U}(\cdot, u_1, u_2, u_3), \mathcal{V}(\cdot, u_1, u_2, u_3)\big)$ to the *complex extended CBITCL Riccati system* is defined as a solution to the following system:

$$\begin{aligned} \mathcal{U}(t, u_1, u_2, u_3) &= \int_0^t \Psi\big(\mathcal{V}(s, u_1, u_2, u_3)\big)\mathrm{d}s, \\ \frac{\partial \mathcal{V}}{\partial t}(t, u_1, u_2, u_3) &= \Phi\big(\mathcal{V}(t, u_1, u_2, u_3)\big) + u_2 + \Xi_Z(u_3), \qquad \mathcal{V}(0, u_1, u_2, u_3) = u_1, \end{aligned} \tag{4.13}$$

up to a time $\mathrm{T}^{(u_1,u_2,u_3)} \in [0, +\infty]$, where $\mathrm{T}^{(u_1,u_2,u_3)}$ denotes the maximum joint lifetime of the functions $\mathcal{U}(\cdot, u_1, u_2, u_3) : [0, \mathrm{T}^{(u_1,u_2,u_3)}) \to \mathbb{C}$ and $\mathcal{V}(\cdot, u_1, u_2, u_3) : [0, \mathrm{T}^{(u_1,u_2,u_3)}) \to \mathcal{O}_1$.

Unlike the extended CBITCL Riccati system of Definition 4.5, a solution to equation (4.13) is necessarily unique since the function Φ is analytic on the entire complex domain $\mathcal{O}_1$ and the function $\mathcal{V}(\cdot, u_1, u_2, u_3)$ is constrained to stay inside $\mathcal{O}_1$ (see [**KRM15**, Remark 2.23]). Furthermore, if a solution to the complex extended CBITCL Riccati system of Definition 4.7 has a real-valued starting point (u_1, u_2, u_3), then the latter solution also solves the extended CBITCL Riccati system.

We are in a position to formulate the next result, which specializes [**KRM15**, Theorem 2.26] to our setting. Indeed, [**KRM15**] had to assume the existence of a solution to the extended Riccati system that remains inside the interior of the effective domain, thus ensuring the uniqueness of the latter. In our setting, there is no necessity to introduce this additional requirement since under Assumption 2.4, we know that there always exists a unique solution $\mathcal{V}(\cdot, x_1, x_2, x_3)$ to equation (4.11), whether this solution starts from the boundary of $\mathcal{D}_1$, or reaches it at a later time.

PROPOSITION 4.8. *Let* $(X_t, Z_t)_{t\geqslant 0}$ *be a* $\mathrm{CBITCL}\big(X_0, \Psi, \Phi, \Xi_Z\big)$. *Suppose that Assumption 2.4 holds. Consider the joint process* $\big(X_t, Y_t, Z_t\big)_{t\geqslant 0}$, *where* $Y_t := \int_0^t X_s \,\mathrm{d}s$, *for all* $t \geqslant 0$. *Then, the joint conditional Laplace transform* (4.12) *can be analytically extended to* $\mathcal{O}_1 \times \mathbb{C} \times \mathcal{O}_2$ *as follows:*

$$\mathbb{E}\Big[e^{\,u_1\,X_T + u_2\,Y_T + u_3\,Z_T}\,\Big|\,\mathcal{F}_t\Big] = \exp\Big(\mathcal{U}(T-t,u_1,u_2,u_3) + \mathcal{V}(T-t,u_1,u_2,u_3)\,X_t + u_2\,Y_t + u_3\,Z_t\Big), \tag{4.14}$$

for all $(u_1, u_2, u_3) \in \mathcal{O}_1 \times \mathbb{C} \times \mathcal{O}_2$ *and* $0 \leqslant t \leqslant T < \mathrm{T}^{(u_1,u_2,u_3)}$, *where* $\big(\mathcal{U}(\cdot, u_1, u_2, u_3), \mathcal{V}(\cdot, u_1, u_2, u_3)\big)$ *is the unique solution to the complex extended CBITCL Riccati system, starting from* (u_1, u_2, u_3) *and defined up to the maximum lifetime* $\mathrm{T}^{(u_1,u_2,u_3)}$, *which verifies*

$$\mathrm{T}^{(u_1,u_2,u_3)} \geqslant \mathrm{T}^{(\mathrm{Re}(u_1),\mathrm{Re}(u_2),\mathrm{Re}(u_3))}, \tag{4.15}$$

where $\mathrm{T}^{(\mathrm{Re}(u_1),\mathrm{Re}(u_2),\mathrm{Re}(u_3))}$ *is the maximum lifetime of the unique solution to the extended CBITCL Riccati system starting from* $(\mathrm{Re}(u_1), \mathrm{Re}(u_2), \mathrm{Re}(u_3))$.

PROOF. Let $(u_1, u_2, u_3) \in \mathcal{O}_1 \times \mathbb{C} \times \mathcal{O}_2$. Under Assumption 2.4, for all $(x_1, x_2, x_3) \in \mathcal{D}_1 \times \mathbb{R} \times \mathcal{D}_2$, there is a unique solution to the extended CBITCL Riccati system up to $\mathrm{T}^{(x_1,x_2,x_3)}$. In particular, this is true for the starting point $(\mathrm{Re}(u_1), \mathrm{Re}(u_2), \mathrm{Re}(u_3))$. By [**KRM15**, Theorem 2.26], there also exists a solution to the complex extended CBITCL Riccati system of Definition 4.7 starting from (u_1, u_2, u_3), which is unique in view of [**KRM15**, Remark 2.23], and whose lifetime $\mathrm{T}^{(u_1,u_2,u_3)}$ is related to $\mathrm{T}^{(\mathrm{Re}(u_1),\mathrm{Re}(u_2),\mathrm{Re}(u_3))}$ via inequality (4.15) due to [**KRM15**, Proposition 5.1]. Under these conditions, again by [**KRM15**, Theorem 2.26], we can then analytically extend the joint conditional Laplace transform (4.12) to the complex domain $\mathcal{O}_1 \times \mathbb{C} \times \mathcal{O}_2$. □

As in Section 2.3, we can rely on [**KRM15**, Proposition 3.3] to assert that the maximum lifetime $\mathrm{T}^{(x_1,x_2,x_3)}$, for all $(x_1, x_2, x_3) \in \mathcal{D}_1 \times \mathbb{R} \times \mathcal{D}_2$, characterizes the finiteness of real exponential moments of CBITCL processes:

$$\mathrm{T}^{(x_1,x_2,x_3)} = \sup\Big\{t \geqslant 0 : \mathbb{E}\big[e^{\,x_1\,X_t + x_2\,Y_t + x_3\,Z_t}\big] < +\infty\Big\}. \tag{4.16}$$

In the following, we propose a generalization of Theorem 2.8 to the class of CBITCL processes, providing an explicit and general characterization of the maximum lifetime $\mathrm{T}^{(x_1,x_2,x_3)}$, for all $(x_1, x_2, x_3) \in \mathcal{D}_1 \times \mathbb{R} \times \mathcal{D}_2$. Because of the presence of $x_3 \in \mathcal{D}_2$, and also due to the fact that the second coordinate x_2 can at present span the whole real line $\mathbb{R}$, we will not be able to state an analogue to Corollary 2.9 for the specific case of CBITCL processes. As in Section 2.4, we proceed by relying on techniques similar to those employed in the proof of [**KR11**, Theorem 4.1]. For $(x_2, x_3) \in \mathbb{R} \times \mathcal{D}_2$, let us introduce the following notation:

$$\mathcal{S} := \Big\{x \in \mathcal{D}_1 : \Phi(x) + x_2 + \Xi_Z(x_3) \leqslant 0\Big\} \quad \text{and} \quad \chi := \sup \mathcal{S} \in [-\infty, \psi \wedge \phi],$$

with the convention $\chi = -\infty$ if $\mathcal{S}$ is empty.

THEOREM 4.9. *Let* $(X_t, Z_t)_{t\geqslant 0}$ *be a* $\mathrm{CBITCL}\big(X_0, \Psi, \Phi, \Xi_Z\big)$. *Suppose that Assumption 2.4 holds. Then, for all* $(x_1, x_2, x_3) \in \mathcal{D}_1 \times \mathbb{R} \times \mathcal{D}_2$, *the lifetime* $\mathrm{T}^{(x_1,x_2,x_3)}$ *is characterized as follows:*

(i) *If* $x_1 \leqslant \chi$, *then* $\mathrm{T}^{(x_1,x_2,x_3)} = +\infty$;

(ii) *If* $x_1 > \chi$, *then*

$$\mathrm{T}^{(x_1,x_2,x_3)} = \int_{x_1}^{\psi\wedge\phi} \frac{\mathrm{d}x}{\Phi(x) + x_2 + \Xi_Z(x_3)}. \tag{4.17}$$

PROOF. Under a slight abuse of notation, it can be easily checked that for the unique solution $\big(\mathcal{U}(\cdot, x_1, x_2, x_3), \mathcal{V}(\cdot, x_1, x_2, x_3)\big)$ to the extended CBITCL Riccati system of Definition 4.5, starting from $(x_1, x_2, x_3) \in \mathcal{D}_1 \times \mathbb{R} \times \mathcal{D}_2$, the following correspondence holds true:

$$\mathcal{V}\big(\cdot, x_1, x_2, x_3\big) = \mathcal{V}\big(\cdot, x_1, x_2 + \Xi_Z(x_3)\big) \quad \text{and} \quad \mathcal{U}\big(\cdot, x_1, x_2, x_3\big) = \mathcal{U}\big(\cdot, x_1, x_2 + \Xi_Z(x_3)\big),$$

where $\big(\mathcal{U}\big(\cdot, x_1, x_2 + \Xi_Z(x_3)\big), \mathcal{V}\big(\cdot, x_1, x_2 + \Xi_Z(x_3)\big)\big)$ is the unique solution to the extended CBI Riccati system of Definition 2.3, starting from $\big(x_1, x_2 + \Xi_Z(x_3)\big) \in \mathcal{D}_1 \times \mathbb{R}$. As a consequence, we can derive an analogous correspondence for their maximum lifetimes, namely $\mathrm{T}^{(x_1,x_2,x_3)} = \mathrm{T}^{(x_1,x_2+\Xi_Z(x_3))}$, which therefore allows us to restrict our attention to the study of the lifetimes $\mathrm{T}^{(x_1,x_2)}$, for all $(x_1, x_2) \in \mathcal{D}_1 \times \mathbb{R}$, where the second coordinate x_2 is from now on allowed to span the entire real line.

We distinguish two cases: $x_2 + \Xi_Z(x_3) \leqslant 0$, corresponding to the setting of Theorem 2.8. In this case, the proof follows exactly the same lines with x_2 replaced by $x_2 + \Xi_Z(x_3)$. We refer the reader to Figure 2.1, where a descriptive illustration of the situation when $x_2 + \Xi_Z(x_3) \leqslant 0$ can be found. The second case $x_2 + \Xi_Z(x_3) > 0$ was not considered in Chapter 2. Figure 4.1 provides a visualization of the situation and contains several possible shapes of the function Φ over $\mathcal{D}_1$ when $x_2 + \Xi_Z(x_3) > 0$. The solid curves refer to the case $\psi \wedge \phi < +\infty$ and the dashed ones to $\psi \wedge \phi = +\infty$.

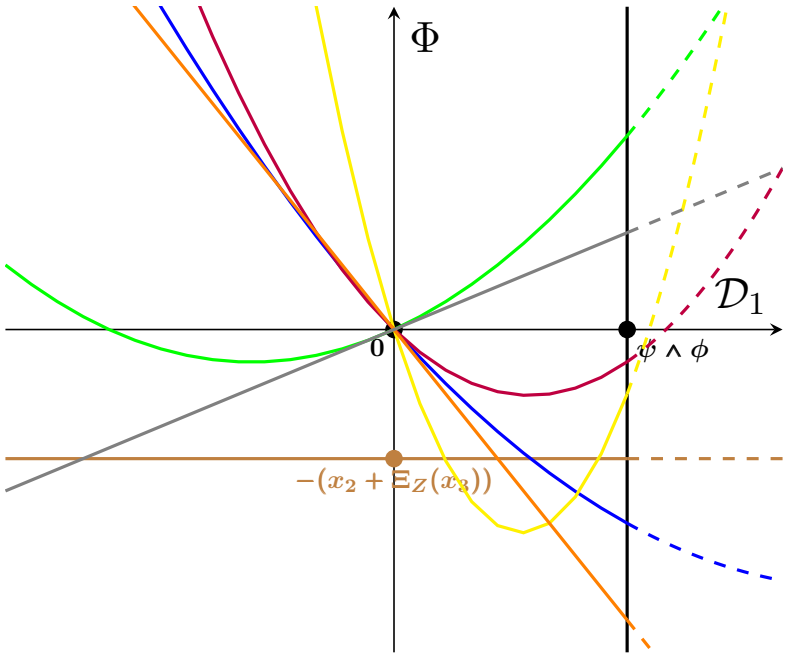

FIGURE 4.1. Case $x_2 + \Xi_Z(x_3) > 0$: Possible shapes of the function Φ over $\mathcal{D}_1$, where the solid curves refer to $\psi \wedge \phi < +\infty$ and the dashed ones to $\psi \wedge \phi = +\infty$.

Observe that when $x_2 + \Xi_Z(x_3) > 0$, the set $\mathcal{S}$ may be empty ($\chi = -\infty$). This is graphically represented by the green and purple curves. In such a situation, we have $\Phi(x_1) + x_2 + \Xi_Z(x_3) > 0$, for all $x_1 > \chi$. We mention that this situation is similar to the case (2) of the proof of Theorem 2.8, namely when $x_2 + \Xi_Z(x_3) \leqslant 0$, $\Phi(\chi) + x_2 + \Xi_Z(x_3) = 0$, but when $x_1 > \chi$. Indeed, we can observe that $\mathcal{V}(\cdot, x_1, x_2, x_3)$ is strictly increasing with values in $[x_1, \phi]$, for all $x_1 > \chi$. In this regard, by using similar techniques, we obtain that $\mathrm{T}^{\mathcal{V}}$ and $\mathrm{T}^{\mathcal{U}}$ are given by (2.18) and (2.19), respectively (with x_2 replaced by $x_2 + \Xi_Z(x_3)$), where we recall that $\mathrm{T}^{\mathcal{V}}$ and $\mathrm{T}^{\mathcal{U}}$ are given by (2.15). Then, by using $\mathrm{T}^{(x_1,x_2,x_3)} = \mathrm{T}^{\mathcal{U}} \wedge \mathrm{T}^{\mathcal{V}}$, we can recover formula (4.17) for $\mathrm{T}^{(x_1,x_2,x_3)}$, for all $x_1 > \chi$.

When the set $\mathcal{S}$ is non-empty, namely when $\chi > -\infty$, as in the proof of Theorem 2.8, two further cases can be distinguished. The first case corresponds to $\chi = \psi \wedge \phi$, which is graphically represented in Figure 4.1 by the blue curve (when $\psi \wedge \phi < +\infty$) and by the orange line (whether ψ is finite or not, representing the linear case $\Phi(x) = -\,b\,x$ with $b > 0$ and $\phi = +\infty$). Arguing similarly to the case (3) of the proof of Theorem 2.8, namely when $x_2 + \Xi_Z(x_3) \leqslant 0$ and $\Phi(\chi) + x_2 + \Xi_Z(x_3) < 0$, there exists a unique $\xi > 0$ such that $\Phi(\xi) + x_2 + \Xi_Z(x_3) = 0$ and $\Phi(x_1) + x_2 + \Xi_Z(x_3) < 0$ for all $\xi < x_1 \leqslant \chi$ by convexity of Φ. By using equation (2.20) (with x_2 replaced by $x_2 + \Xi_Z(x_3)$), $\mathcal{V}(\cdot, x_1, x_2, x_3)$ is strictly decreasing and tends toward ξ as $t \to +\infty$, so that we have $\xi < \mathcal{V}(\cdot, x_1, x_2, x_3) \leqslant x_1$ for all $\xi < x_1 \leqslant \chi$, thus implying that $\mathrm{T}^{\mathcal{V}} = +\infty$. Due to the non-decreasing behavior of the function Ψ, we can deduce that $t\,\Psi(\xi) \leqslant \mathcal{U}(t, x_1, x_2, x_3) \leqslant t\,\Psi(x_1)$ for all $t \geqslant 0$, which yields $\mathrm{T}^{\mathcal{U}} = +\infty$. Hence, we obtain $\mathrm{T}^{(x_1,x_2,x_3)} = +\infty$ for all $\xi < x_1 \leqslant \chi$ and also for all $x_1 \leqslant \xi$ in view of (4.16).

The second case refers to $\chi < \psi \wedge \phi$, which is graphically represented in Figure 4.1 by the blue curve (when $\psi \wedge \phi = +\infty$), the yellow curve (whether $\psi \wedge \phi$ is finite or not) and the gray line ($\Phi(x) = -\,b\,x$ with $b < 0$). Here, we have $\Phi(\chi) + x_2 + \Xi_Z(x_3) = 0$. We proceed as in the case (1) of the proof of Theorem 2.8, i.e. $x_2 + \Xi_Z(x_3) \leqslant 0$ and $\Phi(\chi) + x_2 + \Xi_Z(x_3) = 0$. We then have $\mathcal{V}(\cdot, \chi, x_2, x_3) \equiv \chi$ as the unique solution to equation (4.11), which implies $\mathrm{T}^{(\chi,x_2,x_3)} = +\infty$ and for all $x_1 \leqslant \chi$ in view of (4.16). Next, similarly to the case (2) of the proof of Theorem 2.8, namely $x_2 + \Xi_Z(x_3) \leqslant 0$ and $\Phi(x_1) + x_2 + \Xi_Z(x_3) > 0$ for all $x_1 > \chi$, $\mathcal{V}(\cdot, x_1, x_2, x_3)$ is strictly increasing with values in $[x_1, \phi]$ for all $x_1 > \chi$. As above (when the set $\mathcal{S}$ is empty), by using standard extension results and equation (2.17), we obtain that both $\mathrm{T}^{\mathcal{V}}$ and $\mathrm{T}^{\mathcal{U}}$ are given by (2.18) and (2.19), respectively (with x_2 replaced by $x_2 + \Xi_Z(x_3)$). As a consequence, by $\mathrm{T}^{(x_1,x_2,x_3)} = \mathrm{T}^{\mathcal{U}} \wedge \mathrm{T}^{\mathcal{V}}$, we finally obtain formula (4.17) for $\mathrm{T}^{(x_1,x_2,x_3)}$, for all $x_1 > \chi$. □

4.5. A Girsanov-type theorem

The goal of this section is to characterize a class of equivalent changes of probability of Esscher type that leave invariant CBITCL processes. The result is stated in the form of a Girsanov-type theorem for CBITCL processes. This class of equivalent changes of probability will be used in Chapter 5, where the determination of a class of risk-neutral measures for the multiple currency market, leaving invariant the structure of the model, will represent an important requirement.

As a preliminary, the next lemma presents the differential characteristics of the joint process $\big(X_t, Y_t, Z_t\big)_{t\geqslant 0}$ when seen as a semimartingale, where $(X_t, Z_t)_{t\geqslant 0}$ is a CBITCL process and $Y_t := \int_0^t X_s \,\mathrm{d}s$, for all $t \geqslant 0$. We refer to [**JS03**, Chapter II] for details on semimartingale characteristics.

LEMMA 4.10. *Let* $(X_t, Z_t)_{t\geqslant 0}$ *be a* $\mathrm{CBITCL}\big(X_0, \Psi, \Phi, \Xi_Z\big)$. *Consider also the joint process* $\big(X_t, Y_t, Z_t\big)_{t\geqslant 0}$, *where* $Y_t := \int_0^t X_s \,\mathrm{d}s$, *for all* $t \geqslant 0$. *Then,* $\big(X_t, Y_t, Z_t\big)_{t\geqslant 0}$ *is a semimartingale whose differential characteristics* $\big(\mathcal{A}, \mathcal{B}, \mathcal{C}\big)$ *relative to* $h(x) = x\,\mathbf{1}_{\{|x|<1\}}$ *are given by*

$$\mathcal{A}_t = \begin{pmatrix} \beta + \int_0^1 z\,\nu(\mathrm{d}z) \\ 0 \\ 0 \end{pmatrix} + X_{t-} \begin{pmatrix} -b - \int_1^{+\infty} z\,\pi(\mathrm{d}z) \\ 1 \\ b_Z \end{pmatrix}, \quad \mathcal{B}_t = X_{t-} \begin{pmatrix} \sigma^2 & 0 & 0 \\ 0 & 0 & 0 \\ 0 & 0 & \sigma_Z^2 \end{pmatrix},$$

$$\mathcal{C}_t(\mathrm{d}x) = \nu(\mathrm{d}x_1)\,\delta_{(0,0)}(\mathrm{d}x_2, \mathrm{d}x_3) + X_{t-}\Big(\pi(\mathrm{d}x_1)\,\delta_{(0,0)}(\mathrm{d}x_2, \mathrm{d}x_3) + \delta_{(0,0)}(\mathrm{d}x_1, \mathrm{d}x_2)\,\gamma_Z(\mathrm{d}x_3)\Big),$$

for all $t \geqslant 0$ *and* $x = (x_1, x_2, x_3) \in \mathbb{R}_+ \times \mathbb{R}_+ \times \mathbb{R}$, *where* $\delta_{(0,0)}$ *is the Dirac measure at* $(0, 0)$.

PROOF. By Proposition 4.3, the joint process $\big(X_t, Y_t, Z_t\big)_{t\geqslant 0}$, where $Y_t := \int_0^t X_s \,\mathrm{d}s$, for all $t \geqslant 0$, is affine in the sense of [**DFS03**]. According to the notation of [**DFS03**, Definition 2.6 and Theorem 2.7], and taking $h(x) = x\,\mathbf{1}_{\{|x|<1\}}$ as a truncation function, we can then deduce its admissible parameter set as follows:

- diffusion part:

$$\left(\begin{pmatrix} 0 & 0 & 0 \\ 0 & 0 & 0 \\ 0 & 0 & 0 \end{pmatrix}, \begin{pmatrix} \sigma^2 & 0 & 0 \\ 0 & 0 & 0 \\ 0 & 0 & \sigma_Z^2 \end{pmatrix}, \begin{pmatrix} 0 & 0 & 0 \\ 0 & 0 & 0 \\ 0 & 0 & 0 \end{pmatrix}, \begin{pmatrix} 0 & 0 & 0 \\ 0 & 0 & 0 \\ 0 & 0 & 0 \end{pmatrix}\right); \tag{4.18}$$

- drift part:

$$\left(\begin{pmatrix} \beta + \int_0^1 z\,\nu(\mathrm{d}z) \\ 0 \\ 0 \end{pmatrix}, \begin{pmatrix} -b - \int_1^{+\infty} z\,\pi(\mathrm{d}z) \\ 1 \\ b_Z \end{pmatrix}, \begin{pmatrix} 0 \\ 0 \\ 0 \end{pmatrix}, \begin{pmatrix} 0 \\ 0 \\ 0 \end{pmatrix}\right); \tag{4.19}$$

- jump part:

$$\Big(\nu \times \delta_{(0,0)}, \pi \times \delta_{(0,0)} + \delta_{(0,0)} \times \gamma_Z, 0, 0\Big). \tag{4.20}$$

By [**DFS03**, Theorem 2.12], $\big(X_t, Y_t, Z_t\big)_{t\geqslant 0}$ is a semimartingale whose differential characteristics, which we denote by $\big(\mathcal{A}, \mathcal{B}, \mathcal{C}\big)$ and relative to $h(x) = x\,\mathbf{1}_{\{|x|<1\}}$, are affine functions as follows:

$$\mathcal{A}_t = \begin{pmatrix} \beta + \int_0^1 z\,\nu(\mathrm{d}z) \\ 0 \\ 0 \end{pmatrix} + X_{t-} \begin{pmatrix} -b - \int_1^{+\infty} z\,\pi(\mathrm{d}z) \\ 1 \\ b_Z \end{pmatrix} + Y_{t-} \begin{pmatrix} 0 \\ 0 \\ 0 \end{pmatrix} + Z_{t-} \begin{pmatrix} 0 \\ 0 \\ 0 \end{pmatrix},$$

$$\mathcal{B}_t = \begin{pmatrix} 0 & 0 & 0 \\ 0 & 0 & 0 \\ 0 & 0 & 0 \end{pmatrix} + X_{t-} \begin{pmatrix} \sigma^2 & 0 & 0 \\ 0 & 0 & 0 \\ 0 & 0 & \sigma_Z^2 \end{pmatrix} + Y_{t-} \begin{pmatrix} 0 & 0 & 0 \\ 0 & 0 & 0 \\ 0 & 0 & 0 \end{pmatrix} + Z_{t-} \begin{pmatrix} 0 & 0 & 0 \\ 0 & 0 & 0 \\ 0 & 0 & 0 \end{pmatrix},$$

$$\mathcal{C}_t(\mathrm{d}x) = \Big(\nu \times \delta_{(0,0)}\Big)(\mathrm{d}x) + X_{t-}\Big(\pi \times \delta_{(0,0)} + \delta_{(0,0)} \times \gamma_Z\Big)(\mathrm{d}x) + \Big(Y_{t-} \times 0\Big)(\mathrm{d}x) + \Big(Z_{t-} \times 0\Big)(\mathrm{d}x),$$

for all $t \geqslant 0$ and $x = (x_1, x_2, x_3) \in \mathbb{R}_+ \times \mathbb{R}_+ \times \mathbb{R}$. □

Let us fix two constants $\zeta \in \mathbb{R}$ and $\lambda \in \mathbb{R}$, which will play specific roles in the construction of our multiple currency framework in Chapter 5. Consider the process $\mathcal{W} = (\mathcal{W}_t)_{t\geqslant 0}$ defined by

$$\mathcal{W}_t := \zeta\, X_t + \lambda\, Z_t, \qquad \forall t \geqslant 0. \tag{4.21}$$

By [**JS03**, Proposition II.8.26], it can be easily checked that the process $\mathcal{W} = (\mathcal{W}_t)_{t\geqslant 0}$ is an exponentially special semimartingale if and only if $\zeta \in \mathcal{D}_1$ and $\lambda \in \mathcal{D}_2$. Therefore, $\mathcal{W} = (\mathcal{W}_t)_{t\geqslant 0}$ admits a unique exponential compensator, i.e. a predictable process of finite variation, which we denote by $\mathcal{K} = (\mathcal{K}_t)_{t\geqslant 0}$, such that $\big(e^{\mathcal{W}_t - \zeta\, X_0 - \mathcal{K}_t}\big)_{t\geqslant 0}$ is a local martingale. The following lemma shows that $\mathcal{K} = (\mathcal{K}_t)_{t\geqslant 0}$ can be computed explicitly.

Lemma 4.11. *Let $(X_t, Z_t)_{t\geqslant 0}$ be a $\mathrm{CBITCL}\big(X_0, \Psi, \Phi, \Xi_Z\big)$. Consider the process $\mathcal{W} = (\mathcal{W}_t)_{t\geqslant 0}$ defined by equation (4.21) where $\zeta \in \mathcal{D}_1$ and $\lambda \in \mathcal{D}_2$. Then, the exponential compensator of $\mathcal{W} = (\mathcal{W}_t)_{t\geqslant 0}$, which we denote by $\mathcal{K} = (\mathcal{K}_t)_{t\geqslant 0}$, is given by*

$$\mathcal{K}_t = t\,\Psi(\zeta) + Y_t\,\Big(\Phi(\zeta) + \Xi_Z(\lambda)\Big), \tag{4.22}$$

for all $t \geqslant 0$, where $Y_t := \int_0^t X_s\,\mathrm{d}s$.

Proof. We proceed by relying on the techniques of [**KS02a**]. Indeed, by using [**KS02a**, Theorem 2.19], $\mathcal{K} = (\mathcal{K}_t)_{t\geqslant 0}$ coincides with the *modified Laplace cumulant process* of the joint process $\big(X_t, Y_t, Z_t\big)_{t\geqslant 0}$ at $\theta = (\zeta, 0, \lambda)^\top$ (see [**KS02a**, Defintion 2.16]). Since CBITCL processes are by definition quasi-left-continuous, in view of [**KS02a**, Theorem 2.18], $\mathcal{K} = (\mathcal{K}_t)_{t\leqslant \mathcal{T}}$ can be computed explicitly in terms of the differential characteristics given by Lemma 4.10:

$$\begin{aligned}
\mathcal{K}_t &:= \int_0^t \left(\theta^\top \mathcal{A}_s + \frac{1}{2}\,\theta^\top \mathcal{B}_s\,\theta + \int_{\mathbb{R}^3} \Big(e^{\theta^\top x} - 1 - \theta^\top x\,\mathbf{1}_{\{|x|<1\}}\Big)\,\mathcal{C}_s(\mathrm{d}x)\right)\mathrm{d}s \\
&= t\,\left(\beta\,\zeta + \int_0^{+\infty} \Big(e^{\zeta\, x} - 1\Big)\,\nu(\mathrm{d}x)\right) + Y_t\,\left(-b\,\zeta + \frac{1}{2}\,(\sigma\,\zeta)^2 + \int_0^{+\infty} \Big(e^{\zeta\, x} - 1 - \zeta\, x\Big)\,\pi(\mathrm{d}x)\right) \\
&\quad + Y_t\,\left(b_Z\,\lambda + \frac{1}{2}\,(\sigma_Z\,\lambda)^2 + \int_{\mathbb{R}} \Big(e^{\lambda\, x} - 1 - \lambda\, x\,\mathbf{1}_{\{|x|<1\}}\Big)\,\gamma_Z(\mathrm{d}x)\right) \\
&= t\,\Psi(\zeta) + Y_t\,\Big(\Phi(\zeta) + \Xi_Z(\lambda)\Big), \qquad \forall t \geqslant 0,
\end{aligned}$$

thus yielding the desired result. □

We can now formulate our Girsanov-type theorem for CBITCL processes. To this effect, fix a finite time horizon $\mathcal{T} < +\infty$ and suppose, without loss of generality, that the stochastic basis $\big(\Omega, \mathcal{F}, \mathbb{F}, \mathbb{Q}\big)$ is rich enough so that a CBITCL process $(X_t, Z_t)_{t\leqslant \mathcal{T}}$ admits the extended Dawson–Li representation (4.4)–(4.5). We also invite the reader to compare the next result with Remark 3.9 and other similar Girsanov-type results for CBI processes obtained in the related literature (see [**JMS17, JMSZ21, BBSS21**] among others).

Theorem 4.12. *Let $(X_t, Z_t)_{t\leqslant \mathcal{T}}$ be a $\mathrm{CBITCL}\big(X_0, \Psi, \Phi, \Xi_Z\big)$. Consider the process $\mathcal{W} = (\mathcal{W}_t)_{t\leqslant \mathcal{T}}$ defined by (4.21) where $\zeta \in \mathcal{D}_1$ and $\lambda \in \mathcal{D}_2$, together with its exponential compensator*

$\mathcal{K} = (\mathcal{K}_t)_{t\leqslant\mathcal{T}}$ given by (4.22). Then, the process $\big(e^{\mathcal{W}_t-\zeta X_0-\mathcal{K}_t}\big)_{t\leqslant\mathcal{T}}$ is a true martingale and there exists an equivalent probability measure $\mathbb{Q}'$ defined by

$$\left.\frac{\mathrm{d}\mathbb{Q}'}{\mathrm{d}\mathbb{Q}}\right|_{\mathcal{F}_t} := e^{\mathcal{W}_t-\zeta X_0-\mathcal{K}_t}, \tag{4.23}$$

for all $t \leqslant \mathcal{T}$, under which the joint process $(X_t, Z_t)_{t\leqslant\mathcal{T}}$ remains a CBITCL process with parameters given by $\big(\beta', \nu', b', \sigma', \pi', b'_Z, \sigma'_Z, \gamma'_Z\big)$ in Table 4.1

Proof. Let $\mathcal{Z}_t := e^{\mathcal{W}_t-\zeta X_0-\mathcal{K}_t}$, for all $t \leqslant \mathcal{T}$. By Lemma 4.11, we know that $\mathcal{Z} = (\mathcal{Z}_t)_{t\leqslant\mathcal{T}}$ is a local martingale. Since the latter is non-negative, it is a supermartingale by Fatou's lemma. Hence, in order to prove that it is a true martingale, it suffices to show that $\mathbb{E}\big[\mathcal{Z}_{\mathcal{T}}\big] = 1$. To this effect, in view of (4.16), the lifetime $\mathrm{T}^{(\zeta,-\Phi(\zeta)-\Xi_Z(\lambda),\lambda)}$ should verify $\mathrm{T}^{(\zeta,-\Phi(\zeta)-\Xi_Z(\lambda),\lambda)} > \mathcal{T}$ to ensure $\mathbb{E}\big[\mathcal{Z}_{\mathcal{T}}\big] < +\infty$. By using Theorem 4.9 with $x_1 = \zeta$, $x_2 = -\Phi(\zeta) - \Xi_Z(\lambda)$, and $x_3 = \lambda$, we obtain $\mathcal{S} = \big\{x \in \mathcal{D}_1 : \Phi(x) \leqslant \Phi(\zeta)\big\}$ and this set is therefore always non-empty. Consequently, it holds that $\chi = \sup\mathcal{S} \geqslant \zeta$ and Theorem 4.9 yields $\mathrm{T}^{(\zeta,-\Phi(\zeta)-\Xi_Z(\lambda),\lambda)} = +\infty$, thus leading to $\mathbb{E}\big[\mathcal{Z}_{\mathcal{T}}\big] < +\infty$. By applying now Lemma 4.6, and noting that the function $\mathcal{V}\big(\cdot, \zeta, -\Phi(\zeta) - \Xi_Z(\lambda), \lambda\big) \equiv \zeta$ is the unique solution to

$$\begin{aligned}
\frac{\partial\mathcal{V}}{\partial t}\big(t, \zeta, -\Phi(\zeta) - \Xi_Z(\lambda), \lambda\big) &= \Phi\big(\mathcal{V}\big(t, \zeta, -\Phi(\zeta) - \Xi_Z(\lambda), \lambda\big)\big) - \Phi\big(\zeta\big),\\
\mathcal{V}\big(0, \zeta, -\Phi(\zeta) - \Xi_Z(\lambda), \lambda\big) &= \zeta,
\end{aligned}$$

we obtain $\mathbb{E}\big[\mathcal{Z}_{\mathcal{T}}\big] = 1$. This implies that $\mathcal{Z} = (\mathcal{Z}_t)_{t\leqslant\mathcal{T}}$ is a true martingale and can then be utilized as the density process of a probability measure $\mathbb{Q}'$, equivalent to $\mathbb{Q}$ and defined as follows:

$$\left.\frac{\mathrm{d}\mathbb{Q}'}{\mathrm{d}\mathbb{Q}}\right|_{\mathcal{F}_t} := \mathcal{Z}_t = e^{\mathcal{W}_t-\zeta X_0-\mathcal{K}_t}, \qquad \forall t \leqslant \mathcal{T}.$$

CBITCL parameters under $\mathbb{Q}'$
$\beta' := \beta$
$\nu'(\mathrm{d}z) := e^{\zeta z}\,\nu(\mathrm{d}z)$
$b' := b - \zeta\,\sigma^2 - \int_0^{+\infty} z\,\big(e^{\zeta z} - 1\big)\,\pi(\mathrm{d}z)$
$\sigma' := \sigma$
$\pi'(\mathrm{d}z) := e^{\zeta z}\,\pi(\mathrm{d}z)$
$b'_Z := b_Z + \lambda\,(\sigma_Z)^2 + \int_{\lvert z\rvert<1} z\,\big(e^{\lambda z} - 1\big)\,\gamma_Z(\mathrm{d}z)$
$\sigma'_Z := \sigma_Z$
$\gamma'_Z(\mathrm{d}z) := e^{\lambda z}\,\gamma_Z(\mathrm{d}z)$

Table 4.1. Parameter transformations from $\mathbb{Q}$ to $\mathbb{Q}'$ for the CBITCL process $(X_t, Z_t)_{t\leqslant\mathcal{T}}$.

The next step of the proof consists in using Itô's formula, in order to rewrite the process $\mathcal{Z} = (\mathcal{Z}_t)_{t \leqslant \mathcal{T}}$ as a stochastic exponential:

$$\begin{aligned}\mathcal{Z}_t = \mathcal{E}\left(\zeta\,\sigma\int_0^{\cdot}\sqrt{X_t}\,\mathrm{d}B_s^1 + \lambda\,\sigma_Z\int_0^{\cdot}\sqrt{X_t}\,\mathrm{d}B_s^2 + \int_0^{\cdot}\int_0^{+\infty}\left(e^{\zeta\,x}-1\right)\widetilde{N}_0(\mathrm{d}s,\mathrm{d}x)\right)\\ \times\,\mathcal{E}\left(\int_0^{\cdot}\int_0^{X_{s-}}\int_0^{+\infty}\left(e^{\zeta\,x}-1\right)\widetilde{N}_1(\mathrm{d}s,\mathrm{d}u,\mathrm{d}x) + \int_0^{\cdot}\int_0^{X_{s-}}\int_{\mathbb{R}}\left(e^{\lambda\,x}-1\right)\widetilde{N}_2(\mathrm{d}s,\mathrm{d}u,\mathrm{d}x)\right).\end{aligned}$$

By applying Girsanov's theorem, the processes $(B_t'^{,1})_{t\leqslant\mathcal{T}}$ and $(B_t'^{,2})_{t\leqslant\mathcal{T}}$ defined by

$$\begin{aligned}B_t'^{,1} &:= B_t^1 - \zeta\,\sigma\int_0^t\sqrt{X_s}\,\mathrm{d}s,\\ B_t'^{,2} &:= B_t^2 - \lambda\,\sigma_Z\int_0^t\sqrt{X_s}\,\mathrm{d}s,\end{aligned}$$

for all $t \leqslant \mathcal{T}$, are independent Brownian motions under $\mathbb{Q}'$. Again by Girsanov's theorem (see e.g. [**EK20**, Proposition 3.73]), $N_0(\mathrm{d}t,\mathrm{d}x)$, $N_1(\mathrm{d}t,\mathrm{d}u,\mathrm{d}x)$, and $N_2(\mathrm{d}t,\mathrm{d}u,\mathrm{d}x)$ remain Poisson random measures under $\mathbb{Q}'$, but with modified compensators as follows:

$$\begin{aligned}\widetilde{N}_0'(\mathrm{d}t,\mathrm{d}x) &:= N_0(\mathrm{d}t,\mathrm{d}x) - \mathrm{d}t\,e^{\zeta\,x}\,\nu(\mathrm{d}x),\\ \widetilde{N}_1'(\mathrm{d}t,\mathrm{d}u,\mathrm{d}x) &:= N_1(\mathrm{d}t,\mathrm{d}u,\mathrm{d}x) - \mathrm{d}t\,\mathrm{d}u\,e^{\zeta\,x}\,\pi(\mathrm{d}x),\\ \widetilde{N}_2'(\mathrm{d}t,\mathrm{d}u,\mathrm{d}x) &:= N_2(\mathrm{d}t,\mathrm{d}u,\mathrm{d}x) - \mathrm{d}t\,\mathrm{d}u\,e^{\lambda\,x}\,\gamma_Z(\mathrm{d}x),\end{aligned}$$

In order to show that the joint process $(X_t, Z_t)_{t\leqslant\mathcal{T}}$ remains a CBITCL process under $\mathbb{Q}'$, we need to rewrite its extended Dawson–Li representation (4.4)–(4.5) under $\mathbb{Q}'$ as follows:

$$\begin{aligned}X_t &= X_0 + \int_0^t\left(\beta' - b'\,X_s\right)\mathrm{d}s + \sigma\int_0^t\sqrt{X_s}\,\mathrm{d}B_s'^{,1}\\ &\quad + \int_0^t\int_0^{+\infty}x\,N_0(\mathrm{d}s,\mathrm{d}x) + \int_0^t\int_0^{X_{s-}}\int_0^{+\infty}x\,\widetilde{N}_1'(\mathrm{d}s,\mathrm{d}u,\mathrm{d}x), \qquad \forall t\leqslant\mathcal{T},\\ Z_t &= b_Z'\int_0^t X_s\,\mathrm{d}s + \sigma_Z'\int_0^t\sqrt{X_s}\,\mathrm{d}B_s'^{,2} + \int_0^t\int_0^{X_{s-}}\int_{|x|\geqslant 1}x\,N_2(\mathrm{d}s,\mathrm{d}u,\mathrm{d}x)\\ &\quad + \int_0^t\int_0^{X_{s-}}\int_{|x|<1}x\,\widetilde{N}_2'(\mathrm{d}s,\mathrm{d}u,\mathrm{d}x), \qquad \forall t\leqslant\mathcal{T}.\end{aligned}$$

In view of Lemma 4.2, we can conclude that the joint process $(X_t, Z_t)_{t\leqslant\mathcal{T}}$ remains a CBITCL process under $\mathbb{Q}'$ and associated to the parameters given in Table 4.1. □

In conclusion to this chapter, we briefly investigate the stability under $\mathbb{Q}'$ of some of the examples of CBI processes reported in Table 2.1. More specifically, we restrict our attention to the CIR process, the α-CIR process, and the tempered-stable CBI process, in view of their applications considered in Chapter 5. The next table contains the following observations:

- The first column describes whether the stability under $\mathbb{Q}'$ is ensured or not;
- The second column reports the parameters under $\mathbb{Q}'$ computed with Table 4.1.

	Stability under $\mathbb{Q}'$	Parameters under $\mathbb{Q}'$
CIR process (see [**CIR85**])	Yes, provided that $b > \zeta\,\sigma^2$, where $\zeta \in \mathcal{D}_1 = \mathbb{R}$	$\beta' = \beta$, $b' = b - \zeta\,\sigma^2$, and $\sigma' = \sigma$
α-CIR process, (see [**LM15, JMS17**], and [**JMSZ21**])	No, since for all $z \geqslant 0$: $\pi'(\mathrm{d}z) = \eta^\alpha\,C_\alpha\,z^{-1-\alpha}\,e^{\zeta\,z}\,\mathrm{d}z$, α-CIR processes then become tempered stable where $\zeta \in \mathcal{D}_1 = \mathbb{R}_-$	$\beta' = \beta$, b' is given by $b - \zeta\,\sigma^2 + \alpha\,\eta^\alpha\,C_\alpha\,\Gamma(-\alpha)\,(-\zeta\,\eta)^{\alpha-1}$, $\sigma' = \sigma$, $\eta' = \eta$, $C'_\alpha = C_\alpha$, and $\alpha' = \alpha$
Tempered-stable CBI process (see Section 2.7)	Yes, since for all $z \geqslant 0$: $\pi'(\mathrm{d}z) = \eta^\alpha\,C_\alpha\,z^{-1-\alpha}\,e^{-\frac{\theta-\zeta\,\eta}{\eta}\,z}\,\mathrm{d}z$, where $\theta' := \theta - \zeta\,\eta \geqslant 0$, for $\zeta \in \mathcal{D}_1 = (-\infty, \theta/\eta]$	$\beta' = \beta$, b' is given by $b - \zeta\,\sigma^2 - \alpha\,\eta^\alpha\,C_\alpha\,\Gamma(-\alpha)\,\theta^{\alpha-1} +$ $\alpha\,\eta^\alpha\,C_\alpha\,\Gamma(-\alpha)\,(\theta - \zeta\,\eta)^{\alpha-1}$, $\sigma' = \sigma$, $\eta' = \eta$, $C'_\alpha = C_\alpha$, $\theta' = \theta - \zeta\,\eta$, and $\alpha' = \alpha$

TABLE 4.2. Stability under $\mathbb{Q}'$ of some of the examples of CBI processes reported in Table 2.1 (we refer to Appendix 5.A for the computation of the drift b' in both α-CIR and tempered-stable cases).

CHAPTER 5

CBITCL processes for multiple currency modeling

SUMMARY. We develop a general stochastic volatility modeling framework for multiple currencies based on *CBI-Time-Changed Lévy processes* (CBITCL). Besides capturing the typical sources of risk in the FX market, and preserving the peculiar symmetries of FX rates, our framework allows for self-excitation in the volatility of FX rates, which is generated by the self-exciting behavior of CBI processes. The proposed approach is analytically tractable since it relies on the technology of affine processes, and allows to characterize a class of risk-neutral measures that leave invariant the structure of the framework. Then, we derive a semi-closed-form pricing formula for currency options via Fourier techniques. Finally, we test our model by means of a calibration to an FX triangle where two types of calibration are proposed: *standard* and *deep*, the latter of which uses deep-learning techniques.

Contents

5.1. Introduction

5.1.1. Motivation. The Foreign-Exchange (FX) market has never ceased to grow over the years. According to the Bank for International Settlements (BIS) (see [**BIS19**]), its trading volume attained \$6.6 trillion per day in April 2019, in comparison to \$5.1 trillion three years earlier. This growth can be partly explained by the ever-growing "electronification" of the FX market, i.e. the rise of electronic and automated trading (see e.g. [**Woo19**]). This induces a significant inflow of diverse market participants, which boosts liquidity but is also accompanied by an increased propensity toward riskier investments. In particular, the trading of "soft" currencies[1] grew faster than that of "hard" currencies between 2016 and 2019, attaining 23% of the FX turnover against 19% three years earlier. This has encouraged market participants to manage their risk exposure by relying on financial models capable of capturing the principal risk drivers of the FX market.

When constructing a financial model for multiple currencies, special attention has to be paid to the symmetries that FX rates typically satisfy. To describe these symmetries, consider an FX rate $S^{d,f}$ between the domestic currency d and a foreign currency f (i.e. the value of one unit of currency f measured in units of currency d). The symmetries of FX rates consist in the following:

- If we invert the FX rate $S^{d,f}$, then we must obtain $S^{f,d} = 1/S^{d,f}$, which is the value of one unit of currency d measured in units of currency f. This is referred to as *inversion*;
- Take any additional currency e. The FX rate $S^{d,f}$ must be implied from $S^{d,e}$ and $S^{e,f}$ through multiplication: $S^{d,f} = S^{d,e} \times S^{e,f}$. This is called *triangulation*.

Among the classic sources of risk in the FX market, we find stochastic volatility and jumps in FX rates, whose empirical evidence has been documented in [**GJ87, Jor88, NVW94, Bek95**]. These two features are shared with other financial markets (e.g. equity markets), which has led to employ for FX markets, up to minor modifications, financial models initially conceived for stock returns. We can mention the *Garman–Kohlhagen model* [**GK83**], which is the FX counterpart of the Black–Scholes model. An FX adaptation of the Heston model has also been proposed by [**JKWW11**]. For further examples of such models, we can refer the reader to the volumes [**Lip01, Cas10, Cla11, Wys17**].

We can find two other significant risk factors in the FX market: the presence of stochastic dependence among FX rates, and the stochastic skewness of the FX volatility smile. Concerning the latter, [**CW07**] analyzed the time series of risk-reversals[2], which are in fact known to measure the asymmetry of the FX volatility smile. The authors showed that their values vary greatly over time and exhibit repeated sign changes. They therefore suggested that the skewness of the FX volatility smile should be stochastic and developed a financial model driven by time-changed Lévy processes in order to reproduce this empirical fact.

[1] According to the terminology of [**JFB15**, Section 5.4.2], a "soft" currency corresponds to an emerging country, while a "hard" currency refers to a developed country, i.e. a major currency.

[2] We recall that a risk-reversal, in the context of FX options, measures the difference in implied volatility between an OTM call option and its put counterpart such that they share the same maturity and have symmetric deltas.

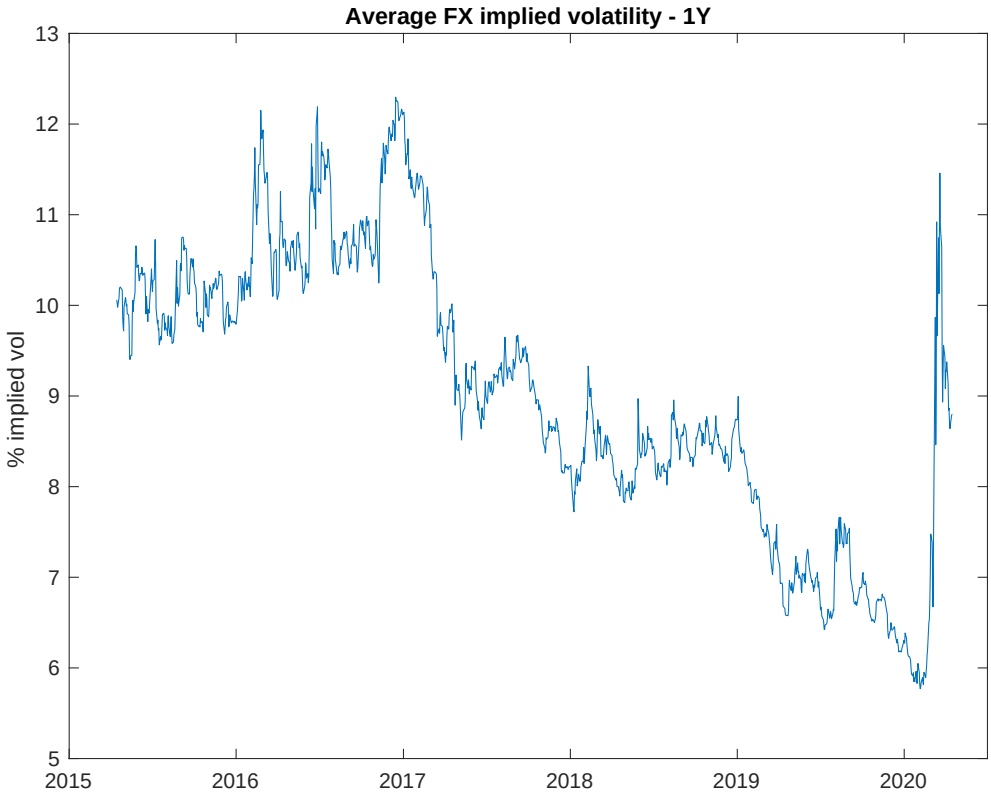

FIGURE 5.1. Weighted average of the 1Y ATM call-implied volatilities of the three major currency pairs USDJPY, EURJPY, and EURUSD, where the weights are represented by the reciprocal bid-ask spreads. The period spans from 2015 to 2020. Source: Bloomberg.

Finally, volatility clustering has been extensively detected across most asset classes (see e.g. [**CT04**, Chapter 7]). This phenomenon tends to be amplified in the FX market, especially due to its electronification (see again [**Woo19**]). Figure 5.1 illustrates the weighted average of the 1Y ATM call-implied volatilities of three major currency pairs (USDJPY, EURJPY, and EURUSD), where the weights are represented by the reciprocal bid-ask spreads. The period spans from 2015 to 2020, thus covering events such as the Brexit referendum, the 2016 United States presidential election, and the first phase of the COVID-19 pandemic. Around these key events, we are able to observe successive jump clusters. This empirical behavior suggests the potential presence of self-excitation in the volatility of FX rates. In particular, one can also expect an amplification of this phenomenon when dealing with currency pairs that involve a hard currency and a soft one.

5.1.2. Contribution. In this chapter, we develop a general stochastic volatility modeling framework for multiple currencies that allows for self-excitation in the volatility of FX rates, while capturing the typical sources of risk in the FX market (such as stochastic dependence among FX rates and stochastic skewness of the FX volatility smile), and preserving the peculiar symmetries of FX rates (i.e. symmetries under inversion and triangulation).

By relying on the technology of *CBI-Time-Changed Lévy processes* (CBITCL, Chapter 4), the proposed approach possesses a remarkable level of analytical tractability. More specifically, by exploiting the affine structure of CBITCL processes (see Proposition 4.3), we can show that CBITCL processes are *coherent* in the sense of [**Gno17**]. This means that if an FX rate is modeled by a CBITCL process, then the inverse FX rate belongs to the same modeling class (we refer to Remark 4.4 for further details). Inspired by [**Gno17**, Section 4], we design our modeling framework by adopting an *artificial currency approach*. The underlying idea consists in expressing each FX rate as the ratio of two primitive processes, with one primitive process associated to each currency. FX rates will therefore satisfy the inversion and triangulation symmetries by construction. As a consequence, this formulation reduces to modeling all primitive processes with a common family of CBITCL processes, assumed to be mutually independent.

By using a Girsanov-type result for CBITCL processes (see Theorem 4.12), we characterize a class of risk-neutral measures that leave invariant the structure of the model. By utilizing the preservation of the affine property, we derive a semi-closed-form pricing formula for currency options by means of Fourier techniques. The proposed approach can also reproduce several features of the FX market. In particular, it allows for non-trivial stochastic dependence between the different currencies, and for non-trivial dependence between FX rates and their volatilities. We emphasize that the latter type of dependence is known to play a relevant role in generating FX volatility smiles that exhibit stochastic skewness.

We assess the empirical performance of our model by means of a calibration to an FX triangle consisting of three major currency pairs (USDJPY, EURJPY, and EURUSD). We restrict our attention to two specifications of our model: the first one simply considers a Brownian motion as the Lévy process of each CBITCL process; the second one consists in choosing the *CGMY process* [**CGMY02**] as the Lévy process of each CBITCL process. For both specifications, each CBI process is set to be a *tempered-stable CBI process* in the sense of Section 2.7. We perform two calibrations: *standard* and *deep*, where the latter uses deep-learning techniques developed by [**HMT21**]. We mention that this type of calibration is here applied for the first time to a multi-currency setting.

Finally, by retaining the calibrated values of the model parameters, we complete our numerical assessment of the proposed approach by carrying out a sensitivity analysis on model-implied volatility smiles. For this empirical study, we restrict our attention to the parameters controlling the self-exciting jump component of each tempered-stable CBI process. The objective behind this sensitivity analysis is to determine the impact of the self-exciting behavior of the tempered-stable CBI processes on the shape of the FX volatility smile.

5.1.3. Related literature. Our modeling framework is based on an *artificial currency approach*. To the best of our knowledge, the idea of introducing a global numéraire, whose value can be expressed in any currency, first appeared in [**FH97**]. Later, [**Dou07**] revisited this framework under a different terminology, i.e. the *intrinsic currency framework*. Then, several stochastic volatility models for multiple currencies have been developed by relying on this approach, see e.g.

[**Dou12, DCGG13, GG14, BGP15**]. From a different standpoint, we can mention the principal component stochastic volatility model of [**EG18**]. We also mention the recent work of [**GGP21**], which unifies [**DCGG13**] and [**BGP15**]. All these frameworks preserve the symmetries of FX rates while taking into account most of the sources of risk in the FX market. Yet, none of them allow for self-excitation in the volatility of FX rates as they can all be considered as generalizations of the Heston model.

A large number of FX models for multiple currencies are based on multi-dimensional extensions of the Heston model. This is justified by the fact that the Heston model is known to be closed under inversion (see e.g. [**DBnR08**]). Motivated by this fact, [**Gno17, GBP20**] have recently characterized all models that remain stable under inversion, allowing for more general modeling approaches beyond the Brownian setting of the Heston model. These models have been termed *coherent* by [**Gno17**] and *consistent* by [**GBP20**]. We will see later that CBITCL processes are coherent in this sense.

Several approaches for the modeling of multiple currencies have gone beyond the Brownian setting, especially using time-changed Lévy processes. We first mention the time-inhomogeneous Lévy framework of [**EK06**], recalling that time-inhomogeneous Lévy processes can be regarded as time-changed Lévy processes with deterministic activity rate. [**CW07**] developed a model based on time-changed Lévy processes with CIR-type activity rate, whose configuration contributed to the stochastic skewness of the FX volatility smile (we also refer the reader to [**Joh02, BCW08, AM09, Itk17**] on this issue).

More recently, [**BDR17**] have developed a multi-currency modeling framework driven by a multi-dimensional Lévy process with dependent components, relying on a factor representation for Lévy processes. In this work, only pure Lévy processes were considered and, therefore, stochastic volatility was not explicitly modeled. This was justified by the short maturities of the contracts considered in the calibration. [**BDR17**] suggested however that time change techniques could be used in future research. In this regard, [**BM18**] have proposed a model based on time-changed Lévy processes for the modeling of a single FX rate (USDJPY).

In their model, the activity rate exhibits self-excitation as well as jumps of infinite activity. Moreover, the presence of a common jump structure between the Lévy process and the activity rate induces non-trivial dependence between the FX rate and its volatility. The objective behind such a mechanism was to introduce correlation between the FX rate and its volatility. By comparing their specification with a benchmark, the authors found evidence of a mild correlation between the FX rate and its volatility, with an indication that this correlation is more pronounced as the interest rate differential broadens (e.g. when the FX rate involves a hard currency and a soft currency).

5.1.4. Structure. In Section 5.2, we describe our general modeling framework. Section 5.3 presents the main features of the proposed approach. Section 5.4 provides a numerical assessment of our model, while Section 5.5 concludes the chapter. Finally, Appendix 5.A contains some aspects of the specifications considered in Section 5.4.

5.2. A CBITCL modeling framework

Let $\mathcal{T} < +\infty$ be a finite time horizon and $\big(\Omega, \mathcal{F}, \mathbb{F}, \mathbb{Q}\big)$ a stochastic basis satisfying the usual conditions, $\mathbb{Q}$ is a probability measure and the structure of $\mathbb{F} = (\mathcal{F}_t)_{t \leqslant \mathcal{T}}$ will be specified later.

5.2.1. Preliminaries on the multiple currency market. The FX market is a financial market where multiple currencies are traded by spot and derivative transactions. Such a market involves different economies, each one associated to a specific currency. The i^{th} and j^{th} currencies are related by the spot FX rate process $S^{i,j} = (S^{i,j}_t)_{t \leqslant \mathcal{T}}$, where $S^{i,j}_t$ denotes the value at time t of one unit of currency j measured in units of currency i. Let us now formally define a multiple currency market. To this end, consider the following ingredients:

(i) Let $N \geqslant 2$ denote the number of currencies traded in the market;
(ii) Let $\boldsymbol{D} = (D^i_t)^{1 \leqslant i \leqslant N}_{t \leqslant \mathcal{T}}$ be an $\mathbb{R}^N$-valued process where each D^i represents the bank account of the i^{th} economy given by $D^i_t := e^{r^i t}$, for all $t \leqslant \mathcal{T}$, where $r^i \geqslant 0$ denotes the short rate;
(iii) Let $\boldsymbol{S} = (S^{i,j}_t)^{1 \leqslant i,j \leqslant N}_{t \leqslant \mathcal{T}}$ be an $\mathbb{R}^{N \times N}$-valued process denoting the spot FX rate processes between the different currencies such that for every $1 \leqslant i \leqslant N$ we have $S^{i,i}_t = 1$ for all $t \leqslant \mathcal{T}$, and for every $1 \leqslant i, j \leqslant N$ with $i \neq j$, $S^{i,j}_t > 0$ for all $t \leqslant \mathcal{T}$.

In line with the classic construction of financial models for multiple currencies (see e.g. [**MR06**, Chapter 4]), we formulate the definition of a multiple currency market as follows.

Definition 5.1. We say that the triplet $\big(N, \boldsymbol{D}, \boldsymbol{S}\big)$ represents a *multiple currency market* if for every $1 \leqslant i \leqslant N$, the following basic assets are traded in the i^{th} economy:

- The bank account $D^i = (D^i_t)_{t \leqslant \mathcal{T}}$;
- For every $1 \leqslant j \leqslant N$ with $j \neq i$, the bank account of the j^{th} economy denominated in units of the i^{th} currency, namely $S^{i,j} D^j$.

For every $1 \leqslant i \leqslant N$, no arbitrage in the sense of *No Free Lunch with Vanishing Risk* (NFLVR) in the i^{th} economy is guaranteed by the existence of a risk-neutral measure $\mathbb{Q}^i$ with respect to the bank account D^i (see [**DS94, DS98**])[3]. However, this does not take into account the elementary no-arbitrage relationships that spot FX rates must satisfy, namely symmetries under inversion and triangulation. To this effect, we propose the following definition, extending [**EG18**, Definition 1] to an FX market consisting of more than three currencies.

Definition 5.2. The multiple currency market $\big(N, \boldsymbol{D}, \boldsymbol{S}\big)$ is *well posed* if the following hold:

(i) No direct arbitrage: For every $1 \leqslant i, j \leqslant N$, $S^{j,i}_t = 1/S^{i,j}_t, \quad \forall t \leqslant \mathcal{T}$;
(ii) No triangular arbitrage: For every $1 \leqslant i, k, j \leqslant N$, $S^{i,j}_t = S^{i,k}_t \times S^{k,j}_t, \quad \forall t \leqslant \mathcal{T}$;
(iii) NFLVR: For every $1 \leqslant i \leqslant N$, there exists a risk-neutral measure $\mathbb{Q}^i$ with respect to the bank account D^i for the i^{th} economy.

[3]Recall that a risk-neutral measure $\mathbb{Q}^i$ with respect to the bank account D^i for the i^{th} economy, for every $1 \leqslant i \leqslant N$, is a probability measure equivalent to $\mathbb{Q}$ such that for every $1 \leqslant j \leqslant N$, the D^i-discounted process $S^{i,j} D^j / D^i$ is a local martingale under $\mathbb{Q}^i$.

REMARK 5.3. [**Moo01**], and [**FKT17, CQTZ20**] more recently, have documented that triangular arbitrage opportunities exist in FX markets, but with a duration of less than one second (there may exist a triplet (i, j, k) such that $S_t^{i,j} \neq S_t^{i,k} \times S_t^{k,j}$ over a short time interval). Allowing for such possibilities is beyond our scope, and then we consider only markets as in Definition 5.2.

In the case of a two-economy market consisting of currencies i and j, well-posedness is automatically satisfied by construction as long as NFLVR holds for both economies. However, assuming that the spot FX rate process $S^{i,j}$ belongs under $\mathbb{Q}^i$ to a certain modeling class, nothing indicates that the inverse process $S^{j,i}$ shares the same modeling class under $\mathbb{Q}^j$. In this respect, the so-called *coherent* models of [**Gno17**] overcome this drawback by being stable under inversion. More specifically, [**Gno17**, Theorem 3.1] shows that affine stochastic volatility models as considered in [**KR11**] are coherent, including in particular CBITCL processes as we will see below.

In general, there is no guarantee that coherent models, when extended to $N \geqslant 3$ currencies, are compatible with well-posedness. Yet, they can be used as building blocks for more general models as discussed in [**Gno17**, Section 4]. Inspired by this fact, we construct our modeling framework for multiple currencies by adopting the *artificial currency approach*. We will proceed along the following steps:

(1) We first express each currency with respect to an artificial currency indexed by 0, which gives rise to N artificial spot FX rates $(S^{0,i})_{1 \leqslant i \leqslant N}$. We then exploit the Girsanov-type result for CBITCL processes that we formulated in Chapter 4 (see Theorem 4.12), in order to characterize a class of risk-neutral measures for the multiple currency market;
(2) The second step consists in the computation of the spot FX rate processes $S^{i,j} = (S_t^{i,j})_{t \leqslant \mathcal{T}}$, for every $1 \leqslant i, j \leqslant N$, with respect to $(S^{0,i})_{1 \leqslant i \leqslant N}$ by taking appropriate ratios, which results in a multiple currency market $\big(N, \boldsymbol{D}, \boldsymbol{S}\big)$ that can be proved to be well posed in the sense of Definition 5.2.

5.2.2. Construction of the CBITCL multi-currency model. Consider the next standing assumption, which is the starting point of the artificial currency approach (see Chapter 1):

ASSUMPTION 5.4. There exists an artificial currency indexed by 0 and related to the i^{th} currency through the artificial spot FX rate process $S^{0,i} = (S_t^{0,i})_{t \leqslant \mathcal{T}}$, for every $1 \leqslant i \leqslant N$.

Our formulation consists in modeling all artificial spot FX rates $(S^{0,i})_{1 \leqslant i \leqslant N}$ with a common family of CBITCL processes, assumed to be mutually independent, where each CBITCL process is directly defined by its extended Dawson–Li stochastic integral representation (4.4)–(4.5) (see Chapter 4). To proceed, fix $d \in \mathbb{N}$ and assume the existence of the following objects, for every $1 \leqslant k \leqslant d$:

- Two standard Brownian motions $B^{k,1} = (B_t^{k,1})_{t \leqslant \mathcal{T}}$ and $B^{k,2} = (B_t^{k,2})_{t \leqslant \mathcal{T}}$;
- A Poisson random measure $N_0^k(\mathrm{d}t, \mathrm{d}x)$ on $[0, \mathcal{T}] \times \mathbb{R}_+$ with compensator $\mathrm{d}t\, \nu^k(\mathrm{d}x)$ and compensated measure $\widetilde{N}_0^k(\mathrm{d}t, \mathrm{d}x) := N_0^k(\mathrm{d}t, \mathrm{d}x) - \mathrm{d}t\, \nu^k(\mathrm{d}x)$, where ν^k is a Lévy measure on $\mathbb{R}_+$ such that $\int_0^1 x\, \nu^k(\mathrm{d}x) < +\infty$;

- A Poisson random measure $N_1^k(\mathrm{d}t, \mathrm{d}u, \mathrm{d}x)$ on $[0, \mathcal{T}]\times\mathbb{R}_+\times\mathbb{R}_+$ with compensator $\mathrm{d}t\,\mathrm{d}u\,\pi^k(\mathrm{d}x)$ and compensated measure $\widetilde{N}_1^k(\mathrm{d}t, \mathrm{d}u, \mathrm{d}x) := N_1^k(\mathrm{d}t, \mathrm{d}u, \mathrm{d}x) - \mathrm{d}t\,\mathrm{d}u\,\pi^k(\mathrm{d}x)$, where π^k is a Lévy measure on $\mathbb{R}_+$ such that $\int_1^{+\infty} x\,\pi^k(\mathrm{d}x) < +\infty$;
- A Poisson random measure $N_2^k(\mathrm{d}t, \mathrm{d}u, \mathrm{d}x)$ on $[0, \mathcal{T}]\times\mathbb{R}_+\times\mathbb{R}$ with compensator $\mathrm{d}t\,\mathrm{d}u\,\gamma_Z^k(\mathrm{d}x)$ and compensated measure $\widetilde{N}_2^k(\mathrm{d}t, \mathrm{d}u, \mathrm{d}x) := N_2^k(\mathrm{d}t, \mathrm{d}u, \mathrm{d}x) - \mathrm{d}t\,\mathrm{d}u\,\gamma_Z^k(\mathrm{d}x)$, where γ_Z^k is a Lévy measure on $\mathbb{R}$.

We suppose that for every $1 \leqslant k \leqslant d$, $B^{k,1}$, $B^{k,2}$, N_0^k, N_1^k, and N_2^k are mutually independent with respect to the filtration

$$\mathcal{F}_t^k := \mathcal{F}_t^{B^{k,1}} \vee \mathcal{F}_t^{B^{k,2}} \vee \mathcal{F}_t^{N_0^k} \vee \mathcal{F}_t^{N_1^k} \vee \mathcal{F}_t^{N_2^k}, \qquad \forall t \leqslant \mathcal{T}, \tag{5.1}$$

and all these processes are also mutually independent across different $1 \leqslant k \leqslant d$.

Let us define, for every $1 \leqslant k \leqslant d$ and for $X_0^k \in \mathbb{R}_+$, the following system of stochastic integral equations

$$\begin{aligned} X_t^k &= X_0^k + \int_0^t \left(\beta^k - b^k\,X_s^k\right)\mathrm{d}s + \sigma^k \int_0^t \sqrt{X_s^k}\,\mathrm{d}B_s^{k,1} \\ &\quad + \int_0^t \int_0^{+\infty} x\,N_0^k(\mathrm{d}s, \mathrm{d}x) + \int_0^t \int_0^{X_{s-}^k} \int_0^{+\infty} x\,\widetilde{N}_1^k(\mathrm{d}s, \mathrm{d}u, \mathrm{d}x), \qquad \forall t \leqslant \mathcal{T}, \end{aligned} \tag{5.2}$$

$$\begin{aligned} Z_t^k &= b_Z^k \int_0^t X_s^k\,\mathrm{d}s + \sigma_Z^k \int_0^t \sqrt{X_s^k}\,\mathrm{d}B_s^{k,2} + \int_0^t \int_0^{X_{s-}^k} \int_{|x|\geqslant 1} x\,N_2^k(\mathrm{d}s, \mathrm{d}u, \mathrm{d}x) \\ &\quad + \int_0^t \int_0^{X_{s-}^k} \int_{|x|<1} x\,\widetilde{N}_2^k(\mathrm{d}s, \mathrm{d}u, \mathrm{d}x), \qquad \forall t \leqslant \mathcal{T}, \end{aligned} \tag{5.3}$$

where $\beta^k \geqslant 0$, $b^k \in \mathbb{R}$, $\sigma^k \geqslant 0$, $b_Z^k \in \mathbb{R}$, and $\sigma_Z^k \geqslant 0$. By Lemma 4.2, the joint process $(X_t^k, Z_t^k)_{t\leqslant\mathcal{T}}$ is a CBITCL$\left(X_0^k, \Psi^k, \Phi^k, \Xi_Z^k\right)$ with respect to the filtration $(\mathcal{F}_t^k)_{t\leqslant\mathcal{T}}$, for every $1 \leqslant k \leqslant d$. We then introduce the following standing assumption on the branching mechanisms $\left(\Phi^k\right)_{1\leqslant k\leqslant d}$.

Assumption 5.5. For every $1 \leqslant k \leqslant d$, Φ^k satisfies Assumption 2.4.

In summary, the global filtration $(\mathcal{F}_t)_{t\leqslant\mathcal{T}}$ is given by

$$\mathcal{F}_t := \bigvee_{1\leqslant k\leqslant d} \mathcal{F}_t^k, \qquad \forall t \leqslant \mathcal{T}. \tag{5.4}$$

Denoting now the factor processes $X = (X_t)_{t\leqslant\mathcal{T}}$ and $Z = (Z_t)_{t\leqslant\mathcal{T}}$ by $X_t := \left(X_t^1, \ldots, X_t^d\right)^\top$ and $Z_t := \left(Z_t^1, \ldots, Z_t^d\right)^\top$ for all $t \leqslant \mathcal{T}$, respectively, we also consider the following objects:

- A family of vectors $\boldsymbol{\zeta} = (\zeta_1, \ldots, \zeta_N)$ with $\zeta_i \in \mathbb{R}^d$, for every $1 \leqslant i \leqslant N$, and where for every $1 \leqslant i \leqslant N$ and $1 \leqslant k \leqslant d$, $\zeta_{i,k} \in \mathcal{D}_1^k$;
- A family of vectors $\boldsymbol{\lambda} = (\lambda_1, \ldots, \lambda_N)$ with $\lambda_i \in \mathbb{R}^d$, for every $1 \leqslant i \leqslant N$, and where for every $1 \leqslant i \leqslant N$ and $1 \leqslant k \leqslant d$, $\lambda_{i,k} \in \mathcal{D}_2^k$;
- A family of stochastic processes $(\mathcal{K}^{i,k})_{1\leqslant k\leqslant d}^{1\leqslant i\leqslant N}$, where for every $1 \leqslant i \leqslant N$ and $1 \leqslant k \leqslant d$, $\mathcal{K}^{i,k} = (\mathcal{K}_t^{i,k})_{t\leqslant\mathcal{T}}$ denotes the exponential compensator of the process $\left(\zeta_{i,k}\,X_t^k + \lambda_{i,k}\,Z_t^k\right)_{t\leqslant\mathcal{T}}$ in the sense of Lemma 4.11,

where we recall from Chapters 2 and 4 that $\mathcal{D}_1^k$ represents the effective domain of the immigration and branching mechanism functions Ψ^k and Φ^k, given by (2.8), while $\mathcal{D}_2^k$ refers to the effective domain of the Lévy exponent Ξ_Z^k, given by (4.10), for every $1 \leqslant k \leqslant d$.

Definition 5.6. The tuple $\big(X, Z, \boldsymbol{\zeta}, \boldsymbol{\lambda}\big)$ is said to generate a *CBITCL multi-currency model* if

$$S_t^{0,i} = S_0^{0,i}\, e^{-\,r^i\, t} \prod_{k=1}^{d} e^{\,\zeta_{i,k}\, X_t^k + \lambda_{i,k}\, Z_t^k - \mathcal{K}_t^{i,k}}, \qquad \forall t \leqslant \mathcal{T}, \tag{5.5}$$

where $S_0^{0,i} > 0$ and $r^i \geqslant 0$ denotes the short rate of the i^{th} economy, for every $1 \leqslant i \leqslant N$.

We point out that the artificial spot FX rates $(S^{0,i})_{1 \leqslant i \leqslant N}$ are modeling quantities that cannot be observed in reality (see Chapter 1). Yet, the constants $\zeta_{i,k}$ and $\lambda_{i,k}$ will play specific roles in the dynamics of the spot FX rate processes. While $\lambda_{i,k}$ will capture the relative importance of the jump risk arising from the k^{th} time-changed Lévy process $Z^k = (Z_t^k)_{t \leqslant \mathcal{T}}$, $\zeta_{i,k}$ will measure the weight of the dependence between the k^{th} CBI process $X^k = (X_t^k)_{t \leqslant \mathcal{T}}$ and the FX rate.

As a preliminary, we can derive the dynamics of each artificial spot FX rate $(S^{0,i})_{1 \leqslant i \leqslant N}$, making use of the standing assumption that each CBITCL process $(X_t^k, Z_t^k)_{t \leqslant \mathcal{T}}$ is defined by its extended Dawson–Li stochastic integral representation (5.2)–(5.3).

Lemma 5.7. *Let $\big(X, Z, \boldsymbol{\zeta}, \boldsymbol{\lambda}\big)$ generate a CBITCL multi-currency model. Then, for every $1 \leqslant i \leqslant N$, the artificial spot FX rate process $S^{0,i} = (S_t^{0,i})_{t \leqslant \mathcal{T}}$ is the unique strong solution to the following stochastic differential equation:*

$$\begin{aligned} \frac{\mathrm{d}S_t^{0,i}}{S_{t-}^{0,i}} &= -\,r^i\,\mathrm{d}t + \sum_{k=1}^{d} \left(\sqrt{X_t^k}\, \left(\zeta_{i,k}\, \sigma^k\, \mathrm{d}B_t^{k,1} + \lambda_{i,k}\, \sigma_Z^k\, \mathrm{d}B_t^{k,2} \right) + \int_0^{+\infty} \left(e^{\,\zeta_{i,k}\, x} - 1 \right)\, \widetilde{N}_0^k(\mathrm{d}t, \mathrm{d}x) \right) \\ &\quad + \sum_{k=1}^{d} \int_0^{X_{t-}^k} \left(\int_0^{+\infty} \left(e^{\,\zeta_{i,k}\, x} - 1 \right)\, \widetilde{N}_1^k(\mathrm{d}t, \mathrm{d}u, \mathrm{d}x) + \int_{\mathbb{R}} \left(e^{\,\lambda_{i,k}\, x} - 1 \right)\, \widetilde{N}_2^k(\mathrm{d}t, \mathrm{d}u, \mathrm{d}x) \right). \end{aligned} \tag{5.6}$$

Proof. A direct application of Itô's formula, combined with system (5.2)–(5.3) and equation (4.22), implies weak existence of the solution to equation (5.6). Pathwise uniqueness then follows from the extended Dawson–Li stochastic integral representation (4.4)–(4.5). By using [**BLP15**, Theorem 2] for example, pathwise uniquess together with weak existence implies strong existence for equation (5.6). □

The next theorem provides a characterization of a class of risk-neutral measures for the multiple currency market, preserving the structure of the CBITCL multi-currency model of Definition 5.6. This result can be regarded as a multi-dimensional extension of the Girsanov-type theorem for CBITCL processes that we formulated in Chapter 4 (see Theorem 4.12).

Theorem 5.8. *Let $\big(X, Z, \boldsymbol{\zeta}, \boldsymbol{\lambda}\big)$ generate a CBITCL multi-currency model. Then, for every $1 \leqslant i \leqslant N$, the stochastic process $S^{0,i}\, D^i$ is a true martingale and there exists an equivalent probability measure $\mathbb{Q}^i$ defined by*

$$\left.\frac{\mathrm{d}\mathbb{Q}^i}{\mathrm{d}\mathbb{Q}}\right|_{\mathcal{F}_t} := \frac{S_t^{0,i}\, D_t^i}{S_0^{0,i}}, \qquad \forall t \leqslant \mathcal{T}, \tag{5.7}$$

CBITCL parameters under $\mathbb{Q}^i$
$\beta^{i,k} := \beta^k$
$\nu^{i,k}(\mathrm{d}z) := e^{\,\zeta_{i,k}\,z}\,\nu^k(\mathrm{d}z)$
$b^{i,k} := b^k - \zeta_{i,k}\,(\sigma^k)^2 - \int_0^{+\infty} z\left(e^{\,\zeta_{i,k}\,z} - 1\right)\pi^k(\mathrm{d}z)$
$\sigma^{i,k} := \sigma^k$
$\pi^{i,k}(\mathrm{d}z) := e^{\,\zeta_{i,k}\,z}\,\pi^k(\mathrm{d}z)$
$b_Z^{i,k} := b_Z^k + \lambda_{i,k}\,(\sigma_Z^k)^2 + \int_{\lvert z\rvert<1} z\left(e^{\,\lambda_{i,k}\,z} - 1\right)\gamma_Z^k(\mathrm{d}z)$
$\sigma_Z^{i,k} := \sigma_Z^k$
$\gamma_Z^{i,k}(\mathrm{d}z) := e^{\,\lambda_{i,k}\,z}\,\gamma_Z^k(\mathrm{d}z)$

TABLE 5.1. Parameter transformations from $\mathbb{Q}$ to $\mathbb{Q}^i$ for the CBITCL process $(X_t^k, Z_t^k)_{t\leqslant\mathcal{T}}$.

which is a risk-neutral measure with respect to the bank account D^i for the i^{th} economy, and under which for every $1 \leqslant k \leqslant d$, the joint process $(X_t^k, Z_t^k)_{t\leqslant\mathcal{T}}$ remains a CBITCL process with parameters given by $\left(\beta^{i,k}, \nu^{i,k}, b^{i,k}, \sigma^{i,k}, \pi^{i,k}, b_Z^{i,k}, \sigma_Z^{i,k}, \gamma_Z^{i,k}\right)$ in Table 5.1.

PROOF. By Theorem 4.12, for every $1 \leqslant i \leqslant N$ and $1 \leqslant k \leqslant d$, the process $\mathcal{Z}^{i,k} = (\mathcal{Z}_t^{i,k})_{t\leqslant\mathcal{T}}$ defined by

$$\mathcal{Z}_t^{i,k} := e^{\,\zeta_{i,k}\,X_t^k + \lambda_{i,k}\,Z_t^k - \mathcal{K}_t^{i,k}}, \qquad \forall t \leqslant \mathcal{T},$$

is a martingale with respect to the filtration $(\mathcal{F}_t^k)_{t\leqslant\mathcal{T}}$. By applying [**Che06**, Theorem 2.1] among others to the product of independent martingales (5.5), for every $1 \leqslant i \leqslant N$, we obtain that the stochastic process $S^{0,i}\,D^i$ is a true martingale, for every $1 \leqslant i \leqslant N$. In turn, this implies the existence of a probability measure $\mathbb{Q}^i$, equivalent to $\mathbb{Q}$ and defined as follows:

$$\left.\frac{\mathrm{d}\mathbb{Q}^i}{\mathrm{d}\mathbb{Q}}\right|_{\mathcal{F}_t} := \frac{S_t^{0,i}\,D_t^i}{S_0^{0,i}}, \qquad \forall t \leqslant \mathcal{T},$$

where it can be easily checked, by referring to [**GEKR95**, Theorem 1] for example, that $\mathbb{Q}^i$ is a risk-neutral measure with respect to the bank account D^i for the i^{th} economy, for every $1 \leqslant i \leqslant N$.

In order to show that the joint processes $(X_t^k, Z_t^k)_{t\leqslant\mathcal{T}}$, for every $1 \leqslant k \leqslant d$, remain CBITCL processes under $\mathbb{Q}^i$, we follow the proof of Theorem 4.12. For convenience of the reader, we give full details. To proceed, we first need to rewrite (5.7) as a stochastic exponential by Lemma 5.7, as follows:

$$\begin{aligned}\left.\frac{\mathrm{d}\mathbb{Q}^i}{\mathrm{d}\mathbb{Q}}\right|_{\mathcal{F}_t} &= \prod_{k=1}^d \mathcal{E}\left(\zeta_{i,k}\,\sigma^k\int_0^\cdot\sqrt{X_t^k}\,\mathrm{d}B_s^{k,1} + \lambda_{i,k}\,\sigma_Z^k\int_0^\cdot\sqrt{X_t^k}\,\mathrm{d}B_s^{k,2} + \int_0^\cdot\int_0^{+\infty}\left(e^{\,\zeta_{i,k}\,x} - 1\right)\widetilde{N}_0^k(\mathrm{d}s,\mathrm{d}x)\right)_t \\ &\quad\times\prod_{k=1}^d \mathcal{E}\left(\int_0^\cdot\int_0^{X_{s-}^k}\int_0^{+\infty}\left(e^{\,\zeta_{i,k}\,x} - 1\right)\widetilde{N}_1^k(\mathrm{d}s,\mathrm{d}u,\mathrm{d}x) + \int_0^\cdot\int_0^{X_{s-}^k}\int_{\mathbb{R}}\left(e^{\,\lambda_{i,k}\,x} - 1\right)\widetilde{N}_2^k(\mathrm{d}s,\mathrm{d}u,\mathrm{d}x)\right)_t,\end{aligned}$$

for all $t \leqslant \mathcal{T}$. By applying Girsanov's theorem, the processes $(B_t^{i,k,1})_{t\leqslant\mathcal{T}}$ and $(B_t^{i,k,2})_{t\leqslant\mathcal{T}}$ defined for every $1 \leqslant i \leqslant N$ and $1 \leqslant k \leqslant d$ by

$$B_t^{i,k,1} := B_t^{k,1} - \zeta_{i,k}\,\sigma^k \int_0^t \sqrt{X_s^k}\,\mathrm{d}s,$$
$$B_t^{i,k,2} := B_t^{k,2} - \lambda_{i,k}\,\sigma_Z^k \int_0^t \sqrt{X_s^k}\,\mathrm{d}s,$$

for all $t \leqslant \mathcal{T}$, are independent Brownian motions under $\mathbb{Q}^i$. Again by Girsanov's theorem, $N_0^k(\mathrm{d}t,\mathrm{d}x)$, $N_1^k(\mathrm{d}t,\mathrm{d}u,\mathrm{d}x)$, and $N_2^k(\mathrm{d}t,\mathrm{d}u,\mathrm{d}x)$ remain Poisson random measures under $\mathbb{Q}^i$, but with modified compensators as follows:

$$\widetilde{N}_0^{i,k}(\mathrm{d}t,\mathrm{d}x) := N_0^k(\mathrm{d}t,\mathrm{d}x) - \mathrm{d}t\,e^{\,\zeta_{i,k}\,x}\,\nu^k(\mathrm{d}x),$$
$$\widetilde{N}_1^{i,k}(\mathrm{d}t,\mathrm{d}u,\mathrm{d}x) := N_1^k(\mathrm{d}t,\mathrm{d}u,\mathrm{d}x) - \mathrm{d}t\,\mathrm{d}u\,e^{\,\zeta_{i,k}\,x}\,\pi^k(\mathrm{d}x),$$
$$\widetilde{N}_2^{i,k}(\mathrm{d}t,\mathrm{d}u,\mathrm{d}x) := N_2^k(\mathrm{d}t,\mathrm{d}u,\mathrm{d}x) - \mathrm{d}t\,\mathrm{d}u\,e^{\,\lambda_{i,k}\,x}\,\gamma_Z^k(\mathrm{d}x),$$

for every $1 \leqslant i \leqslant N$ and $1 \leqslant k \leqslant d$. Finally, we rewrite system (5.2)–(5.3) under $\mathbb{Q}^i$ as follows:

$$\begin{aligned}
X_t^k &= X_0^k + \int_0^t \big(\beta^{i,k} - b^{i,k}\,X_s^k\big)\,\mathrm{d}s + \sigma^{i,k}\int_0^t \sqrt{X_s^k}\,\mathrm{d}B_s^{i,k,1} \\
&\quad + \int_0^t\int_0^{+\infty} x\,N_0^k(\mathrm{d}s,\mathrm{d}x) + \int_0^t\int_0^{X_{s-}^k}\int_0^{+\infty} x\,\widetilde{N}_1^{i,k}(\mathrm{d}s,\mathrm{d}u,\mathrm{d}x), \qquad \forall t \geqslant 0, \\
Z_t^k &= b_Z^{i,k}\int_0^t X_s^k\,\mathrm{d}s + \sigma_Z^{i,k}\int_0^t \sqrt{X_s^k}\,\mathrm{d}B_s^{i,k,2} + \int_0^t\int_0^{X_{s-}^k}\int_{|x|\geqslant 1} x\,N_2^k(\mathrm{d}s,\mathrm{d}u,\mathrm{d}x) \\
&\quad + \int_0^t\int_0^{X_{s-}^k}\int_{|x|<1} x\,\widetilde{N}_2^{i,k}(\mathrm{d}s,\mathrm{d}u,\mathrm{d}x), \qquad \forall t \geqslant 0.
\end{aligned}$$

In view of Lemma 4.2, we can conclude that the joint process $(X_t^k, Z_t^k)_{t\leqslant\mathcal{T}}$ remains a CBITCL process under $\mathbb{Q}^i$ with parameters given in Table 5.1, for every $1 \leqslant i \leqslant N$ and $1 \leqslant k \leqslant d$. □

We define the spot FX rate process $S^{i,j} = (S_t^{i,j})_{t\leqslant\mathcal{T}}$, for every $1 \leqslant i,j \leqslant N$, as follows:

$$S_t^{i,j} := \frac{S_t^{0,j}}{S_t^{0,i}}, \qquad \forall t \leqslant \mathcal{T}. \tag{5.8}$$

In the next result, we first show that the triplet $\big(N, \boldsymbol{D}, \boldsymbol{S}\big)$ is a well-posed multiple currency market in the sense of Definitions 5.1 and 5.2. We then provide each spot FX rate process $S^{i,j} = (S_t^{i,j})_{t\leqslant\mathcal{T}}$ with a stochastic integral representation under $\mathbb{Q}^i$. In particular, we will notice that their dynamics are functionally symmetric with respect to ratios/products, which is a direct consequence of the fact that CBITCL processes are coherent in the sense of [**Gno17**].

Corollary 5.9. *Let $\big(X, Z, \boldsymbol{\zeta}, \boldsymbol{\lambda}\big)$ generate a CBITCL multi-currency model. Then:*

(i) *The triplet $\big(N, \boldsymbol{D}, \boldsymbol{S}\big)$ is a well-posed multiple currency market;*

(ii) *For every $1 \leqslant i, j \leqslant N$ with $i \neq j$, under $\mathbb{Q}^i$, the spot FX rate process $S^{i,j} = (S_t^{i,j})_{t \leqslant \mathcal{T}}$ is the unique strong solution to the following stochastic differential equation:*

$$\begin{aligned}
\frac{\mathrm{d}S_t^{i,j}}{S_{t-}^{i,j}} &= \left(r^i - r^j\right)\mathrm{d}t + \sum_{k=1}^{d} \sqrt{X_t^k}\left(\sigma^k\left(\zeta_{j,k} - \zeta_{i,k}\right)\mathrm{d}B_t^{i,k,1} + \sigma_Z^k\left(\lambda_{j,k} - \lambda_{i,k}\right)\mathrm{d}B_t^{i,k,2}\right) \\
&\quad + \sum_{k=1}^{d} \int_0^{+\infty} \left(e^{\left(\zeta_{j,k} - \zeta_{i,k}\right)x} - 1\right) \widetilde{N}_0^{i,k}(\mathrm{d}t, \mathrm{d}x) \\
&\quad + \sum_{k=1}^{d} \int_0^{X_{t-}^k} \int_0^{+\infty} \left(e^{\left(\zeta_{j,k} - \zeta_{i,k}\right)x} - 1\right) \widetilde{N}_1^{i,k}(\mathrm{d}t, \mathrm{d}u, \mathrm{d}x) \\
&\quad + \sum_{k=1}^{d} \int_0^{X_{t-}^k} \int_{\mathbb{R}} \left(e^{\left(\lambda_{j,k} - \lambda_{i,k}\right)x} - 1\right) \widetilde{N}_2^{i,k}(\mathrm{d}t, \mathrm{d}u, \mathrm{d}x). \qquad (5.9)
\end{aligned}$$

Proof. The well-posedness of the multiple currency market $\left(N, \boldsymbol{D}, \boldsymbol{S}\right)$ directly follows from Theorem 5.8 and equation (5.8). Concerning part (ii), the product rule for semimartingales reads

$$\mathrm{d}S_t^{i,j} = \mathrm{d}\left(S_t^{0,j} \times \frac{1}{S_t^{0,i}}\right) = S_{t-}^{0,j}\,\mathrm{d}\frac{1}{S_t^{0,i}} + \frac{1}{S_{t-}^{0,i}}\,\mathrm{d}S_t^{0,j} + \mathrm{d}\left[S^{0,j}, \frac{1}{S^{0,i}}\right]_t, \qquad (5.10)$$

where, by using Itô's formula, we can show that the inverse process of $S^{0,i} = (S_t^{0,i})_{t \leqslant \mathcal{T}}$ satisfies

$$\begin{aligned}
S_{t-}^{0,i}\,\mathrm{d}\frac{1}{S_t^{0,i}} &= r^i\,\mathrm{d}t - \sum_{k=1}^{d} \sqrt{X_t^k}\,\left(\zeta_{i,k}\,\sigma^k\,\mathrm{d}B_t^{i,k,1} + \lambda_{i,k}\,\sigma_Z^k\,\mathrm{d}B_t^{i,k,2}\right) \\
&\quad + \sum_{k=1}^{d} \int_0^{+\infty} \left(e^{-\zeta_{i,k}\,x} - 1\right) \widetilde{N}_0^{i,k}(\mathrm{d}t, \mathrm{d}x) \\
&\quad + \sum_{k=1}^{d} \int_0^{X_{t-}^k} \int_0^{+\infty} \left(e^{-\zeta_{i,k}\,x} - 1\right) \widetilde{N}_1^{i,k}(\mathrm{d}t, \mathrm{d}u, \mathrm{d}x) \\
&\quad + \sum_{k=1}^{d} \int_0^{X_{t-}^k} \int_{\mathbb{R}} \left(e^{-\lambda_{i,k}\,x} - 1\right) \widetilde{N}_2^{i,k}(\mathrm{d}t, \mathrm{d}u, \mathrm{d}x),
\end{aligned}$$

and the co-variation $\left[S^{0,j}, \frac{1}{S^{0,i}}\right]$ is determined by

$$\begin{aligned}
\frac{1}{S_{t-}^{i,j}}\,\mathrm{d}\left[S^{0,j}, \frac{1}{S^{0,i}}\right]_t &= -\sum_{k=1}^{d} X_t^k \left(\zeta_{i,k}\,\zeta_{j,k}\,(\sigma^k)^2 + \lambda_{i,k}\,\lambda_{j,k}\,(\sigma_Z^k)^2\right)\mathrm{d}t \\
&\quad + \sum_{k=1}^{d} \int_0^{+\infty} \left(e^{-\zeta_{i,k}\,x} - 1\right)\left(e^{\zeta_{j,k}\,x} - 1\right) N_0^k(\mathrm{d}t, \mathrm{d}x) \\
&\quad + \sum_{k=1}^{d} \int_0^{X_{t-}^k} \int_0^{+\infty} \left(e^{-\zeta_{i,k}\,x} - 1\right)\left(e^{\zeta_{j,k}\,x} - 1\right) N_1^k(\mathrm{d}t, \mathrm{d}u, \mathrm{d}x) \\
&\quad + \sum_{k=1}^{d} \int_0^{X_{t-}^k} \int_{\mathbb{R}} \left(e^{-\lambda_{i,k}\,x} - 1\right)\left(e^{\lambda_{j,k}\,x} - 1\right) N_2^k(\mathrm{d}t, \mathrm{d}u, \mathrm{d}x).
\end{aligned}$$

□

5.3. Features of the model

5.3.1. Stochastic volatility and jumps. Corollary 5.9 highlights the presence of stochastic volatility and jumps in the dynamics of the spot FX rate processes. Let us fix a couple (i,j) with $1 \leqslant i,j \leqslant N$ and $i \neq j$, omitting the index k for simplicity, the dynamics of the spot FX rate process $S^{i,j} = (S_t^{i,j})_{t \leqslant \mathcal{T}}$ are then influenced by the following sources of randomness: a diffusive component driven by the two Brownian motions $(B_t^{i,1})_{t \leqslant \mathcal{T}}$ and $(B_t^{i,2})_{t \leqslant \mathcal{T}}$, and three jump components driven by the three compensated Poisson random measures $\widetilde{N}_0^i$, $\widetilde{N}_1^i$, and $\widetilde{N}_2^i$. Let us now comment on the interpretation of these different sources of randomness.

We start with the diffusive component, which is proportional to the square root of the CBI process $X = (X_t)_{t \leqslant \mathcal{T}}$, thus giving rise to stochastic volatility. Moreover, this shows that our modeling framework allows for self-excitation in the volatility of FX rates, which directly derives from the self-exciting behavior of CBI processes. The first jump component driven by $\widetilde{N}_0^i$ results from the immigration of the CBI process $X = (X_t)_{t \leqslant \mathcal{T}}$, whose magnitude is controlled by the difference $\zeta_j - \zeta_i$.

The second jump component driven by $\widetilde{N}_1^i$ represents the dependence of self-exciting type between the CBI process $X = (X_t)_{t \leqslant \mathcal{T}}$ and the FX rate, whose magnitude is again controlled by the difference $\zeta_j - \zeta_i$. When this difference is large, e.g. between a hard currency and a soft one, it indicates strong dependence between the CBI process $X = (X_t)_{t \leqslant \mathcal{T}}$ and the FX rate. If the quantity $\zeta_j - \zeta_i$ is small, e.g. between two hard currencies, then it suggests moderate dependence, in line with the findings of [**BM18**].

The third jump component driven by $\widetilde{N}_2^i$ represents the jump risk of self-exciting type generated by the time-changed Lévy process $Z = (Z_t)_{t \leqslant \mathcal{T}}$, whose magnitude is controlled by the difference $\lambda_j - \lambda_i$. If this difference is large, then it implies an important contribution of the time-changed Lévy process $Z = (Z_t)_{t \leqslant \mathcal{T}}$ to the jump risk of the FX rate. If the quantity $\lambda_j - \lambda_i$, then it implies a weaker contribution.

5.3.2. Stochastic dependence and skewness. We investigate whether our framework can generate stochastic dependence among FX rates and FX volatility smiles with stochastic skewness. To this end, we compute the co-variations between the different FX rates and examine, for each FX rate, the instantaneous correlation between the FX rate and the sum of the d CBI processes $(X^k)_{1 \leqslant k \leqslant d}$ driving the volatility of the FX rate. This quantity is known to be intimately related to the skewness of the FX volatility smile (see e.g. [**CHJ09**, Section 3] and [**DFG11**, Section 3]).

For every $1 \leqslant i,j \leqslant N$ with $i \neq j$, consider, for $t \leqslant \mathcal{T}$, the time-t instantaneous correlation between the spot FX rate process $S^{i,j} = (S_t^{i,j})_{t \leqslant \mathcal{T}}$ and the sum of the CBI processes $(X^k)_{1 \leqslant k \leqslant d}$, denoted by $\mathrm{d}\,\mathrm{Corr}_t\big(S^{i,j}, \sum_{k=1}^d X^k\big)$. By [**DFG11**, Section 3], it can be informally defined as

$$\mathrm{d}\,\mathrm{Corr}_t\bigg(S^{i,j}, \sum_{k=1}^d X^k\bigg) := \frac{\mathrm{d}\Big[S^{i,j}, \sum_{k=1}^d X^k\Big]_t}{\sqrt{\mathrm{d}\Big[S^{i,j}\Big]_t}\sqrt{\mathrm{d}\Big[\sum_{k=1}^d X^k\Big]_t}}. \tag{5.11}$$

We shall verify the following two properties:

(1) If for every $1 \leqslant i \leqslant N$ and every $1 \leqslant p, q \leqslant N$ with $p \neq i$, $q \neq i$, and $p \neq q$, the co-variation $\left[S^{i,p}, S^{i,q}\right]$ is a stochastic process, then we can say that there exists stochastic dependence among FX rates;
(2) If for every $1 \leqslant i, j \leqslant N$ with $i \neq j$, and for all $t \leqslant \mathcal{T}$, the time-t instantaneous correlation $\mathrm{d}\,\mathrm{Corr}_t\big(S^{i,j}, \sum_{k=1}^d X^k\big)$ is stochastic, then we can say that every FX rate of the market generates a volatility smile with stochastic skewness.

We first compute $\left[S^{i,p}, S^{i,q}\right]$ by using (5.9), for every $1 \leqslant i, p, q \leqslant N$ with $p \neq i$, $q \neq i$, and $p \neq q$:

$$\begin{aligned}
\frac{1}{S^{i,p}_{t-}\, S^{i,q}_{t-}}\,\mathrm{d}\Big[S^{i,p}, S^{i,q}\Big]_t &= \sum_{k=1}^d X^k_t \left((\sigma^k)^2 \left(\zeta_{p,k} - \zeta_{i,k}\right)\left(\zeta_{q,k} - \zeta_{i,k}\right) + (\sigma^k_Z)^2 \left(\lambda_{p,k} - \lambda_{i,k}\right)\left(\lambda_{q,k} - \lambda_{i,k}\right)\right)\mathrm{d}t \\
&\quad + \sum_{k=1}^d \int_0^{+\infty} \left(e^{\left(\zeta_{p,k} - \zeta_{i,k}\right)x} - 1\right)\left(e^{\left(\zeta_{q,k} - \zeta_{i,k}\right)x} - 1\right) N^k_0(\mathrm{d}t, \mathrm{d}x) \\
&\quad + \sum_{k=1}^d \int_0^{X^k_{t-}} \int_0^{+\infty} \left(e^{\left(\zeta_{p,k} - \zeta_{i,k}\right)x} - 1\right)\left(e^{\left(\zeta_{q,k} - \zeta_{i,k}\right)x} - 1\right) N^k_1(\mathrm{d}t, \mathrm{d}u, \mathrm{d}x) \\
&\quad + \sum_{k=1}^d \int_0^{X^k_{t-}} \int_{\mathbb{R}} \left(e^{\left(\lambda_{p,k} - \lambda_{i,k}\right)x} - 1\right)\left(e^{\left(\lambda_{q,k} - \lambda_{i,k}\right)x} - 1\right) N^k_2(\mathrm{d}t, \mathrm{d}u, \mathrm{d}x),
\end{aligned}$$

thus showing evidence of stochastic dependence among FX rates. As far as the time-t instantaneous correlation $\mathrm{d}\,\mathrm{Corr}_t\big(S^{i,j}, \sum_{k=1}^d X^k\big)$ is concerned, for every $1 \leqslant i, j \leqslant N$ with $i \neq j$, and for all $t \leqslant \mathcal{T}$, the latter is determined by the (quadratic) co-variations $\left[\sum_{k=1}^d X^k\right]$, $\left[S^{i,j}\right]$, and $\left[S^{i,j}, \sum_{k=1}^d X^k\right]$:

$$\begin{aligned}
\mathrm{d}\left[\sum_{k=1}^d X^k\right]_t &= \sum_{k=1}^d \left(X^k_t\,(\sigma^k)^2\,\mathrm{d}t + \int_0^{+\infty} x^2\, N^k_0(\mathrm{d}t, \mathrm{d}x) + \int_0^{X^k_{t-}} \int_0^{+\infty} x^2\, N^k_1(\mathrm{d}t, \mathrm{d}u, \mathrm{d}x)\right), \\
\frac{\mathrm{d}\big[S^{i,j}\big]_t}{\left(S^{i,j}_{t-}\right)^2} &= \sum_{k=1}^d X^k_t \left(\Big(\sigma^k\left(\zeta_{j,k} - \zeta_{i,k}\right)\Big)^2 + \Big(\sigma^k_Z\left(\lambda_{j,k} - \lambda_{i,k}\right)\Big)^2\right)\mathrm{d}t \\
&\quad + \sum_{k=1}^d \int_0^{+\infty} \left(e^{\left(\zeta_{j,k} - \zeta_{i,k}\right)x} - 1\right)^2 N^k_0(\mathrm{d}t, \mathrm{d}x) \\
&\quad + \sum_{k=1}^d \int_0^{X^k_{t-}} \int_0^{+\infty} \left(e^{\left(\zeta_{j,k} - \zeta_{i,k}\right)x} - 1\right)^2 N^k_1(\mathrm{d}t, \mathrm{d}u, \mathrm{d}x) \\
&\quad + \sum_{k=1}^d \int_0^{X^k_{t-}} \int_0^{+\infty} \left(e^{\left(\lambda_{j,k} - \lambda_{i,k}\right)x} - 1\right)^2 N^k_2(\mathrm{d}t, \mathrm{d}u, \mathrm{d}x), \\
\frac{1}{S^{i,j}_{t-}}\,\mathrm{d}\left[S^{i,j}, \sum_{k=1}^d X^k\right]_t &= \sum_{k=1}^d \left(X^k_t\,(\sigma^k)^2\left(\zeta_{j,k} - \zeta_{i,k}\right)\mathrm{d}t + \int_0^{+\infty} x\left(e^{\left(\zeta_{j,k} - \zeta_{i,k}\right)x} - 1\right) N^k_0(\mathrm{d}t, \mathrm{d}x)\right) \\
&\quad + \sum_{k=1}^d \int_0^{X^k_{t-}} \int_0^{+\infty} x\left(e^{\left(\zeta_{j,k} - \zeta_{i,k}\right)x} - 1\right) N^k_1(\mathrm{d}t, \mathrm{d}u, \mathrm{d}x).
\end{aligned}$$

Replacing all the terms into (5.11), we obviously find a rich stochastic structure for the instantaneous correlation, showing that every FX rate generates a volatility smile with stochastic skewness.

5.3.3. Currency option pricing. In view of Theorem 5.8, our modeling framework retains analytical tractability under a suitable class of risk-neutral measures. By relying on this result, we derive a semi-closed-form representation of the characteristic function of each spot FX rate process. We denote the expectation under $\mathbb{Q}^i$ by $\mathbb{E}^i$, for every $1 \leqslant i \leqslant N$.

LEMMA 5.10. *Let $\big(X, Z, \boldsymbol{\zeta}, \boldsymbol{\lambda}\big)$ generate a CBITCL multi-currency model. Then, for every $1 \leqslant i, j \leqslant N$ with $i \neq j$, the characteristic function of $\log S^{i,j} = \big(\log S^{i,j}_t\big)_{t \leqslant \mathcal{T}}$ under $\mathbb{Q}^i$ is given by*

$$\mathbb{E}^i\left[e^{\mathsf{i}\,u\,\log S^{i,j}_t}\right] = e^{\mathsf{i}\,u\left(\log S^{i,j}_0 + \left(r^i - r^j\right)t\right)} \times \prod_{k=1}^{d} e^{\mathsf{i}\,u\left(\Psi^k(\zeta_{i,k}) - \Psi^k(\zeta_{j,k})\right)t}$$

$$\times \prod_{k=1}^{d} \exp\Big(\mathcal{U}^{i,k}\big(t, u^k_1, u^k_2, u^k_3\big) + \mathcal{V}^{i,k}\big(t, u^k_1, u^k_2, u^k_3\big)\, X^k_0\Big), \qquad \forall (u,t) \in \mathbb{R} \times [0, \mathcal{T}],$$

where for every $1 \leqslant k \leqslant d$, $\big(\mathcal{U}^{i,k}\big(\cdot, u^k_1, u^k_2, u^k_3\big), \mathcal{V}^{i,k}\big(\cdot, u^k_1, u^k_2, u^k_3\big)\big)$ is the unique solution to the CBITCL Riccati system associated to $(X^k_t, Z^k_t)_{t \leqslant \mathcal{T}}$ under $\mathbb{Q}^i$ with

$$u^k_1 = \mathsf{i}\,u\left(\zeta_{j,k} - \zeta_{i,k}\right), \quad u^k_2 = \mathsf{i}\,u\left(\Phi^k(\zeta_{i,k}) + \Xi^k_Z(\lambda_{i,k}) - \Phi^k(\zeta_{j,k}) - \Xi^k_Z(\lambda_{j,k})\right), \quad \textit{and} \quad u^k_3 = \mathsf{i}\,u\left(\lambda_{j,k} - \lambda_{i,k}\right).$$

PROOF. The logarithm of the spot FX rate process $S^{i,j} = (S^{i,j}_t)_{t \leqslant \mathcal{T}}$, for every $1 \leqslant i, j \leqslant N$ with $i \neq j$, has the following form

$$\log S^{i,j}_t = \log S^{i,j}_0 + \left(r^i - r^j\right)t + \sum_{k=1}^{d}\Big(\left(\zeta_{j,k} - \zeta_{i,k}\right)X^k_t + \left(\lambda_{j,k} - \lambda_{i,k}\right)Z^k_t + \mathcal{K}^{i,k}_t - \mathcal{K}^{j,k}_t\Big),$$

for all $t \leqslant \mathcal{T}$. Since the CBITCL processes are mutually independent, we have

$$\mathbb{E}^i\left[e^{\mathsf{i}\,u\,\log S^{i,j}_t}\right] = e^{\mathsf{i}\,u\left(\log S^{i,j}_0 + \left(r^i - r^j\right)t\right)} \times \prod_{k=1}^{d} \mathbb{E}^i\left[e^{\mathsf{i}\,u\left(\left(\zeta_{j,k} - \zeta_{i,k}\right)X^k_t + \left(\lambda_{j,k} - \lambda_{i,k}\right)Z^k_t + \mathcal{K}^{i,k}_t - \mathcal{K}^{j,k}_t\right)}\right].$$

By inserting equation (4.22), we obtain

$$\mathbb{E}^i\left[e^{\mathsf{i}\,u\,\log S^{i,j}_t}\right] = e^{\mathsf{i}\,u\left(\log S^{i,j}_0 + \left(r^i - r^j\right)t\right)} \times \prod_{k=1}^{d} e^{\mathsf{i}\,u\left(\Psi^k(\zeta_{i,k}) - \Psi^k(\zeta_{j,k})\right)t}$$

$$\times \prod_{k=1}^{d} \mathbb{E}^i\left[e^{\mathsf{i}\,u\left(\zeta_{j,k} - \zeta_{i,k}\right)X^k_t + \mathsf{i}\,u\left(\Phi^k(\zeta_{i,k}) + \Xi^k_Z(\lambda_{i,k}) - \Phi^k(\zeta_{j,k}) - \Xi^k_Z(\lambda_{j,k})\right)Y^k_t + \mathsf{i}\,u\left(\lambda_{j,k} - \lambda_{i,k}\right)Z^k_t}\right].$$

where $Y^k_t := \int_0^t X^k_s \,\mathrm{d}s$, for all $t \leqslant \mathcal{T}$ and for every $1 \leqslant k \leqslant d$. The conclusion then follows from the preservation of the affine property of CBITCL processes under $\mathbb{Q}^i$ (see Theorem 5.8), for every $1 \leqslant i \leqslant N$, and a direct application of Proposition 4.3 to each joint process $\big(X^k_t, Y^k_t, Z^k_t\big)_{t \leqslant \mathcal{T}}$. □

The availability of a semi-closed-form expression for the characteristic function of each spot FX rate process allows for currency option pricing via Fourier techniques. Unlike in Chapter 3, where the approach of [**Lee04**] was followed for caplet pricing, here we adopt the COS method developed by [**FO09**]. The latter presents the advantage of utilizing only the characteristic function of the underlying process, without requiring any domain extensions as in other Fourier pricing techniques.

In our setting, such domain extensions would require additional constraints on the parameters. We proceed as follows:

- Consider a European call option in the i^{th} economy written on the spot FX rate process $S^{i,j} = (S_t^{i,j})_{t \leqslant \mathcal{T}}$ for $1 \leqslant j \neq i \leqslant N$ with maturity $T \leqslant \mathcal{T}$ and strike $K > 0$. Thanks to the well-posedness of the multiple currency market $\big(N, \boldsymbol{D}, \boldsymbol{S}\big)$, we can apply the risk-neutral valuation formula under $\mathbb{Q}^i$ to this European call option. The resulting arbitrage-free price $C(T,K)$, considered at $t = 0$ for simplicity, is given by

$$C(T,K) = e^{-r^i\,T}\,\mathbb{E}^i\left[\left(S_T^{i,j} - K\right)^+\right] = e^{-r^i\,T}\int_{\mathbb{R}} K\left(e^x - 1\right)^+ f_T^{i,j}(x)\,\mathrm{d}x, \tag{5.12}$$

  where $f_T^{i,j}$ represents the density function of $\log\big(S_T^{i,j}/K\big)$ under $\mathbb{Q}^i$;
- Introduce an appropriately chosen truncation range $[a,b] \subset \mathbb{R}$ such that $C(T,K)$ can be approximated with good accuracy by

$$C(T,K) \approx e^{-r^i\,T}\int_a^b K\left(e^x - 1\right)^+ f_T^{i,j}(x)\,\mathrm{d}x. \tag{5.13}$$

Let us now propose a simple semi-closed-form pricing formula for currency options based on the COS method of [**FO09**]. We emphasize that this pricing formula does not involve any additional assumptions or domain extensions of the characteristic function given by Lemma 5.10.

PROPOSITION 5.11. *Let $\big(X, Z, \boldsymbol{\zeta}, \boldsymbol{\lambda}\big)$ generate a CBITCL multi-currency model. Then, the arbitrage-free price $C(T,K)$ of a European call option written on the spot FX rate process $S^{i,j} = (S_t^{i,j})_{t \leqslant \mathcal{T}}$ with maturity $T \leqslant \mathcal{T}$ and strike $K > 0$, can be approximated by*

$$C(T,K) \approx e^{-r^i\,T}\,K\sum_{k=0}^{N-1}\left(1 - \frac{\delta_0(k)}{2}\right)\mathrm{Re}\left(e^{\mathrm{i}\frac{k\,\pi}{a-b}(a+\log K)}\mathbb{E}^i\left[e^{\mathrm{i}\frac{k\,\pi}{b-a}\log S_T^{i,j}}\right]\right)B_k, \tag{5.14}$$

where δ_0 denotes the Kronecker delta at 0, $N \in \mathbb{N}$, $B_0 = \frac{1}{b-a}\left(e^{\,b} - 1 - b\right)$, and where B_k, for every $1 \leqslant k \leqslant N-1$, is given by

$$B_k = \frac{2}{b-a}\left(\frac{1}{1 + \left(\frac{k\,\pi}{b-a}\right)^2}\left((-1)^k\,e^{\,b} - \cos\left(\frac{k\,\pi\,a}{b-a}\right) + \frac{k\,\pi}{b-a}\sin\left(\frac{k\,\pi\,a}{b-a}\right)\right) - \frac{b-a}{k\,\pi}\sin\left(\frac{k\,\pi\,a}{b-a}\right)\right).$$

PROOF. We proceed along the lines of [**FO09**, Section 3]. The starting point for deriving formula (5.14) is the approximation (5.13) of the arbitrage-free price $C(T,K)$. We replace $f_T^{i,j}$ with its cosine expansion on $[a,b]$, given by

$$f_T^{i,j}(x) = \sum_{k=0}^{+\infty}\left(1 - \frac{\delta_0(k)}{2}\right)A_k\cos\left(k\,\pi\,\frac{x-a}{b-a}\right), \tag{5.15}$$

for all $a \leqslant x \leqslant b$, where

$$A_k := \frac{2}{b-a}\int_a^b f_T^{i,j}(x)\cos\left(k\,\pi\,\frac{x-a}{b-a}\right)\mathrm{d}x, \tag{5.16}$$

for every $k \in \mathbb{N}$. Then, inserting equation (5.15) into approximation (5.13) and interchanging summation and integration, we obtain

$$C(T,K) \approx \frac{b-a}{2}\, e^{-r^i\, T}\, K \sum_{k=0}^{+\infty} \left(1 - \frac{\delta_0(k)}{2}\right) A_k\, B_k, \tag{5.17}$$

where we define the coefficients B_k by

$$B_k := \frac{2}{b-a} \int_a^b (e^x - 1)^+ \cos\left(k\,\pi\,\frac{x-a}{b-a}\right) \mathrm{d}x = \frac{2}{b-a} \int_0^b (e^x - 1) \cos\left(k\,\pi\,\frac{x-a}{b-a}\right) \mathrm{d}x,$$

for every $k \in \mathbb{N}$. The values of B_k have been computed explicitly in [**FO09**, Section 3.1] in the case of a European call option. We now truncate the series in (5.17) as justified by [**FO09**, Section 3] due to the rapid decay of the coefficients A_k and B_k as $k \to +\infty$, thus yielding

$$C(T,K) \approx \frac{b-a}{2}\, e^{-r^i\, T}\, K \sum_{k=0}^{N-1} \left(1 - \frac{\delta_0(k)}{2}\right) A_k\, B_k, \tag{5.18}$$

where $N \in \mathbb{N}^*$. We then recover formula (5.14) by making use of the characteristic function of $\log S_T^{i,j}$, as given by Lemma 5.10. We proceed as follows

$$\begin{aligned} A_k &\approx \frac{2}{b-a} \int_{\mathbb{R}} f_T^{i,j}(x) \cos\left(k\,\pi\,\frac{x-a}{b-a}\right) \mathrm{d}x \\ &= \frac{2}{b-a}\, \mathrm{Re}\left(e^{-\,\mathrm{i}\,k\,\pi\,\frac{a}{b-a}} \int_{\mathbb{R}} f_T^{i,j}(x)\, e^{\,\mathrm{i}\,\frac{k\,\pi}{b-a}\,x}\, \mathrm{d}x\right) \\ &= \frac{2}{b-a}\, \mathrm{Re}\left(e^{-\,\mathrm{i}\,k\,\pi\,\frac{a+\log K}{b-a}}\, \mathbb{E}^i\left[e^{\,\mathrm{i}\,\frac{k\,\pi}{b-a}\log S_T^{i,j}}\right]\right), \end{aligned} \tag{5.19}$$

which finally enables us to conclude the proof by inserting (5.19) into (5.18). □

Remark 5.12. In order to preserve the accuracy of formula (5.14), one needs to select the truncation range $[a,b]$ properly. Inspired by [**FO09**, Section 5.1], one can choose it as follows:

$$[a,b] = \left[c_1 - L\sqrt{c_2 + \sqrt{c_4}},\quad c_1 + L\sqrt{c_2 + \sqrt{c_4}}\right], \tag{5.20}$$

with $L = 10$ and where c_n, for $n = 1, 2, 4$, represents the n^{th} cumulant of $\log\big(S_T^{i,j}/K\big)$. In our framework, the cumulants are not available in closed form. However, they can be approximated by using finite differences since they are by definition given by the derivatives at zero of the cumulant-generating function of $\log\big(S_T^{i,j}/K\big)$ (see [**FO09**, Appendix A] for further details).

Remark 5.13. As in [**FO09**, Section 3.3], formula (5.14) can be readily extended to a multi-strike setting, which is practically important when one needs to price many European options at once, with the same maturity but associated to different strikes, e.g. during a calibration routine. Suppose that we are given M European call options with the same maturity $T \leqslant \mathcal{T}$ but associated to M different strikes denoted by $K_i > 0$ for every $1 \leqslant i \leqslant M$. Consider the following objects:

- Let $\vec{K} = (K_i)_{1 \leqslant i \leqslant M}^\top$ represent the vector containing M different strikes;
- Let $\vec{C}(T,\vec{K}) = (C(T,K_i))_{1 \leqslant i \leqslant M}^\top$ be the vector containing the corresponding prices.

Denote the spot FX rate process by $S = (S_t)_{t \leqslant \mathcal{T}}$ where we omit the indexes i and j for simplicity of notation. Following Remark 5.12, the quantities $b-a$ and $a+\log K$ in formula (5.14) do not depend on the strike K. By introducing the diagonal matrix $\mathrm{diag}(B_k) = \mathrm{diag}\big(B_k(K_1), \dots, B_k(K_M)\big)$ for every $0 \leqslant k \leqslant N-1$, we can derive the following multi-strike version of formula (5.14)

$$\vec{C}(T, \vec{K}) \approx e^{-r^i T} \sum_{k=0}^{N-1} \left(1 - \frac{\delta_0(k)}{2}\right) \mathrm{Re}\left(e^{\mathrm{i}\, \frac{k\pi}{a-b}(a+\log K)} \mathbb{E}^i\left[e^{\mathrm{i}\, \frac{k\pi}{b-a} \log S_T}\right]\right) \mathrm{diag}(B_k)\, \vec{K}, \tag{5.21}$$

where each term $\mathrm{diag}(B_k)\, \vec{K}$ refers to a matrix-vector product and each real part in the summation is a scalar. The characteristic function of $\log S_T$ needs to be evaluated only $N-1$ times for the pricing of a European option smile, thus reducing the computation time in a calibration.

5.4. Numerical analysis

5.4.1. FX market data. We start by describing the market data. For a given trading date (April 15, 2020), we consider three FX implied volatility surfaces: EURUSD, EURJPY, along with USDJPY. The latter are quoted according to the FORDOM convention, meaning that the second currency in each pair represents the domestic one. We emphasize that the quoting convention for FX implied volatility surfaces differs from what we observe in equity markets: implied volatilities are not quoted in terms of strikes and maturities, but in terms of deltas and maturities.

Furthermore, excluding ATM, single volatilities are not directly quoted: the market practice consists in quoting certain combinations of contracts (risk-reversals and butterflies) from which, by means of conversion formulas, one can recover implied volatilities for single contracts in terms of maturities and deltas. The conversion between deltas and strikes is then performed by suitable inversions of the Black–Scholes formula. We stress that also the definition of ATM poses some challenges in FX markets, which depends on how the currency pair is quoted. We refer to [**Cla11**] for a complete overview of quoting convention and smile construction in the FX market.

For each surface and each maturity considered (ranging from one week to one year, all of our surfaces share the same maturity range), we retrieved from Bloomberg the following market quotes: ATM implied volatility, 10Δ and 25Δ risk-reversals and butterflies. For 25Δ[4], we have

$$\begin{aligned} RR_{25\Delta} &= \sigma_{25\Delta Call} - \sigma_{25\Delta Put}, \\ BF_{25\Delta} &= \frac{\sigma_{25\Delta Call} + \sigma_{25\Delta Put}}{2} - \sigma_{ATM}, \end{aligned}$$

from which, by straightforward computations, we are able to obtain

$$\begin{aligned} \sigma_{25\Delta Call} &= \sigma_{ATM} + \frac{1}{2} RR_{25\Delta} + BF_{25\Delta}, \\ \sigma_{25\Delta Put} &= \sigma_{ATM} - \frac{1}{2} RR_{25\Delta} + BF_{25\Delta}, \end{aligned}$$

and similarly for 10Δ. In summary, for each surface and each maturity, we have the implied volatilities of 5 contracts at our disposal. Market data not corresponding to the 5 points above is typically interpolated (see again [**Cla11**] for a discussion of different interpolation techniques).

[4]By 25Δ, we mean an OTM call option with a delta of 25% and its put counterpart with a delta of -25%.

In order to reconstruct observed market prices, we also retrieved from Bloomberg FX spots and FX forward points, which enable us to build FX forward curves by adding the spot and the forward points. Equipped with such data, we have all the information needed to convert deltas into strikes and implies volatilities into prices. We performed these tasks by using the open-source Java library Strata by OpenGamma [**Ope16**].

5.4.2. Two types of calibration. In general, the objective of a calibration to an FX triangle ($N = 3$ FX implied volatility surfaces) is to solve the following problem: let p denote a vector of model parameters, belonging to some set of admissible parameters $\mathcal{P}$. Let $\#T$ be the number of maturities and $\#K$ be the number of strikes that we consider. For simplicity of presentation, we assume that all smiles have the same strike range and the same number of strikes. We aim at solving the following minimization problem:

$$\min_{p\in\mathcal{P}} \sum_{u=1}^{N}\sum_{i=1}^{\#T}\sum_{j=1}^{\#K}\left(\sigma_{imp}^{mkt}(u,T_i,K_j)-\sigma_{imp}^{mod(p)}(u,T_i,K_j)\right)^2, \tag{5.22}$$

where $\sigma_{mkt}^{imp}(u,T_i,K_j)$ denotes the market-observed implied volatility for surface u, maturity T_i, and strike K_j, while $\sigma_{imp}^{mod(p)}(u,T_i,K_j)$ denotes its model-implied counterpart for a given vector of parameters $p \in \mathcal{P}$. The penalty function in (5.22) is one of the many possible alternatives that can be found in the literature. A popular alternative involves the use of prices in place of implied volatilities, also the introduction of weights in terms of bid-ask spreads or by using greeks (most notably the vega) is common.

We now present two types of calibration. The first one, to which we refer as *standard calibration*, utilizes the semi-closed-form pricing formula for currency options of Proposition 5.11 (or its multi-strike version considered in Remark 5.13), in order to produce model prices for a given choice of model parameters. Such prices are then converted into model-implied volatilities by means of a standard implied volatility bootstrapper, and inserted into minimization problem (5.22). This gives rise to a multi-dimensional pricing function $\Sigma : \mathcal{P} \to \mathbb{R}^{N\times\#T\times\#K}$ such that for all $p \in \mathcal{P}$, for every $1 \leqslant u \leqslant N$, $1 \leqslant i \leqslant \#T$, and $1 \leqslant j \leqslant \#K$, we have $\Sigma(p)_{(u,i,j)} = \sigma_{imp}^{mod(p)}(u,T_i,K_j)$.

The second type of calibration, which we name *deep calibration*, adopts the two-step approach developed by [**HMT21**] for the resolution of minimization problem (5.22). We proceed as follows:

Grid-based implicit training: The goal is to approximate the non-linear function Σ by a fully-connected feed-forward neural network $\mathcal{N}^w : \mathcal{P} \to \mathbb{R}^{N\times\#T\times\#K}$ in the sense of [**HMT21**, Definition 1], where w denotes some vector of network parameters (weights and biases). We first generate a training set $\left\{(p_n,\Sigma(p_n))\right\}_{1\leqslant n\leqslant N_{train}}$ of size N_{train}, where each vector of parameters p_n is generated randomly and where we have fixed the grid (u,T_i,K_j), for every $1 \leqslant u \leqslant N$, $1 \leqslant i \leqslant \#T$, and $1 \leqslant j \leqslant \#K$, throughout the generation (hence the term "grid-based"). We then solve the following minimization problem called "training" of the neural network:

$$\min_{w} \sum_{n=1}^{N_{train}}\sum_{u=1}^{N}\sum_{i=1}^{\#T}\sum_{j=1}^{\#K}\left(\Sigma(p_n)_{(u,i,j)}-\mathcal{N}^w(p_n)_{(u,i,j)}\right)^2, \tag{5.23}$$

whose solution represents an optimal vector of network parameters $\widehat{w}$ such that the neural network $\mathcal{N} := \mathcal{N}^{\widehat{w}}$ best approximates the observations $\left\{\Sigma(p_n)\right\}_{1 \leqslant n \leqslant N_{train}}$. Notice that $\widehat{w}$ depends on the grid that we have fixed, thus explaining the term "implicit";

Deterministic calibration: We rewrite minimization problem (5.22) by means of the trained neural network $\mathcal{N}$ as follows:

$$\min_{p \in \mathcal{P}} \sum_{u=1}^{N} \sum_{i=1}^{\#T} \sum_{j=1}^{\#K} \left(\sigma_{imp}^{mkt}(u, T_i, K_j) - \mathcal{N}(p)_{(u,i,j)} \right)^2. \tag{5.24}$$

Given the linear structure of the trained neural network $\mathcal{N}$, the resolution of problem (5.24) is considerably faster than a standard calibration problem.

Inspired by [**HMT21**], we choose the following neural network architecture:

- 3 hidden layers with 30 nodes on each;
- $N = 3$ surfaces, all sharing the same maturity range of size $\#T = 6$, where all smiles have the same number of strikes $\#K = 5$, which yields an output layer of $3 \times 6 \times 5 = 90$ nodes. The size of the input layer is simply the number of model parameters;
- All input and hidden layers equipped with the Exponential Linear Unit (ELU) activation function. The output layer is in turn equipped with the Sigmoid function.

Figure 5.2 provides a visualization of the chosen neural network architecture.

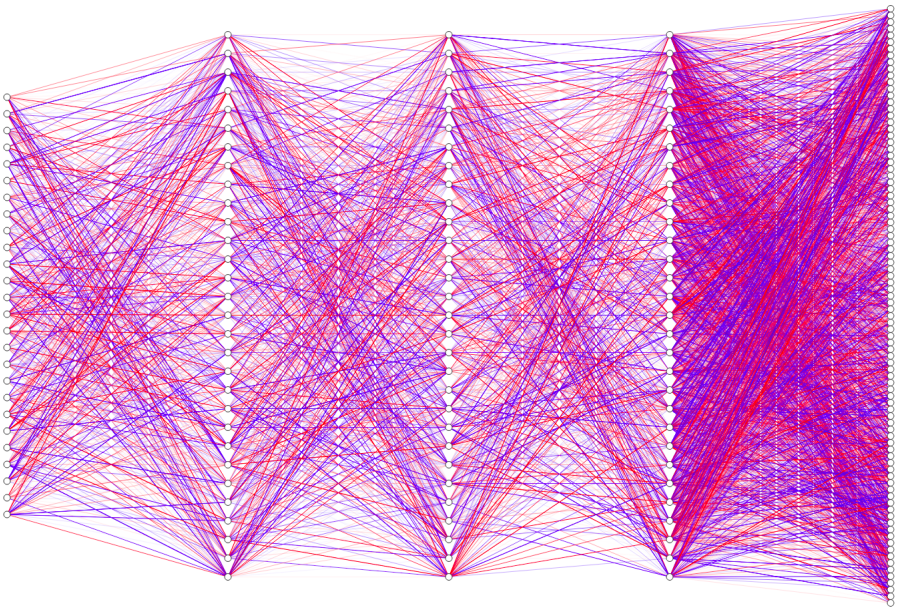

FIGURE 5.2. Illustration of the chosen neural network architecture, where all weights have been generated randomly. The width of an edge is proportional to the weight. The color of an edge defines the sign of the weight, namely if the latter is positive, then the edge color is red; if it is negative, then the color is blue.
Source: NN-SVG schematic generator developed by [**LeN19**].

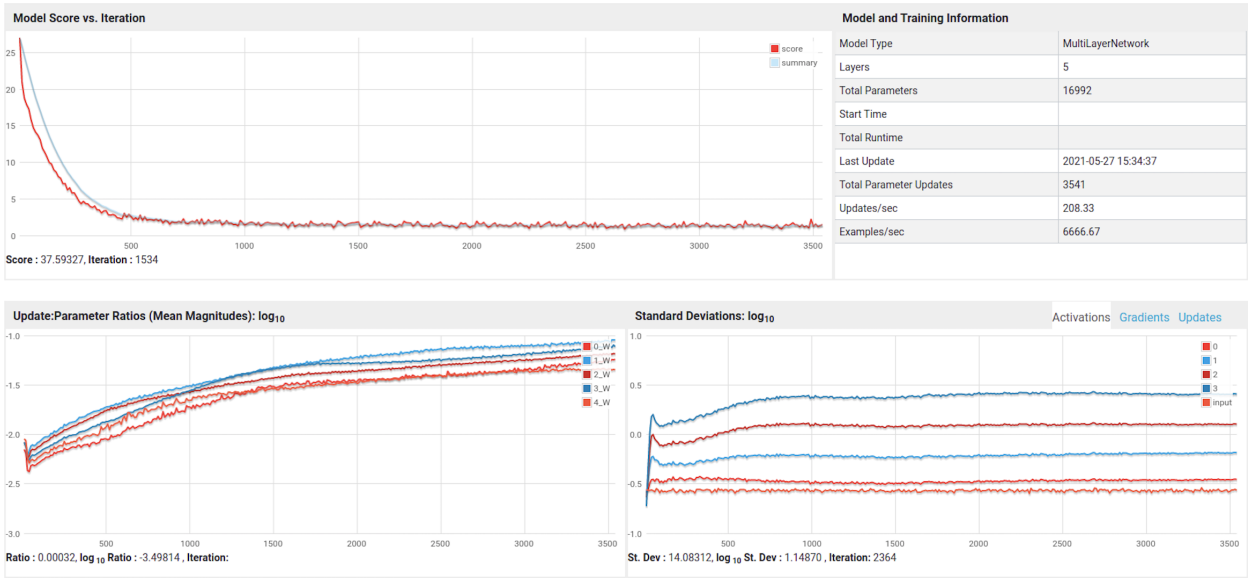

FIGURE 5.3. Monitoring of the neural network training presented in Figure 5.2. Source: Eclipse Deeplearning4j.

Concerning the training step, we start with the random generation of a training set of size $N_{train} = 10,000$. After suitably normalizing the data, we proceed with the training of the neural network corresponding to the resolution of minimization problem (5.23). The common practice is to use a stochastic optimization algorithm based on "mini-batch" gradient descent (see [**GBC16**]), whose updater can be further specified following the *Adam* scheme (see [**KB17**]). We then set the mini-batch size to 32 and the number of epochs to 150 with potential early stopping.

For its implementation, we rely on the open-source Java library Eclipse Deeplearning4j [**Tea16**], which offers a convenient monitoring interface. Figure 5.3 gives an overview of the latter at the end of the training of the neural network of Figure 5.2. The top left panel, called "score versus iteration", plots the value of the loss function over successive iterations. The top right panel provides a description of the neural network being trained and also further details on how the training process has been carried out. In particular, we also have the exact total number of network parameters to be calibrated, corresponding to the dimension of the vector w appearing in (5.23). The other two panels provide further checks on the state of the hyper-parameters employed during the training phase.

5.4.3. Calibration results. For the resolution of minimization problems (5.22) and (5.24), we use the Levenberg–Marquardt optimizer of the open-source Finmath Java library (see [**Fri21**]). We recall that we consider on April 15, 2020 the three FX implied volatility surfaces EURUSD, EURJPY, and USDJPY ($N = 3$ currencies), all sharing the same maturity range: 1 and 2 weeks, 1, 3, and 6 months, and 1 year. These maturities cover the most liquid segment of the implied volatility surface for FX pairs.

We work under the modeling framework presented in Section 5.2.2 with $d = 2$ and consider two specifications: the first one assumes that the Lévy process of each CBITCL process is simply a Brownian motion; the second specification uses the *CGMY process* [**CGMY02**] as the Lévy process of each CBITCL process. For both specifications, each CBI process is a *tempered-stable CBI process* (see Section 2.7). We refer to Appendix 5.A for an overview of these models.

We first consider the Brownian specification. We perform both standard and deep calibrations. Concerning the standard one, we obtain a root-mean-square error of 0.06119 in 929.086 seconds. Figure 5.4 provides a comparison of model and market prices that demonstrates the capability of the Brownian specification to obtain a satisfactory fit to market data. The quality of the fit is better for shorter maturities and worsens when considering the 6-month and 1-year maturities. The deep calibration performs better: we obtain a root-mean-square error of 0.04157 in 0.218 seconds. The better quality of the fit can be appreciated from Figure 5.5, where it appears that the fit is improving for longer maturities.

We now discuss the CGMY specification. As above, we perform standard and deep calibrations. For the standard, we obtain a root-mean-square error of 0.07557 in 709.977 seconds. Figure 5.6 shows a satisfactory fit that slightly worsens for longer maturities. Similarly to the Brownian specification, we observe that the deep calibration outperforms the standard one since we obtain a root-mean-square error of 0.04092 in 0.269 seconds. We report in Figure 5.7 the comparison between model and market prices from which is visible an improvement for longer maturities.

The calibrated values of the model parameters can be found in Table 5.2 for the four calibrations considered. We can first observe that all the differences $\zeta_{\text{EUR}} - \zeta_{\text{USD}}$, $\zeta_{\text{EUR}} - \zeta_{\text{JPY}}$, and $\zeta_{\text{USD}} - \zeta_{\text{JPY}}$, are relatively small in absolute value, which brings evidence of moderate dependence between the FX rates considered and their volatility. This is in line with the findings of [**BM18**] since in the present calibration we are considering only hard currencies. We also remark that these differences are slightly larger in the case of the CGMY specification.

By inspecting the calibrated values of the parameters of the tempered-stable CBI processes, we can notice a non-trivial contribution from their self-exciting jumps. This documents the presence of self-excitation in the volatility of FX rates (see Figure 5.1). It is also interesting to remark that the calibrated values of the parameters of the CGMY specification are surprisingly stable across the two types of calibration, which might be ascribed to the non-injectivity issue that one typically faces during a deep calibration (refer to [**BDL21**, Appendix B]). In particular, this issue can be addressed by reducing the number of input parameters, which explains why this phenomenon appears to be mitigated in the case of the Brownian specification.

We can discern a strong discrepancy between the calibrated values obtained by standard calibration and those obtained by deep calibration in the case of the Brownian motion. This may be justified by the fact that the calibrated values obtained by deep calibration tend to underestimate the real contribution of the tempered-stable CBI processes. This is because the neural network returns slightly lower volatilities than the original pricing function, which is a direct consequence of the normalization process applied to the training set before solving minimization problem (5.23).

When restricting our attention to the deep calibration, which outperforms the standard one for both specifications considered, it appears that the CGMY specification marginally improves the quality of the fit compared to the Brownian one. This suggests that incorporating self-exciting jumps into the activity rate allows to replicate FX market-implied volatility surfaces in the presence of self-excitation in the volatility of FX rates. Taking into account the observation that the non-injectivity of the neural network appears to be more pronounced in the case of the CGMY specification, this also suggests that introducing extra jumps into the base process might be redundant.

5.4.4. Sensitivity analysis. In this last section, we study the impact of the self-exciting behavior of the tempered-stable CBI processes on the shape of the FX volatility smile. We focus on the smile at maturity 2 weeks of the FX implied volatility surface USDJPY (smallest RMSE), and restrict our attention to the parameters controlling the self-exciting jumps of the tempered-stable CBI processes (α, η, and θ). We fix $d = 1$ for simplicity.

We start with the sensitivity with respect to the stability index α, which can be visualized in Figure 5.8. First, we decrease the calibrated value by 40%, witnessing a significant increase of the first extremity of the smile, seeking to attain the level of the opposite extremity. We then reduce the obtained value by a further 40%, observing a slight rightward shift of the local minimum together with an increase of the global level of the smile. When looking at smaller values in $(1, 2)$, we observe that the entire smile stabilizes along a symmetric shape around the local minimum. This limit shape of the smile is compatible with an increased likelihood of large jumps along with stronger compensation effects in the dynamics of the tempered-stable CBI process, which happens when α gets smaller in $(1, 2)$ (compare with the discussion before Remark 3.9 in Chapter 3). Indeed, as far as the FX rate is concerned, this is reflected by prolonged periods of stability during which a relatively large jump of the FX rate, whose direction is unknown, is very likely to occur. Investors then seek to protect themselves against a potential fall/rise of the FX rate, hence the presence of higher volatilities at both ends of the smile.

We then proceed with the study of the sensitivity with respect to η and θ, which can be visualized in Figures 5.9 and 5.10, respectively. In particular, we can observe that when θ gets closer to 0 and when η gets bigger, the smile curvature changes from a convex shape to a concave one, while the global level of the smile increases significantly, where the sign of the slope depends on how the currency pair is quoted. While the increased level of the smile can be justified by higher demand for protection among investors as in the case of smaller values of α in $(1, 2)$, the curvature change might be caused by the the fact that the parameters ζ_{JPY}, ζ_{USD}, and ζ_{EUR} must be lower than θ/η (we recall that $\mathcal{D}_1 = (-\infty, \theta/\eta]$ in the case of a tempered-stable CBI process, see Appendix 5.A), with the consequence that these parameters are forced to become either extremely small or negative to comply with this constraint. In view of the discussion in Section 5.3.1, this can give rise to stronger dependence effects between FX rates and their volatility, which translate into the appearance of "frowns" or "smirks" instead of smiles when looking at model-implied volatilities (see [**JFB15**, Section 5.4.2] and [**BM18**]).

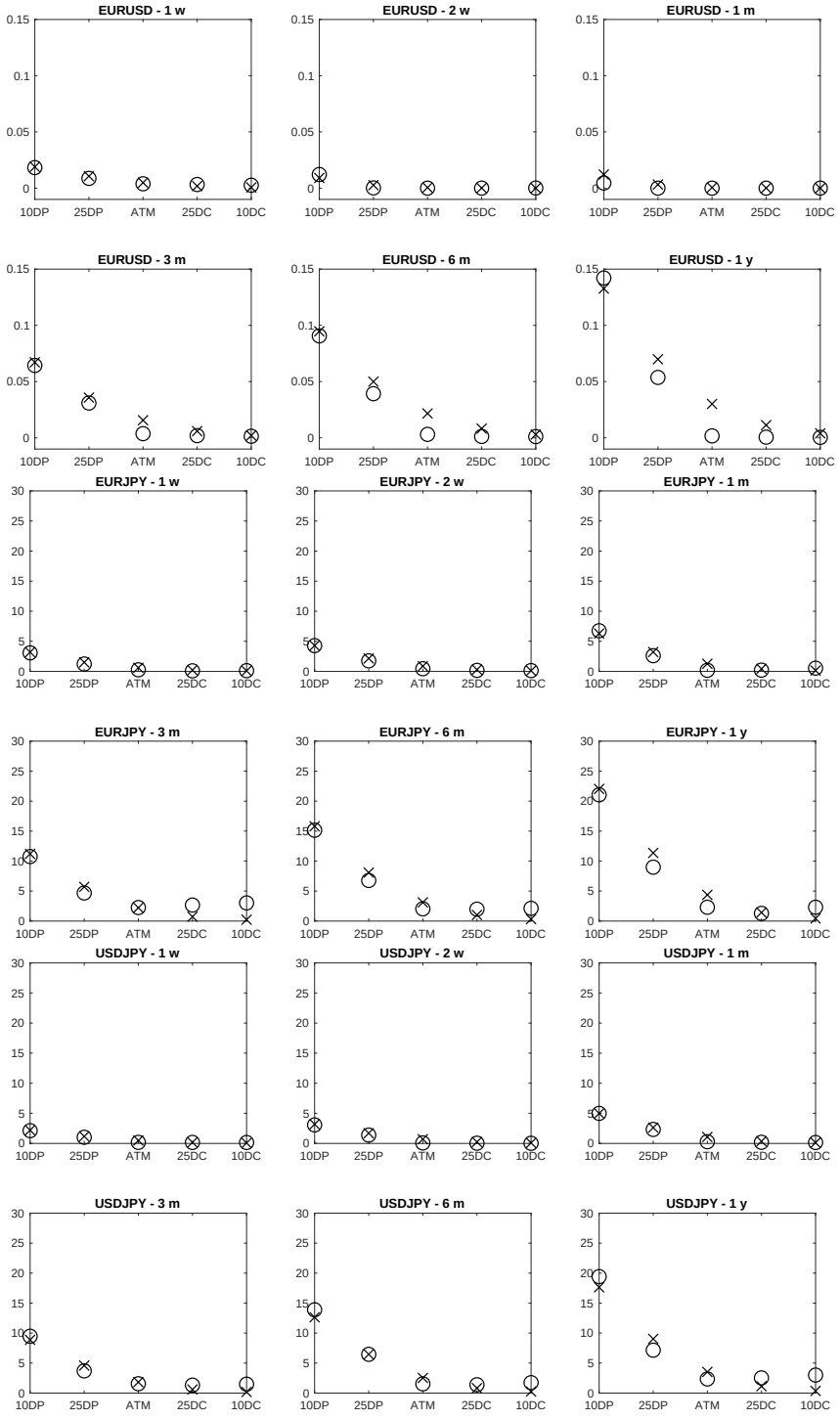

FIGURE 5.4. Calibration results obtained by standard calibration for the Brownian specification. Market prices are denoted by crosses, model prices are denoted by circles. Moneyness levels follow the standard Delta quoting convention in the FX option market. DC and DP stand for "delta call" and "delta put", respectively.

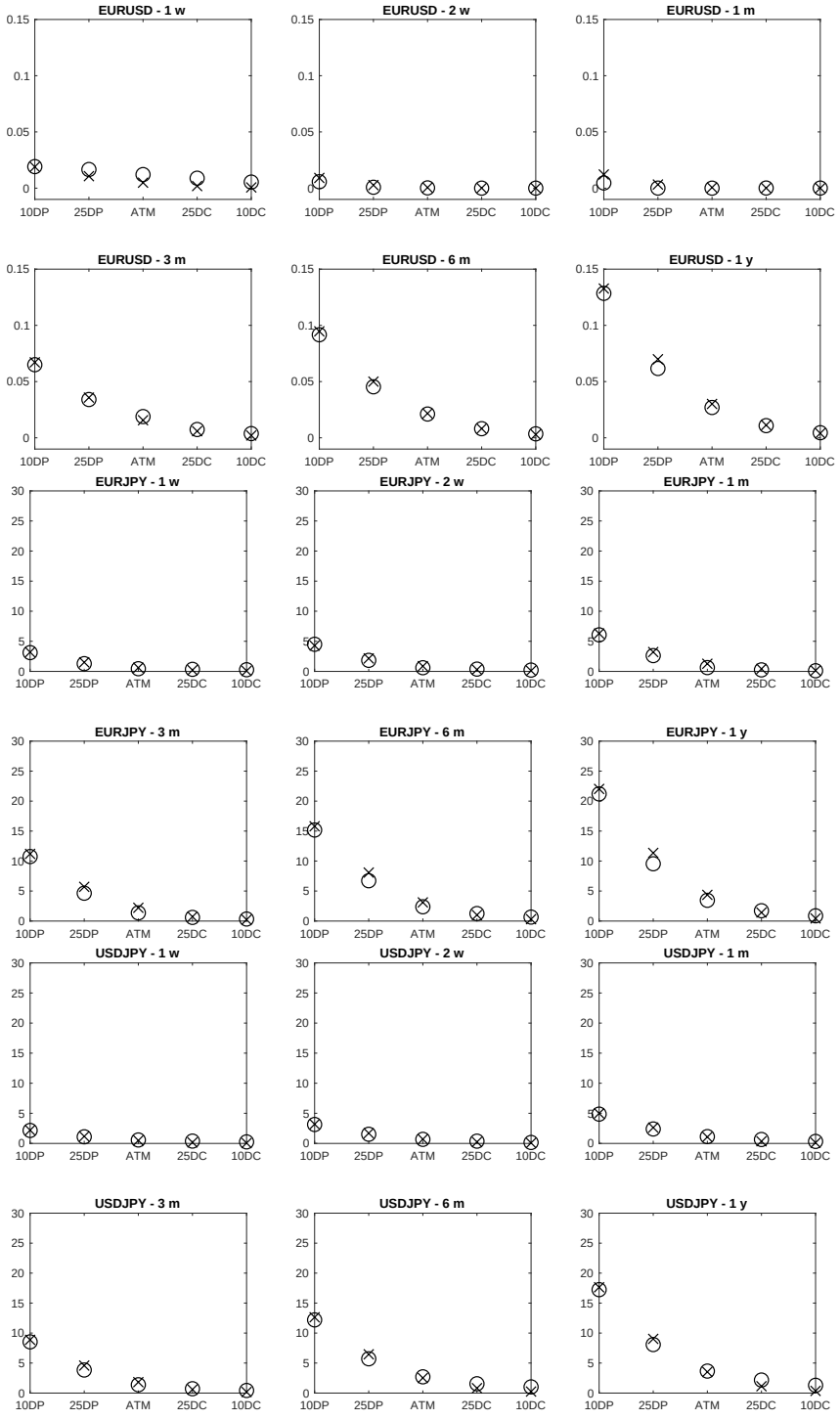

FIGURE 5.5. Calibration results obtained by deep calibration for the Brownian specification. Market prices are denoted by crosses, model prices are denoted by circles. Moneyness levels follow the standard Delta quoting convention in the FX option market. DC and DP stand for "delta call" and "delta put", respectively.

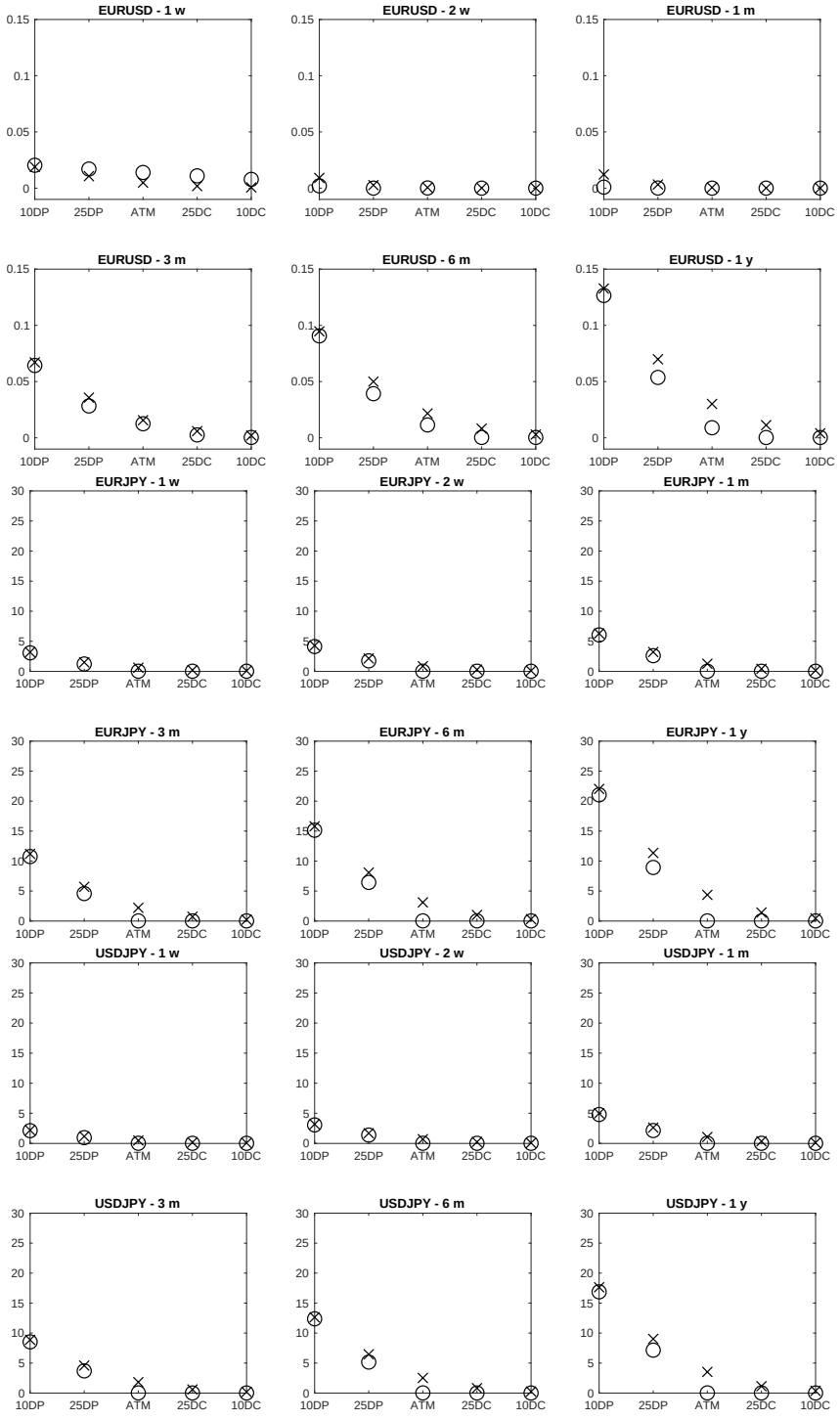

FIGURE 5.6. Calibration results obtained by standard calibration for the CGMY specification. Market prices are denoted by crosses, model prices are denoted by circles. Moneyness levels follow the standard Delta quoting convention in the FX option market. DC and DP stand for "delta call" and "delta put", respectively.

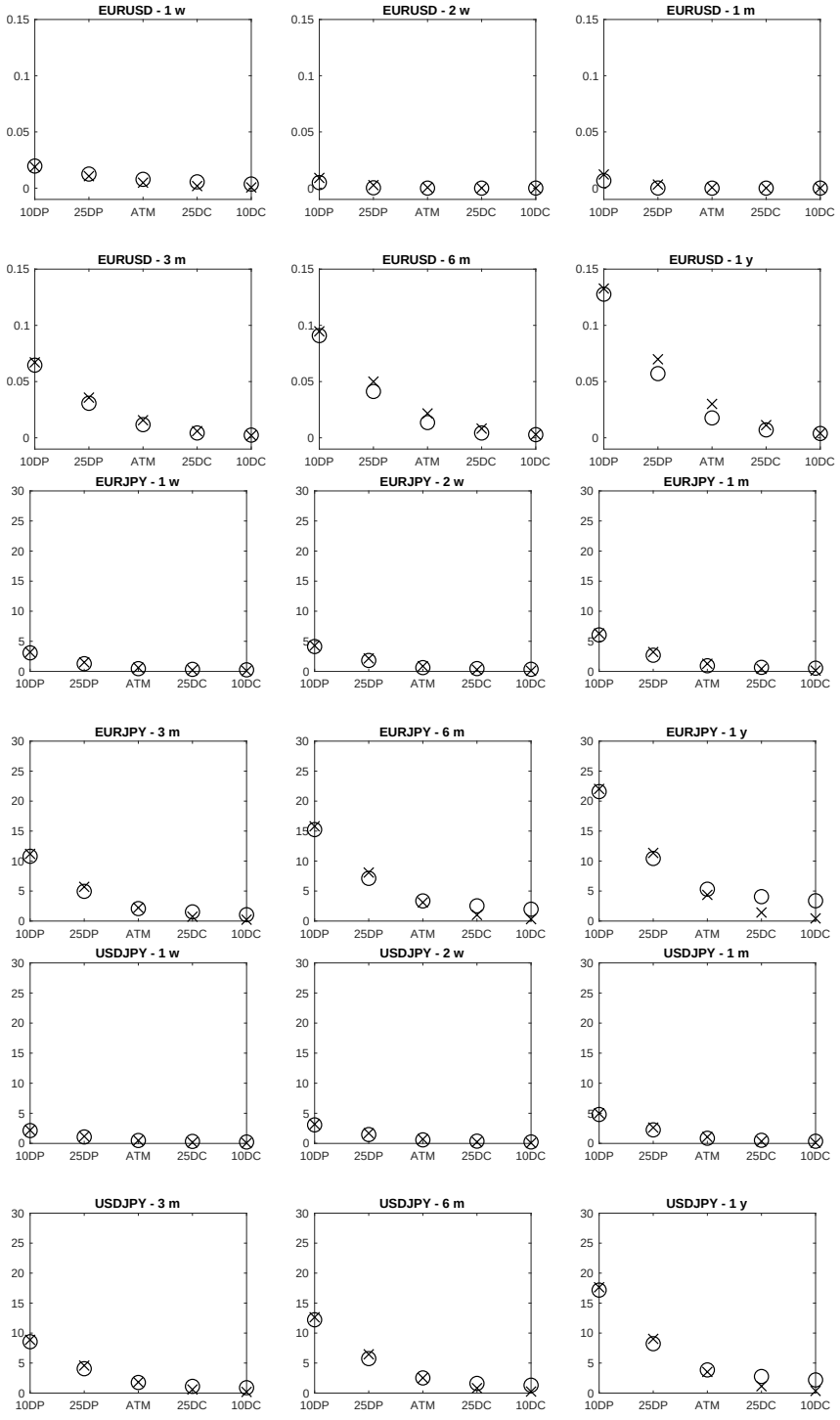

FIGURE 5.7. Calibration results obtained by deep calibration for the CGMY specification. Market prices are denoted by crosses, model prices are denoted by circles. Moneyness levels follow the standard Delta quoting convention in the FX option market. DC and DP stand for "delta call" and "delta put", respectively.

Brownian			CGMY		
	Standard	Deep		Standard	Deep
X_0^1	1.5079	1.3234	X_0^1	1.1040	1.1106
β^1	0.87413	1.2538	β^1	0.37721	0.65766
b^1	-0.47807	-1.5635	b^1	0.43082	0.43082
σ^1	3.8930	1.1439	σ^1	2.1473	2.1473
η^1	9.5007	0.76198	η^1	1.7208	1.7208
θ^1	0.26712	0.43398	θ^1	1.9338	1.9338
α^1	1.9999	1.8677	α^1	1.1697	1.1697
			β_Z^1	-0.16220	-0.16220
			G^1	3.0313	3.0313
			M^1	0.79529	0.79529
			Y^1	1.7675	1.7675
$\zeta_{JPY,1}$	0.013356	0.021699	$\zeta_{JPY,1}$	1.12323	1.12366
$\zeta_{USD,1}$	0.0043576	0.012494	$\zeta_{USD,1}$	0.27244	0.27244
$\zeta_{EUR,1}$	0.0070923	0.00087200	$\zeta_{EUR,1}$	0.089747	0.097352
$\lambda_{JPY,1}$	0.56295	0.56517	$\lambda_{JPY,1}$	0.39764	0.39764
$\lambda_{USD,1}$	0.49695	0.39581	$\lambda_{USD,1}$	0.32863	0.32863
$\lambda_{EUR,1}$	0.58852	0.58201	$\lambda_{EUR,1}$	0.16260	0.16260
X_0^2	0.37404	0.44963	X_0^2	0.19652	0.18549
β^2	1.6333	0.51905	β^2	1.7524	1.7782
b^2	0.96291	-0.16185	b^2	-0.73467	-0.73467
σ^2	0.19556	1.1141	σ^2	1.1174	1.1174
η^2	0.51939	1.0396	η^2	2.1855	2.1855
θ^2	0.30117	0.26946	θ^2	0.65273	0.65273
α^2	1.7560	1.8584	α^2	1.1122	1.1122
			β_Z^2	0.88065	0.88065
			G^2	0.59711	0.59711
			M^2	0.22821	0.22821
			Y^2	1.2390	1.2390
$\zeta_{JPY,2}$	0.15058	0.13473	$\zeta_{JPY,2}$	0.232636	0.232636
$\zeta_{USD,2}$	0.094102	0.065180	$\zeta_{USD,2}$	0.092184	0.060470
$\zeta_{EUR,2}$	0.030499	0.029955	$\zeta_{EUR,2}$	0.025973	0.024422
$\lambda_{JPY,2}$	1.3190	1.3190	$\lambda_{JPY,2}$	0.11410	0.11410
$\lambda_{USD,2}$	0.72105	0.67472	$\lambda_{USD,2}$	-0.014839	-0.014839
$\lambda_{EUR,2}$	0.88728	1.0493	$\lambda_{EUR,2}$	0.040496	0.040496
RMSE	0.06119	0.04157	RMSE	0.07557	0.04092
Time (in sec.)	929.086	0.218	Time (in sec.)	709.977	0.269

TABLE 5.2. Calibrated values of the model parameters. We can observe that all parameter constraints set in Section 5.2.2 are satisfied.

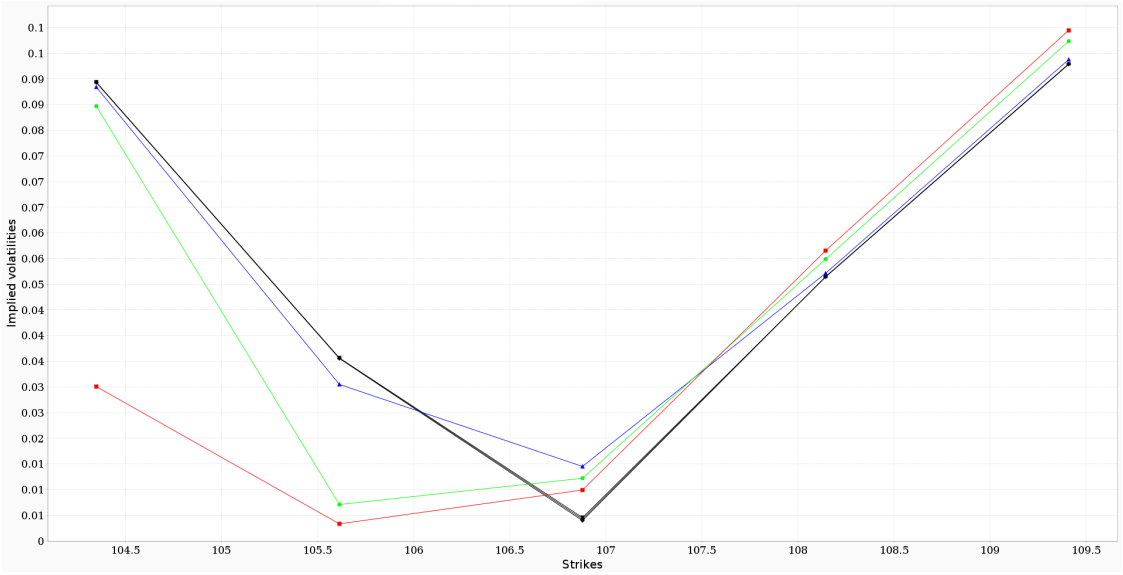

FIGURE 5.8. Sensitivity with respect to α, where each smile is generated by shifting α by a certain decrement. The plot contains six smiles: the red smile corresponds to the calibrated value of Table 5.2; the green one to $\alpha - 40\%$; the blue one to $\alpha - 80\%$; and three black ones almost overlapping perfectly corresponding to $\alpha - 83\%$, $\alpha - 84\%$, and $\alpha - 85\%$, thus demonstrating convergence to a limit shape.

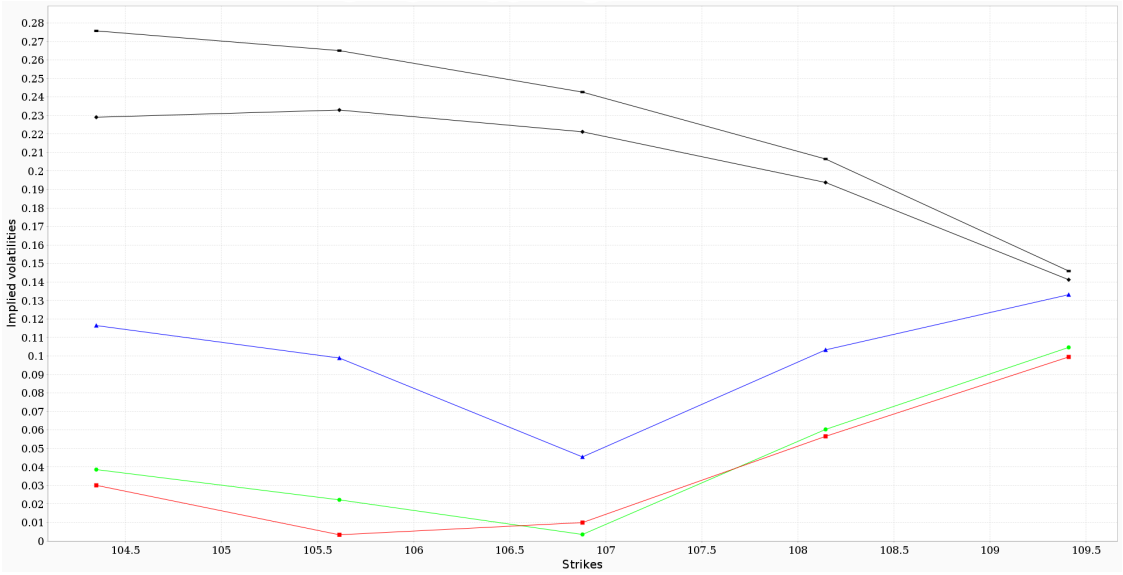

FIGURE 5.9. Sensitivity with respect to η, where each smile is generated by shifting η by a certain increment. The plot contains five smiles: the red smile corresponds to the calibrated value of Table 5.2; the green one to $\eta + 30\%$; the blue one to $\eta + 60\%$; and the two black ones to $\eta + 90\%$ and $\eta + 120\%$.

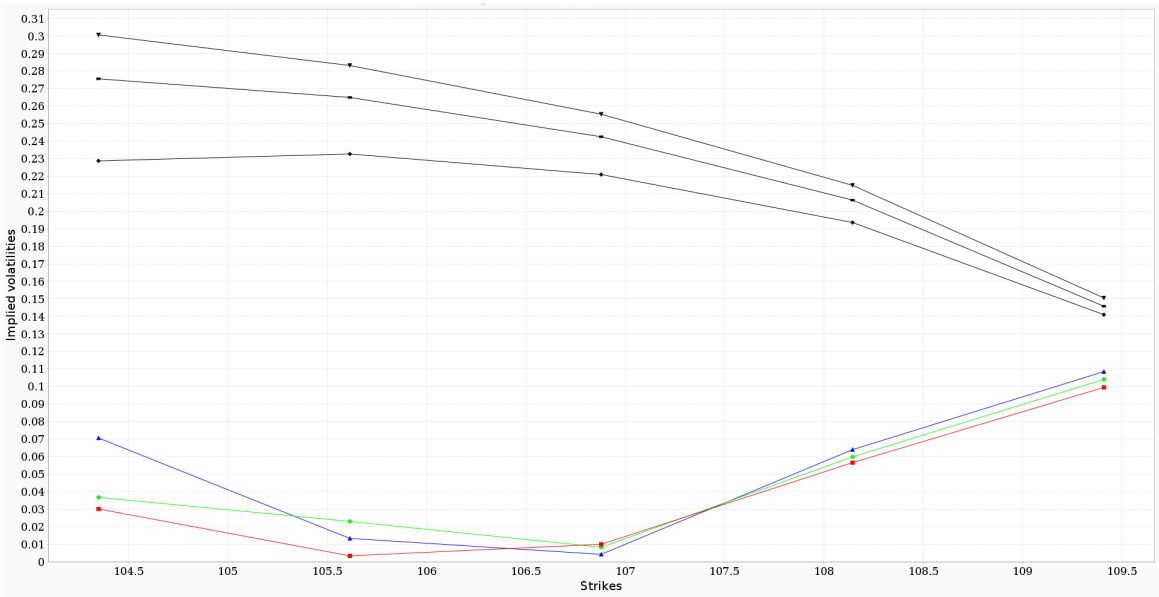

FIGURE 5.10. Sensitivity with respect to θ, where each smile is generated by multiplying θ by some factor. The plot contains six smiles: the red smile corresponds to the calibrated value of Table 5.2; the green one to 60% of θ; the blue one to 30% of θ; and the three black ones to 10% of θ, 5% of θ, and 3% of θ.

5.5. Conclusion

We have proposed a stochastic volatility modeling framework for multiple currencies based on *CBI-Time-Changed Lévy processes* (CBITCL). The characteristic feature of the proposed approach consists in the self-excitation of the volatility of FX rates (which directly derives from the self-exciting behavior of CBI processes), while preserving the peculiar symmetries that FX rates satisfy. Our framework retains a remarkable level of analytical tractability since we have been able to characterize a class of risk-neutral measures leaving invariant the structure of the model. By relying on this result, we have derived a semi-closed-form pricing formula for currency options.

We have tested our framework via a calibration to an FX triangle. Two specifications of the model have been introduced: Brownian and CGMY, where each CBI process has been chosen tempered stable. Two types of calibration have been implemented: standard and deep, where the latter uses deep-learning techniques. We have observed that the deep calibration outperforms the standard one. We have also found that the CGMY specification marginally improves the quality of the fit over the Brownian one. Taking into account the observed non-injectivity of the neural network in the case of the CGMY specification, this suggests that adding jumps into the base process, when the activity rate exhibits self-excitation, might be redundant.

We have performed a sensitivity analysis on model-implied volatility smiles, restricting our attention to the parameters controlling the self-exciting behavior of the tempered-stable CBI processes. In particular, we have documented a prevailing role of the tempering parameter in the sense that when this parameter approaches zero, the smile curvature radically changes from a convex shape to a concave one, which is a major impact on the shape of the FX volatility smile.

There are many avenues of further research. The first avenue would be to incorporate stochasticity into the short rates appearing in the dynamics of the FX rates, and then relate the present framework to that of Chapter 3. However, special attention should be paid to the growing number of parameters. Another avenue would be to extend the numerical assessment of Section 5.4 by also introducing soft currencies.

5.A. Appendix: Model specifications

In this appendix, we provide more information on the specifications considered in Section 5.4. For every $1 \leqslant k \leqslant 2$, $X^k = (X^k_t)_{t \leqslant \mathcal{T}}$ is chosen to be a *tempered-stable CBI process* in the sense of Section 2.7, which is defined by $\nu^k = 0$ and π^k given by

$$\pi^k(\mathrm{d}z) = (\eta^k)^{\alpha^k} C^k_\alpha \, z^{-1-\alpha^k} \, e^{-\frac{\theta^k}{\eta^k} z} \, \mathbf{1}_{\{z>0\}} \, \mathrm{d}z, \tag{5.25}$$

where we fix

$$C^k_\alpha = \frac{1}{\Gamma(-\alpha^k)}, \tag{5.26}$$

where $\eta^k > 0$ serves as a volatility parameter for the jump part, $\theta^k > 0$ denotes the tempering parameter, and $\alpha^k \in (1,2)$, called *stability index*, determines the local behavior (see Section 2.7).

We recall from Section 2.7 that in the case of a tempered stable CBI processes $X^k = (X^k_t)_{t\leqslant\mathcal{T}}$, we have $\mathcal{D}^k_1 = \big(-\infty, \theta^k/\eta^k\big]$. We also rewrite the expressions associated to the immigration and branching mechanisms Ψ^k and Φ^k, given by $\Psi^k(x) = \beta^k\, x$ and

$$\Phi^k(x) = -\,b^k\, x + \frac{1}{2}\left(\sigma^k\, x\right)^2 + \left(\theta^k - \eta^k\, x\right)^{\alpha^k} - \left(\theta^k\right)^{\alpha^k} + \alpha^k\left(\theta^k\right)^{\alpha^k-1}\eta^k\, x, \tag{5.27}$$

for all $x \leqslant \theta^k/\eta^k$, where we recall that Φ^k satisfies Assumption 2.4.

We then consider two different specifications for each Lévy triplet $\big(b^k_Z, \sigma^k_Z, \gamma^k_Z\big)$. The first one consists in taking $b^k_Z = 0$, $\sigma^k_Z = 1$, and $\gamma^k_Z = 0$, which reduces to a Brownian motion. We then have $\mathcal{D}^k_2 = \mathbb{R}$ and $\Xi^k_Z(u) = \frac{1}{2}\left(\sigma^k_Z\, u\right)^2$, for all $u \in \mathbb{C}$. The second specification makes use of the *CGMY process* [**CGMY02**] as the Lévy process of each CBITCL process so that the Lévy measure γ^k_Z is given by

$$\gamma^k_Z(\mathrm{d}z) = C^k_Y\left(z^{-1-Y^k}\, e^{-\,M^k\, z}\,\mathbf{1}_{\{z>0\}} + |z|^{-1-Y^k}\, e^{-\,G^k\,|z|}\,\mathbf{1}_{\{z<0\}}\right)\mathrm{d}z, \tag{5.28}$$

where we fix

$$C^k_Y = \frac{1}{\Gamma(-Y^k)}. \tag{5.29}$$

While $G^k > 0$ tempers the downward jumps, $M^k > 0$ tempers the upward ones, and $Y^k \in (1,2)$ controls the local behavior similarly to α^k. We also recall that any CGMY process is determined by a Lévy triplet of the form $\big(\beta^k_Z, 0, \gamma^k_Z\big)$. The associated Lévy exponent Ξ^k_Z is then given by

$$\Xi^k_Z(u) := \beta^k_Z\, u + \int_{\mathbb{R}}\left(e^{\,z\,u} - 1 - z\,u\right)\gamma^k_Z(\mathrm{d}z), \qquad \forall u \in \mathrm{i}\,\mathbb{R}, \tag{5.30}$$

where the correspondence between β^k_Z and b^k_Z is given by

$$\beta^k_Z := b^k_Z + \int_{|z|\geqslant 1} z\,\gamma^k_Z(\mathrm{d}z), \tag{5.31}$$

where the integral is finite since $\int_{|z|\geqslant 1}|z|\,\gamma^k_Z(\mathrm{d}z) < +\infty$ for γ^k_Z given by (5.28).

It can be easily checked that in the case of a CGMY process, we have $\mathcal{D}^k_2 = \big[-G^k, M^k\big]$, and the Lévy exponent Ξ^k_Z given by (5.30) takes the following form:

$$\Xi^k_Z(x) = \beta^k_Z\, x + \left(M^k - x\right)^{Y^k} - \left(M^k\right)^{Y^k} + \left(G^k + x\right)^{Y^k} - \left(G^k\right)^{Y^k} + x\,Y^k\left(\left(M^k\right)^{Y^k-1} - \left(G^k\right)^{Y^k-1}\right),$$

for all $-G^k \leqslant x \leqslant M^k$.

In the present context, thanks to the explicit form of the sets $\mathcal{D}^k_1$ and $\mathcal{D}^k_2$ and in view of satisfying $\zeta_{i,k} \in \mathcal{D}^k_1$ and $\lambda_{i,k} \in \mathcal{D}^k_2$ (see Section 5.2.2), it suffices to verify $\max\limits_{1\leqslant i\leqslant 3}\zeta_{i,k} \leqslant \theta^k/\eta^k$ in the case of the Brownian specification and

$$\max_{1\leqslant i\leqslant 3}\zeta_{i,k} \leqslant \theta^k/\eta^k, \quad -G^k \leqslant \min_{1\leqslant i\leqslant 3}\lambda_{i,k}, \quad \text{and} \quad \max_{1\leqslant i\leqslant 3}\lambda_{i,k} \leqslant M^k,$$

in the case of the CGMY specification.

We now investigate the stability of both specifications under (5.7). In view of Theorem 5.8, we start by inserting (5.25) into $\pi^{i,k}$ of Table 5.1:

$$\pi^{i,k}(dz) = (\eta^k)^{\alpha^k}\, C^k_\alpha\, z^{-1-\alpha^k}\, e^{-\,\frac{\theta^k - \zeta_{i,k}\,\eta^k}{\eta^k}\,z}\,\mathbf{1}_{\{z>0\}}\,\mathrm{d}z.$$

By taking $\eta^{i,k} := \eta^k$, $\theta^{i,k} := \theta^k - \zeta_{i,k}\,\eta^k$, and $\alpha^{i,k} := \alpha^k$, we notice that $X^k = (X^k_t)_{t\leqslant\mathcal{T}}$ remains a tempered-stable CBI process under $\mathbb{Q}^i$ (compare with Table 4.2). Concerning the Lévy processes, two situations can occur: the Brownian specification is preserved under $\mathbb{Q}^i$ since we have $\gamma^{i,k}_Z = 0$, but also $b^{i,k}_Z = \lambda_{i,k}$ by Table 5.1 ($\sigma^{i,k}_Z = \sigma^k_Z = 1$ in any case). Regarding the CGMY specification, we plug (5.28) into $\gamma^{i,k}_Z$ of Table 5.1:

$$\gamma^{i,k}_Z(\mathrm{d}z) = C^k_Y \left(z^{-1-Y^k}\, e^{-\left(M^k-\lambda_{i,k}\right) z}\, \mathbf{1}_{\{z>0\}} + |z|^{1+Y^k}\, e^{-\left(G^k+\lambda_{i,k}\right)|z|}\, \mathbf{1}_{\{z<0\}} \right) \mathrm{d}z,$$

where, by defining $G^{i,k} := G^k + \lambda_{i,k}$, $M^{i,k} := M^k - \lambda_{i,k}$, and $Y^{i,k} := Y^k$, we observe that each Lévy process remains a CGMY process under $\mathbb{Q}^i$.

The computation of the drifts $b^{i,k}$ and $\beta^{i,k}_Z$ follows the lines of the proof of Lemma 2.19:

$$b^{i,k} := b^k - \zeta_{i,k}\left(\sigma^k\right)^2 - \int_0^{+\infty} z\left(e^{\,\zeta_{i,k}\,z} - 1\right)\pi^k(\mathrm{d}z) \quad \text{and} \quad \beta^{i,k}_Z := \beta^k_Z + \int_{\mathbb{R}} z\left(e^{\,\lambda_{i,k}\,z} - 1\right)\gamma^k_Z(\mathrm{d}z),$$

where we have moved from $(b^k_Z, b^{i,k}_Z)$ to $(\beta^k_Z, \beta^{i,k}_Z)$ by (5.31). As in the proof of Lemma 2.19, we replace the exponential with its Maclaurin series expansion:

$$b^{i,k} = b^k - \zeta_{i,k}\,(\sigma^k)^2 - \frac{(\eta^k)^{\alpha^k}}{\Gamma(-\alpha^k)} \int_0^{+\infty} \sum_{n=1}^{+\infty} \frac{(\zeta_{i,k}\,z)^n}{n!\,z^{\alpha^k}}\, e^{-\frac{\theta^k}{\eta^k}\,z}\,\mathrm{d}z,$$

$$\beta^{i,k}_Z = \beta^k_Z + \frac{1}{\Gamma(-Y^k)} \left(\int_0^{+\infty} \sum_{n=1}^{+\infty} \frac{(\lambda_{i,k}\,z)^n}{n!\,z^{Y^k}}\, e^{-M^k\,z}\,\mathrm{d}z + \int_0^{+\infty} \sum_{n=1}^{+\infty} \frac{(-\lambda_{i,k}\,z)^n}{n!\,z^{Y^k}}\, e^{-G^k\,z}\,\mathrm{d}z \right).$$

Then, by applying Fubini's theorem and by making use of the Gamma function, we obtain

$$b^{i,k} = b^k - \zeta_{i,k}\,(\sigma^k)^2 - \frac{(\eta^k)^{\alpha^k}(\theta^k)^{\alpha^k-1}}{\Gamma(-\alpha^k)} \sum_{n=1}^{+\infty} \frac{\left(\zeta_{i,k}\,\eta^k/\theta^k\right)^n}{n!}\,\Gamma\big(n-(\alpha^k-1)\big),$$

$$\beta^{i,k}_Z = \beta^k_Z + \frac{(M^k)^{Y^k-1}}{\Gamma(-Y^k)} \sum_{n=1}^{+\infty} \frac{\left(\lambda_{i,k}/M^k\right)^n}{n!}\,\Gamma\big(n-(Y^k-1)\big) + \frac{(G^k)^{Y^k-1}}{\Gamma(-Y^k)} \sum_{n=1}^{+\infty} \frac{\left(-\lambda_{i,k}/G^k\right)^n}{n!}\,\Gamma\big(n-(Y^k-1)\big).$$

By inserting $\Gamma\big(n-(\delta-1)\big) = -\delta\,(-1)^n\,n!\,\binom{\delta-1}{n}\,\Gamma(-\delta)$ into the summations, while introducing the Maclaurin series expansion of $x \mapsto (1+x)^{\delta-1}$ for $\delta = \alpha^k$ or Y^k, we finally obtain

$$b^{i,k} = b^k - \zeta_{i,k}\,(\sigma^k)^2 - \alpha^k\,(\eta^k)^{\alpha^k}\Big(\left(\theta^k\right)^{\alpha^k-1} - \left(\theta^k - \zeta_{i,k}\,\eta^k\right)^{\alpha^k-1}\Big), \tag{5.32}$$

$$\beta^{i,k}_Z = \beta^k_Z + Y^k\left(\left(M^k\right)^{Y^k-1} - \left(M^k-\lambda_{i,k}\right)^{Y^k-1} + \left(G^k\right)^{Y^k-1} - \left(G^k+\lambda_{i,k}\right)^{Y^k-1}\right). \tag{5.33}$$

Bibliography

[AB13] F.M. Ametrano and M. Bianchetti. Everything you always wanted to know about multiple interest rate curve bootstrapping but were afraid to ask. SSRN working paper available at `http://ssrn.com/abstract=2219548`, 2013.

[AB20] L. B. G. Andersen and D. R. A. Bang. Spike modeling for interest rate derivatives with an application to SOFR caplets. SSRN working paper available at `https://ssrn.com/abstract=3700446`, 2020.

[AG00] T. Ané and H. Geman. Order flow, transaction clock, and normality of asset returns. *The Journal of Finance*, 55(5):2259–2284, 2000.

[AGS20] M. Alfeus, M. Grasselli, and E. Schlögl. A consistent stochastic model of the term structure of interest rates for multiple tenors. *Journal of Economic Dynamics and Control*, 114:103861, 2020.

[AJ91] K. I. Amin and R. A. Jarrow. Pricing foreign currency options under stochastic interest rates. *Journal of International Money and Finance*, 10(3):310–329, 1991.

[AM09] C. Albanese and A. Mijatović. A stochastic volatility model for risk-riversals in foreign exchange. *International Journal of Theoretical and Applied Finance*, 12(6):877–899, 2009.

[AR01] S. Asmussen and J. Rosinski. Approximations of small jumps of Lévy processes with a view towards simulation. *Journal of Applied Probability*, 38(2):482–493, 2001.

[BBSS21] G. Bernis, R. Brignone, S. Scotti, and C. Sgarra. A Gamma Ornstein-Uhlenbeck model driven by a Hawkes process. To appear in *Mathematics and Financial Economics*, 2021.

[BCW08] G. Bakshi, P. Carr, and L. Wu. Stochastic risk premiums, stochastic skewness in currency options, and stochastic discount factors in international economies. *Journal of Financial Economics*, 87(1):132–156, 2008.

[BDL21] F. E. Benth, N. Detering, and S. Lavagnini. Accuracy of deep learning in calibrating HJM forward curves. To appear in *Digital Finance*, 2021.

[BDR17] L. Ballotta, G. Deelstra, and G. Raye. Multivariate FX models with jumps: Triangles, quantos and implied correlation. *European Journal of Operational Research*, 260(3):1181–1199, 2017.

[Bek95] G. Bekaert. The time variation of expected returns and volatility in foreign-exchange markets. *Journal of Business and Economic Statistics*, 13(4):397–408, 1995.

[BGP15] J. Baldeaux, M. Grasselli, and E. Platen. Pricing currency derivatives under the benchmark approach. *Journal of Banking and Finance*, 53:34–48, 2015.

[Bia10] M. Bianchetti. Two curves, one price. *Risk Magazine*, pages 74–80, August 2010.

[Bie45] I. J. Bienaymé. De la loi de multiplication et de la durée des families. *Société Philomathique de Paris Extraits*, 5:37–39, 1845.

[BIS19] BIS Triennial Central Bank Survey: Foreign exchange turnover in April 2019. Technical report, Bank for International Settlements (BIS), Monetary and Economic Department, April 2019.

[BLP15] M. Barczy, Z. Li, and G. Pap. Yamada–Watanabe results for stochastic differential equations with jumps. *International Journal of Stochastic Analysis*, 2015.

[BM96] P. Brémaud and L. Massoulié. Stability of nonlinear Hawkes processes. *The Annals of Probability*, 24(3):1563–1588, 1996.

[BM02] P. Brémaud and L. Massoulié. Power spectra of general shot noises and Hawkes point processes with a random excitation. *Advances in Applied Probability*, 34(1):205–222, 2002.

[BM13] M. Bianchetti and M. Morini, editors. *Interest Rate Modelling After the Financial Crisis*. Risk Books, 2013.

[BM18] L. Ballotta and A. Morico. Hidden correlations: A self-exciting tale from the FX world. SSRN working paper available at `https://ssrn.com/abstract=3245149`, 2018.

[BMSS19] A. Backwell, A. Macrina, E. Schlögl, and D. Skovmand. Term rates, multicurve term structures and overnight rate benchmarks: A roll-over risk approach. SSRN working paper available at `https://ssrn.com/abstract=3399680`, 2019.

[BNT02] P. Brémaud, G. Nappo, and G. L. Torrisi. Rate of convergence to equilibrium of marked Hawkes processes. *Journal of Applied Probability*, 39(1):123–136, 2002.

[BS20] G. Bernis and S. Scotti. Clustering effects via Hawkes processes. In Y. Jiao, editor, *From Probability to Finance - Lecture Notes of BICMR Summer School on Financial Mathematics*. Springer, Singapore, 2020.

[BSS18] G. Bernis, K. Salhi, and S. Scotti. Sensitivity analysis for marked Hawkes processes: application to CLO pricing. *Mathematics and Financial Economics*, 12:541–559, 2018.

[Cas10] A. Castagna. *FX Options and Smile Risk*. The Wiley Finance Series. Wiley, 2010.

[CD13] S. Crépey and R. Douady. Lois: credit and liquidity. *Risk Magazine*, pages 82–86, June 2013.

[CDS01] P. Collin-Dufresne and B. Solnik. On the term structure of default premia in the swap and LIBOR markets. *The Journal of Finance*, 56(3):1095–1115, 2001.

[CFG16] C. Cuchiero, C. Fontana, and A. Gnoatto. A general HJM framework for multiple yield curve modeling. *Finance and Stochastics*, 20(2):267–320, 2016.

[CFG19a] G. Callegaro, L. Fiorin, and M. Grasselli. Quantization meets Fourier: a new technology for pricing options. *Annals of Operations Research*, 282(1):59–86, 2019.

[CFG19b] C. Cuchiero, C. Fontana, and A. Gnoatto. Affine multiple yield curve models. *Mathematical Finance*, 29(2):568–611, 2019.

[CGMY02] P. Carr, H. Geman, D. B. Madan, and M. Yor. The fine structure of asset returns: An empirical investigation. *The Journal of Business*, 75(2):305–332, 2002.

[CGMY03] P. Carr, H. Geman, D. B. Madan, and M. Yor. Stochastic volatility for Lévy processes. *Mathematical Finance*, 13(3):345–382, 2003.

[CGNS15] S. Crépey, Z. Grbac, N. Ngor, and D. Skovmand. A Lévy HJM multiple-curve model with application to CVA computation. *Quantitative Finance*, 15(3):401–419, 2015.

[Che06] A. Cherny. Some particular problems of martingale theory. In Y. Kabanov, R. Lipster, and J. Stoyanov, editors, *From stochastic calculus to mathematical finance - The Shiryaev Festschrift*, pages 109–124. Springer, Berlin, 2006.

[CHJ09] P. Christoffersen, S. Heston, and K. Jacobs. The shape and term structure of the index option smirk: Why multifactor stochastic volatility models work so well. *Management Science*, 55(12):1914–1932, 2009.

[CIR85] J. C. Cox, J. E. Ingersoll, and S. A. Ross. A theory of the term structure of interest rates. *Econometrica*, 53(2):385–407, 1985.

[CKT16] C. Cuchiero, I. Klein, and J. Teichmann. A new perspective on the fundamental theorem of asset pricing for large financial markets. *Theory of Probability and its Applications*, 60(4):561–579, 2016.

[Cla73] P. K. Clark. A subordinated stochastic process model with finite variance for speculative prices. *Econometrica*, 41(1):135–155, 1973.

[Cla11] I. J. Clark. *Foreign Exchange Option Pricing: A Practitioner's Guide*. The Wiley Finance Series. Wiley, 2011.

[CM99] P. Carr and D. B. Madan. Option valuation using the fast Fourier transform. *Journal of Computational Finance*, 2(4):61–73, 1999.

[CMNS16] S. Crépey, A. Macrina, T. M. Nguyen, and D. Skovmand. Rational multi-curve models with counterparty-risk valuation adjustments. *Quantitative Finance*, 16(6):847–866, 2016.

[CMS19] G. Callegaro, A. Mazzoran, and C. Sgarra. A self-exciting modelling framework for forward prices in power markets. ArXiv working paper available at `https://arxiv.org/abs/1910.13286`, 2019.

[CQTZ20] Z. Cui, W. Qian, S. Taylor, and L. Zhu. Detecting and identifying arbitrage in the spot foreign exchange market. *Quantitative Finance*, 20(1):119–132, 2020.

[CT04] R. Cont and P. Tankov. *Financial Modelling with Jump Processes*. Chapman and Hall CRC, London, 2004.

[CW03] P. Carr and L. Wu. What type of process underlies options? A simple robust test. *The Journal of Finance*, 58(6):2581–2610, 2003.

[CW04] P. Carr and L. Wu. Time-changed Lévy processes and option pricing. *Journal of Financial Economics*, 71:113–141, 2004.

[CW07] P. Carr and L. Wu. Stochastic skew in currency options. *Journal of Financial Economics*, 86(1):213–247, 2007.

[DBnR08] S. Del Baño Rollin. Spot inversion in the Heston model. Working paper available at `https://core.ac.uk/display/13283041`, 2008.

[DCGG13] A. De Col, A. Gnoatto, and M. Grasselli. Smiles all around: FX joint calibration in a multi-Heston model. *Journal of Banking and Finance*, 37(10):3799–3818, 2013.

[DFG11] J. Da Fonseca and M. Grasselli. Riding on the smiles. *Quantitative Finance*, 11(11):1609–1632, 2011.

[DFM14] X. Duhalde, C. Foucart, and C. Ma. On the hitting times of continuous-state branching processes with immigration. *Stochastic Processes and their Applications*, 124(12):4182–4201, 2014.

[DFS03] D. Duffie, D. Filipović, and W. Schachermayer. Affine processes and applications in finance. *Annals of Applied Probability*, 13(3):984–1053, 2003.

[DFZ14] J. Da Fonseca and R. Zaatour. Hawkes process: Fast calibration, application to trade clustering, and diffusive limit. *Journal of Futures Markets*, 34(6):548–579, 2014.

[Die69] J. Dieudonné. *Foundations of Modern Analysis*, volume 1 of *Elément d'analyse*. Academic Press, 1969.

[DL06] D. A. Dawson and Z. Li. Skew convolution semigroups and affine Markov processes. *Annals of Probability*, 34(3):1103–1142, 2006.

[DL12] D. A. Dawson and Z. Li. Stochastic equations, flows and measure-valued processes. *The Annals of Probability*, 40(2):813–857, 2012.

[Dou07] P. Doust. The intrinsic currency valuation framework. *Risk Magazine*, March:76–81, 2007.

[Dou12] P. Doust. The stochastic intrinsic currency volatility model: A consistent framework for multiple FX rates and their volatilities. *Applied Mathematical Finance*, 19(5):381–445, 2012.

[DS94] F. Delbaen and W. Schachermayer. A general version of the fundamental theorem of asset pricing. *Mathematische Annalen*, 300(3):463–520, 1994.

[DS98] F. Delbaen and W. Schachermayer. The fundamental theorem of asset pricing for unbounded stochastic processes. *Mathematische Annalen*, 312:215–250, 1998.

[DS15] D. Duffie and J. C. Stein. Reforming LIBOR and other financial market benchmarks. *Journal of Economic Perspectives*, 29(2):191–212, 2015.

[DVJ08] D. J. Daley and D. Vere-Jones. *An introduction to the theory of point processes; 2nd ed.* Probability and its Applications. Springer, New York, 2008.

[ECPGUB13] M. Emilia Caballero, J. L. Pérez Garmendia, and G. Uribe Bravo. A Lamperti-type representation of continuous-state branching processes with immigration. *The Annals of Probability*, 41(3):1585–1627, 2013.

[EG18] M. Escobar and C. Gschnaidtner. A multivariate stochastic volatility model with applications in the foreign exchange market. *Review of Derivatives Research*, 21(1):1–43, 2018.

[EGG20] E. Eberlein, C. Gerhart, and Z. Grbac. Multiple curve Lévy forward price model allowing for negative interest rates. *Mathematical Finance*, 30(1):167–195, 2020.

[EK06] E. Eberlein and N. Koval. A cross-currency Lévy market model. *Quantitative Finance*, 6(6):465–480, 2006.

[EK20] E. Eberlein and J. Kallsen. *Mathematical Finance*. Springer finance. Springer, 2020.

[Fel51] W. Feller. Diffusion processes in genetics. In: Proceedings of the 2nd Berkeley Symposium on Mathematical Statistics and Probability (1951), University of California Press, Berkeley and Los Angeles, pp. 227–246, 1951.

[FGGS20] C. Fontana, Z. Grbac, S. Gümbel, and T. Schmidt. Term structure modeling for multiple curves with stochastic discontinuities. *Finance and Stochastics*, 24:465–511, 2020.

[FH97] B. Flesaker and L. P. Hughston. International models for interest rates and foreign exchange. 1997. Reprinted as Chapter 13 in: Hughston, L.P. (ed.) *The new interest rate models*. US: Risk Publications 2000, pp. 217–235.

[Fil01] D. Filipović. A general characterization of one factor affine term structure models. *Finance and Stochastics*, 5(3):389–412, 2001.

[Fil09] D. Filipović. *Term-structure models: A graduate course*. Springer Finance. Springer, Berlin–Heidelberg, 2009.

[FKT17] T. Foucault, R. Kozhan, and W. W. Tham. Toxic arbitrage. *The Review of Financial Studies*, 30(4):1053–1094, 2017.

[FL10] Z. Fu and Z. Li. Stochastic equations of non-negative processes with jumps. *Stochastic Processes and their Applications*, 120(3):306–330, 2010.

[FO09] F. Fang and C. W. Oosterlee. A novel pricing method for European options based on Fourier-cosine series expansions. *SIAM Journal on Scientific Computing*, 31(2):826–848, 2009.

[Fri21] C. Fries. Finmath lib v5.1.3: Algorithms and methodologies related to mathematical finance, Apache Software Foundation License v2.0. `https://www.finmath.net/finmath-lib`, 2021.

[FST11] M. Fujii, A. Shimada, and A. Takahashi. A market model of interest rates with dynamic basis spreads in the presence of collateral and multiple currencies. *Wilmott*, 54:61–73, 2011.

[FT13] D. Filipović and A. B. Trolle. The term structure of interbank risk. *Journal of Financial Economics*, 109(3):707–733, 2013.

[FUB14] C. Foucart and G. Uribe Bravo. Local extinction in continuous-state branching processes with immigration. *Bernoulli*, 20(4):1819–1844, 2014.

[GBC16] I. Goodfellow, Y. Bengio, and A. Courville. *Deep Learning*. MIT Press, 2016. Available at `http://www.deeplearningbook.org`.

[GBP20] F. Graceffa, D. Brigo, and A. Pallavicini. On the consistency of jump-diffusion dynamics for FX rates under inversion. *International Journal of Financial Engineering*, 7(4):2050046, 2020.

[GCF17] A. M. Gambaro, R. Caldana, and G. Fusai. Approximate pricing of swaptions in affine and quadratic models. *Quantitative Finance*, 17(9):1325–1345, 2017.

[GEKR95] H. Geman, N. El Karoui, and J. C. Rochet. Changes of numraire, changes of probability measure and option pricing. *Journal of Applied Probability*, 32(2):443–458, 1995.

[GG14] A. Gnoatto and M. Grasselli. An affine multi-currency model with stochastic volatility and stochastic interest rates. *SIAM Journal on Financial Mathematics*, 5(1):493–531, 2014.

[GGP21] A. Gnoatto, M. Grasselli, and E. Platen. Calibration to FX triangles of the 4/2 model under the benchmark approach. To appear in *Decisions in Economics and Finance*, 2021.

[GJ87] A. Giovannini and P. Jorion. Interest rates and risk premia in the stock market and in the foreign exchange market. *Journal of International Money and Finance*, 6(1):107–123, 1987.

[GK83] M. B. Garman and S. W. Kohlhagen. Foreign currency option values. *Journal of International Money and Finance*, 2(3):231–237, 1983.

[GKP11] D. Gefang, G. Koop, and S. M. Potter. Understanding liquidity and credit risks in the financial crisis. *Journal of Empirical Finance*, 18(5):903–914, 2011.

[GL00] S. Graf and H. Luschgy. *Foundations of Quantization for Probability Distributions*, volume 1730 of *Lecture Notes in Mathematics*. Springer, Berlin–Heidelberg, 2000.

[GM16] M. Grasselli and G. Miglietta. A flexible spot multiple-curve model. *Quantitative Finance*, 16(10):1465–1477, 2016.

[GMY01] H. Geman, D. B. Madan, and M. Yor. Time changes for Lévy processes. *Mathematical Finance*, 11(1):79–96, 2001.

[Gno17] A. Gnoatto. Coherent foreign exchange market models. *International Journal of Theoretical and Applied Finance*, 20(1):1750007, 2017.

[GPSS15] Z. Grbac, A. Papapantoleon, J. Schoenmakers, and D. Skovmand. Affine LIBOR models with multiple curves: Theory, examples and calibration. *SIAM Journal on Financial Mathematics*, 6:984–1025, 2015.

[GR15] Z. Grbac and W. J. Runggaldier. *Interest Rate Modeling: Post-Crisis Challenges and Approaches*. SpringerBriefs in Quantitative Finance. Springer, Cham, 2015.

[Gre74] D. R. Grey. Asymptotic behaviour of continuous time, continuous state-space branching processes. *Journal of Applied Probability*, 11(4):669–677, 1974.

[Gri74] A. Grimvall. On the convergence of sequences of branching processes. *The Annals of Probability*, 2(6):1027–1045, 1974.

[GS21] K. Gellert and E. Schlögl. Short rate dynamics: A Fed Funds and SOFR perspective. ArXiv working paper available at `https://arxiv.org/abs/2101.04308`, 2021.

[GSS17] J. Gallitschke, S. Seifried, and F. T. Seifried. Interbank interest rates: Funding liquidity risk and XIBOR basis spreads. *Journal of Banking and Finance*, 78:142–152, 2017.

[GT05] K. Giesecke and P. Tomecek. Dependent events and changes of time. Cornell University. Project 2 Modeling and Predicting the Volatility. Working paper available at `http://citeseerx.ist.psu.edu/viewdoc/summary?doi=10.1.1.139.2668`, 2005.

[Har82] P. Hartman. *Ordinary Differential Equations; 2nd ed.* Classics in Applied Mathematics. Society for Industrial and Applied Mathematics (SIAM), 3600 Market Street, Floor 6, Philadelphia, PA 19104, 1982.

[Haw71] A. G. Hawkes. Spectra of some self-exciting and mutually exciting point processes. *Biometrika*, 58(1):83–90, 1971.

[Haw18] A. G. Hawkes. Hawkes processes and their applications to finance: a review. *Quantitative Finance*, 18(2):193–198, 2018.

[Hen14] M. Henrard. *Interest Rate Modelling in the Multi-Curve Framework*. Palgrave Macmillan, 2014.

[Hes93] S. L. Heston. A closed-form solution for options with stochastic volatility with applications to bond and currency options. *Review of Financial Studies*, 6(2):327–343, 1993.

[HMT21] B. Horvath, A. Muguruza, and M. Tomas. Deep learning volatility. *Quantitative Finance*, 21(1):11–27, 2021.

[HO74] A. G. Hawkes and D. Oakes. A cluster process representation of a self-exciting process. *Journal of Applied Probability*, 11(3):493–503, 1974.

[HW04] J. Z. Huang and L. Wu. Specification analysis of option pricing models based on time-changed Lévy processes. *The Journal of Finance*, 59(3):1405–1439, 2004.

[Itk17] A. Itkin. Modelling stochastic skew of FX options using SLV models with stochastic spot/vol correlation and correlated jumps. *Applied Mathematical Finance*, 24(6):485–519, 2017.

[IW89] N. Ikeda and S. Watanabe. *Stochastic differential equations and diffusion processes; 2nd ed.* North-Holland mathematical library. North-Holland, Amsterdam–Oxford–New York, 1989.

[Jac79] J. Jacod. *Calcul Stochastique et Problèmes de Martingales*, volume 714 of *Lecture Notes in Mathematics*. Springer, Berlin–Heidelberg–New York, 1979.

[JFB15] J. James, J. Fullwood, and P. Billington. *FX Option Performance: An Analysis of the Value Delivered by FX Options since the Start of the Market*. The Wiley Finance Series. Wiley, 2015.

[Jir58] M. Jirina. Stochastic branching processes with continuous state space. *Czechoslovak Mathematical Journal*, 8:292–312, 1958.

[JKWW11] A. Janek, T. Kluge, R. Weron, and U. Wystup. FX smile in the Heston model. In P. Cizek, W. K. Härdle, and R. Weron, editors, *Statistical Tools for Finance and Insurance*, pages 133–162. Springer, Berlin–Heidelberg, 2011.

[JMS17] Y. Jiao, C. Ma, and S. Scotti. Alpha-CIR model with branching processes in sovereign interest rate modeling. *Finance and Stochastics*, 21(3):789–813, 2017.

[JMSS19] Y. Jiao, C. Ma, S. Scotti, and C. Sgarra. A branching process approach to power markets. *Energy Economics*, 79:144–156, 2019.

[JMSZ21] Y. Jiao, C. Ma, S. Scotti, and C. Zhou. The Alpha-Heston stochastic volatility model. To appear in *Mathematical Finance*, 2021.

[Joh02] T. C. Johnson. Volatility, momentum, and time-varying skewness in foreign exchange returns. *Journal of Business and Economic Statistics*, 20(3):390–411, 2002.

[Jor88] P. Jorion. On jump processes in the foreign exchange and stock markets. *The Review of Financial Studies*, 1(4):427–445, 1988.

[JS03] J. Jacod and A. Shiryaev. *Limit Theorems for Stochastic Processes; 2nd ed.*, volume 288 of *Grundlehren der mathematischen Wissenschaften*. Springer, Berlin–Heidelberg–New York, 2003.

[JT98] R. Jarrow and S. M. Turnbull. A unified approach for pricing contingent claims on multiple term structures. *Review of Quantitative Finance and Accounting*, 10:5–19, 1998.

[Kal06] J. Kallsen. A didactic note on affine stochastic volatility models. In Y. Kabanov, R. Lipster, and J. Stoyanov, editors, *From stochastic calculus to mathematical finance - The Shiryaev Festschrift*, pages 343–368. Springer, Berlin, 2006.

[KB17] D. P. Kingma and J. Ba. Adam: A method for stochastic optimization. ArXiv working paper available at `https://arxiv.org/abs/1412.6980`, 2017.

[Ken10] C. Kenyon. Post-shock short-rate pricing. *Risk Magazine*, 23:83–87, November 2010.

[KMK10] J. Kallsen and J. Muhle-Karbe. Exponentially affine martingales, affine measure changes and exponential moments of affine processes. *Stochastic Processes and their Applications*, 120(2):163–181, 2010.

[KR09] M. Keller-Ressel. *Affine Processes - Theory and Applications in Finance*. PhD thesis, Vienna University of Technology, 2009.

[KR11] M. Keller-Ressel. Moment explosions and long-term behavior of affine stochastic volatility models. *Mathematical Finance*, 21(1):73–98, 2011.

[KRM15] M. Keller-Ressel and E. Mayerhofer. Exponential moments of affine processes. *Annals of Applied Probability*, 25(2):714–752, 2015.

[KS02a] J. Kallsen and A. Shiryaev. The cumulant process and Esscher's change of measure. *Finance and Stochastics*, 6:397–428, 2002.

[KS02b] J. Kallsen and A. Shiryaev. Time change representation of stochastic integrals. *Theory of Probability and Its Applications*, 46(3):522–528, 2002.

[KS21] S. Klingler and O. Syrstad. Life after LIBOR. *Journal of Financial Economics*, 141(2):783–801, 2021.

[KTW09] M. Kijima, K. Tanaka, and T. Wong. A multi-quality model of interest rates. *Quantitative Finance*, 9(2):133–145, 2009.

[KW71] K. Kawazu and S. Watanabe. Branching processes with immigration and related limit theorems. *Theory of Probability and its Applications*, 16(1):36–54, 1971.

[Kyp14] A. E. Kyprianou. *Fluctuations of Lévy Processes with Applications: Introductory Lectures; 2nd ed.* Universitext. Springer, Berlin–Heidelberg, 2014.

[Lam67a] J. Lamperti. Continuous state branching processes. *Bulletin of the American Mathematical Society*, 73(3):382–386, 1967.

[Lam67b] J. Lamperti. The limit of a sequence of branching processes. *Zeitschrift für Wahrscheinlichkeitstheorie und Verwandte Gebiete*, 7:271–288, 1967.

[Leb72] N. N. Lebedev. *Special Functions and their Applications*. Prentice-Hall, Englewood Cliffs (N.J.), 1972.

[Lee04] R. Lee. Option pricing by transform methods: Extensions, unification and error control. *Journal of Computational Finance*, 7(3):51–86, 2004.

[LeN19] A. LeNail. NN-SVG: Publication-ready neural network architecture schematics. *Journal of Open Source Software*, 4(33):747, 2019.

[LH20] C. G. N. Leunga and D. Hainaut. Interbank credit risk modeling with self-exciting jump processes. *International Journal of Theoretical and Applied Finance*, 23(06):2050039, 2020.

[Li11] Z. Li. *Measure-Valued Branching Markov Processes*. Springer, Berlin–Heidelberg, 2011.

[Li20] Z. Li. Continuous-state branching processes with immigration. In Y. Jiao, editor, *From Probability to Finance - Lecture Notes of BICMR Summer School on Financial Mathematics*. Springer, Singapore, 2020.

[Lip01] A. Lipton. *Mathematical Methods For Foreign Exchange: A Financial Engineer's Approach*. World Scientific, 2001.

[LM15] Z. Li and C. Ma. Asymptotic properties of estimators in a stable Cox–Ingersoll–Ross model. *Stochastic Processes and their Applications*, 125(8):3196–3233, 2015.

[LM19] A. Lyashenko and F. Mercurio. Looking forward to backward-looking rates: A modeling framework for term rates replacing LIBOR. SSRN working paper available at `https://ssrn.com/abstract=3330240`, 2019.

[Mer10] F. Mercurio. Modern Libor market models: using different curves for projecting rates and discounting. *International Journal of Theoretical and Applied Finance*, 13(1):113–137, 2010.

[Mer13] F. Mercurio. A Libor market model with a stochastic basis. *Risk Magazine*, pages 96–101, December 2013.

[Mer18a] F. Mercurio. The present of futures. *Risk Magazine*, pages 1–6, March 2018.

[Mer18b] F. Mercurio. A simple multi-curve model for pricing SOFR futures and other derivatives. SSRN working paper available at `https://ssrn.com/abstract=3225872`, 2018.

[MM18] A. Macrina and O. Mahomed. Consistent valuation across curves using pricing kernels. *Risks*, 6(1):18, 2018.

[Moo01] I. Moosa. Triangular arbitrage in the spot and forward foreign exchange markets. *Quantitative Finance*, 1(4):387–390, 2001.

[MP14] N. Moreni and A. Pallavicini. Parsimonious HJM modelling for multiple yield-curve dynamics. *Quantitative Finance*, 14(2):199–210, 2014.

[MR06] M. Musiela and M. Rutkowski. *Martingale Methods in Financial Modelling*. Springer, Berlin–Heidelberg, 2006.

[MS20] A. Macrina and D. Skovmand. Rational savings account models for backward-looking interest rate benchmarks. *Risks*, 8(1):23, 2020.

[MU08] F. L. Michaud and C. Upper. What drives interbank rates? Evidence from the Libor panel. *BIS Quarterly Review*, March 2008.

[MX12] F. Mercurio and Z. Xie. The basis goes stochastic. *Risk Magazine*, pages 78–83, December 2012.

[NS15] T. A. Nguyen and F. T. Seifried. The multi-curve potential model. *International Journal of Theoretical and Applied Finance*, 18(07):1550049, 2015.

[NVW94] F. Nieuwland, W. Verschoor, and C. Wolff. Stochastic trends and jumps in EMS exchange rates. *Journal of International Money and Finance*, 13(6):699–727, 1994.

[Ope16] OpenGamma. Strata. `https://github.com/OpenGamma/Strata`, 2016.

[Orn14] C. Ornthanalai. Lévy jump risk: Evidence from options and returns. *Journal of Financial Economics*, 112(1):69–90, 2014.

[Pag15] G. Pagès. Introduction to vector quantization and its applications for numerics. *ESAIM: Proceedings and Surveys*, 48:29–79, 2015.

[Par16] E. Pardoux. *Probabilistic models of population evolution: Scaling limits, genealogies and interactions*. Stochastics in biological systems. Springer, Switzerland, 2016.

[PBL10] E. Platen and N. Bruti-Liberati. *Numerical Solution of Stochastic Differential Equations with Jumps in Finance*. Springer, Berlin–Heidelberg, 2010.

[Roc70] R.T. Rockafellar. *Convex Analysis*. Princeton Landmarks in Mathematics and Physics. Princeton University Press, 1970.

[RY99] D. Revuz and M. Yor. *Continuous Martingales and Brownian motion; 3rd ed.*, volume 293 of *Grundlehren der mathematischen Wissenschaften*. Springer, Berlin–Heidelberg, 1999.

[Sat99] K. Sato. *Lévy Processes and Infinitely Divisible Distributions*, volume 68 of *Cambridge Studies in Advanced Mathematics*. Cambridge Univ. Press, Cambridge, 1999.

[Sil69] M. L. Silverstein. Continuous state branching semi-groups. *Zeitschrift für Wahrscheinlichkeitstheorie und Verwandte Gebiete*, 14:96–112, 1969.

[SS19] A. Schrimpf and V. Sushko. Beyond LIBOR: a primer on the new benchmark rates. *BIS Quarterly Review*, March 2019.

[SS21] J. B. Skov and D. Skovmand. Dynamic term structure models for SOFR futures. To appear in *Journal of Futures Markets*, 2021.

[Swi21] A. Swishchuk. Modelling of limit order books by general compound Hawkes processes with implementations. *Methodology and Computing in Applied Probability*, 23(1):399–428, 2021.

[SZZ21] A. Swishchuk, R. Zagst, and G. Zeller. Hawkes processes in insurance: Risk model, application to empirical data and optimal investment. To appear in *Insurance: Mathematics and Economics*, 2021.

[Tea16] Eclipse Deeplearning4j Development Team. Deeplearning4j: Open-source distributed deep learning for the JVM, Apache Software Foundation License v2.0. `http://deeplearning4j.org`, 2016.

[Wal86] J. B. Walsh. An introduction to stochastic partial differential equations. In P. L. Hennequin, editor, *École d'Été de Probabilités de Saint Flour XIV - 1984*, pages 265–439. Springer, Berlin–Heidelberg, 1986.

[WG75] H. W. Watson and F. Galton. On the probability of the extinction of families. *The Journal of the Anthropological Institute of Great Britain and Ireland*, 4:138–144, 1875.

[Woo19] P. Wooldridge. FX and OTC derivatives markets through the lens of the Triennial Survey. *BIS Quarterly Review*, December 2019.

[Wys17] U. Wystup. *FX Options and Structured Products; 2nd ed.* The Wiley Finance Series. Wiley, 2017.

Appendix

CV of the author

Guillaume Szulda

Via Trieste, 63 – 35122 Padova (PD) – Italia
✉ szulda@math.unipd.it

Current affiliation

Department of Mathematics "Tullio Levi-Civita" **Padova (Italy)**
University of Padova
Research associate in Mathematical Finance *2021–2022*
Assignments among others:
- Tutoring of *Mathematical Finance* (30 hours);
- Refereeing for *Annals of Operations Research*.

Education

Laboratoire de Probabilités, Statistiques et Modélisation (LPSM) **Paris (France)**
Université de Paris, Sorbonne Paris Cité (USPC)
Doctoral program (Ph.D.) in Mathematical Finance *2017–2021*
Thesis title: *Branching processes and multiple term structure modeling*
Under the supervision of Prof. Claudio Fontana (University of Padova)
Defended publicly on December 10, 2021

Université de Paris, ENSAE and Université Panthéon Sorbonne **Paris (France)**
Master of Research M2MO (ex DEA Laure Elie) in Mathematical Finance *2016–2017*
Master thesis:
- Title: *An alpha-CIR interest rate model for multiple yield curves*;
- Supervisor: Prof. Claudio Fontana.

Université Paris Dauphine – PSL **Paris (France)**
Master of Science M1MA in Applied Mathematics *2015–2016*

Université de Lille **Lille (France)**
Bachelor of Science in Mathematics *2011–2015*

Publications

1. C. Fontana, A. Gnoatto, and G. Szulda. Multiple yield curve modeling with CBI processes. *Mathematics and Financial Economics*, **15**:579–610, 2021;
2. C. Fontana, A. Gnoatto, and G. Szulda. CBI-time-changed Lévy processes for multi-currency modeling. Submitted to *Annals of Operations Research*, 2021;
3. C. Fontana, A. Gnoatto, and G. Szulda. CBI-time-changed Lévy processes: An analytical framework. In preparation, 2022.

Fellowships

École Doctorale Sciences Mathématiques de Paris Centre (ED386) **Paris (France)**
Doctoral fellowship *October 2017–March 2021*

Fondation Sciences Mathématiques de Paris **Paris and Freiburg**
Research grant *April–July 2019*
Visiting period at the Albert-Ludwigs University of Freiburg (Germany)
under the supervision of Prof. Thorsten Schmidt and JProf. Philipp Harms
Project title: *Energy modeling with measure-valued processes*

Department of Economics, University of Verona **Verona (Italy)**
Research grant *September–December 2019*
Visiting period under the supervision of Prof. Alesandro Gnoatto
Project title: *Branching time change for the modeling of foreign exchange markets*

Presentations

12th European Summer School in Financial Mathematics — **Padova (Italy)**
Contributed talk: Multiple yield curve modeling with CBI processes — *September 02–06, 2019*

Brown Bag Seminar, University of Verona — **Verona (Italy)**
Talk: Multiple yield curve modeling with CBI processes — *October 29, 2019*

13th European Summer School in Financial Mathematics — **Vienna (Austria)**
Contributed talk: CBI-time-changed processes for multi-currency modeling — *August 31–September 04, 2020*

QFW2021, XXII Workshop on Quantitative Finance — **Verona (Italy)**
Contributed poster: CBI-time-changed processes for multi-currency modeling — *January 28–29, 2021*

London-Paris Bachelier Workshop in Financial Mathematics — **London and Paris**
Contributed poster: Multiple yield curve modeling with CBI processes — *March 11–12, 2021*

SIAM Conference on Financial Mathematics (FM21) — **Philadelphia (U.S.)**
Invited talk: Multiple yield curve modeling with CBI processes — *June 01–04, 2021*

10th General AMaMeF Conference — **Padova (Italy)**
Contributed talk: CBI-time-changed processes for multi-currency modeling — *June 22–25, 2021*

Seminario dottorato, University of Padova — **Padova (Italy)**
Talk: Mathematical finance: a tale of stochastic processes — *December 01, 2021*

Conferences

4th Workshop on Branching Processes and Related Topics — **ECNU Shanghai (China)**, *May 21–25, 2018*

11th European Summer School in Financial Mathematics — **ENSAE Paris (France)**, *August 27–31, 2018*

12th Financial Risks International Forum — **CCI Paris (France)**, *March 18–19, 2019*

Languages

French: Mother tongue
English: Professional knowledge
Italian: Good knowledge

Computing

Software

Typesetting: LaTeX
Office: Adobe, Excel, Word, PowerPoint
OS: Windows, Debian and Ubuntu (Linux)

Programming

Good: C, C++, Java
Medium: Python, R project
Basic: Scilab, Maple, Matlab

References

Prof. Claudio Fontana
- Senior Lecturer
- University of Padova – Dep. of Mathematics
- fontana@math.unipd.it
- sites.google.com/site/fontanaclaud/

Prof. Alessandro Gnoatto
- Associate Professor
- University of Verona – Dep. of Economics
- alessandro.gnoatto@univr.it
- alessandrognoatto.com

By **Guillaume Szulda** on January 27, 2022